AUTOMATED TECHNIQUES FOR ECG WAVEFORM FIDUCIAL POINT RECOGNITION.

Parveen Chishti, B. Sc.

Thesis Submitted for the degree of Ph.D.

To: The Faculty of Medicine
University of Glasgow

The research described in this thesis was carried out in the University Department of Medical Cardiology, Royal Infirmary, Glasgow.

Parveen Chishti

Signed:

Date:

ProQuest LLC.
789 East Eisenhower Parkway
P.O. Box 1346
Ann Arbor, MI 48106 – 1346

TABLE OF CONTENTS

CHAPTER TWO:

REFERENCE DATABASES FOR THE STANDARDISATION OF COMPUTER-DERIVED ECG MEASUREMENTS 69

LIST OF TABLES

LIST OF FIGURES

DECLARATION

I hereby certify that this thesis has been researched and written entirely by myself and that it has not been submitted previously for any degree.

Signed:

Date:

ACKNOWLEDGEMENTS

I would like to thank Professor P. W. Macfarlane for his guidance and assistance throughout the duration of my PhD.

Equally, I would like to thank Mr T. C. Aitchison for his support and guidance over the past few years.

The completion of this PhD would not have been possible without the support of many people in the department of Medical Cardiology. I would like to thank Mr B. Devine for all his programming assistance and his helpful advice and assistance in the field of Neural Networks. Most of all, I am grateful for the support and friendship which he has given me throughout the past few years. I could not have done it without him. I am deeply grateful to Mrs J. Watson for all the genuine words of encouragement and support she has given me, thanks Janice.

I would also like to take the opportunity to thank all my friends in the Department of Medical Cardiology and Statistics for all their advice and friendship.

Finally I wish to thank my family for the encouragement and support that they have given me.

ABSTRACT

The aim of this project was to provide methodology to improve ECG wave measurements within the Glasgow Program both in the absence and presence of noise. To this end a database of 125 ECGs (including 'true' values for the fiducial points) was obtained from the Common Standards for Quantitative Electrocardiography (CSE) multilead reference library.

The first technique investigated, effectively involved splitting an ECG several times and averaging the resulting waveforms (the Glasgow smoothing filter). This splitting technique was indeed tried and subsequently implemented as a filter. An initial set of 21 ECGs with 'true' duration and interval values provided was assessed. Standard deviations of the differences (estimated-'true' values) about zero were calculated for each of the P-duration, QRS-duration, PR and QT intervals. For these 21 ECGs, the standard deviations were considerably lower after applying the Glasgow smoothing filter than using the Glasgow Program alone, with the greatest improvement in the P-duration. Five types of noise were added separately to each of these 21 ECGs and tested. Most estimation problems encountered by the conventional program were eliminated when the Glasgow smoothing filter was used.

An alternative method investigated for fiducial point estimation was that of software based neural networks. Several networks were trained using a training set of 75 CSE ECGs to locate the corresponding QRS onsets. Each network was then tested using a validation set of 50 noisy CSE ECGs. A test set of 48 CSE ECGs was next tested. Using the

validation ECGs, the best neural network accurately detected more QRS-onsets than either the Glasgow smoothing filter or the conventional Glasgow program. Based on the test set, the same networks performed poorly. It was clear that the Glasgow smoothing filter performed better than any of the neural networks.

The final technique investigated was that of individualised linear templates. Individualised templates were constructed using 24 filtered (using the Glasgow smoothing filter) CSE ECGs for the P-onset, P-offset, QRS-onset, QRS-offset and T-end, respectively. Results from a test set of 88 CSE ECGs, showed that the individualised templates were extremely successful in estimating the P-onset and T-end. The Glasgow smoothing filter seemed to perform best when locating the P-offset and QRS-onset and QRS-offset. This also appeared true when the five noise types were added to these ECGs. The pattern of improvement was consistent across the different program versions for the different noise types. However, the addition of high frequency noise proved detrimental to the conventional program's ability to accurately estimate the P-onset, P-offset, QRS-onset and QRS-offset. This problem was alleviated by the use of the Glasgow smoothing filter as well as the template.

Although the Glasgow Program is an invaluable ECG analysis program, the techniques described here can be used in conjunction with the Glasgow program to improve the accuracy of ECG wave measurement estimation. It is clear that the Glasgow smoothing filter is best at locating the P-offset, QRS-onset and QRS offset, while the template performs best when estimating the P-onset and T-end.

SUMMARY

Electrocardiography is one of the most widely used clinical tests in hospital practice and is used to record the electrical activity generated by the heart. With the introduction of digital computers in this field, it has been possible to analyse ECGs and cope with the increase in workload. One of the important benefits gained by automating ECG analysis was the increase in accuracy of the estimation of wave measurements compared to those of cardiologists. This reduced observer bias and variation in "visual" analysis, thereby leading to more consistent interpretation. However, since all measurement programs have their own philosophies with respect to optimum waveform analysis, this too can lead to the problem of variations in the estimation of wave measurements.

It is important that ECG wave fiducial point estimation and more importantly duration and interval estimation is as accurate as possible, since it is these measurements that are later used in the diagnostic criteria within an ECG analysis program, such as the Glasgow Program. Inaccurate estimation of wave measurements is even more prevalent in cases where the ECG signal has been contaminated with noise. Whether through powerline interference or other artefacts, these inaccuracies can have the effect of producing erroneous diagnoses and hamper the exchange of diagnostic criteria. It was therefore the aim of this project to provide methodology to improve ECG wave measurements in the absence and presence of noise.

The main database of ECGs used in this project was obtained from the Common Standards for Quantitative Electrocardiography multilead reference library. This library consisted of a training set of 125 ECGs along with corresponding 'true' values produced by a group of five experienced referees as well as 16 European ECG analysis programs. Due to the absence of a reference beat (used in the CSE coordinating centre to align beats produced by different programs) for the alignment of the beats processed by the Glasgow program, a separate set of reference fiducial points was later produced visually by an experienced electrocardiographer. It was important that any results produced through modification of the Glasgow Program or through the introduction of new techniques would match the corresponding 'true' value as closely as possible.

The first technique investigated was that of splitting an ECG. An initial set of 21 ECGs with 'true' duration and interval values provided, was assessed. Initial results were obtained by splitting a 500 sample per second waveform into two 250 sample per second traces, performing linear interpolation on each to once again produce 500 sample per second ECGs and averaging the resulting measurements after processing. Further splitting was performed on the two interpolated split waveforms to produce four traces. After further interpolation, these were then averaged within the program and a final set of smoothed measurements was produced. With the splitting and averaging technique performing the same function as a filter, which was effectively how the technique was implemented, the resulting waveforms were considerably smoother than the original recordings. (The filter was thereafter referred to as the "Glasgow smoothing filter"). Standard deviations of the differences (estimated-'true' values)

about zero were calculated for each of the P-duration, QRS-duration, PR and QT intervals. For this particular set of 21 ECGs the standard deviations were considerably lower after applying the Glasgow smoothing filter. The greatest improvement observed was in the P-duration, where the standard deviation dropped from 16.5ms for the original program to 6.1ms for the Glasgow smoothing filter. Five types of high and low frequency noise were also added to each of these 21 ECGs and tested using both the conventional Glasgow program and Glasgow smoothing filter. Most problems encountered by the conventional program when estimating durations and intervals were eliminated when the Glasgow smoothing filter was used.

An alternative method for fiducial point estimation investigated was that of software based neural networks. Artificial neural networks adopting a back propagation algorithm were trained using 75 CSE ECGs in an attempt to locate the QRS onset of an initial validation set of 50 noisy CSE ECGs (taken from the training set and then contaminated with high frequency 25μV RMS noise). All ECGs were initially filtered using the Glasgow smoothing filter. A "new" test set of 48 CSE ECGs was also tested. Results showed that for the first set of validation ECGs, the best neural network detected more QRS-onsets than either the Glasgow smoothing filter technique or the conventional Glasgow program. However, through closer inspection of the output data it was evident that there was a lot more deviation between the 'true' QRS-onset point and the estimated QRS-onset for certain ECGs when compared to the estimates produced using the Glasgow smoothing filter. Based on the "new" test set of 48 CSE ECGs, neural networks performed poorly, overall. Although certain networks estimated more exact QRS onsets than the Glasgow smoothing filter,

they also estimated more QRS onsets 3 or 4 samples away from the "true" onset compared to the Glasgow smoothing filter. It was also observed that the network which performed best on the validation set did not do as well on the "new" independent test set. It was clear, therefore, that the Glasgow smoothing filter once again performed better than the other methods in estimating the QRS-onset.

The final technique investigated was that of individualised linear templates. Individualised templates were constructed using 24 filtered (using the Glasgow smoothing filter) CSE ECGs for the P-onset, P-offset, QRS-onset, QRS-offset and T-end. Templates for the P-onset, offset and QRS-onset and offset were all designed to locate a global (i.e. across all 15 leads) fiducial point, whereas the template for the T-end was designed to locate a T-end for every available lead of a 15 lead ECG. It was from these T-ends that an overall global T-end was chosen using conventional methods (in the Glasgow program). Results from a test set consisting of 88 CSE ECGs, showed that the individualised templates were extremely successful in improving the location of both the P-onset and T-end. After computing differences between each of the estimated results and the 'true' values for each method, the median difference dropped from 4ms for the conventional program to 0ms for the individualised template in the case of the P-onset. Similarly, when comparing the median difference of the conventional program estimated T-end to that of the templates, the median dropped from 11ms to 2ms. In general, the Glasgow smoothing filter seemed to perform best when locating the P-offset and QRS-onset and QRS-offset. This was also evident when the previous five noise types were added to these ECGs. The pattern of improvement was consistent across the different program versions for the different noise types. However, the

addition of high frequency noise proved detrimental to the conventional program's ability to accurately estimate the P-onset, P-offset, QRS-onset and QRS-offset. This problem was alleviated by the use of the Glasgow smoothing filter as well as the template.

Table 1 summarises the subset of ECGs used in this thesis. Each chapter is listed along with the ECGs used and the reason for using them.

Chapter	Subset of ECGs Used	Reason
Chapter 3 **SPLITTING AN ECG**	21 CSE ECGs 16 CTS ECGs	"True" values were selected for 25 CSE ECGs initially out of a total of 125. These were reduced to 21 ECGs due to compression problems when later adding noise. Total number of calibration ECGs.
Chapter 4 **SPLITTING + NOISE**	21 CSE ECGs + 21 CSE ECGs * 5 Noise types 16 CTS ECGs + 16 CTS ECGs * 5 Noise types	This resulted in 126 ECGs including the original noise-free ECGs. i.e. 6*21 ECGs. This resulted in 96 CTS ECGs including the original noise-free ECGs. i.e. 6*16 ECGs.
Chapter 5 **ARTIFICIAL NEURAL NETORKS**	75 CSE ECGs -Training Set 50 CSE ECGs - Test Set 48 CSE ECGs - Test Set	A total of 75 CSE ECGs had fiducial points visually determined (using CSE durations as a guide) by a referee. 50 of these 75 ECGs randomly selected from training set and contaminated with high frequency noise (25μV) to create an initial test set. "True" values determined for remaining 50 CSE ECGs. 2 ECGs discarded due to presence of pacemaker or noise spikes.
Chapter 6 **TEMPLATES**	24 CSE ECGs - Training Set 88 CSE ECGs - Test Set 77 CSE ECGs + 77 CSE ECGs * 5 Noise types	24 CSE ECGs used since these were the ECGs visually determined by the referee. Originally 25 however 1 ECG discarded due to the absence of a P-wave caused by atrial fibrillation. These were the remaining CSE ECGs out of the total 125. Originally there were 100 (minus 25 for training set) however, 12 were excluded due to problems of artial fibrillation or spikes. The 88 test set ECGs were reduced to 77 when noise was added, due to problems of data compression. This resulted in a total of 462 ECGs including the original 77 noise-free ECGs. i.e. 6*77 ECGs.

Table 1 Subsets of ECGs used

Table 2 recommends the best technique coupled with the existing Glasgow program logic for estimating each fiducial point.

Fiducial Point	Recommended Technique
P Onset	GP & GSF & IT
P Offset	GP & GSF
QRS Onset	GP & GSF
QRS Offset	GP & GSF
T End	GP & GSF & IT

Table 2 Recommendations for the estimation of ECG wave fiducial points within the Glasgow Program. GSF=Glasgow smoothing filter and IT=individualised template

It has been shown in this thesis that, although the Glasgow Program is an invaluable analysis program, the techniques described here can be used in conjunction with the program to improve the accuracy of ECG wave measurement estimation. It is not the most elaborate method which proved to be successful (i.e. in the use of neural networks) and in fact the simpler methods (i.e. the Glasgow smoothing filter and linear templates) produced the greatest improvement.

CHAPTER ONE

ELECTROCARDIOGRAPHY

1.1 INTRODUCTION

An electrocardiogram is the name given to the graphical recording of the electrical activity generated by the heart. Electrocardiography is a valuable aid in the diagnosis of heart disease and complements other cardiac investigations. There is no doubt that the ECG is still the most non-invasive, inexpensive and simplest technique available. (Fisch, 1980). Furthermore, in recent years it has been demonstrated that the ECG can be rapidly and effectively recorded using portable computer-aided equipment. In fact, one of the reasons for using digital computers for interpreting ECGs was to cope with the increase in workload. Other benefits expected were an increase in the accuracy of wave measurements when compared to a cardiologist and the elimination of observer bias, thereby leading to more consistent interpretation. As well as the practical considerations, a significant amount of research has resulted from the introduction of computers into the field of electrocardiography.

1.2 THE HEART

The heart has four chambers, namely the left and right atria and the left and right ventricles (Figure 1.1). Blood is transported to the right atrium from the rest of the body, which then pumps the blood into the right ventricle. It is then transported to the lungs for oxygenation via the pulmonary arteries. Once oxygenated, the blood is transported to

the right atrium via the pulmonary veins, where it is pumped into the left ventricle. The oxygenated blood then exits the left ventricle through the aorta and is then circulated around the body once more.

Each heart beat is controlled by the electrical activity initiated by the sinoatrial (SA) node, more commonly known as the pacemaker of the heart, which is situated in the wall of the right atrium. Impulses from the SA node initiate atrial contraction and then travel via the atria to the atrio-ventricular (AV) node, which lies just above the atrio-ventricular septum (the wall which separates the atria and ventricles).

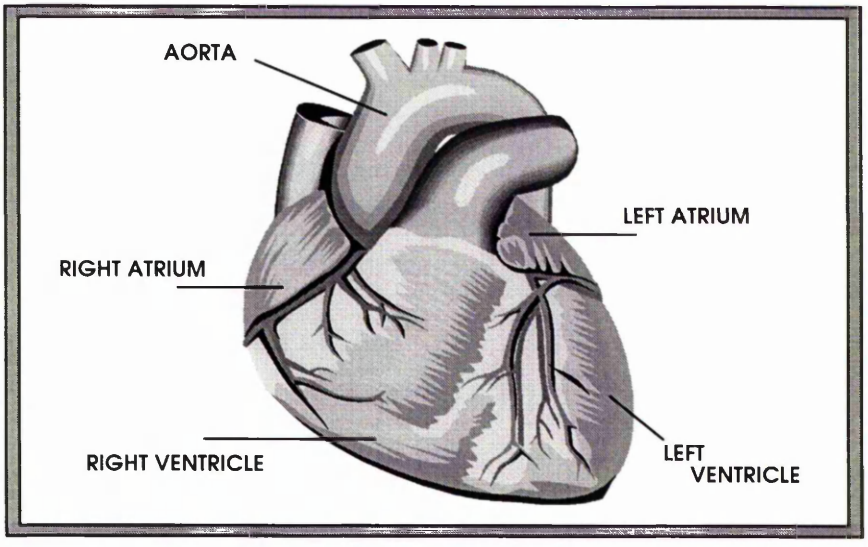

Figure 1.1 The Heart

The electrical impulses then travel down the bundle of His which is divided into two main branches, left and right. Conduction then spreads through the Purkinje fibres, a specialised tissue contained within the ventricles, and then finally into the actual cardiac muscle. It is excitation of these muscle cells which then result in ventricular contraction. During muscular activity, there are two major electrical processes. These are:

Depolarisation : Activation

Repolarisation : Recovery

During the resting state, the muscle cells are said to be polarised.

1.3 HISTORY OF THE ECG

The idea of electrocardiography first came about in the mid-nineteenth century when Galvani (Snellen, 1984) initiated researchers into exploring the idea of electrical activity generated by muscles and nerves. It was in 1856 that bioelectric potentials were demonstrated in a frog's heart (Kolliker & Muller, 1856).

It was in 1876 that the electrical activity of a frog's heart was recorded photographically, using Lippmann's electrometer (Marey, 1876). There were others who were also among the first to do so (Engelmann, 1878; Burdon Sanderson & Page, 1878). It could be said that it was refinement of all this previous work that led to the first known human ECG recording (Waller, 1887). The ECG shown below was obtained from electrodes placed on the front and back of the chest.

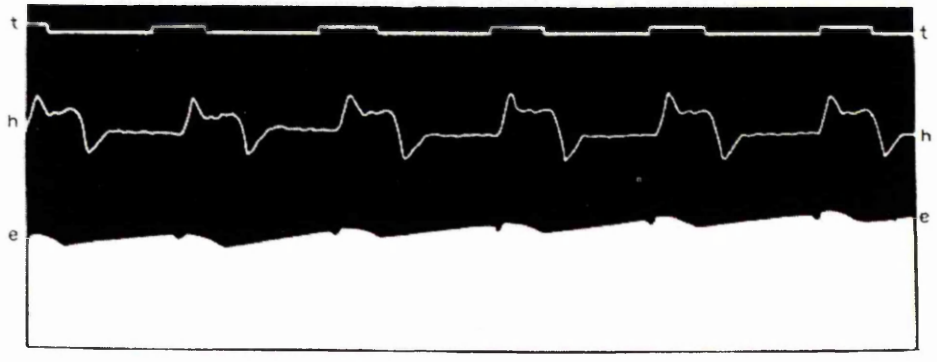

Figure 1.2 The first published human ECG recorded by Waller in 1887
t = time in seconds, h = chest wall movement,
e = electrocardiogram

It was around the turn of the century that the Dutch physician Willem Einthoven developed a string galvanometer sensitive enough to record electrical potentials from the surface of the body (Einthoven, 1901). The methodology applied involved directing a beam of light onto the string of the galvanometer and its image was in turn recorded onto a photographic plate falling under gravity at a constant rate. However, it was not until 1908 in the U.K., that the first commercial version of the Einthoven electrocardiograph was produced, by the Cambridge Instrument Company, and thereafter other models became available throughout Europe.

1.4 ECG LEAD SYSTEMS

1.4.1 12 Lead Electrocardiography

The 12 lead ECG consists of a system of (10) electrodes which measure specific potential differences when connected to the various limbs and the anterior chest. The first set of leads to be introduced were the bipolar limb leads. These were followed by the augmented unipolar limb leads and the unipolar precordial leads.

Bipolar Limb Leads - These leads measure the potential differences between pairs of limbs, i.e. between two points, hence the term 'bipolar'. There are three such leads which were introduced (Einthoven, Fahr and de Waart 1913):

Lead I - Measures the potential difference between the left and right arm.

Lead II - Measures the potential difference between the left leg and the right arm.

Lead III - Measures the potential difference between the left leg and the left arm.

This can be represented in a triangular form better known as Einthoven's Triangle (see Figure 1.3).

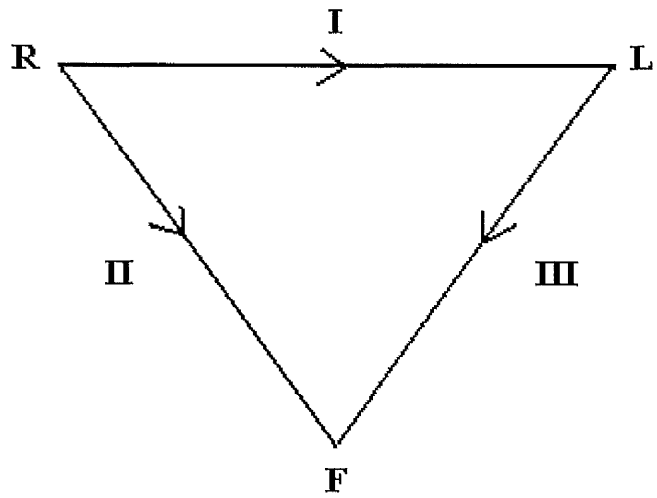

Figure 1.3 Einthoven's Triangle

Einthoven, Fahr and de Waart regarded this triangle as an approximation of the frontal plane of the human body, which was assumed to be electrically homogeneous. However the problem of inhomogeneties was investigated by Burger and van Milaan (Burger & van Milaan, 1946), who subsequently modified the shape of the Einthoven triangle from an equilateral to a scalene triangle, which was named the Burger triangle. Nevertheless, Einthoven's triangle being the idealistic shape continues to be used to illustrate the approximate relationships between the directions associated with the bipolar limb leads.

If E_R, E_L and E_F denote the potentials at the right arm, left arm and left leg respectively then the three bipolar limb leads can be represented in mathematical form as follows :

$$\text{Lead I} = \text{I} = E_L - E_R \quad (1.1)$$

$$\text{Lead II} = \text{II} = E_F - E_R \quad (1.2)$$

$$\text{Lead III} = \text{III} = E_F - E_L \quad (1.3)$$

It thus follows that, at any instant in the cardiac cycle :

$$\text{I} + \text{III} = \text{II} \quad (1.4)$$

the advantage being that if any of the two leads are available, then the third can be immediately derived.

Unipolar Limb Leads - The 'Wilson Central Terminal' was developed in 1934 by Wilson and associates (Wilson, Johnston, Macleod & Barker, 1934). The voltage at this terminal, denoted E_{WCT}, represented the average of the potentials at the right and left arms and the left leg, i.e.

$$E_{WCT} = \tfrac{1}{3}(E_R + E_L + E_F) \quad (1.5)$$

where E_{WCT} was a relatively constant value obtained throughout each cardiac cycle. Now if E_P denotes the potential of an exploring electrode P, seen in Figure 1.4, then the potential variation, V_P, measured at a single point is :

$$V_P = E_P - E_{WCT}$$
$$= E_P - \tfrac{1}{3}(E_R + E_L + E_F) \quad (1.6)$$

Since E_{WCT} is a relatively constant potential then this allows the potential variation to be recorded at a selected point, in this case the exploring electrode P. Hence the term given to a lead which records the potential variation at a single point is 'unipolar'.

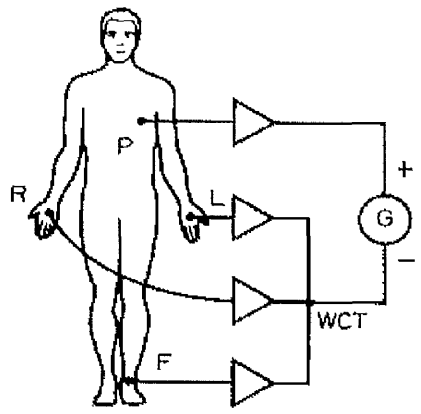

Figure 1.4 The circuitry used to record a unipolar lead. P is the exploring electrode and WCT is the Wilson Central Terminal. (From Comprehensive Electrocardiology, Eds. P. W. Macfarlane and T. D. V. Lawrie)

Similarly, it is possible to derive the unipolar limb leads VR, VL and VF, which measure the potential variation at the right arm, the left arm and the left leg respectively. It is then possible to write:

$$VR = E_R - E_{WCT} \quad (1.7)$$
$$VL = E_L - E_{WCT} \quad (1.8)$$
$$VF = E_F - E_{WCT} \quad (1.9)$$

From equations 1.5 and 1.7-1.9 it follows that :

$$VR + VL + VF = 0 \tag{1.10}$$

However, the disadvantage of these leads was that the voltage recorded was undesirably low and so in 1942 Goldberger produced a modification to the Wilson Central Terminal (Goldberger, 1942). This modification involved removing one of the connecting electrodes from the terminal in order to increase the voltage readings obtained by a unipolar limb lead. For example, by removing the electrode connected to the right arm, the new central terminal consisted of the average of the potentials at the left arm and left leg. Figure 1.5 illustrates the circuitry required to derive the augmented lead, aVR.

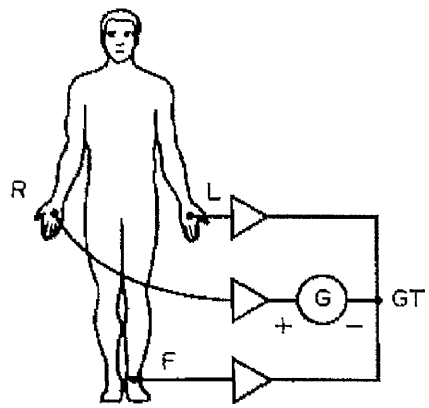

Figure 1.5 The circuitry used to record the augmented unipolar limb lead aVR. Here GT represents the Goldberger Terminal. (From Comprehensive Electrocardiology, Eds. P. W. Macfarlane and T. D. V. Lawrie)

If E_{GT} denotes the potential at the modified terminal, then it follows that:

$$
\begin{aligned}
aVR &= E_R - E_{GT} \\
&= E_R - \tfrac{1}{2}(E_L + E_F) \\
&= \tfrac{3}{2}E_R - \tfrac{1}{2}(E_R + E_L + E_F) \\
&= \tfrac{3}{2}\left\{E_R - \tfrac{1}{3}(E_R + E_L + E_F)\right\} \\
&= \tfrac{3}{2}V_R
\end{aligned}
\tag{1.11}
$$

The results obtained by removing connections corresponding to the left arm and left leg would be similar producing aVL and aVF respectively. In summary :

$$aVR = \tfrac{3}{2}VR \tag{1.12}$$

$$aVL = \tfrac{3}{2}VL \tag{1.13}$$

$$aVF = \tfrac{3}{2}VF \tag{1.14}$$

These leads were named the **Augmented Unipolar Limb Leads** due to the fact that the potential of the particular augmented lead increased by 50% when compared to the original lead. It then automatically follows that

$$aVR + aVL + aVF = 0 \tag{1.15}$$

at any instant in the cardiac cycle.

Unipolar Precordial Leads - The development of the Wilson Central Terminal made it possible to measure the potential variation at any point on the body, e.g. on the anterior chest. It was therefore not surprising that additional information could be gained by placing electrodes closer to the heart and moving them around the thorax to obtain 'views' of the heart from different angles. A committee of the American Heart Association (1938 & 1943) selected six positions on the

precordium in order to standardise recordings. The positions of the electrodes V1-V6 on the chest are illustrated in Figure 1.6.

These leads together with the aforementioned 6 leads, form the conventional 12-lead ECG which is the most frequently recorded ECG in routine use.

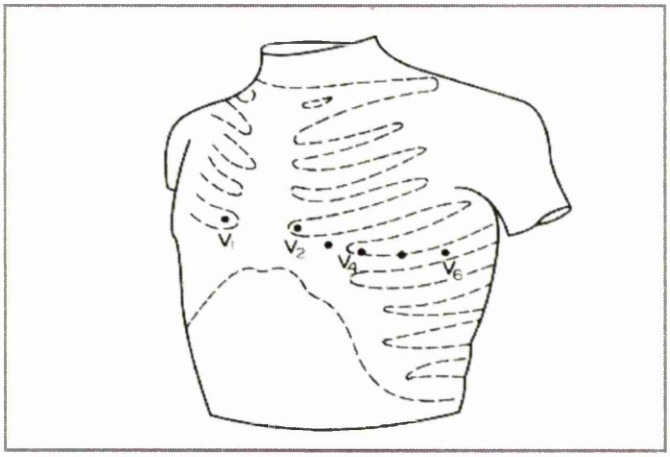

Figure 1.6 The six electrode positions used to record unipolar chest leads.
(From Comprehensive Electrocardiology, Eds. P. W. Macfarlane and T. D. V. Lawrie)

1.4.2 Vectorcardiography

Einthoven et al. (Einthoven, Fahr & De Waart, 1913) came to the conclusion that by summing the individual electrical forces at any instant in a single cardiac cycle, it was possible to produce a single resultant force which could be represented by a vector that had a direction and a magnitude. This idea of a single resultant vector could be extended throughout the cardiac cycle. As a result, a loop could be produced by joining the tips of these vectors. This was done both in 1920 and again in 1938 (Maan, 1920; Wilson & Johnston, 1938). In order to derive a vector loop in the frontal plane, both leads I and VF

were applied simultaneously to the horizontal and vertical axes of an oscilloscope respectively. A line joining the origin of the loop to any point on its circumference represented the relative magnitude and orientation of the resultant cardiac vector in the frontal plane at one particular instant in the cardiac cycle.

The concept of a resultant vector in a plane could be extended to that of a spatial vector loop. By recording three leads simultaneously, denoted X, Y and Z, it was possible to derive a vector which moved throughout 3-dimensional space. Projection of this spatial vector loop onto three mutually perpendicular planes called frontal, sagittal and transverse gave rise to the vectorcardiogram (see Figure 1.7). However, due to the fact that these leads were not electrically orthogonal, (i.e. they did not record the potential differences in the desired mutually perpendicular directions for the resultant vector to be calculated accurately at any instant) these lead systems were termed 'uncorrected systems'.

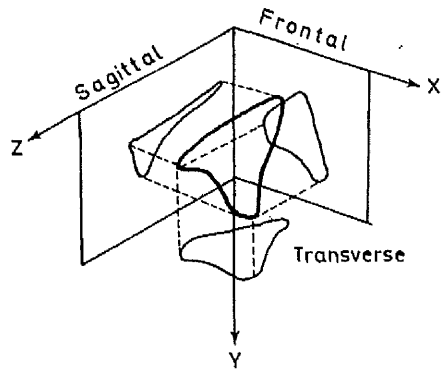

Figure 1.7 **A spatial vector loop, with its projections onto three mutually perpendicular planes, called frontal, sagittal and transverse** **(From An Introduction to Automated Electrocardiogram Interpretation. Eds P.W. Macfarlane and T.D.V. Lawrie, 1974).**

The concept behind using a corrected lead system was to produce an electrode network that resulted in potential differences that were of equal magnitude and at the same time, mutually perpendicular, at least in theory. It was Frank who developed the first truly corrected orthogonal lead system (Frank, 1956). The characteristics of this system were that the leads were equally sensitive and measured the components of the cardiac dipole in approximately the desired orthogonal direction. These leads were thus referred to as Frank XYZ leads.

1.5 THE PQRST WAVEFORM

The PQRST waveform is the term used to describe the basic ECG morphology. The terminology first originated from Einthoven's earlier papers, where he used the term to describe the deflections of the electrocardiogram. This choice of letters meant that it was possible to leave room for further discoveries such as the U wave which was later discovered by Einthoven himself, using his string galvanometer.

The PQRST waveform consists of three main components. These are the P-wave, the QRS complex and the T-wave. An 'idealistic' example is shown in Figure 1.8. Each deflection is produced by an electrical process, depolarisation and repolarisation, both of which were mentioned in the previous section. The three major deflections and their corresponding electrical states can be summarised as follows:

(i) P-wave : atrial depolarisation

(ii) QRS-complex : ventricular depolarisation

(iii) T-wave : ventricular repolarisation

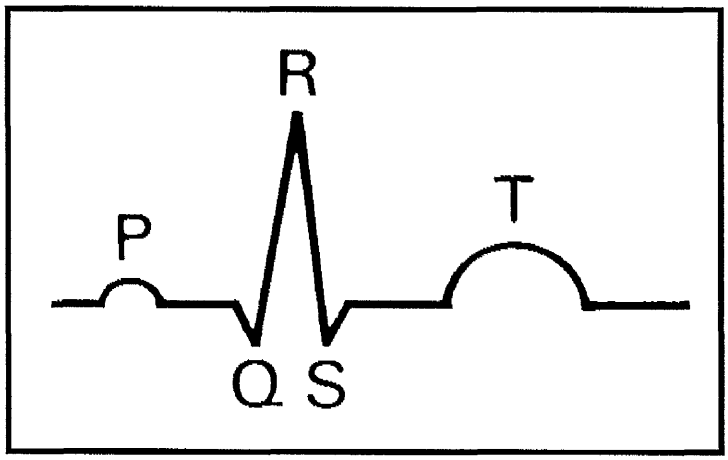

Figure 1.8 Schematic interpretation of an ECG waveform

Cardiac abnormalities are determined by parameters such as the duration and amplitude of a particular waveform. Time intervals and durations are evaluated by taking the difference of certain fiducial points of the wave components. The magnitude of the P-wave can be seen to be much smaller than that of the QRS complex. The underlying reason is that the atrial mass is smaller than the ventricular mass and therefore a smaller deflection is recorded during depolarisation of the atria.

The determining factor of the direction of the deflection of an ECG waveform is in part the positioning of the electrodes. By convention, when an electrical impulse flows towards a unipolar electrode or the positive electrode of a bipolar lead, a positive, upwards deflection is recorded by the galvanometer. However, when an electrical impulse flows away from these electrodes, a negative downwards deflection is recorded. It is these deflections that are arbitrarily and sequentially named P, QRS, and T.

1.6 Spatio-Temporal Relationship of ECG Waveforms

A 12-lead ECG can be considered as a projection of the resultant cardiac vector onto 12 different axes (or lead directions). This is demonstrated in Figure 1.9.

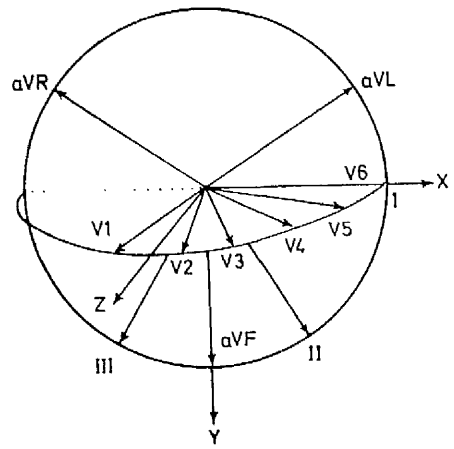

Figure 1.9 **The projection of the resultant cardiac vector onto the assumed lead directions of the 12-lead ECG. (From An Introduction to Automated Electrocardiogram Interpretation. Eds P.W. Macfarlane and T.D.V. Lawrie, 1974).**

In terms of spatio-temporal relationships, the orientation of a vector loop, for example a T-vector loop, critically affects the location of the end-point of the wave, in this case the T-wave (Kors, van Herpen and van Bemmel; 1999). From Figure 1.10 it can be seen that as the vector loop becomes perpendicular to a lead axis, the amplitude of the resulting T-wave becomes smaller. Note also, that as a result, the end of the T-wave is apparently located earlier (cf time point 3 in Figure 1.10, B compared to A). Conversely, if the loop becomes more parallel to a lead axis, the T-wave amplitude increases.

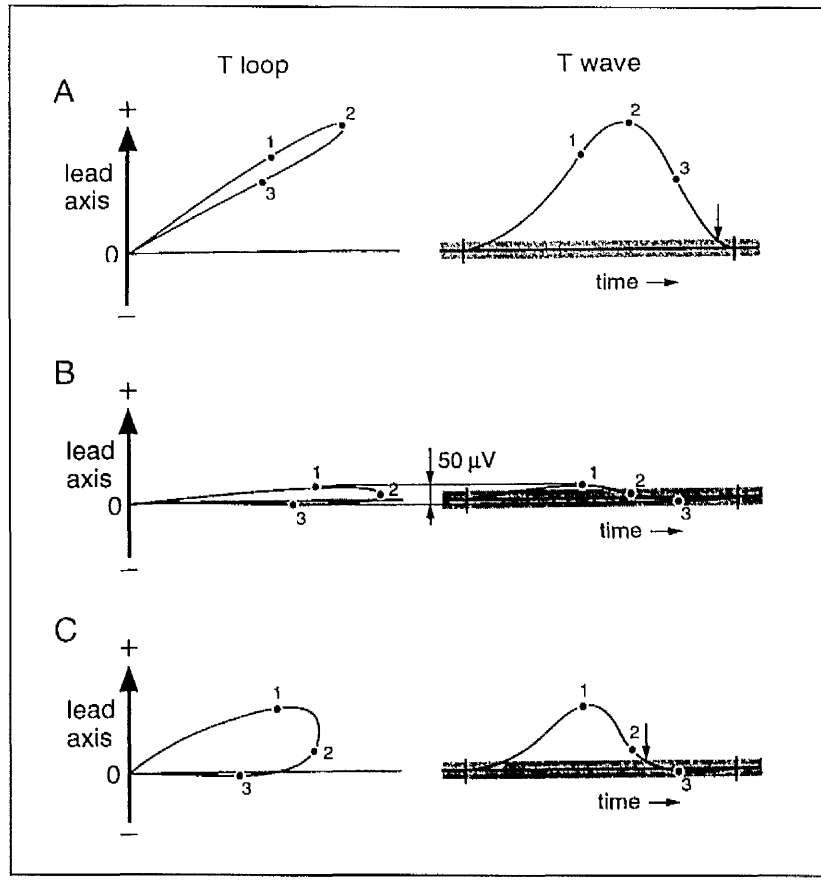

Figure 1.10 Projection of T loops on hypothetical lead axis plotted against time. (From QT Dispersion as an Attribute of T-Loop Morphology. J.A. Kors, G. van Herpen J.H. van Bemmel, 1999).

In certain forms of disease, the T vector loop is more likely to deviate from the normal direction, giving rise to a greater probability of T-wave abnormalities and dispersion about the true end of the T-wave, depending on the leads involved. From Figure 1.11 the presence of some different and distinct cardiac 'diseases' can be seen to affect the morphology of each of the components of the ECG waveform. Also included are the corresponding spatial velocities [$s.v.=\sum_{l=1}^{12}|\Delta x_i|$, where l represents the lead number and i, the ith sample point] for each illustration. The spatial velocity is basically a transformation of all the available leads and is used commonly to improve fiducial point detection (see

Section 1.8). The first column of ECGs in Figure 1.11 is representative of a normal 12-lead ECG. In the case of left ventricular hypertrophy (LVH), there is increased muscle mass of the left ventricle, with increased electrical activity. This is typically reflected by tall R waves in leads V5 and V6 with occasional T-wave inversion, and deep S waves in leads V1 and V2. Left bundle branch block (LBBB) occurs when there is a block in conduction through the main branch of the left bundle of His. Here, the QRS complex becomes widened and the R-wave usually becomes wide and notched in leads I, aVL, V5 and V6. With myocardial infarction (MI), the sequence of ECG changes is usually as follows: the T-wave normally becomes tall and upright, the ST segment becomes elevated, a Q wave appears and the T wave become inverted. Over a few days the ST segment should gradually return to the isoelectric line and the T-wave may eventually become upright. The Q-wave may persist.

It is **therefore** important that any method of detecting fiducial points has to acknowledge the wide variation in the morphology of ECG waveforms.

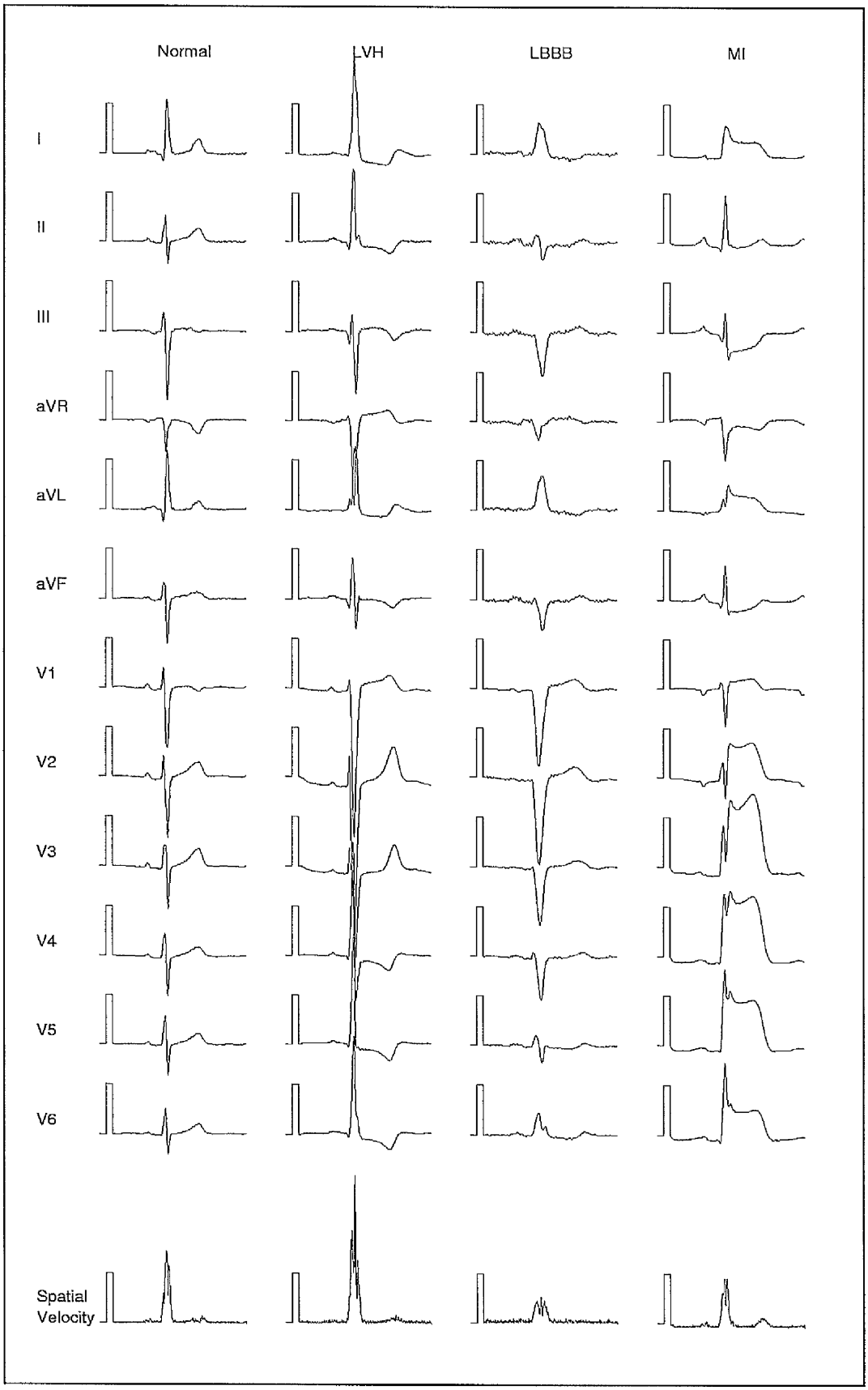

Figure 1.11 The effect of different diseases on a 12-lead ECG

1.7 COMPUTER ANALYSIS OF THE ECG

Electrocardiography is one of the most widely used clinical tests in hospital practice. The continuing growth of ECGs recorded annually over the years, stimulated the development of automated methods of ECG interpretation (Macfarlane, 1974).

The application of the digital computer to analysis of ECGs was initiated in the 1950's and continued into the next decade. The first task was to construct a device that allowed the conversion of electrical signals generated by an electrocardiograph into digital data. It was only then that this data could be handled by a computer (Pipberger, Freis, Taback & Mason, 1960). However, at that time analogue-to-digital (A-D) conversion systems were not available and so as a result a special purpose A-D converter was developed. XYZ leads were simultaneously recorded on an analogue tape recorder and a single cycle was selected by a technician. This cycle was then converted to digital form at a rate of 1000 times per second and stored on digital tape (Pipberger et al, 1960). It was in 1961 that the first automatic wave recognition program was developed (Stallman & Pipberger, 1961). This program involved the construction of a function which was dependent on the three simultaneously recorded XYZ leads. This function was then used to detect the required fiducial points. By 1962, one of the first programs for analysis of the 12 lead ECG became available (Caceres, Steinberg, Rikli et al., 1962). Cady and associates (Cady, Woddburgy, Gelertner et al., 1961) and Young and Huggins (1964) were just some of the other researchers who investigated alternative approaches to the computer interpretation of the ECG during the early 1960's.

It was not long before European and Japanese researchers began to show great interest. With the cooperation of American researchers, a Japanese team published their first paper in 1963 (Okajima, Stark, Yasui et al., 1963). By 1964 some Europeans began their research into this field, but it was not until 1968 that the first paper discussing the future of computerised electrocardiography was published (Lawrie & Macfarlane, 1968). Other early European researchers were Van Bemmel (Van Bemmel, Duisterhout, Versteeg et al., 1971) and Zywietz, the latter of whom was active in organising an international meeting in 1971, where the most up to date developments in computerised electrocardiography were presented (Zywietz & Schneider, 1973).

The early 1970's saw the advent of the microprocessor on a single chip. This major technological advancement meant that it was possible to automate ECG analysis at the bedside. This would replace the process of transmitting ECG recordings in analogue form to processing centres hundreds of miles away via telephone lines (Macfarlane, 1990).

Such advances in technology have allowed the simultaneous recording of all 12 ECG leads in digital form, using a microprocessor controlled electrocardiograph. Once the recordings are completed, an interpretation is produced in a matter of seconds. Such automated methods are capable of producing results very close to those produced manually by physicians, although these results do require confirmation by an authorised member of the medical staff.

1.8 ECG WAVE MEASUREMENT PROGRAMS

One of the main tasks of ECG-processing computer systems is the calculation of wave measurements. Techniques for the detection of QRS complexes include those algorithms of single lead QRS detection where implementation of a threshold means that when a band pass filtered signal exceeds a predefined level, the signal is assumed to be a QRS complex. As well as the single lead detection algorithm there exists the multiple lead algorithm. In this case, the formation of a detection function is required to transform the leads and increase the fiducial point detection rate. One common type of transformation is the construction of a spatial velocity. The concept of spatial velocities has progressed from the 3 simultaneously recorded orthogonal leads to combining several leads from the 12 lead ECG. This spatial velocity function is defined as follows :

$$s.v.(t) = \sum_{n=1}^{L} \frac{|x_n(t+k) - x_n(t)|}{|k.\Delta t|} \tag{1.16}$$

Here $x_n(t)$ represents the amplitude in lead n at time t (Δt being the sampling interval) and L is the total number of leads over which the spatial velocity is being calculated. Δt should be kept as small as possible with k=1 if an accurate estimate of the first derivative is desired. As the contribution of $k.\Delta t$ is a constant, the spatial velocity is often expressed as the sum of the absolute first difference of all the available leads and can be represented as follows :

$$s.v.(t) = \sum_{n=1}^{L} |x_n(t+1) - x_n(t)| \tag{1.17}$$

Throughout the years there have been many QRS detection methods developed (Plokker, 1978) and a more elaborate method based on pattern recognition (Talmon, 1983). More recent algorithms include a wavelet transform-based QRS complex detector (Kadambe, Murray & Boudreaux-Bartels, 1999), a real-time microprocessor QRS detector system (Ruha, Sallinen & Nissila, 1997), a microcontroller-based real-time QRS detection method (Sun, Suppappola and Wrublewski, 1992, 1995) and a single channel, arrhythmia-monitoring QRS detection algorithm (Forbes & Jimison, 1987). Alternative approaches for QRS-detection have included artificial neural networks (Vijaya, Kumar & Verma, 1998; Xue, Hu & Tompkins,1992).

An example of a T-wave detection algorithm is that by Daskalov and Christov (Daskalov and Christov, 1999) which consisted of adequate selection of the T-end search interval, improved T-wave peak detection and computation of the angle between two 10ms long adjacent segments along the search interval.

Automated techniques used for the location of the T-end have been discussed previously (McLaughlin, Campbell & Murray; 1995, 1996; Murray, McLaughlin & Campbell, 1997). These include the 'threshold' method, the 'differential threshold' method, the 'slope intercept' method and the 'peak slope' intercept method. Both threshold methods determine the T-wave end as the interception of a threshold level with the T-wave and the differential of the T-wave. The threshold levels are calculated as a fraction of the amplitude of the T-wave or differential T-wave for the threshold and differential threshold techniques respectively. Threshold crossing points are determined using a left to right scan of the data from the waveform peaks.

The 'slope intercept' and 'peak slope intercept' techniques are based on slope features of the T wave. The 'slope intercept' technique identifies the end of the T-wave as the intercept of an isoelectric level and a line tangential to the point of maximum T wave slope. Technique 'peak slope intercept' calculates the end of the T wave as the intersection point between an isoelectric level and the line which passes through the peak of the T wave and the point of maximum T-wave slope.

Unlike the QRS complex, detection of the P wave still remains the most difficult task in automated ECG analysis (Willems & Pipberger, 1972). Alternative techniques used in the past have included a microcomputer based P-wave synchronisation system for an artificial heart (Li, Han & Yang, 1986) and the use of a new atrial pacemaker lead which improves stability and detection of the P-wave (Hughes, Bertolet & Brownlee, 1983). Neither of these are however suited or relevant to 12-lead electrocardiography. In situations where a P wave is undetected or inaccurately measured, the resulting interpretation will undoubtedly be affected, thus producing an inaccurate diagnosis. In an attempt to detect P waves successfully, it is important that the processing time is kept to a level which is practically feasible (van Bemmel, 1982). A compromise must be reached where the amount of signal processing required does not far exceed the practical use (i.e. there is no point implementing a technique with a long run time only to produce results which are slightly better than the existing methodology). This may prove to be difficult but, nevertheless, necessary.

1.9 THE GLASGOW PROGRAM

The very first wave recognition program became available in 1961 (Stallman & Pipberger, 1961) which allowed more detailed analysis of ECG records. This original program was based on the Frank XYZ leads. It was in 1962 that the first program for conventional 12-lead ECG analysis was introduced (Caceres, Steinberg, Abraham et al., 1962). Since then several other operational systems have been developed, one of which includes the Royal Infirmary's Glasgow Program (Macfarlane, Devine, Watts et al., 1990). The current Glasgow 12 lead ECG program originates from 1977 when it was decided, after many years of developing techniques for computer analysis (Macfarlane, Watts, Lawrie et al., 1976), that the 3-orthogonal lead ECG display was not going to be readily accepted by clinicians even though studies had shown that, from a clinical point of view, the 3-orthogonal lead ECG was at least as accurate in the diagnostic sense as the 12-lead ECG (Macfarlane, Lorimer & Lawrie, 1971).

Due to improvements in the development of microprocessor technology in the 1970's it became possible to record all leads simultaneously and so it was decided to develop a new lead system that combined both the 12-lead and the 3-orthogonal lead ECG. As a result, the hybrid lead system was introduced in 1978 (Macfarlane, 1979).

The current 12-lead ECG program is implemented on several electrocardiographic devices. Those currently in use in the Glasgow Royal Infirmary are the Siemens 440, 740 and the Siemens Megacart which are used for recording routine ECGs within the hospital. Other

devices being used in locations outwith the Glasgow Royal Infirmary but in collaboration with the department are the Siemens 460 and the Burdick 850i. ECG reports can be obtained directly from the ECG machines, although in situations where it is of interest to store the ECG data such as for serial comparisons or clinical trials in which the department may be involved, the ECG can be transmitted directly from the carts into an ECG management system via a serial or ethernet link. ECGs recorded outwith the hospital are transmitted via modems to the central ECG management systems through telephone lines.

The development version of the Glasgow Program is run on a MICROVAX system under the ULTRIX-32 operating system. This version is solely used for research and development purposes within the Department of Medical Cardiology.

1.10 WAVE MEASUREMENT WITHIN THE GLASGOW PROGRAM

The wave measurement section of the Glasgow program begins with applying a 50 or 60 Hz filter to the ECG data to remove any excess noise, depending on the mains frequency. Leads which fail to be recorded properly are removed from any further processing.

The next section of the program generates floating point data files from the original integer lead data files. Also those leads which are not recorded by the ECG machines, namely, leads III, aVR, aVL, aVF and if required, leads X, Y and Z, are derived using a set of predefined equations.

Provisional QRS onsets and terminations are next located by forming a spatial velocity function using all the available leads. The peaks of QRS complexes are located and the corresponding spatial velocities are used to calculate threshold values. These thresholds are then used to located the required QRS onsets and terminations.

Excessive baseline drift is then detected. The severity of drift is determined by a detection criteria for each lead individually. When a significant amount of baseline drift is present, it is removed by forming a cubic spline interpolation between each of the QRS onsets and subtracting this 'curve' from the ECG signal. The leads are then rewritten with the drift removed.

The next stage involves wave typing. This process involves categorising different beat morphologies within a lead into different classes. Optimum alignment of two beats (by comparing first differences) determines to which class the beats are allocated. If the difference between two cycles in terms of the parameter under consideration is less than a certain threshold value then they are said to be of the same class. For example the first and second beat of lead I are compared. If they are below the stated threshold then they are classified as type 1. If they are dissimilar (i.e. if the defined threshold is exceeded) then the second beat is classified as type 2. All remaining beats are then compared to both classes and allocated accordingly. If a new type of wave morphology is encountered then a third class type is established and so on. This results in clusters consisting of similar complexes. The process is repeated for all the remaining leads.

The next stage is to form an average, modal or median beat (this is an option available within the program). However, first of all a single class is isolated from those established in the wave typing section. Different circumstances influence this choice although most often the class type with the narrowest QRS width is chosen (Macfarlane, Peden & Lawrie et al., 1977). These beats are already aligned timewise and so first differences are computed, at each sampling point where each is assigned a definite weight which is determined by an equation which takes into account the value of the first difference. Those differences which are most common or closest together are allocated a large weight and any of which are different are assigned a small weight. These values are therefore integrated and a weighted average is computed (Macfarlane et al., 1977).

The final stage of the procedure is the wave measurement section. At this point, the various measurements of the 3, 12 or 15 lead averaged beats are computed depending on which type of ECG is being analysed. A preassigned software switch setting is available within the Glasgow program as to which type of lead analysis is required, i.e. 3, 12 or 15. Initially, global QRS onset and termination points are located by forming a spatial velocity from all the available leads. The spatial velocity is assumed to take the form of an M-shape. Maxima are located on each side of the waveform. Critical or threshold values are then used to locate the fiducial points on the appropriate side of the two peaks. Fiducial points are revised in case the 'true' onset or termination point had been missed. Individual lead onsets and terminations are then found in isolation including the morphology of the averaged beats. Once all the QRS fiducial points have been located for the various leads, the earliest point is taken to be the overall QRS

onset. The same procedure is applied to the QRS offset and T termination and the latest points are regarded as being the overall offsets after having checked for and removed outliers. These outliers are those fiducial points which lie 10 or more samples away from their nearest neighbour.

The case of the P onset and termination points is entirely different. Due to the problem of low amplitude P-waves it was decided that the P onsets would be regarded as being simultaneous in all leads. This also applied to the P terminations.

Figure 1.12 depicts the individual stages of the Glasgow program, including the diagnostic phase, in the form of a flow diagram. The text to the right of each 'box' represent the names of the individual analysis procedures within the Glasgow Program.

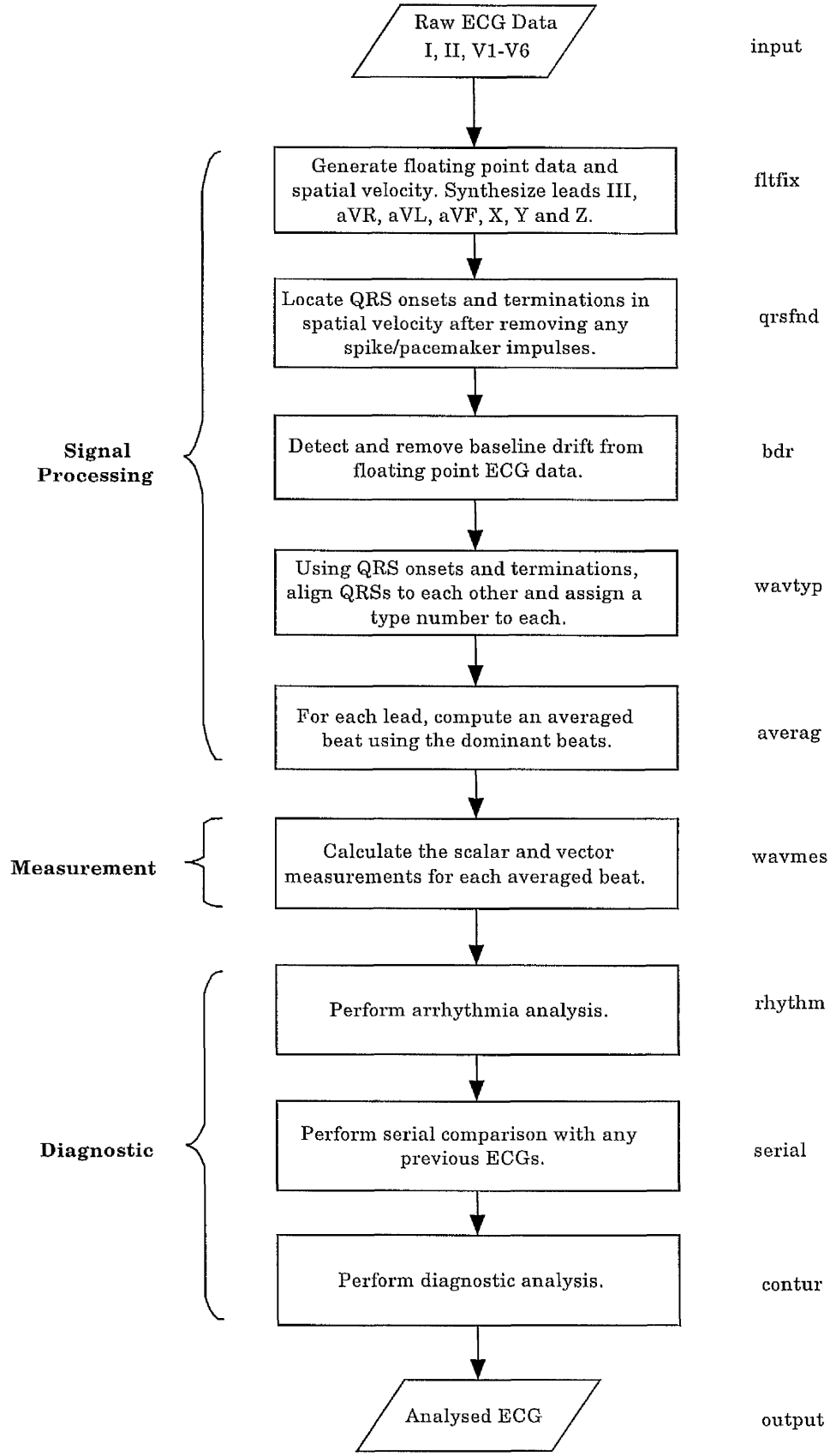

Figure 1.12 Flow diagram representing the stages of ECG analysis within the Glasgow Program.

1.11 EFFECTS OF NOISE

Inaccuracy of wave measurements is even more prevalent in cases where the ECG signal has been contaminated with noise. Whether through powerline interference or other artifacts, these inaccuracies can have the effect of producing false diagnoses and hamper the exchange of diagnostic criteria. An example of a noisy 12-lead ECG can be seen in Figure 1.13

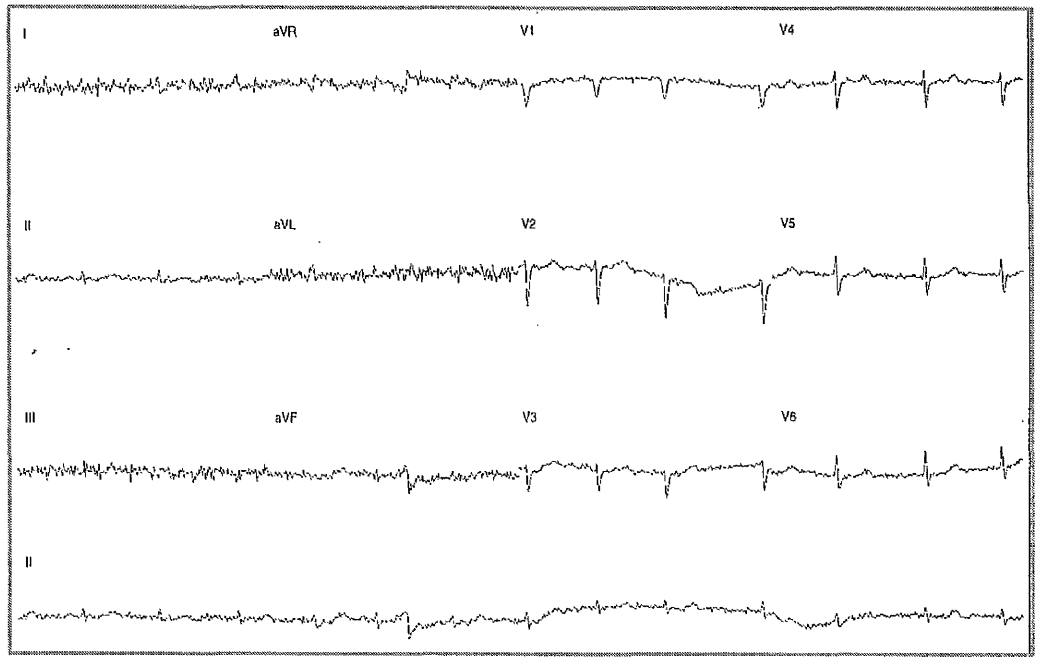

Figure 1.13 A noisy 12-lead ECG

It is of utmost importance that, in order to obtain optimal performance in ECG processing, the ECG data should be of good quality (Talmon, 1983). Different techniques have been designed in previous years to correct for artifacts such as powerline interference, baseline wander and spikes, most of which incorporate digital-filtering methods such as that by Mortara (Mortara, 1977). Different programs apply different filters to the ECG signal and each of its components,

specific to the task at hand. Correction for baseline 'wander' and spike removal are just some of the techniques which have been incorporated into existing ECG programs. There are many types of digital filters, examples of which are: infinite and finite impulse response filters, integer filters and adaptive filters (Tompkins, 1993; Thakor, 1991). Some have used an inverse loop method for eliminating interference by electromagnetic induction from powerlines (Adli, Yamamoto, Nakamura, 1999) while others involve a two step procedure of selective filtering of the ECG and removal of residual error in order to enhance the precision of ECG baseline correction (Shusterman, Shah, Beigel & Anderson, 2000). However, although these filters attempt to eliminate excess noise, there is still difficulty in producing accurate measurements for ECGs similar to the contaminated version seen in Figure 1.12 above.

Inaccurate measurements are also a problem when the repeatability of ECGs is investigated. ECGs recorded several minutes apart or days apart, can lack repeatability in the overall diagnostic sense due to small changes in ECG measurements. This is possible because the ECGs are recorded and analysed independently of each other even though all the conditions remain unchanged. Changes in ECG measurements from one recording to another cause threshold values to be crossed within the diagnostic section of the program, therefore producing different diagnoses.

1.12 SUMMARY

This thesis aims to tackle the problem of inaccurate fiducial point estimation in the absence and presence of noise. The presence of excess

noise in an ECG signal is a common problem faced by many cardiologists and automated analysis systems and in turn causes difficulties in interpreting the recordings.

The following chapter discusses in detail the data sets which were used in this thesis. The underlying reasons behind the construction of the databases is discussed as well as results from subsequent studies performed.

CHAPTER TWO

REFERENCE DATABASES FOR THE STANDARDISATION OF COMPUTER-DERIVED ECG MEASUREMENTS

2.1 THE CSE DATABASE

2.1.1 Introduction

Recommendations for standardisation in electrocardiography were first published by the American Heart Association and the Cardiac Society of Great Britain and Ireland (1938). Updates were subsequently made by different Committees on electrocardiography of the American Heart Association (1943, 1954, 1967, 1975). Due to the rapid growth in computer electrocardiographic processing, it was necessary to develop standards for computer-derived ECG measurements. However, the nomenclature and most of the definitions outlined by the various committees of the American Heart Association were intended mainly for visual analysis and were not specific enough for computer interpretation of the ECG. Requirements for rules which would help to reduce the wide variation in ECG measurements from program to program and lead to better levels of agreement led to the initiation of an international project within the European community in 1979, entitled Common Standards for Quantitative Electrocardiography, better known as the CSE study (Willems, Arnaud, Zywietz, et al., 1980, 1981, 1982, 1983, 1984, 1985; Bourdillon, Denis, Willems, et al., 1982; Macfarlane & Willems, 1983). This later led to the development of the very first CSE reference library (Willems, Arnaud, Zywietz et al, 1985). The databases within this measurement reference library were

constructed solely for measurement testing. The library allowed for the evaluation of three ECG leads recorded simultaneously from the standard 12-leads as well as the Frank XYZ leads. Following on from this a second study was subsequently performed to establish the CSE multilead reference library (Willems, Arnaud, Zywietz et al, 1987). The development of a multilead library was necessary since most advanced micro-computer based ECG systems operate only on multilead ECGs where all the leads (12 or 15) are recorded simultaneously. This chapter summarises the results from the aforementioned publications and is intended to introduce the CSE database, its usefulness and its relevance to studies on ECG signal processing.

2.1.2 The Analysis Process

The multilead database consisted of 250 original ECG recordings which represented a wide variety of ECG configurations; 26% were normal and the remainder were abnormal. However, due to different ECG measurement programs having their own philosophies with respect to analysis, 250 artificial ECGs were created. These ECGs were formed on the basis of a selected beat taken from the original recordings and reproduced to create a string of identical beats with stable RR intervals over ten seconds for all 12/15 simultaneous leads. These 250 original and corresponding artificial ECGs were then randomly divided (in pairs) into two sets containing nearly equal samples of normal and abnormal pathologic entities. The first set of original and artificial ECGs was used for training and the second was kept for future testing.

The 250 original ECGs and corresponding 250 artificial ECGs were visually analysed by five expert CSE referee cardiologists and processed by a total of six XYZ and eleven standard 12-lead ECG analysis programs. These are shown in Table 2.1. Programs 2, 11 and 13 based their wave recognition on all leads simultaneously. Program 4 analysed six leads at a time (I-aVF and V1-V6). Program 15 performed global wave recognition on three semiorthogonal standard leads (II, V2 and V6), whereas program 12 processed all 15 leads (12 standard leads and the Frank XYZ leads) simultaneously. These six programs were grouped under the label 12 simultaneous leads (12SL). Programs 5, 7, 8, 14 and 16 performed wave boundary detection using the conventional standard lead group combination of 3 leads at a time (I-III, aVR-aVF, V1-V3 and V4-V6), hence the labelling 3 simultaneous leads (3SL).

For each computer program, onset and offset points of the P, QRS and T waves were requested with respect to the beginning of the record or of the reference beat. For those programs which used an averaged or modal beat, the raw data was requested. These averaged beats were sent to the coordinating centre in Leuven, Belgium where onset and termination points were adjusted by alignment of these beats with the beat selected for the artificial library, using methods of cross correlation. Basic interval measurements were also computed for each program in the coordinating centre.

NO.	PROGRAM NAME	12 LEAD ECG	NUMBER OF SL	XYZ LEADS
2	MARQUETTE	YES	12	
3	LOUVAIN			YES
4	HANOVER	YES	6	
5	HP	YES	3	
7	IBM	YES	3	YES
8	NAGOYA	YES	3	
9	LYON			YES
10	AVA			YES
11	GLASGOW	YES	12	YES
12	HALIFAX	YES	15*	
13	PADOVA	YES	12	
14	TELEMED	YES	3	
15	MODULAR	YES	3**	YES
16	SICARD	YES	3	

Table 2.1 Programs examined in the Multilead Study.
*** All 15 leads analysed simultaneously.**
**** II, V2, V6 used to derive global fiducial points.**
S.L. =simultaneously recorded leads.

All 12-lead and XYZ programs also sent in one set of global fiducial points. For those programs which analysed three leads at a time, the earliest onset and the latest offset was determined in each of the four lead groups. A procedure was carried out in the coordinating centre to eliminate any outliers. If the earliest onset lay more than a certain delta value away from its neighbouring onset within the 4 lead

groups then it was removed and likewise for the case of the latest offset. These delta values can be seen in table 2.2 :

FIDUCIAL POINT	DELTA VALUE
P Onset	12 ms
P Termination	12 ms
QRS Onset	8 ms
QRS Offset	12 ms
T End	30 ms

Table 2.2 Delta Values for Program Estimates

Median values of each fiducial point were calculated from the eleven standard 12 lead programs, six XYZ programs separately as well as from all the fourteen programs combined (XYZ leads were also analysed by three of the 12SL programs). Medians of each fiducial point were also calculated for the six multilead programs and the five conventional 3-lead programs. ECGs which exhibited certain cardiac abnormalities affecting the P-wave, as well as those cases with electronic pacemakers were eliminated leaving a total of 112 cases with P wave measurements in each dataset (training and test sets).

The referees determined overall onset and offset points for every fifth case out of the 250 ECGs from the artificial library (50 ECGs in total). Visual analysis was made on highly amplified tracings where 50 or 60Hz noise was filtered out using a filter designed by Mortara (1977). Using a translucent ruler, earliest and latest offset points of the various waves were determined by each referee. The median of each fiducial point, from the five referee estimates, was obtained. If at least four out of the five referees agreed within a delta value set for that fiducial point then the median of the five measurements was accepted as the 'true' fiducial point for that ECG. The delta values for this visual analysis are given in Table 2.3 :

FIDUCIAL POINT	DELTA VALUE
P Onset	8 ms
P Termination	10 ms
QRS Onset	4 ms
QRS Offset	8 ms
T End	22 ms

Table 2.3 Delta Values for Visual Analysis Estimates

A second review was required for cases where the delta value was exceeded by more than one referee for a particular case. This took place in the coordinating centre by using a modified Delphi approach (Willems, Arnaud, Zywietz, 1985). The Delphi approach is an iterative procedure in which experts are supposed to judge or measure a certain event whilst provided with identified previous results. In the case of the CSE approach, the first round results were made available although kept anonymous. All the cases which had exceeded the delta values were reviewed once again and a consensus was reached. In addition to this, forty measurements for which the program results indicated too large a scatter around the median were also analysed visually by the referees.

2.1.3 Results

2.1.3.1 A Comparison of the Median Program Results with respect to Fiducial Point Estimation.

Differences were computed between the median of the multilead (15SL, 12SL, 6SL & 3SL) program-determined fiducial points and the median of the XYZ program fiducial points. Results from paired t-tests indicated significantly earlier P and QRS onsets as well as later P and T offsets in the multilead program results when compared to the XYZ programs ($p<0.001$). The QRS offset was time coherent for both program types, i.e. there was no significant difference in the estimation

of the QRS offset by both program types. Significant differences were also present when the median results of the 12SL (15SL, 12SL & 6SL) and conventional 3SL program differences were computed. Wave onsets occurred earlier and offsets later for the standard 3SL case compared to the 12SL. With the exclusion of the P offset and T end results, there appeared to be a better level of agreement between the multilead (15SL, 12SL, 6SL & 3SL) and XYZ program estimates than the 3SL and XYZ estimates. The results are tabulated in table 2.4. On average, results were almost identical for the original and artificial ECGs.

When the individual program results were examined for both original and artificial ECGs, it was observed that on average the largest difference (original-original or artificial-artificial) between two programs was 15ms for the P onset, 19ms for the P offset, 8ms for the QRS onset, 12ms for the QRS offset and 15ms for the end of the T wave.

Comparison of the Glasgow program results with the program median showed that the worst fiducial point to be estimated was the T-end which differed by approximately 4ms (original ECGs) to 8ms (artificial ECGs) from the program median, (i.e. the Glasgow program located the T-end much later than the program median). The P-onset and QRS-onset estimates were estimated well, however, the P offset was located slightly later by 2-3ms for the original and artificial ECGs, respectively. The QRS-offset was also estimated approximately 3ms later than the program median in the case of the artificial ECGs only.

Measurement	Type of ECG	No.	XYZ vs Multilead		3SL vs 12SL	
			Mean	SD	Mean	SD
P Onset	Original	218	3.2	4.4	6.0	4.8
	Artificial	218	3.6	4.6	6.0	4.6
P Offset	Original	218	-6.0	4.0	-2.6	5.4
	Artificial	218	-5.6	3.8	-3.2	5.0
QRS Onset	Original	240	2.0	2.6	5.6	3.8
	Artificial	240	2.8	3.0	4.2	3.2
QRS Offset	Original	240	1.0	3.6	-2.4	4.4
	Artificial	240	0.4	3.4	-3.8	4.4
T End	Original	238	-3.2	7.4	-0.8	10.2
	Artificial	238	-3.2	8.0	0.1	9.4

Table 2.4 **Mean differences and corresponding standard deviations (in milliseconds) between the XYZ and multilead (15SL,12SL,6SL&3SL) results, as well as the 3SL and 12SL (15SL,12SL&6SL) results. Differences were computed for median results after elimination of four pacemaker cases and three outliers for P and QRS cases and four for the T end case in each data set.**

2.1.3.2 A Comparison of the Median Referee and Program Results with respect to Fiducial Point Estimation.

Differences were computed between the median referee fiducial points (50 original and 50 artificial ECGs where the referee values were available plus the 40 individual measurements for which the program results showed too large a scatter) and the median fiducial points from all the programs combined (multilead and XYZ) as well as the corresponding medians of the individual program types (3SL, 12SL, multilead, XYZ, 12SL+XYZ). The referee results compared best with the results of all the programs combined than with the individual program types. Mean differences for the onsets and offsets of the P wave and QRS complex were less than 2ms for the combined program estimates and referee medians, although the T end was estimated significantly later (<0.05) by the referees.

Sample mean differences and corresponding standard deviations of the differences, between each of the program and referee medians are presented in Tables 2.5 and 2.6 respectively.

Measurement	ECG Type	No.	3SL	12SL	Multi Lead	XYZ	XYZ+12SL	All Combined
P Onset	Orig.	56	-2.0	3.4	1.2	3.6	2.2	2.0
	Art.	56	-1.8	3.6	1.0	3.0	1.8	1.4
P Offset	Orig.	52	3.2	1.2	1.6	-4.4	-0.8	0.0
	Art.	52	3.2	0.4	1.2	-5.2	-1.6	-0.2
QRS Onset	Orig.	58	-3.6	2.2	0.4	2.6	1.8	1.2
	Art.	58	-3.2	1.0	-0.8	2.8	1.2	0.4
QRS Offset	Orig.	51	3.0	-0.6	0.6	-0.8	-0.2	0.2
	Art.	51	2.4	-2.6	-0.4	-0.6	-0.8	-0.6
T End	Orig.	55	-6.2	-9.0	-6.2	-10.8	-7.0	-6.4
	Art.	55	-4.8	-5.4	-4.4	-10.8	-6.2	-5.6

Table 2.5 **Sample mean differences (in milliseconds) between the individual program medians and referee median results.**
3SL=3 simultaneously recorded leads
12SL=15SL,12SL&6SL
Multilead=3SL&12SL
All Combined = Multilead + XYZ

Measurement	ECG Type	No.	3SL	12SL	Multi Lead	XYZ	XYZ+12SL	All Combined
P Onset	Orig.	56	6.2	6.6	5.6	5.8	4.6	4.8
	Art.	56	6.4	4.8	5.4	7.6	4.2	5.0
P Offset	Orig.	52	6.4	5.2	4.6	6.8	4.8	4.8
	Art.	52	5.6	7.4	5.2	7.2	5.8	4.6
QRS Onset	Orig.	58	5.6	2.8	3.6	3.8	3.0	3.4
	Art.	58	5.2	2.8	3.4	4.0	2.8	3.0
QRS Offset	Orig.	51	4.6	5.6	4.8	5.6	5.8	5.4
	Art.	51	5.8	5.6	5.2	5.8	5.8	6.0
T End	Orig.	55	13.8	15.2	13.6	17.6	13.6	13.2
	Art.	55	12.0	17.2	15.0	18.8	16.6	12.8

Table 2.6 **Standard deviations (milliseconds) of the differences between the individual program medians and referee median results.**
3SL=3 simultaneously recorded leads
12SL=15SL,12SL&6SL
Multilead=3SL&12SL
All Combined = Multilead + XYZ

2.1.3.3 A Comparison of the Median Program Results to each other and to the Median Referee Results with respect to Interval Measurements.

By comparing the median XYZ program results and multilead program results, it was observed that the XYZ programs estimated P durations and QT intervals on average to be 6 to 8ms shorter ($P<0.001$). By comparing the overall combined program medians (XYZ and multilead) to the median referee results, it was observed that the sample mean difference was less than 1ms for the average P duration, QRS duration and PR interval. However, the program-determined QT interval median was 5ms shorter than the visual measurement.

2.1.4 Performance of ECG Programs in the Presence of Noise

2.1.4.1 Introduction

The accuracy of wave measurements is influenced greatly by the quality of the ECG recording and is largely dependent on the signal to noise ratio. It was therefore decided by the CSE working party to evaluate quantitatively the performance of the programs listed in table 2.7 in the presence of several different types of noise (Willems, Zywietz, Macfarlane et al., 1997).

The next section discusses the selection of the ECGs and the noise types examined. The results of the noisy ECGs were compared to the corresponding noise-free ECG results. Each program would act as its own control where 'ideally' the resulting measurements would be the same for noise-free and noisy ECGs. All programs applied appropriate filtering techniques which already existed within the respective programs before any analysis took place.

NO.	PROGRAM NAME	12-LEAD ECG	XYZ LEADS
3	LOUVAIN		YES
4	HANOVER		YES
5	HP	YES	
7	IBM	YES	YES
8	NAGOYA	YES	
9	LYON		YES
10	AVA		YES
12	HALIFAX	YES	
13	PADOVA	YES	
14	TELEMED	YES	
15	MODULAR	YES	YES
16	SICARD	YES	

Table 2.7 Programs Examined in the CSE Noise Study

2.1.4.2 Data Selection and Noise Types

Ten ECGs were selected from the original 3-lead CSE library where each ECG had a different QRS waveform and low noise content. Naturally occurring noise in an ECG can be due to powerline interference, poor electrode/skin contact at the time of recording or other artefacts such as somatic tremor. The ten corresponding ECGs were also taken from the artificial library. Seven different types of noise were investigated (Alraun, Zywietz, Willems et al., 1983) and added to each of the ECG signals. Including the corresponding noise-free recordings, the data set consisted of a total of 160 ECGs. However, it was decided to leave out the original ECG recordings when analysing the programs due to different programs having different philosophies

on beat selection and analysis. Since some programs base their analysis on single beats and others analyse averaged beats, in order to avoid different beat selection algorithms influencing the overall measurement results it was decided to use only the artificial ECGs. The types of noise investigated in this study are listed in Table 2.8, including examples of sources of such noise types in practical ECG monitoring.

No.	Noise Type	Example
1	High Frequency (HF), 15μV rms	Somatic Tremor
2	High Frequency, 25μV rms	Somatic Tremor
3	High Frequency, 35μV rms	Somatic Tremor
4	Line Frequency, 50Hz, 25μV Peak	AC Interference
5	Low Frequency (LF), 0.3Hz, 500μV Peak	Respiration
6	Sawtooth Signal, 0.3Hz, 500μV Peak	Atrial flutter, Artificial Noise
7	HF, 15μV & LF, 0.3Hz, 500μV	Combination of 1 & 5

Table 2.8 Noise Types Investigated in the CSE Study

The data was analysed by eight multilead ECG and six XYZ programs. Results from each centre were sent in as before, in an agreed form, to the coordinating centre. Time locations with respect to the beginning of the record were requested as was the raw data for the averaged or modal beat when applicable. Averaged beats of the noise recordings were aligned with their respective noise-free recordings by means of cross-correlation methods in the coordinating centre.

2.1.4.3 Results:-

Influence of Noise on P Onset and Offset Location

For the case of the ten artificial ECGs, sample mean differences and corresponding standard deviations were calculated between the noise and noise-free recordings for the P onset and offset. Results for the four lead groups in the 3SL case (I-III, aVR-aVF, V1-V3 and V4-V6) were combined and an average was computed. An extreme outlier was removed from each lead group for each noise type.

Results showed that line frequency noise and the sawtooth signal (linear baseline shift) had the least effect on most results produced by the individual programs. Increasing high frequency noise had the net effect of producing earlier P onsets and later offsets for several programs in both the multilead and Frank XYZ cases. Several programs failed to detect P-waves for 30-40% of the cases when 35μV rms high frequency noise was added. Low frequency noise had an intermediate effect whereas the combination of high frequency and low frequency noise showed greater error in estimation when compared to the corresponding noise-free recordings, at least for those programs which analysed each QRS complex separately. In general, programs which analysed an averaged beat exhibited significantly less variability than programs measuring beats individually.

2.1.4.4 Results:-

Influence of Noise on QRS Onset and Offset Location

Sample mean differences for QRS onsets, between the noise and noise free cases were calculated as well as the standard deviations of the

differences in the presence of high and low frequency noise, respectively, after the exclusion of one extreme outlier. Once again, the addition of high frequency noise had the net effect of producing earlier QRS onsets for three of the programs although on average, results were relatively stable for the other programs. It was seen that by the addition of noise type 3, 35μV rms high frequency noise, the program estimates varied significantly ($p<0.001$) within the multilead programs (5.4-11.5ms) and even more so within the XYZ programs (1-26ms).

With respect to the QRS offsets, it was seen that the QRS onset estimates produced by program 12 were on average fairly stable in the presence of high frequency noise. However examination of the same program (program 12) for the QRS offset estimates showed that there was on average a much greater difference between the no noise ECGs and the equivalent high frequency contaminated ECGs, in particular for 35μV rms noise (noise type 3). Similarly as with the P wave, line frequency and baseline drift noise had no significant effect on most of the program results. Further, it could be concluded that programs which analysed an average beat produced more stable QRS-onset results than those which analysed single beats. However, the results for the QRS-offsets were not so consistent indicating that some multilead programs which analysed single beats produced better estimates of the QRS-offsets than those which analysed an averaged beat and vice versa.

2.1.4.5 Results:-

Influence of Noise on T End Location

Sample mean differences between the noise and noise-free results for the end of the T wave and corresponding standard deviations, with the exclusion of an extreme outlier, were calculated. Due to the addition of noise, programs 5, 14 and 16 failed to detect the T-end for 15% of the cases. The addition of high frequency noise again produced a significant increase in the variability of T-end estimation. Programs 7, 8, 9, 10, 13 and 15 demonstrated significantly later T-ends in the presence of high frequency noise and programs 4, 5, 7, 10 and 14 proved to be significantly more sensitive to low frequency noise. The XYZ programs were seen to be more stable than the multilead programs and again measurements produced by programs analysing averaged beats showed less variability than those which used a single beat.

2.2 THE CTS DATABASE

In 1989, the Council of European Communities (concerned with the standardisation of computer assisted medical equipment) initiated a project known as Conformance Testing Services (CTS) for Computerised Electrocardiography, the purpose being to develop the basis for a consistent testing service in Europe. In 1993, the Council adopted the directive on medical devices which stated that devices with a measuring function had to be designed and manufactured in such a way as to provide sufficient accuracy and stability with appropriate limits of accuracy whilst taking into account the intended purpose of the device.

As part of the CTS project, pilot test centres were established at the University of Leuven and at the Medical School in Hanover. A CTS-ECG test bench was set up containing a computer, which was used for controlling the various test devices and for documenting the results.

Test signals were developed which had the same characteristics as an ECG sampled at 500 or 1000 samples per second. These signals could be used for testing both analogue based conventional electrocardiographs, which only record ECGs, and electrocardiographs with integrated signal processing capabilities, which provide measurements and interpretative statements. These ECGs, known as calibration ECGs, made up part of the CTS-ECG test database. Characteristics of the calibration ECGs were :

1. The eight leads I, II, V1, V2, V3, V4, V5 and V6 were identical for each calibration ECG. This allowed for programs with different analysis techniques to be tested.

2. Flat maximum amplitudes were created to ensure that the maximum amplitudes of the relatively short QRS deflections were picked up reliably.

3. Most of the calibration ECGs had a long QRS duration of 100 milliseconds similar to that of an adult ECG. These had biphasic QRS complexes with QR and RS configurations. Others had a monophasic QRS configuration (duration=56ms) with only a Q or an R wave. Two of the calibration ECGs had exceptionally short QRS durations to simulate neonatal ECGs.

In total, there were 16 CTS calibration ECGs. For each, the global P and QRS duration, as well as the global PR and QT interval, were provided as reference values.

One of the other main reasons behind the construction of the CTS database was to test the performance of ECG systems in the presence of noise. To enable the testing of such systems, the testing service provided five different types of noise in addition to the database of ECGs. The characteristics of these five noise types are discussed later.

2.3 SUMMARY

In summary, the construction of the CSE multi-lead reference library has resulted in a useful facility with which future improvements in ECG analysis within Europe, and particularly within the Glasgow Royal Infirmary, can be assessed and evaluated. It has been recommended by the CSE Working Party (Willems, Zywietz, Macfarlane et al., 1987) that computer programs which perform selective averaging be used in favour of those which analyse one beat at a time or a selected beat. An underlying condition is that averaging should be performed only if proper alignment and precise waveform comparisons have been carried out beforehand in order to eliminate dissimilar wave morphologies.

The CSE study had demonstrated that there is still room for improvement in the field of computerised electrocardiography as far as wave measurements are concerned and in particular for situations

where the ECG signals have been contaminated with high frequency noise.

In addition, the CTS data base has been constructed to enable the testing of the hardware and software of ECG systems, as well as providing five noise types. These noise types can be added to test ECGs in order to observe the performance of analysis programs in extreme conditions and serve as a useful tool in their improvement.

Other databases have been created such as the MIT database and the European STT database (Taddei, Distante, Emdin et al., 1992). However, neither of these are '12 lead ECG' databases. The MIT (Massachusetts Institute of Technology) database is predominantly used for assessment of QRS and arrhythmia detection during Holter monitoring while the ST-T database is intended for evaluation of algorithms analysing ST and T-wave changes also during Holter recording. Each database consists of annotated excerpts of ambulatory ECG recordings.

CHAPTER THREE

MEASUREMENT EVALUATION OF THE CURRENT GLASGOW PROGRAM AND THE EFFECTS OF SPLITTING ECG SIGNALS INTO MULTIPLE WAVEFORMS

3.1. THE GOLD STANDARD

With any type of investigation or experiment concerning comparisons, a gold standard is required with which results produced by current or future methods can be compared. With respect to the present study, a gold standard was required in order to assess the performance of the Glasgow program with respect to the estimation of fiducial points. The CSE database library offered such a standard by providing median program and referee fiducial points together with the database of 125 ECGs. The median referee results (see Chapter 2) were provided for every fifth case of the CSE database. The exclusion of four cases due to data compression problems encountered later when adding noise (this is discussed in more detail in Chapter 6) resulted in the availability of 21 ECGs. The referee medians were taken to be the "gold standard" or "true" value since the human eye was considered to be more precise in its estimation than any automated method available.

For each of the 21 ECGs, the referee median P-onset, P-offset, QRS-onset, QRS-Offset and T-end estimates were provided with the database. However, it was not possible to perform a direct comparison of the onset and termination estimates produced by the Glasgow program with these referee measurements. In order to do this, the original reference beat used earlier in the CSE coordinating centre

would have been required to be aligned with the modal beat produced by the Glasgow approach. A cross correlation method would then have had to be applied similar to that in the coordinating centre. However, as the reference beat was not provided, duration and interval measurements had to be used instead. These standard measurements were calculated as follows :

P Duration	=	P Offset - P Onset
QRS Duration	=	QRS Offset - QRS Onset
PR Interval	=	QRS Onset - P Onset
QT Interval	=	T Offset - QRS Onset

3.2 THE GLASGOW PROGRAM VS THE GOLD STANDARD

The aim of this part of the work was to compare the referee durations to those produced by the conventional Glasgow program. Duration and interval measurements were extracted from the program output and as an initial step, each of the measurements produced by the Glasgow program was plotted against the corresponding referee estimates with the line of equality superimposed. These can be seen in Figure 3.1. All measurements were in milliseconds.

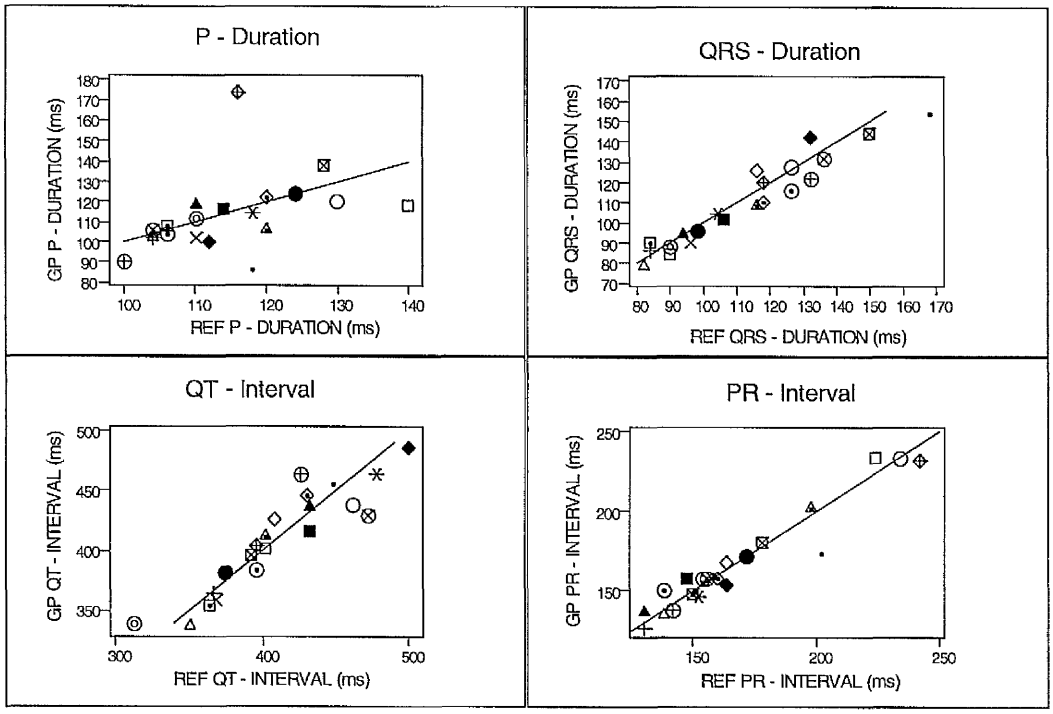

Figure 3.1 Glasgow Program measurements (G.P.) Vs the Referee measurements (REF.) including the line of equality.

Clearly, the P-duration estimates were the poorest, whereas the QRS-duration and PR-interval estimates appeared to be the best. For almost all the intervals, there were approximately equal amounts of points on either side of the line of equality implying that the Glasgow program did not seem to be overestimating or underestimating the measurements when compared to the referee standard. However, there was a suggestion from the plot that the Glasgow program may have been slightly underestimating the QRS-duration. Clearly any biases present in the data were not dependent on the magnitude of the fiducial interval measurements and as such the differences of the "Glasgow-Referee" values could be used to investigate systematic biases and variability.

To assess the level of agreement between the CSE referee durations and those produced by the Glasgow program, correlations

were computed. Furthermore, to investigate the presence of systematic biases, the Glasgow program estimates (for each set of durations/intervals) were modelled on the referee values using simple linear regression as follows:

If x_i represents the 21 Glasgow program estimates and t_i denotes the CSE referee measurements, then the data can be modelled as follows :

$$x_i = \alpha + \beta t_i + \varepsilon_i \tag{3.1}$$

where i=1,..n (n=21) and $\varepsilon_i \sim N(0,\sigma^2)$ represents the error term in the model which accounts for the variation due to an individual. Also, α represents the intercept of the regression line and β the slope. The hypothesis which would then be tested would be :

$$\begin{array}{cccccc} & H0 & : & \alpha = 0 & \text{and} & \beta = 1 \\ \text{vs} & H1 & : & \alpha \neq 0 & \text{or} & \beta \neq 1 \end{array}$$

An exact test for this null hypothesis, H0 against H1 would be based on the result

$$F = \frac{(r_0 - r_1)/2}{r_1/n-2} \quad \sim \quad F(2, n-2) \text{ under H0} \tag{3.2}$$

where n=21 and F is the test statistic used to decide whether or not to reject the null hypothesis H0. Also, r_0 and r_1 represent the residual sum of squares under H0 and H1, respectively. As a result, large values of F are evidence in favour of H1. However, if H0 cannot be rejected then this suggests that there is no difference between the referee medians and the Glasgow program estimates, subject to some

variability. A summary of the results, as well as the relevant sample correlation coefficients for each of the corresponding program and referee interval measurements, is presented in Table 3.1. P-values for a test of equality i.e. intercept=0 and slope=1, have also been provided.

Interval	Sample Correlation	Evidence of a Bias? (H0 : $\alpha=0,\beta=1$)	Test of "H0"
P Duration	0.42	No	p=0.70
QRS Duration	0.96	No	p=0.09
QT Interval	0.92	No	p=0.83
PR Interval	0.97	No	p=0.66

Table 3.1 Conventional Glasgow Program and Referee correlations

From Table 3.1, it is evident that there is poor correlation between the Glasgow program and the referees for estimates of the P wave duration. From the accompanying plot in Figure 3.1, it can be seen that this poor correlation may possibly be due to the single outlier at the top of the plot. Removal of this outlier increased the sample correlation to 0.61. However, there was no justifiable reason to omit this outlier since it represented a real occurrence in routine ECG processing. The remainder of the results indicated a good level of agreement between the referee medians and the Glasgow program estimates for the other fiducial intervals. There was no evidence to suggest that the Glasgow program did in fact overestimate or underestimate any of the four sets of fiducial interval measurements when compared to those of the referee, although there was a suggestion (p=0.09) that the Glasgow program underestimated the QRS duration compared to the referee medians.

Before any standard deviations could be calculated, differences between each of the referee medians and corresponding Glasgow program fiducial intervals were calculated. Normality of these differences was then assessed graphically in the form of boxplots which are depicted in Figure 3.2. It is clear that all four plots look normally distributed with the median difference lying approximately equidistant from each quartile. However, it is evident that there are outliers for the P-duration and PR-interval. The exclusion of these outliers would result in a drop in the standard deviations for both fiducial intervals, although more so in the case of the P-duration. To exclude these possible outliers would not be acceptable since these cases appear to be representative of routinely occurring ECG recordings.

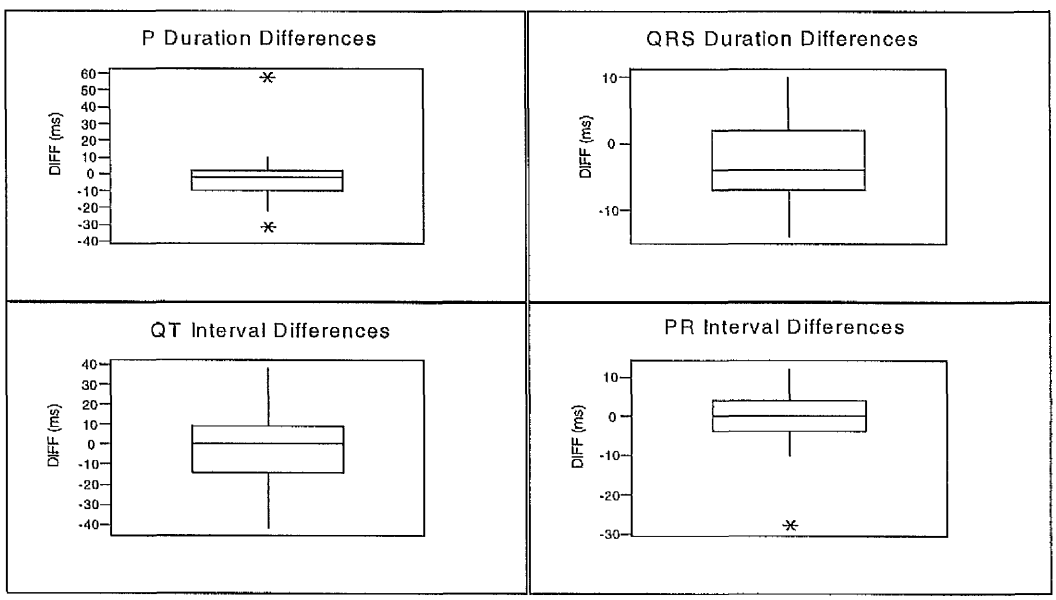

Figure 3.2 **Check for the assumption of normality of the Glasgow Program and Referee differences.**
Diff = Glasgow program - Referee Median

It was now possible to calculate the standard deviations of the fiducial interval differences which simply quoted the variability in the differences assuming no systematic bias (Table 3.2). For example, for the case of the P-duration, let Diff = $PDur_{GP}$ - $PDur_{Ref}$ where

GP=Glasgow Program and Ref=Referee. The sample standard deviation (about zero) was then estimated by

$$\sqrt{\frac{\sum_{i=1}^{n} Diff^2}{n}}, \qquad \text{where } n = 21 \ .$$

It is evident from Table 3.2 that the standard deviations about zero for the P-duration and QT-interval cases are quite high. A possible explanation for the poor performance could be due to poor estimation of the P-offset and T-end. This is deduced from the better estimation of both the QRS-duration and PR-interval, which obviously depend on the QRS-onset and P-onset, respectively. However, by excluding the outliers illustrated in Figure 3.2, the standard deviation is reduced to 7.9ms and 5.9ms for the P-duration and PR-interval, respectively.

Interval	Standard Deviation About Zero
P Duration	16.5
QRS Duration	6.7
QT Interval	17.7
PR Interval	8.5

Table 3.2 Standard deviations of the Differences in ms (i.e. Glasgow Program - Referee) .

3.3 SPLITTING AN ECG

The idea of "splitting" an ECG into two traces was first investigated by Bailey in 1974 for the purposes of analysing reproducibility of ECG interpretations (Bailey, Horton & Itscoitz, 1974). In order to test

reproducibility in ECG computer program performance results, Bailey et al. produced two digital representations of the same analogue ECG tracing to assess the reproducibility of diagnostic statements in a set of 217 ECGs and again in a set of 33 ECGs, using a different program on each occasion. The technique used by Bailey et al. for splitting an ECG involved digitising an ECG at 1000 samples per second. The EGG was then split by separating odd and even samples (one from the other by a one millisecond phase lag in sample points) resulting in two traces, the first consisting of all odd sample points i.e. 1, 3, 5 and so on, for each lead and the second consisting of all even samples i.e. 2, 4, 6 etc. Each trace therefore had a sampling rate of 500 samples per second. This technique was then applied to each ECG in Bailey's dataset where each of the two split traces of a single ECG was analysed and hence assessed for reproducibility in terms of diagnostic statements.

This approach used by Bailey et al. was implemented into the Glasgow Program. The splitting approach was identical to that of Bailey's. However, in this case the ECG was digitised at 500 samples per second. This resulted in both split traces having a sampling rate of 250 samples per second. To reproduce waveforms with a sampling rate of 500 samples per second (since the Glasgow program analyses ECGs sampled at 500 samples per second), linear interpolation was performed between each pair of consecutive points on each of the traces separately (Figure 3.3). To illustrate the effect of this procedure (hereinafter called the Glasgow Program (GP) filter), a noisy calibration ECG was selected and the technique applied (Figure 3.4). Here the original beat and the resulting two interpolated split traces have been depicted.

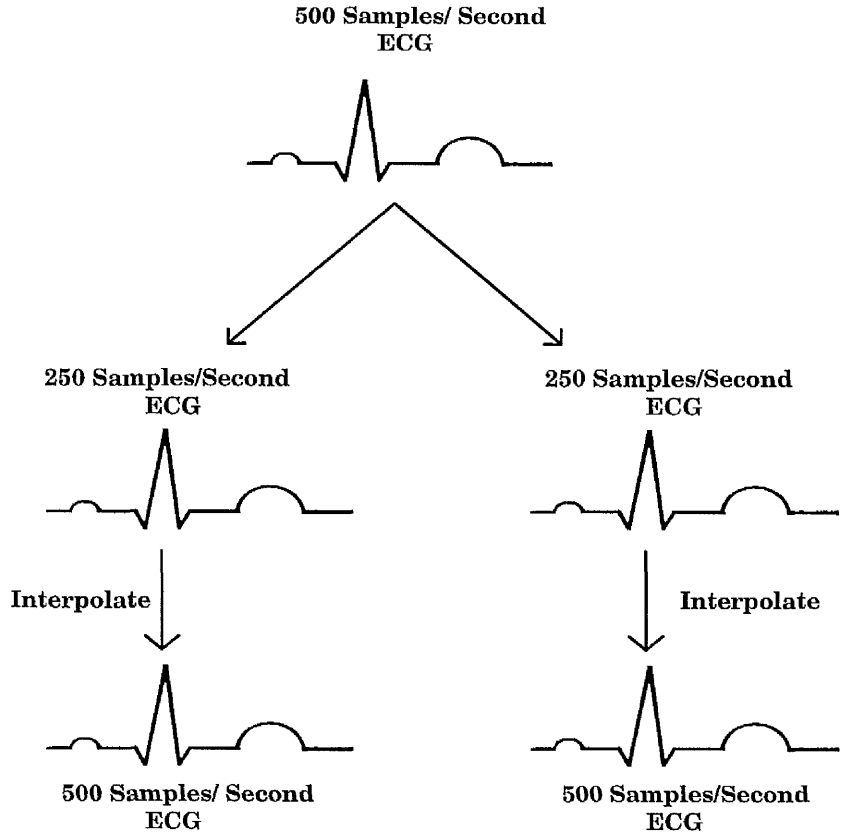

Figure 3.3 Illustration of splitting a waveform into two and linearly interpolating the resulting split traces.

In the present study, it was of interest to average the actual measurement outputs of the resulting two digital representations in an attempt to improve the accuracy of the measurements produced by the Glasgow program.

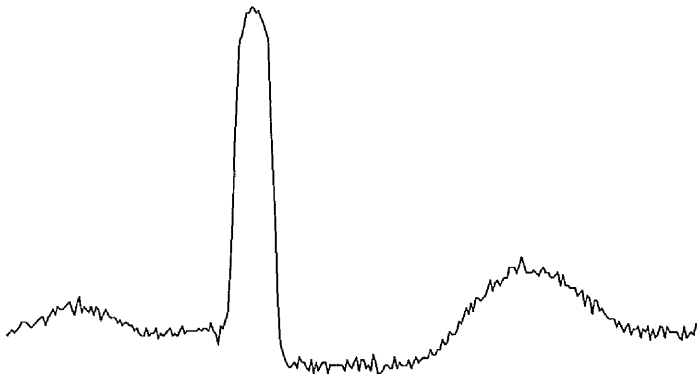

ORIGINAL ECG (500samples/sec)

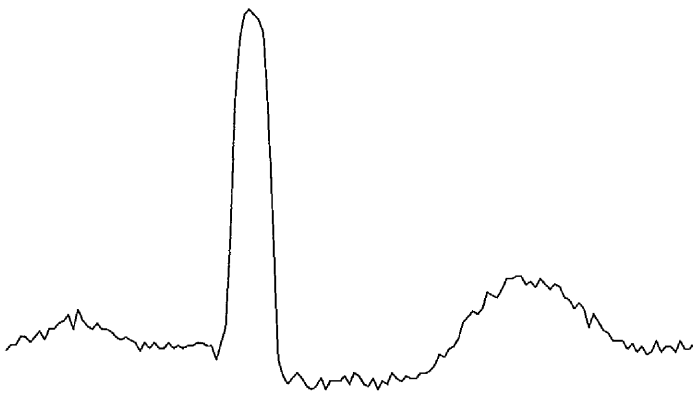

INTERPOLATED 'ODD SAMPLE POINTS' TRACE (500samples/sec)

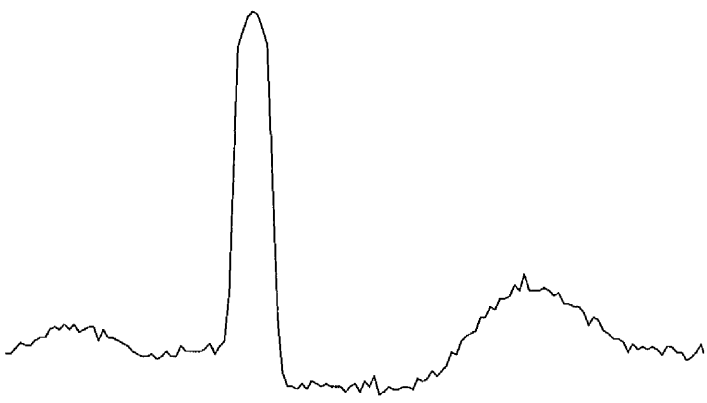

INTERPOLATED 'EVEN SAMPLE POINTS' TRACE (500samples/sec)

Figure 3.4 Result of splitting a noisy 500 sample/second calibration ECG

The GP filter was then applied to all 21 CSE ECGs producing 42 split traces, two for each ECG. For all the traces, estimates of the relevant points were obtained (P-onset, P-offset, QRS-onset, QRS-offset and T-end). Each corresponding pair of fiducial points (from trace 1 and trace 2) were then averaged to produce a single onset and offset, resulting in 21 sets of fiducial point estimates. For example:

$$P\text{-}onset = [P\text{-}onset\ (trace1) + P\text{-}onset\ (trace2)]\ /\ 2$$

Based on these 'averaged' estimates, the relevant durations and intervals were computed. These new measurements were plotted against the corresponding median referee estimates (Figure 3.5). Techniques of simple linear regression were applied once again to check for systematic biases by testing for a line of equality with slope equal to one and intercept zero. The results of these, as well as the corresponding sample correlations between the GP filter and referee estimates, are presented in Table 3.3.

From the table, it can be observed that the level of agreement between the GP filter estimates and referee estimates has improved for each of the fiducial intervals. From the plot of the P-duration in Figure 3.5, it appears that the previously existing outlier has now been pulled in towards the line of equality implying a more precise estimation of the P wave duration by using the GP filter.

Since there was no strong evidence of a clear systematic bias in any of the fiducial intervals, differences of the GP filter estimates and the referee estimates were computed and standard deviations about zero were calculated. Table 3.4 summarises these standard deviations

(ms) as well as those for the conventional Glasgow program. A consistent pattern of improvement in estimation of fiducial intervals is evident when compared to the conventional program results. It can be seen that the standard deviation about zero has decreased for all four fiducial intervals, in particular for the case of the P duration where the standard deviation of the differences has dropped by around one third.

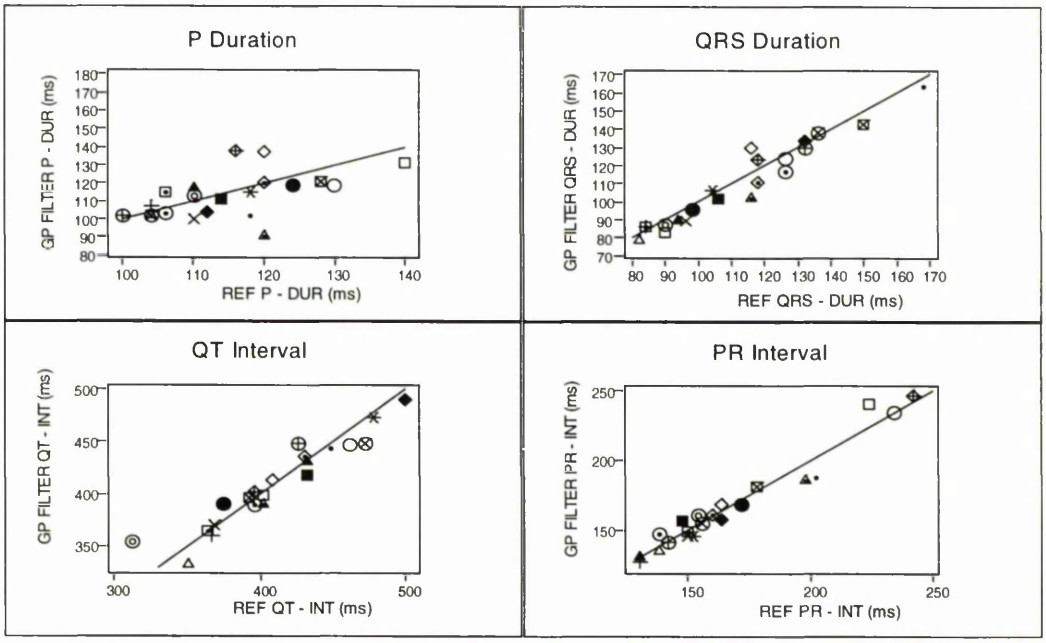

Figure 3.5 Measurements (ms) produced by using the Glasgow Program Filter (GP Filter) Vs the referee measurements (REF.) including the line of equality.

Interval	GP Sample Correlation	Evidence of a Bias? Test of H0	GP Filter Sample Correlation	Evidence of a Bias? Test of H0
P Duration	0.40	No , p=0.70	0.54	No , p=0.38
QRS Duration	0.96	No , p=0.09	0.97	No , p=0.09
QT Interval	0.92	No , p=0.83	0.95	No , p=0.77
PR Interval	0.97	No , p=0.66	0.98	No , p=0.86

Table 3.3 Comparison between the conventional Glasgow Program (GP) & referee correlations and the Glasgow Program Filter & referee correlations.

Difference	Standard Deviation about Zero GP	Standard Deviation about Zero GP Filter
P Duration	16.5	11.0
QRS Duration	6.7	6.2
QT Interval	17.7	14.5
PR Interval	8.5	7.2

Table 3.4 Comparison of the Standard deviations of the differences about zero for the conventional Glasgow Program estimates (GP) & referee values and Glasgow Program Filter estimates (GP Filter) & referee values.

3.4 DOUBLE SPLITTING

It was clear from the results in the previous section that the idea of splitting an ECG had proved to be a beneficial exercise and so it was decided to take this a stage further. As before, an ECG lead digitised at 500 samples per second was split into two separate 250 sample per second ECGs. Once again the first split trace consisted of all odd samples and the second contained all even samples. As before, each waveform was linearly interpolated back to 500 samples per second. However, these interpolated waveforms were then split for a second time to produce a total of four waveforms, each sampled at 250 samples per second. Linear interpolation was once again performed on each of the four waveforms, resulting in four ECG waveforms derived from a single lead, with each signal representing a smoother ECG waveform sampled at the standard rate of 500 samples per second. Figure 3.6 illustrates this process of splitting and averaging. In the previous case of the two split traces (GP filter), the ECG measurements were extracted and averaged. However, in this case it seemed more realistic to average the four ECG waveforms to produce a single smoothed

version of the original waveform. Figure 3.7 shows the overall effect of this approach (designated as the "Glasgow smoothing filter") on a noisy calibration ECG. Essentially, this "filter" is an example of a linear phase finite impulse response filter (FIR). A FIR filter has a unit impulse response with a limited number of terms (in this case a limited number of samples) to compute the filtered point. FIR filters are generally nonrecursive, which means that there is no feedback involved in computation of the output (Tompkins, 1993). Later in this chapter, the frequency response of this filter is assessed.

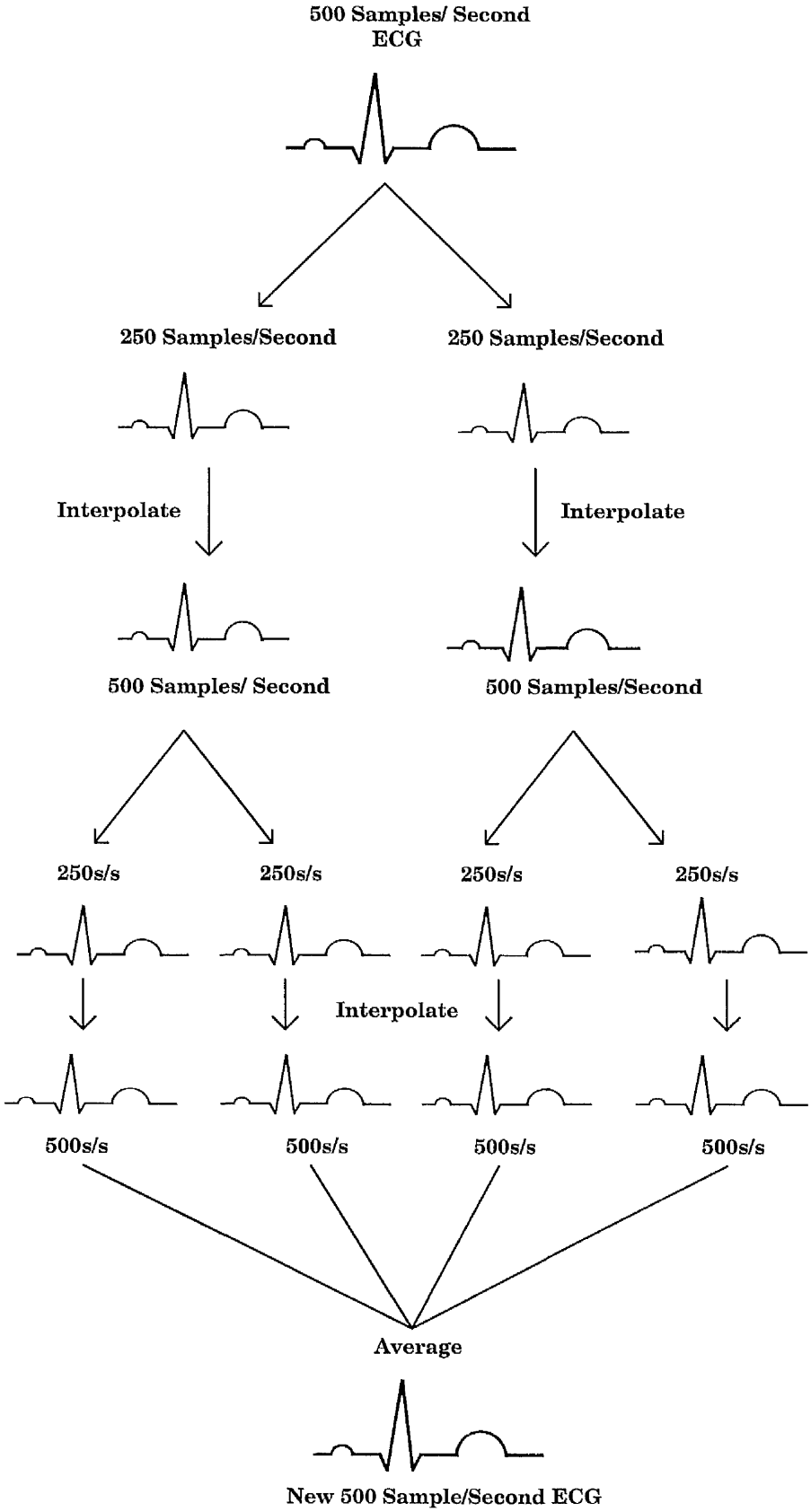

Figure 3.6 Illustration of the double splitting and averaging technique

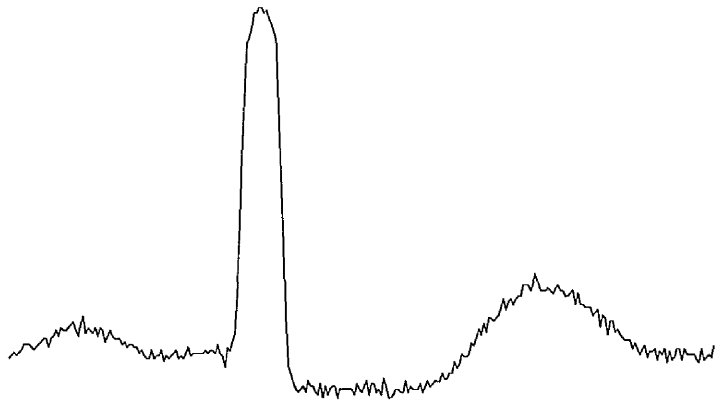

ORIGINAL ECG

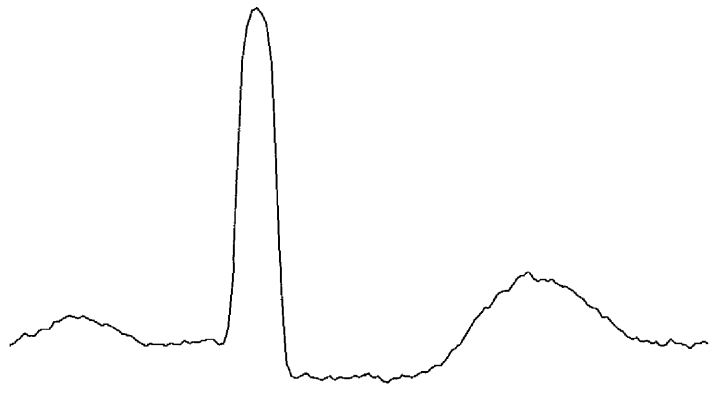

ECG AFTER SPLITTING AND AVERAGING

Figure 3.7 Result of applying the Glasgow smoothing filter to a noisy calibration ECG.

The Glasgow smoothing filter is of the form

$$a(i)=\frac{x(i-2)+4x(i-1)+6x(i)+4x(i+1)+x(i+2)}{16}\ , \qquad (3.3)$$

for i = 3, 4, 5,....., N-2

where a(i) is the 'smoothed' signal at the ith sample point and x(i) is the original signal. The first and last two sample points could not be 'smoothed' since the construction of a(i) required the first and last two

points of the original data to make up its first point a(3). For this reason, a(1) and a(2) were set equal to a(3) and a(N) and a(N-1) were set equal to a(N-2) to keep the samples numbers consistent with the original waveform.

This equation was applied to the data of the 21 CSE ECGs, producing new "smoother" waveforms for each case. Revised fiducial points were then estimated and fiducial intervals based on these were then computed. These measurements can be seen plotted in milliseconds against the corresponding referee estimates in Figure 3.8. By superimposing the line of equality onto each of the plots, it is clear that in the case of the P-duration, the variability has reduced noticeably. Also, the slight reduction in variability in the case of the QRS duration has allowed clearer identification of a bias.

Sample correlations for the corresponding "Glasgow smoothing filter" and median referee fiducial intervals together with formal checks for systematic biases have been summarised in Table 3.5 as well as those for the case of the previous GP filter and the conventional Glasgow program results.

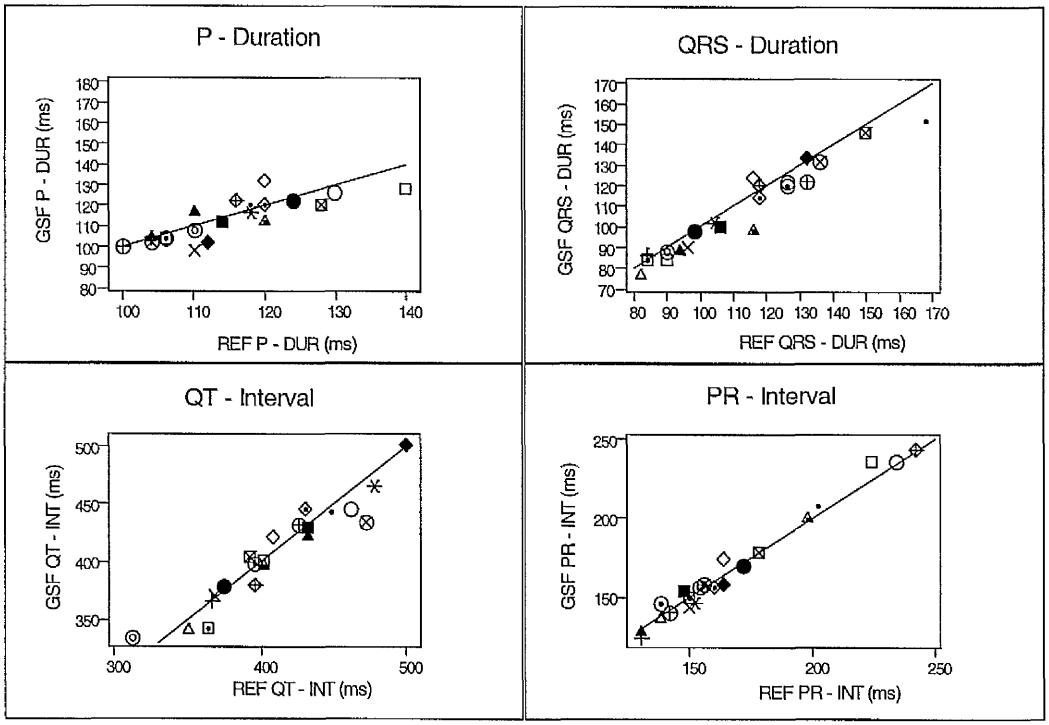

Figure 3.8 Measurements produced by the Glasgow smoothing filter (GSF) Vs the Referee measurements (REF.) including the line of equality.

Interval	GP Sample Correlation	Bias? Test of H0	GP Filter Sample Correlation	Bias? Test of H0	Glasgow Smoothing Filter Sample Correlation	Bias? Test of H0
P Duration	0.40	No p=0.70	0.54	No p=0.38	0.83	No p=0.14
QRS Duration	0.96	No p=0.09	0.97	No p=0.09	0.97	Yes p=0.01
QT Interval	0.92	No p=0.83	0.95	No p=0.77	0.96	No p=0.37
PR Interval	0.97	No p=0.66	0.98	No p=0.86	0.99	No p=0.52

Table 3.5 Comparisons between the conventional Glasgow Program (GP) & referee sample correlations, Glasgow Program filter & referee sample correlations and Glasgow smoothing filter & referee sample correlations.

It is clear from each set of sample correlations that the variability about the line of equality is reduced after the introduction of each of the GP filter and the Glasgow smoothing filter, particularly in the case of the P-duration. It is also seen that there is in fact evidence of a systematic bias for the case of the Glasgow smoothing filter determined QRS duration with p-value=0.01. However, it should be noted that the corresponding p-values (0.09) for the conventional program and GP filter also suggested a bias may exist. It is only after applying the Glasgow smoothing filter that the variation about the line of equality has decreased making the bias clearer. The line of equality is seen to fit the data marginally better using the Glasgow smoothing filter than in the case of the GP filter and the conventional Glasgow program.

The improvement in the estimation of the fiducial intervals is further illustrated in Table 3.6 where the standard deviations of the differences, "Glasgow smoothing filter" - "referee", were computed about zero for those cases where no bias was present. For the case where a significant bias did exist (i.e. QRS-durations), the standard deviation about the mean was quoted as well as for the corresponding conventional program and GP filter. The overall improvements using the Glasgow smoothing filter are evident across all four durations/intervals with consistently the lowest standard deviations of the differences (about zero or the mean) across the three possible techniques for estimating fiducial intervals.

Interval	GP	GP Filter	Glasgow Smoothing Filter
P Duration	16.5	11.0	6.1
QRS Duration	6.4 (6.7)	5.9 (6.2)	*5.9
QT Interval	17.7	14.5	13.8
PR Interval	8.5	7.2	5.2

Table 3.6 Comparison of the Standard Deviations (S.D.) of the differences about zero for the conventional program - referee and the two filtering versions of the program - referee.
*** represents the case where there was evidence of a bias and so the S.D. about the mean has been quoted for all QRS durations. S.D.s about zero in ( ).**

3.5 RESULTS OF THE CTS TEST SET

As described in Chapter 2, the Conformance Testing Services (CTS) provided a database of 16 calibration ECGs along with Global reference values for the P and QRS durations and the PR and QT intervals. The purpose of these ECGs was to test the hardware and software of automated ECG analysis systems and therefore develop the basis for a harmonised conformance testing service in Europe.

Each ECG was processed by both the conventional Glasgow program (GP) and the modified versions which included the Glasgow Program filter and the Glasgow smoothing filter, respectively. Once again the program estimates were plotted against the median referee values for each of the three versions of the program. These are depicted in Figures 3.9, 3.10 and 3.11 respectively. A line of equality was included so that the level of agreement between the program and referee could be seen more easily. As can be seen in Figures 3.9, 3.10 and 3.11, there is little or no variability in the sample of reference cases for the P-duration and PR-interval values. It is dubious but not impossible to compare the performances of the different programs on

such artificial and clinically atypical samples. A wider range of "durations" and "intervals" would have been preferable. It is clear, however, that the P-duration and the PR-interval are consistently being under-estimated by the conventional Glasgow program and each of the two filters. In the case of the QRS duration and QT interval, there is not much variation in the estimates derived from the different methods (ie. the conventional program, GP filter and the Glasgow smoothing filter).

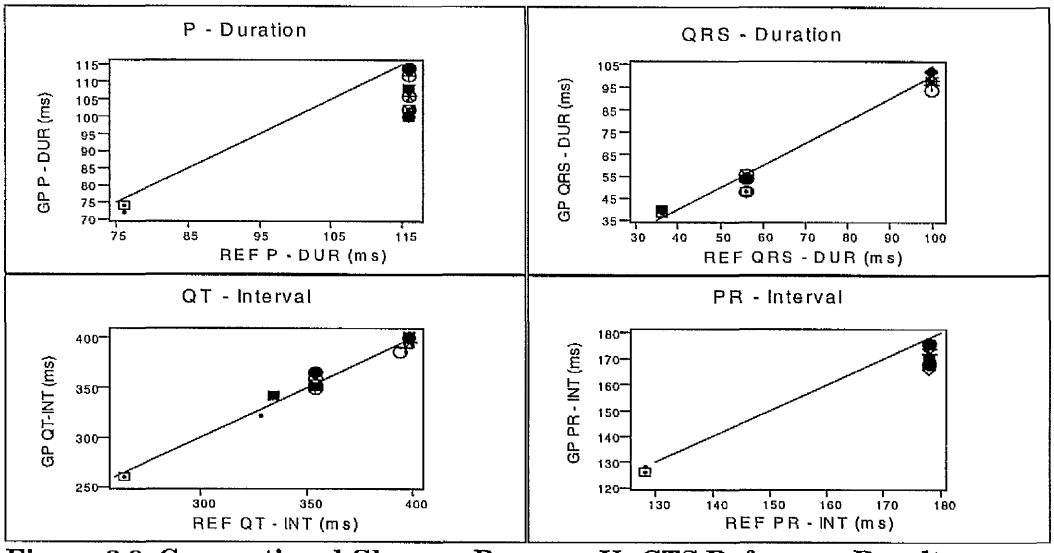

Figure 3.9 Conventional Glasgow Program Vs CTS Reference Results

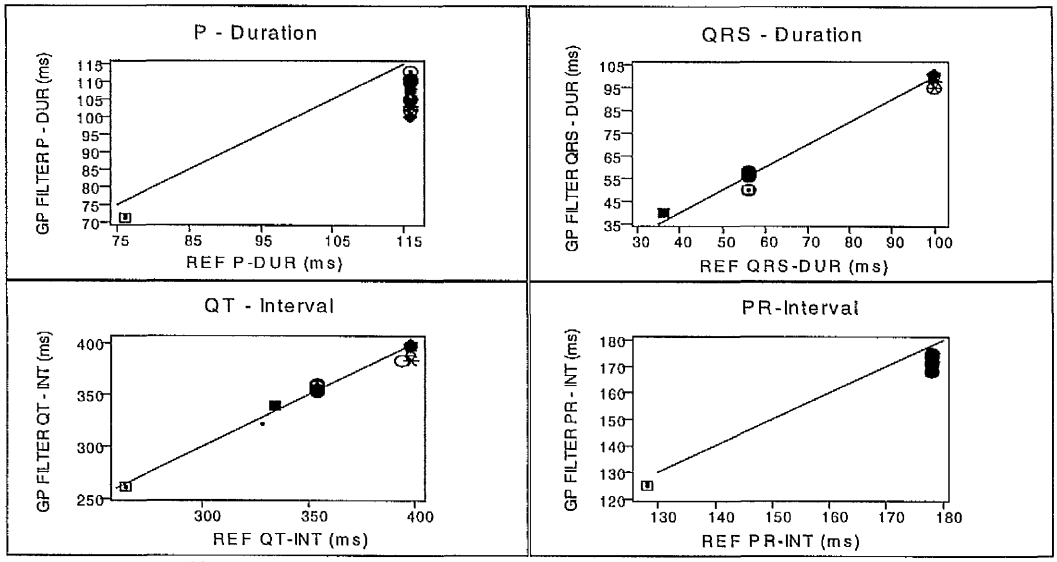

Figure 3.10 Glasgow Program Filter Vs CTS Reference Results

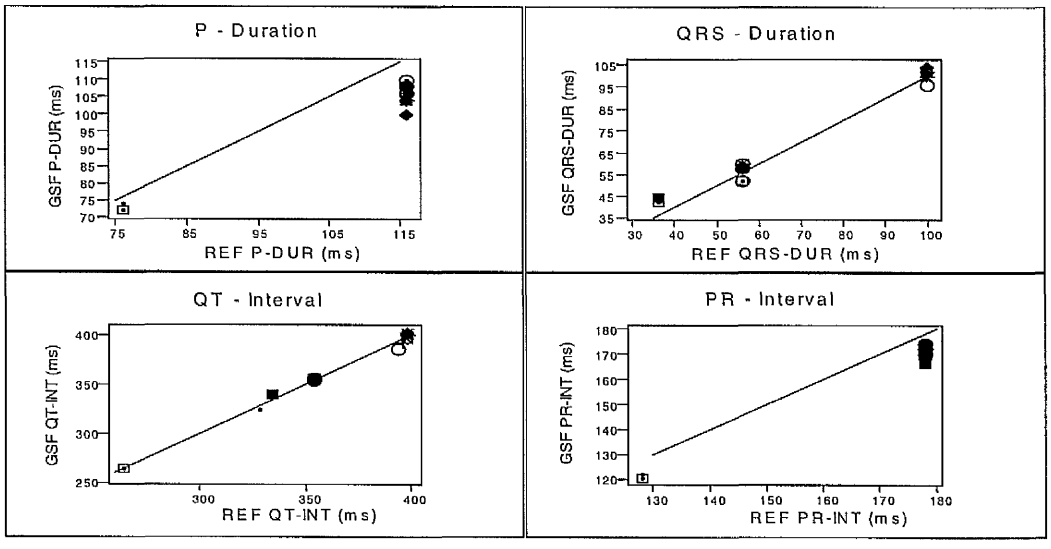

Figure 3.11 Glasgow Smoothing Filter Vs CTS Reference Results

Figure 3.12 depicts boxplots of the differences between the estimated and reference interval measurements. It is clear that the estimates produced by the Glasgow smoothing filter show least variability. It is also apparent that the GP filter (single split) shows less variability in its estimates than the conventional program. In general, it can be seen that there is a clear bias in the P-duration and PR-Interval estimates. Standard deviations about the mean difference (since most results showed a clear or borderline bias), are presented in Table 3.7. It is clear that the two filters (independently of each other) do equally as well as the conventional program in the case of QRS duration and better for the other intervals in terms of reducing the variability of the estimates. In most cases the Glasgow smoothing filter, once again, performs best.

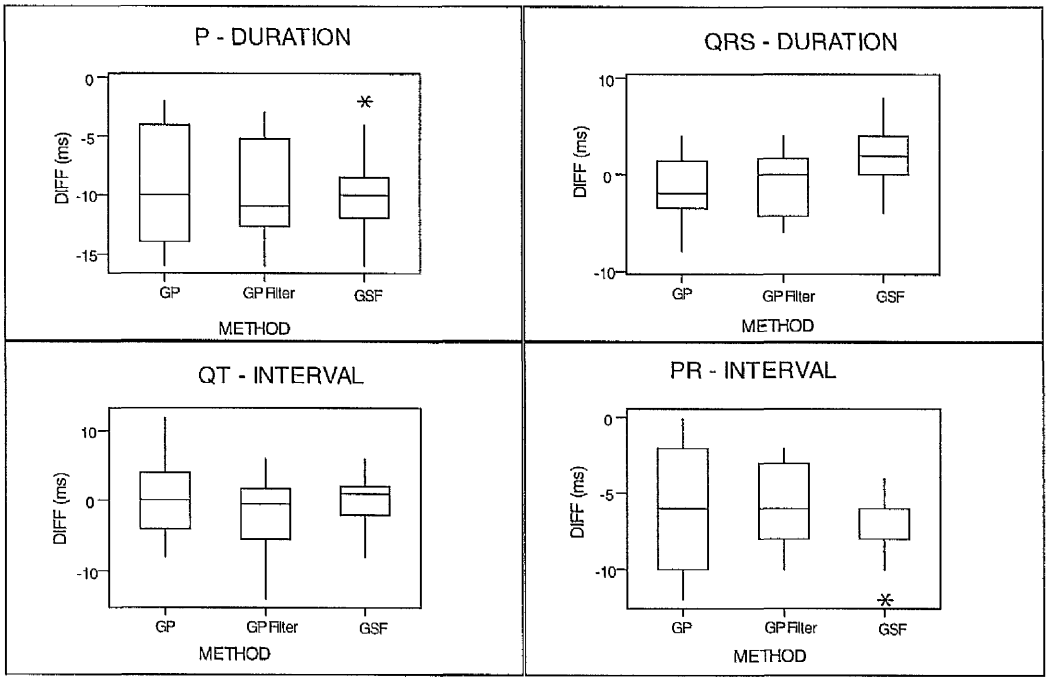

Figure 3.12 Performance of the conventional Glasgow Program (GP), Glasgow Program Filter (GP Filter) and Glasgow Smoothing Filter (GSF) in terms of the measurement differences (program-reference) .

Interval	GP	GP Filter	Glasgow Smoothing Filter
P Duration	5.30	4.06	3.42
QRS Duration	3.49	3.30	3.54
QT Interval	5.51	5.45	3.57
PR Interval	3.90	2.86	2.03

Table 3.7 **Standard Deviations for the Program-Reference differences (milliseconds) for the 16 CTS calibration ECGs. GP=Glasgow Program.**

3.6 FREQUENCY RESPONSE

For any type of filtering technique, it is always useful to determine the frequency response of a filter. Since the method of splitting and averaging was implemented as a filter, it was appropriate to determined the frequency response of the filter. Ideally, the peak amplitude of any ECG waveform should remain unchanged after the application of a low pass filtering technique. However, realistically it is reasonable to assume that the peak amplitude would decrease slightly.

The frequency response of the Glasgow smoothing filter was determined using MATLAB. The appropriate functions were used to assess the effect of filtering signals in the range 0-250Hz. The results can be seen in graphical form in Figure 3.13(a)

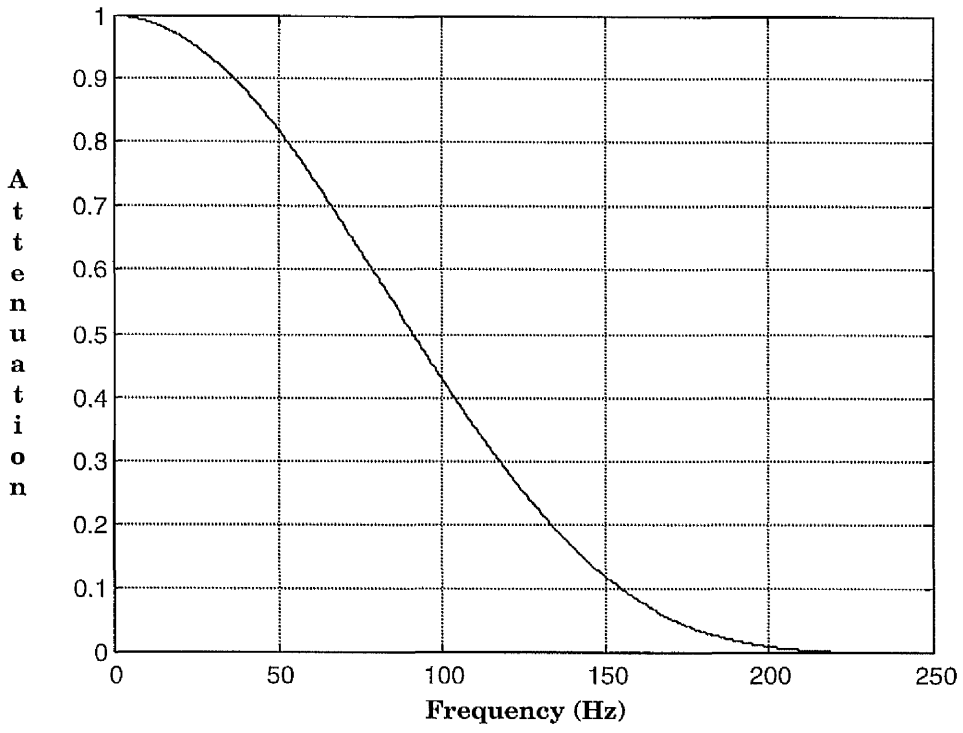

Figure 3.13(a) Frequency Response of the Glasgow Smoothing Filter

The amount of attenuation increases as the frequency increases and above 220Hz the Glasgow smoothing filter has zero response. The frequency response in decibels (db) can be seen in Figure 3.13(b). At the 3db the frequency is 65-70Hz and at this point the filter begins to have an effect on the signal i.e. the frequency response of the filter is flat to that point.

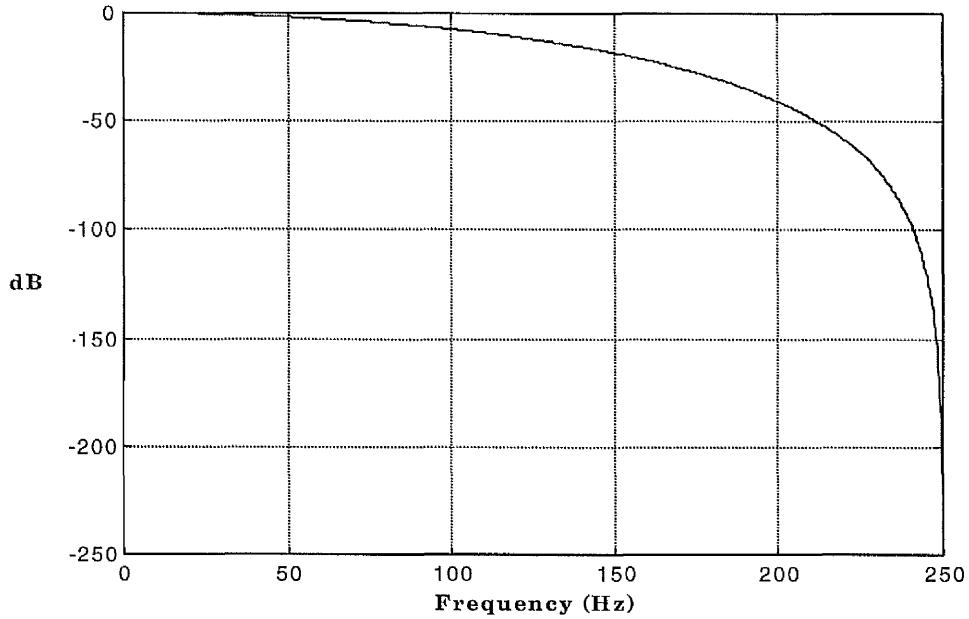

Figure 3.13(b) Frequency Response of the Glasgow Smoothing Filter in decibels

3.7 SUMMARY

It has been shown in this chapter that splitting an ECG signal into 2 or 4 waveforms and averaging the resulting interpolated waveforms has proved equivalent to a beneficial filtering technique that results in more accurate wave duration estimates. In fact, the standard deviation of the P duration decreased by approximately two thirds when compared to the conventional Glasgow program estimates in a set of 21 CSE ECGs.

In the case of the CTS database, due to the lack of variability in the P-duration and PR-interval reference values, it proved difficult to make an overall assessment of the different methods. However, in general it was clear that both filters showed a reduction in the amount of variability in the estimates of the fiducial intervals when compared to the conventional program, more so in the case of the Glasgow smoothing filter.

CHAPTER FOUR

ASSESSMENT OF THE CONVENTIONAL AND MODIFIED GLASGOW PROGRAM-DERIVED MEASUREMENTS IN THE PRESENCE OF NOISE

4.1 INTRODUCTION

As mentioned earlier, inaccuracy of wave measurements is more prevalent in cases where the ECG signal has been contaminated with noise. This can be due to reasons such as powerline interference or poor electrode/skin contact at the time of the recording. It is important for an automated analysis system to overcome such problems by minimising any excess noise present in the signal.

In an attempt to tackle the problem of mains frequency interference, the initial phase of the Glasgow program incorporates a notch filter in order to eliminate any 50Hz noise present within the ECG signal. An alternative 60Hz filter can be set up for those ECGs which may have been recorded in a location where the mains frequency is 60Hz.

In the previous chapter, it was seen that the technique of splitting and averaging was effectively performing as a filter, i.e. it was smoothing out some of the excess noise present in the ECG signals. It was shown that "Glasgow smoothing filter" (double splitting) had proved to be successful with respect to fiducial point interval estimation in a set of 21 ECGs. As a further test, it was decided to

assess how well the Glasgow smoothing filter measurements compared with the referee results and in turn the conventional Glasgow program estimates in extreme conditions, when five different noise signals were added to the same 21 CSE ECGs as well as the 16 CTS ECGs already studied.

4.2 CHARACTERISTICS OF NOISE

Five types of noise were added to the ECGs. The noise types were provided by the European Conformance Testing Services (CTS) in order to test how reliably an ECG system could produce measurements under adverse operating conditions. The characteristics of the five noise signals can be seen in Figure 4.1(a).

Possible sources of each of the chosen noise types in practical ECG monitoring are:

Noise 1	:	somatic tremor
Noise 2 & 3	:	AC interference
Noise 4	:	respiration
Noise 5	:	combination of respiration and somatic tremor

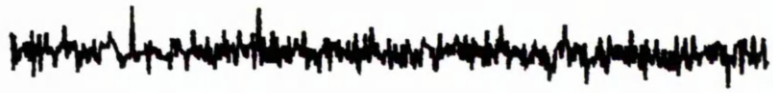

Noise 1 : High Frequency Noise 25μV

Noise 2 : Line Frequency Noise 50Hz, 25μV peak

Noise 3 : Line Frequency Noise 60Hz, 25μV peak

Noise 4 : Baseline Noise 0.3Hz, 0.5mV peak

Noise 5 : Baseline and High Frequency Noise
0.3Hz, 0.5mV peak; 15μV RMS

Figure 4.1(a) Characteristics of Noise Types obtained from the CTS database.

Each of these five noise signals was added separately to each of the leads for all the 21 CSE ECGs assessed before any processing had occurred. This provided 105 noisy ECGs and 126 ECGs in total for the purposes of this study. An illustration of the effect of adding each of these noise types to a single ECG lead (V1) is given in Figure 4.1(b).

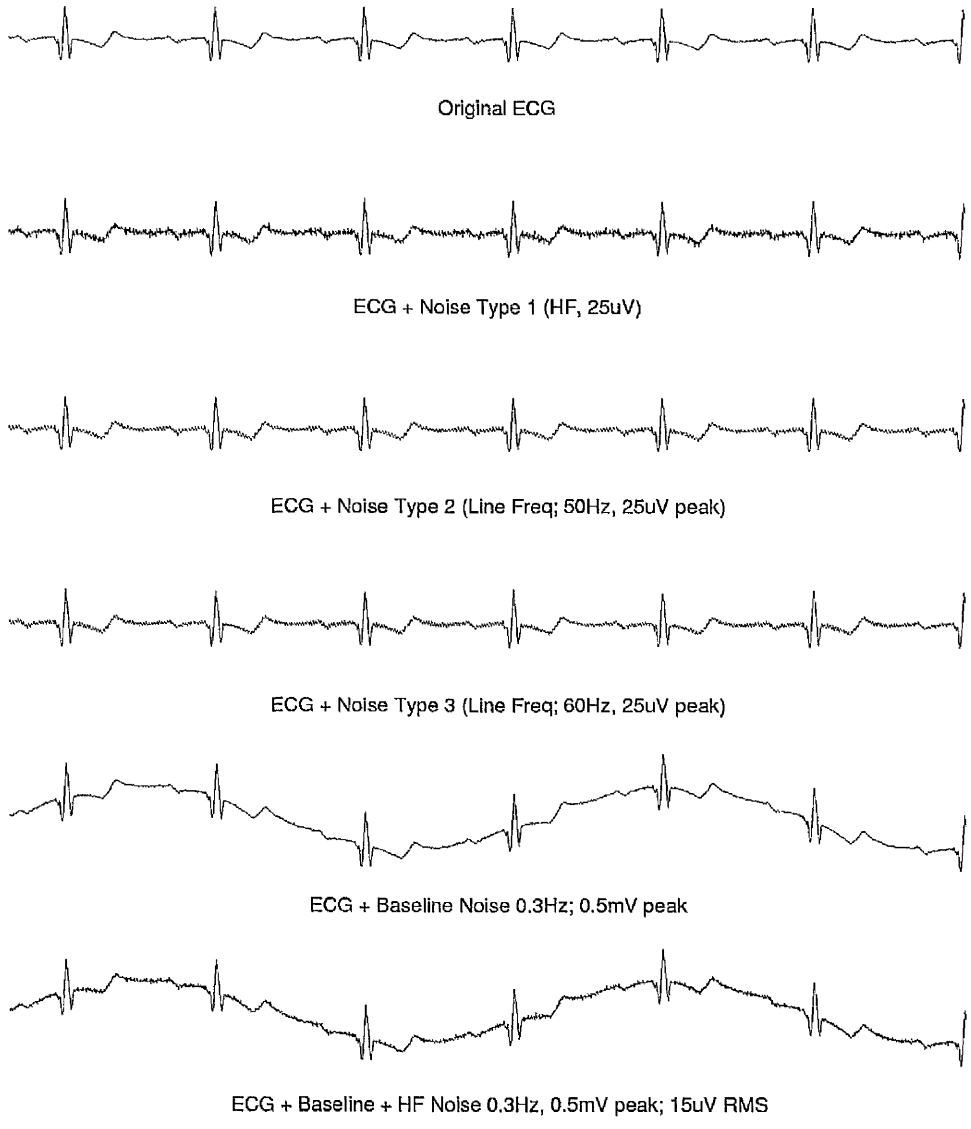

Figure 4.1(b) Illustration of the effect of the 5 CTS noise types on a typical ECG lead.

The effects of the high frequency and two line frequency noise types is clearly visible when compared to the original lead. The effect of the baseline wander (noise 4) is also clearly observed from the cyclic nature of the noise. Table 4.1 summarises the signal to noise ratio for each of the components (i.e. P-wave, QRS-complex or T-wave) of this lead and each of the noise types depicted in Figure 4.1(a). The following equation was used to compute the signal to noise ratio (SNR):

$$SNR = \frac{RMS_s}{RMS_n} = \frac{\sqrt{\frac{1}{N}\sum_{i=1}^{N} s_i^2}}{\sqrt{\frac{1}{M}\sum_{j=1}^{M} n_j^2}} = \sqrt{\frac{M}{N}\left(\sum_{i=1}^{N} s_i^2 \Big/ \sum_{j=1}^{M} n_j^2\right)} \qquad (4.1)$$

where N represents the number of sample points in the signal component and M is the number of sample points in the equivalent noise portion (for noise types 1-3 M=N; for noise types 4 and 5, N remained the same but M=3.3seconds*500, since there is 1 full cycle in 3.3 seconds of data for these two noise types and the sampling rate is 500 samples per second). Further, s_i represents the signal amplitude at sample point i (i=1,..,N) and n_j is the amplitude of the noise at sample point j (j=1,...,M). In the case of noise types 4 and 5 the value of RMS_n was divided by the ratio M/N in order for RMS_s and RMS_n to be computed over equal time intervals.

Waveform	SNR (Noise 1)	SNR (Noise 2)	SNR (Noise 3)	SNR (Noise 4)	SNR (Noise 5)
P-Wave	1.5	2.3	2.3	2.4	2.4
QRS Complex	10.7	13.9	14.2	18.1	18.2
T-Wave	3.5	5.6	5.7	4.1	4.1

Table 4.1 Signal to noise ratio (SNR) of a single lead (V1) obtained from a 12 lead ECG (same lead as Figure 4.1(b)) and the noise types from the CTS database.

Clearly the signal to noise ratio is poorest for the P-wave. This is only to be expected since the P-wave has the smallest amplitude of all the components.

It should be noted that the 'cyclic' nature of the ECG which has been contaminated with noise types 4 and 5, is removed automatically within the Glasgow Program by the application of the "baseline drift removal" algorithm (Macfarlane, Watts, Podolski, Shoat & Lawrie, 1986).

4.3 THE CSE STUDY

4.3.1 Graphical Display of Data

All 126 ECGs were processed by both the conventional Glasgow program and the Glasgow smoothing filter. P, PR, QRS and QT intervals were then estimated. The resulting P-duration estimates are presented in the form of line plots in Figures 4.2 and 4.3 for the conventional Glasgow program and Glasgow smoothing filter, respectively. Each main plot contains 4 subplots. The 4 subplots are basically just the 21 ECGs split up into groups of 5, 5 ,5 and 6 ECGs. One line in a subplot represents a single ECG and its measured P-durations in the presence of the 5 noise types as well as in the absence of noise. The corresponding referee value is also included for comparison. These results (in milliseconds), as well as those for the other three fiducial intervals considered, are summarised by boxplots in Figure 4.4 for both the conventional Glasgow program and Glasgow smoothing filter.

P-DURATION : CONVENTIONAL GLASGOW PROGRAM

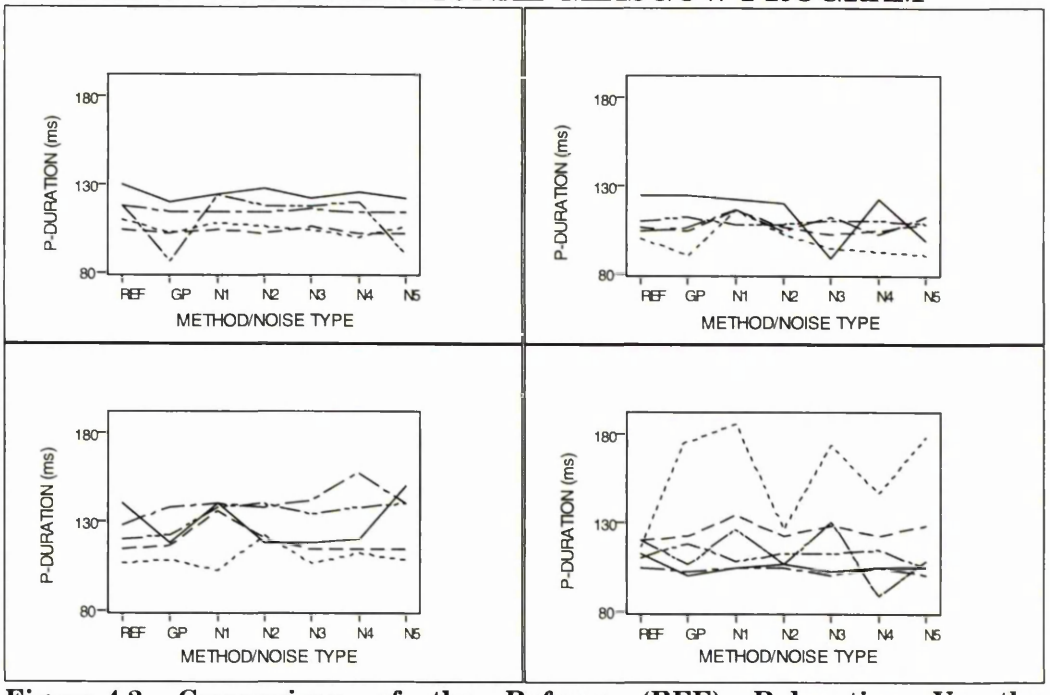

Figure 4.2 Comparison of the Referee (REF) P-duration Vs the Conventional Glasgow Program (GP) P-duration in the absence and presence of noise types 1 to 5 (N1-N5). Each line represents one ECG - 21 CSE ECGs.

P-DURATION : GLASGOW SMOOTHING FILTER

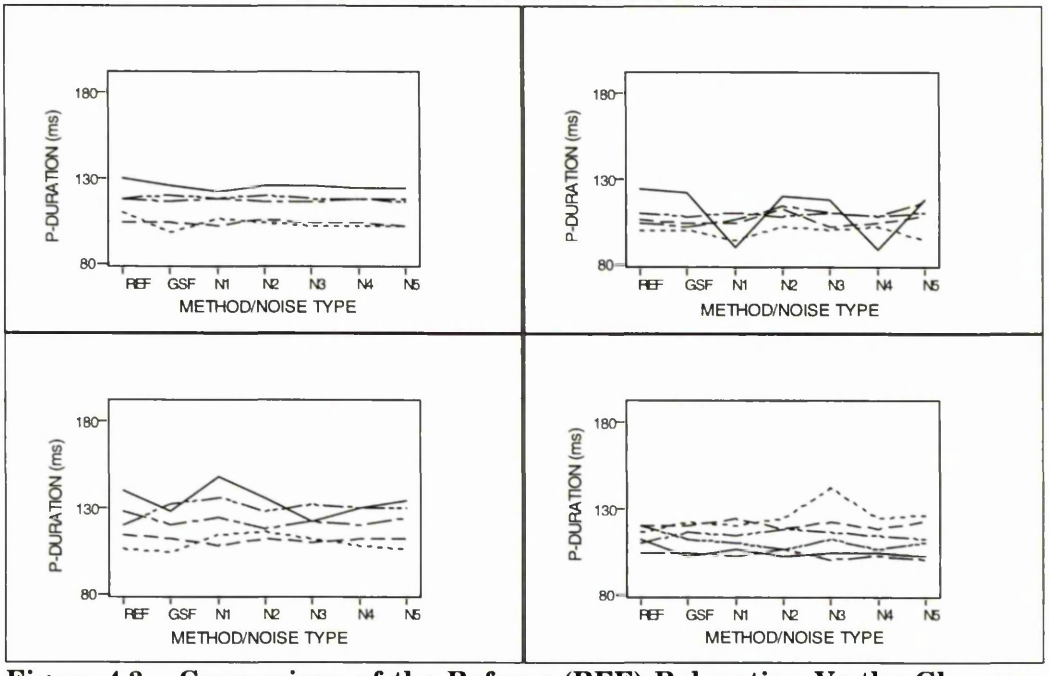

Figure 4.3 Comparison of the Referee (REF) P-duration Vs the Glasgow Smoothing Filter P-duration (GSF) in the absence and presence of noise types 1 to 5 (N1-N5). Each line represents a single ECG - 21 CSE ECGs.

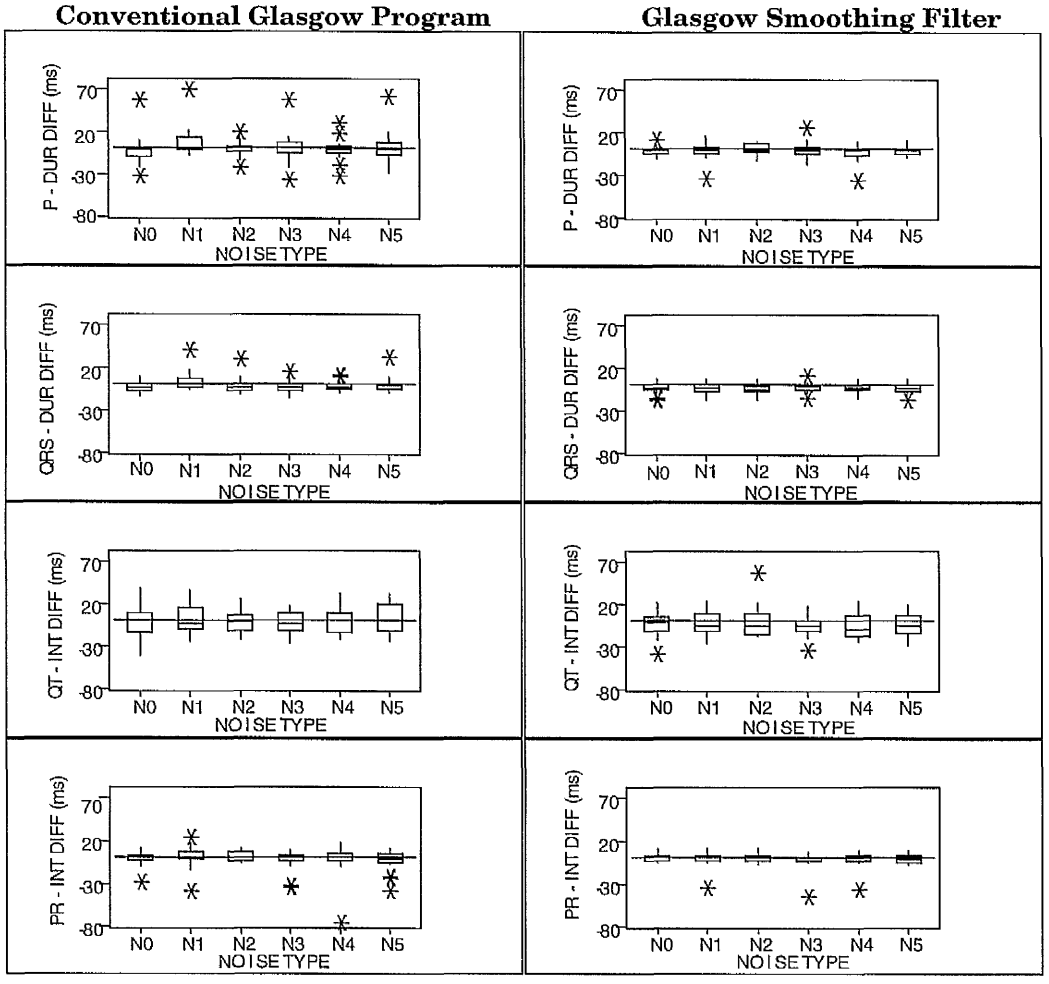

Figure 4.4 Performance of the Glasgow Program and Glasgow Smoothing Filter in the absence (N0) and presence of 5 types of noise (N1-N5) - 21 CSE ECGs
Diff = Estimate - Referee

From Figure 4.4, it can be seen that the addition of noise type 2 slightly improves the P-duration estimation by reducing the variability in the differences (estimate - referee) when using the conventional program compared to the equivalent noise-free case (N0). For the remaining durations/intervals, the addition of any of the types of noise showed no sign of a detrimental effect or improvement in the estimation of the fiducial intervals using the conventional program when compared to the noise-free (N0) case.

There is an overall improvement in P-duration estimation after applying the Glasgow smoothing filter (Figure 4.3) compared to the corresponding conventional program (Figure 4.2). The majority of the results are relatively consistent and contamination of the data with noise does not, in general, affect the program's ability to accurately detect the P-wave duration once the Glasgow smoothing filter is applied. The second set of boxplots in Figure 4.4 summarises the Glasgow smoothing filter results for all four fiducial intervals being examined, once again, by taking differences of the estimates with respect to the median referee estimates. As with the P-duration, the improvement in PR-interval estimation is clearly visible when compared to the corresponding boxplots for the conventional Glasgow program case. It can be seen that, even with the presence of excess noise, the program is still able to detect the PR interval relatively accurately once the Glasgow smoothing filter has been applied to the data. The boxplots of the QRS-duration estimate differences produced by the Glasgow smoothing filter (with respect to the referee medians) seem to indicate that there is now a systematic bias present, suggesting that the QRS-duration is now being clearly under-estimated by the Glasgow smoothing filter.

4.3.2 Formal Analysis

From the graphs, it appeared that the Glasgow smoothing filter seemed to be performing effectively. To further assess the performance of the programs more formally, sample correlations between the program and referee estimates were computed as were standard deviations of the differences, Estimate-Referee, about zero for both the conventional program and the modified version. For those cases where

there was significant evidence of a bias in the method, the standard deviation of the difference about the mean was quoted. The sample correlations have been tabulated in Tables 4.2(a) and 4.2(b) and the standard deviations (ms) in Tables 4.3 and 4.4 for the conventional Glasgow program and Glasgow smoothing filter, respectively. P-values have also been included indicating the absence or presence of a systematic bias.

From Tables 4.2(a) and 4.2(b), it can be seen that there is a considerable improvement in the agreement between the referee and Glasgow program P-duration estimates once the Glasgow smoothing filter is incorporated into the program. This is true across most of the noise types. This is also true for the QRS-duration, QT and PR interval, although the agreement between the referee and program estimates was initially good. However, in the case of the QRS-duration, there is significant evidence of a systematic measurement bias existing both in the absence (as seen in chapter three) and presence of all the noise types after applying the Glasgow smoothing filter. This bias is once again made significant due to the improved estimation of the QRS-duration estimates allowing an already existing bias to be made clearly identifiable.

CONVENTIONAL GLASGOW PROGRAM

Interval	No Noise	Noise 1	Noise 2	Noise 3	Noise 4	Noise 5
P Duration	0.42 p = 0.70	0.50 p = 0.06	0.64 p = 0.85	0.41 p = 0.82	0.58 p = 0.98	0.54 p = 0.91
QRS Duration	0.96 p = 0.09	0.91 p = 0.08	0.93 p = 0.29	0.99 p = 0.19	0.97 p = 0.07	0.93 p = 0.85
QT Interval	0.92 p = 0.83	0.93 p = 0.62	0.96 p = 0.66	0.96 p = 0.38	0.95 p = 0.93	0.93 p = 0.31
PR Interval	0.97 p = 0.66	0.93 p = 0.81	0.99 p = 0.08	0.94 p = 0.43	0.86 p = 0.62	0.93 p = 0.28

Table 4.2(a) **Sample correlations for the conventional Glasgow Program and the CSE median referee results.**
The p-values relate to the test of the null hypothesis of "no bias" (Bias present if $p<0.05$).

GLASGOW SMOOTHING FILTER

Interval	No Noise	Noise 1	Noise 2	Noise 3	Noise 4	Noise 5
P Duration	0.83 p = 0.14	0.70 p = 0.40	0.75 p = 0.95	0.65 p = 0.73	0.58 p = 0.12	0.82 p = 0.34
QRS Duration	0.97 p = 0.01	0.96 p = 0.03	0.97 p < 0.001	0.97 p = 0.04	0.97 p = 0.02	0.95 p = 0.02
QT Interval	0.96 p = 0.37	0.95 p = 0.52	0.92 p = 0.91	0.96 p = 0.07	0.95 p = 0.13	0.96 p = 0.23
PR Interval	0.99 p = 0.52	0.97 p = 0.67	0.99 p = 0.44	0.95 p = 0.50	0.97 p = 0.52	0.99 p = 0.87

Table 4.2(b) **Sample correlations for the Glasgow Smoothing Filter and the median CSE Referee results.**
The p-values relate to the test of the null hypothesis of "no bias" (Bias present if $p<0.05$).

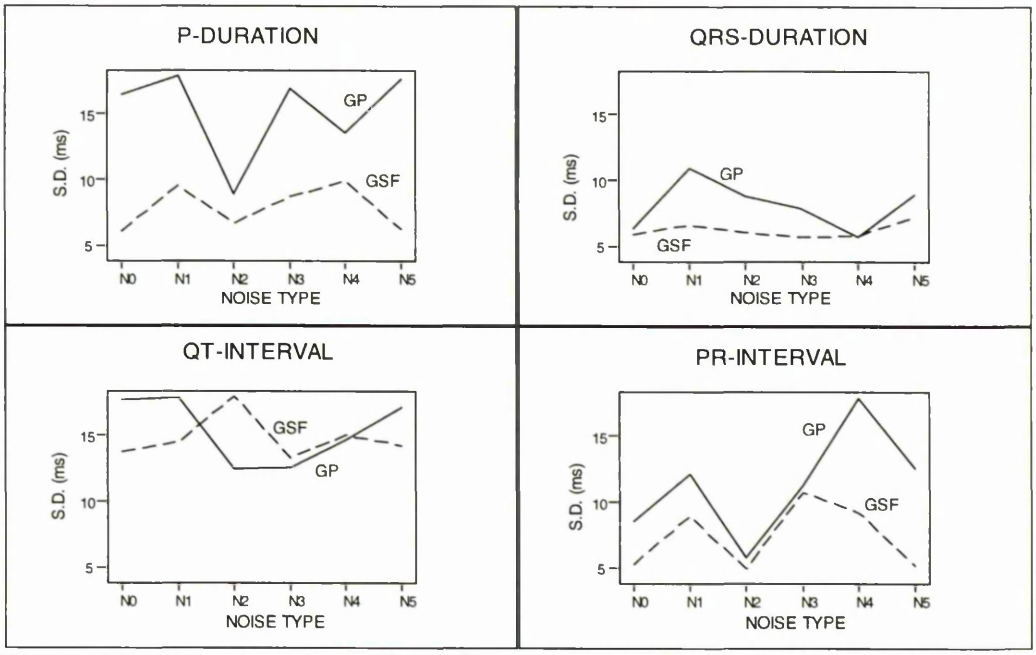

Figure 4.5 Standard deviations about zero for P-duration, QT-interval and PR-interval differences and about the mean for QRS-duration differences - 21 CSE ECGs. GP=conventional Glasgow program; GSF=Glasgow smoothing filter.
Difference = Estimate -Reference

From Figure 4.5 it is seen that the improvement in estimation of the P-duration is consistent across all the five noise types, on the basis of reduced standard deviations. This improvement is also clearly reflected in the case of the PR interval suggesting perhaps a more accurate P-onset estimation using the Glasgow smoothing filter, since both durations involve the P-onset in their calculation. Standard deviations for the QRS duration indicate that the results produced by the Glasgow smoothing filter are in general more stable than those produced by the conventional Glasgow program across virtually all of the noise types. However, in the case of the QT-interval, it is seen that the Glasgow smoothing filter performs more poorly than the conventional program in terms of the standard deviation in the presence of noise type 2 as well as noises 3 and 4, but not to the same extent.

Overall, it has been found that, for this particular data set, the addition of noise has not had a detrimental effect, in general, on the Glasgow program's ability to determine the intervals of interest. Again, it has been shown that after applying the Glasgow smoothing filter to noisy data, the net effect has been the production of better and more stable estimates of the P duration, QRS-duration and PR interval and in some cases the QT-interval when compared to the conventional Glasgow program.

4.4 THE CTS STUDY

4.4.1 Graphical Display of Data

As mentioned previously, the Conformance Testing Services (CTS) provided a database of 16 calibration ECGs along with reference values for the P and QRS durations and the PR and QT intervals. As with the CSE ECGs, the five different noise signals were added to these calibration ECGs before any processing was undertaken by the Glasgow program. This resulted in an additional set of 80 noisy ECGs together with the 16 original signals.

Each ECG was processed by both the conventional Glasgow program and the Glasgow smoothing filter. In order to assess the effects of both versions in the presence of noise, plots were once again constructed in order to demonstrate the performance of both the conventional Glasgow program and Glasgow smoothing filter. The line plots for the P-duration only, can be seen in Figures 4.6 for the conventional Glasgow program and Figure 4.7 for the Glasgow smoothing filter. The ECGs have been plotted in groups of four in order

to allow the effects of the different types of noise to be more clearly visible.

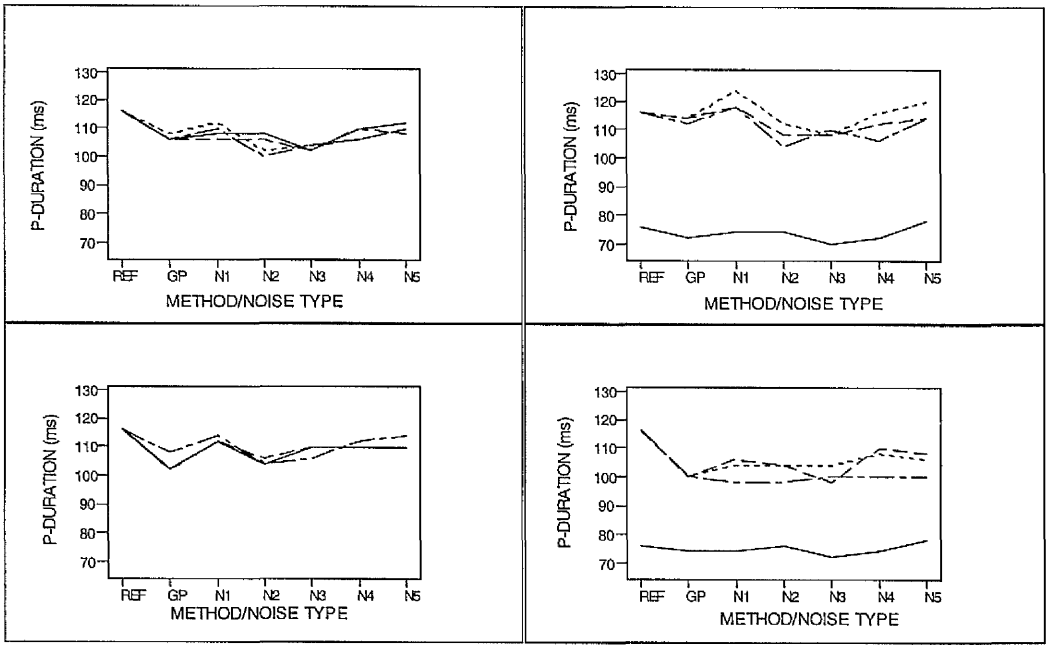

Figure 4.6 Comparison of the Reference (REF) P-duration Vs the conventional Glasgow Program (GP) P-duration in the absence and presence of noise types 1 to 5 (N1-N5). Each line represents one ECG - 16 CTS ECGs

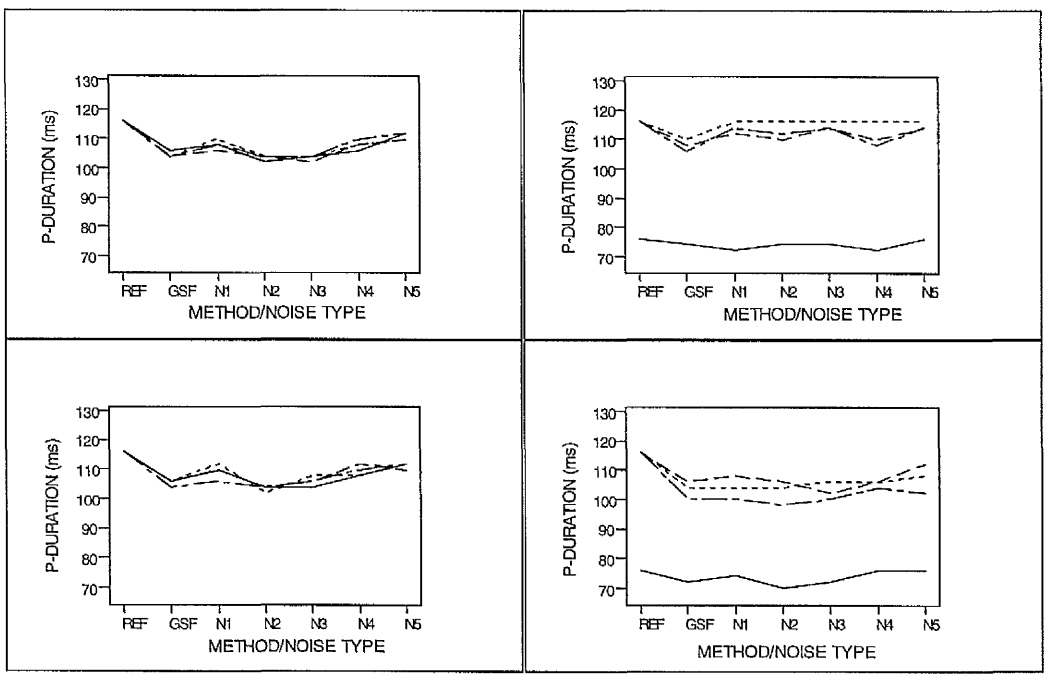

Figure 4.7 Comparison of the Reference (REF) P-duration Vs the Glasgow smoothing Filter P-duration in the absence and presence of noise types 1 to 5 (N1-N5). Each line represents one ECG - 16 CTS ECGs

From the two graphs, it can be seen that the Glasgow smoothing filter appears to reduce the measurement variability to a limited extent. It is clear that the addition of noise has not had a detrimental affect on the performance of either version of the program, in particular the Glasgow smoothing filter.

Figure 4.8 summarises all the duration and interval measurement differences estimated by the conventional Glasgow program and Glasgow smoothing filter with respect to the median referee results. When the two sets of equivalent measurements are compared, it is seen that in the case of the QRS-durations the median differences for the conventional program are all mostly negative whereas, for the filtered cases, the median differences are positive. The addition of noise types 2 and 3 seems to have introduced a bias into the conventional program QRS-duration estimates. However, this seems to be removed after the Glasgow smoothing filter is applied. In terms of QT-interval estimation, noise types 1 and 5 seem to have the worst effect on both the conventional program and Glasgow smoothing filter estimates (with respect to the CTS reference results). The P-duration and PR-interval plots are not very informative, once again due to the lack of variability in the reference values resulting in a clear bias in both the conventional Glasgow program and Glasgow smoothing filter cases.

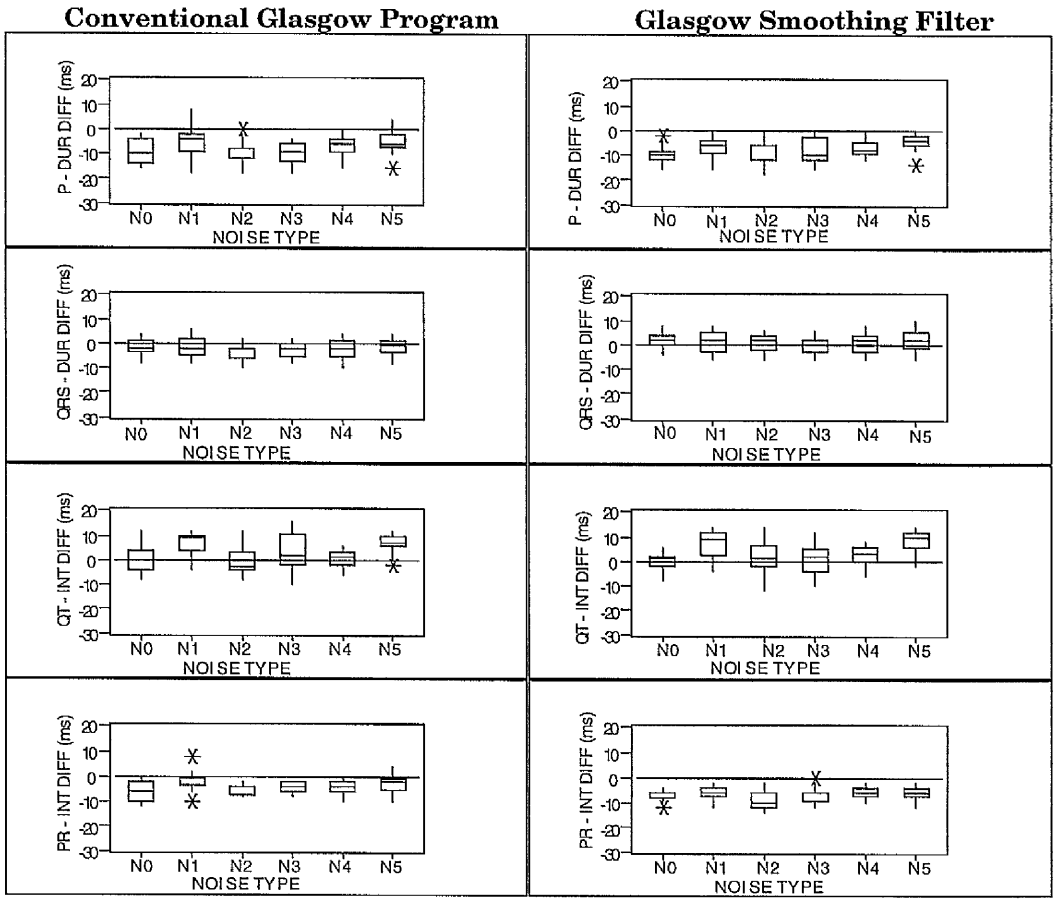

Figure 4.8 Performance of the Glasgow Program and Glasgow Smoothing Filter in the absence (N0) and presence of 5 types of noise (N1-N5) - 16 CTS ECGs
Diff = Estimate - Reference

4.4.2 Formal Analysis

Due to the presence of a bias in most of the fiducial intervals, standard deviations were computed for the differences about their means. Rather than provide a direct comparison of the performances of the conventional Glasgow program and Glasgow smoothing filter, these standard deviations give an indication of the stability of the measurements in the presence of the different noise types. The standard deviations for each interval and noise type are plotted in Figure 4.9 for both the conventional Glasgow program and Glasgow smoothing filter. The solid line represents those measurements

estimated by the Conventional Glasgow program (CGP) in the absence and presence of noise and the dashed line represents those measurements estimated by the Glasgow smoothing filter (GSF) in the absence and presence of noise.

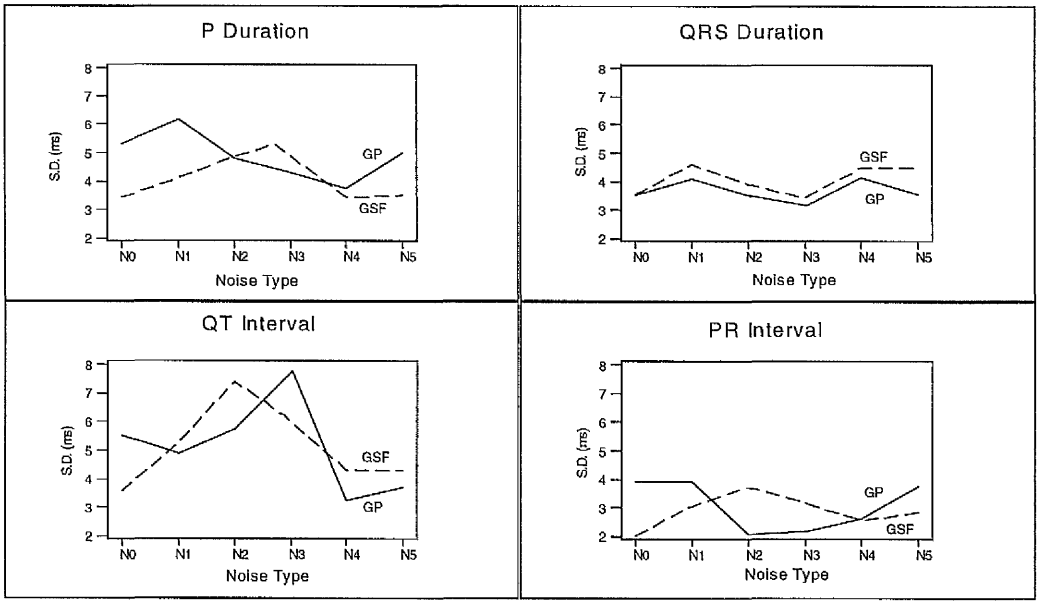

Figure 4.9 **Standard deviations about the mean for P-duration, QRS-duration, QT-interval and PR-interval differences - 16 CTS ECGs.**
GP=Cconventional Glasgow program; GSF=Glasgow smoothing filter.
Difference = Estimate - Reference

A comparison of the two sets of standard deviations indicates that there is no convincing evidence of a difference between the conventional Glasgow program and Glasgow smoothing filter results across all the noise types, i.e. neither method does consistently better than the other for this data set.

4.5 SUMMARY

It has been demonstrated in this chapter that, when excess noise was added to the ECGs being tested, the estimates of fiducial intervals did not deteriorate substantially. When the Glasgow smoothing filter was applied to the CSE database the resulting estimates improved compared to the conventional program both in the absence and presence of noise. In general, the fiducial interval estimates based on the Glasgow smoothing filter seemed to be more stable than those from the conventional program across the selection of noise types investigated.

An examination of the CTS database indicated that the performance of the conventional Glasgow program and Glasgow smoothing filter showed little difference in fiducial interval estimation in the presence of noise. It was seen that the database was not very helpful for the purposes of comparing the two methods of estimation due to the lack of variability in reference values.

CHAPTER FIVE

QRS ONSET LOCATION USING SOFTWARE BASED NEURAL NETWORKS

5.1 GENERAL INTRODUCTION

Although chapters 3 and 4 concentrated on testing the accuracy of wave duration and interval measurements estimated by the conventional Glasgow program and the new Glasgow smoothing filter, it was important to investigate alternative methods for improving the estimation of fiducial points. One method of particular interest was that of software-based neural networks. Previous medical applications of neural networks have included identifying ST-T abnormalities (Devine, 1990), classification of electrocardiographic ST-T segments (Edenbrandt, Devine & Macfarlane, 1992) and diagnosis of atrial fibrillation and myocardial infarction (Yang, 1995).

5.2 BACKGROUND

5.2.1 Introduction

Intelligent behaviour in a human seems to emerge from interactions involving huge numbers of neurons. These neurons are living nerve cells, and neural networks are essentially networks of such cells. An artificial neural network (ANN) is a model which attempts to simulate the same behaviour as a biological neural network. Although advances in technology have led to an increase in performance of many complex tasks by computer, which is far better and faster than the human brain, these advances have failed to produce devices that can approach

the capability of human intelligence in pattern recognition, innovation and creativity.

Research into neural networks dates back to when McCulloch and Pitts (1943) applied their knowledge of the human brain to the binary decision neuron. The formal model of the neuron was described as a threshold logic unit having a preset threshold which was used to separate the two states 'yes' or 'no', 'on' or 'off' etc. (Branscombe, 1990). This later became known as the McCulloch-Pitts or M-P neuron.

5.2.2 The McCulloch-Pitts Neuron

The M-P neuron is characterised by a finite number of inputs (n) defined by x_i (i=1,...,n), a threshold level, L and an output, y. The inputs to and output from the M-P neuron can assume the binary values 0 or 1. The output y of an "isolated" M-P neuron can be described as a function, g, of its inputs, better known as an **activation function**, and can be expressed mathematically as :

$$y = g\left(\sum w_i x_i - L\right) \tag{5.1}$$

Here, w_i is a weight attached to input x_i, where w_i represents a value assigned at each connection of an input to a neuron and L is any positive integer. Let

$$p = \sum w_i x_i - L, \tag{5.2}$$

then

$$\begin{aligned} g(p) &= 0 \quad p < 0 \\ &= 1 \quad p \geq 0 \end{aligned}$$

In other words, this means that a neuron can "fire" if the total excitation it receives reaches or exceeds the threshold value.

This idea can be extended to that of a group of M-P neurons forming a layer. A simple ANN consisting of a single layer can be created from an array of n neurons. Each of these neurons then receives inputs from m sources, $x_1,x_2,....,x_m$, via weights w_{ij}, resulting in outputs $y_1,y_2,.....,y_n$. The output for the jth neuron can be written as :

$$y_j = g\left(\sum_{i=1}^{m} w_{ij}x_i - L_j \right) \qquad \text{for } j=1,...n \tag{5.3}$$

where, L_j is the threshold for the jth neuron.

5.2.3 The Perceptron

In 1949, Hebb published a paper entitled "The Organisation of Behaviour" in which he proposed that the connectivity of the brain was continually changing as it was learning. He further postulated that the repeated activation of one neuron by another through a particular synapse increased its conductance. This implied that groups of weakly connected neurons, if activated synchronously, had the tendency to organise themselves into more strongly connected assemblies.

In 1958, Rosenblatt published a paper showing how an M-P network with adjustable weights could be "trained" to classify certain sets of patterns. Rosenblatt labelled these networks Perceptrons. Initially, the weight settings are arbitrary, so that any stimulation of the network produces an arbitrary response. To obtain the desired

response, the weights are adjusted by a procedure known as training or learning. The perceptron which Rosenblatt popularised was the two layer neural network (see Figure 5.1). The first layer consisted of the inputs and the second consisted of a single unit with a threshold activation function which produced a binary output.

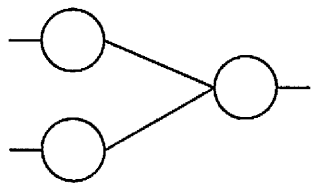

Figure 5.1 Basic Structure of the Perceptron

Minsky and Papert (1969) pointed out a fundamental problem with the single layer perceptron. It was shown that perceptrons could not handle even relatively simple problems such as distinguishing between the letters T and C. This publication had a devastating effect on research into the field of artificial neural networks resulting in little work being done on neural networks in the late 60's and early 70's.

5.2.4 Multi-Layer Perceptrons

To overcome the problem associated with single layer perceptrons, an extra hidden layer of neurons had to be added between the input layer and the output layer of the network, as shown in Figure 5.2. The term used to describe these types of networks was **"multi-layer perceptrons"** or **"multi-layer networks"**. However the addition of this extra layer presented a problem since the relationship between the outputs from the hidden neurons and the outputs from the network were not known. It was Rumelhart and associates (1986) who

developed an effective training algorithm that could adjust the weights of the hidden neurons.

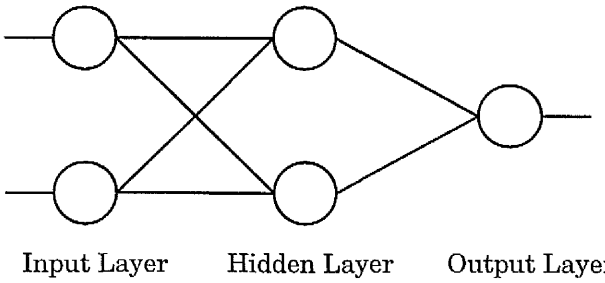

Figure 5.2 Basic Structure of a Multi-Layer Network

5.3 NEURAL NETWORK ARCHITECTURE

5.3.1 Feed-Forward Networks

The design of a neural network is mainly concerned with the number of layers in the network and the number of neurons in these layers. A network consists of an input layer, hidden layer(s) and an output layer. The manner in which the neurons of a neural network are structured is intimately linked with the learning algorithm used to train the network which in turn is influenced by the problem to be solved.

The network design used in this study is known as **feed-forward**. The architecture of a feed-forward network is such that each of the neurons in a particular layer can be connected only to those neurons in the following layers. Typically, the neurons in each layer of the network have, as their inputs, the output signals of the preceding layer only. The set of resulting signals of the neurons in the output layer of the network, constitute the overall response of the network to the activation pattern supplied by the input layer. The main advantage of

a feed-forward network is that the output from the network can be calculated quickly using a single forward pass.

When every neuron in each layer is connected to every other neuron in the adjacent forward layer then the network is said to be **fully connected.**

The optimal choice of the number of layers and neurons per layer cannot be predicted although the more neurons used, the greater the capacity of the network to learn and store associations. However, sometimes there is a danger that a network may 'overtrain', thus compromising its performance on new problems of a similar nature.

5.3.2 Supervised Learning Algorithm

A learning algorithm is simply a training technique which is designed to produce a series of weights which allow a network to perform a function. The learning algorithm used in this chapter was a **supervised learning algorithm.**

Supervised learning algorithms require each neuron to be trained to produce an ideal response to the input signals. Networks are iteratively trained on a given set of training inputs until learning is completed. During each training iteration, the weights are adjusted to minimise the overall network error (difference between the actual output and desired output), which is achieved when all the input and output patterns are successfully learned.

5.3.3 Transfer Functions

A **transfer function** is a function applied to the value (activation value) output by the activation function (see section 5.2.2). The purpose of a transfer function is to define how the activation value, (sum of the weighted inputs of a neuron at a particular time), is to be output (see Figure 5.3).

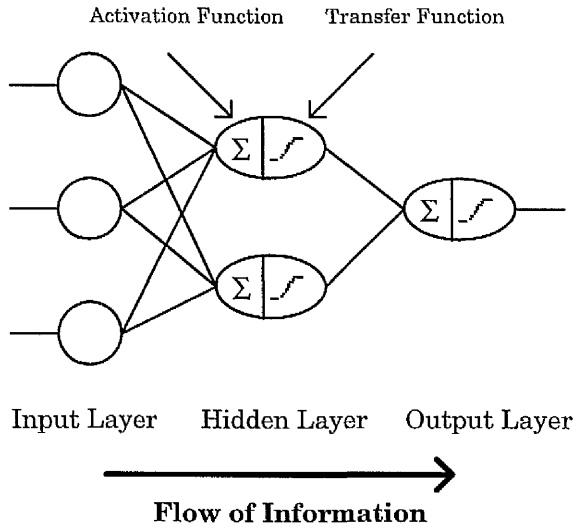

Figure 5.3 Example of a Fully connected, Feed-Forward Network

The transfer function utilised in this study was the commonly used **sigmoidal function**, of the form:

$$f(g(p)) = \frac{1}{1+e^{-g(p)}} \qquad (5.4)$$

where the value of g(p) represents the activation value (sum of the weighted inputs) and e is the exponential function. In this case f(g(p)) can take any value between 0 and 1. An example of the output which can be expected from this function can be seen in Figure 5.4. The activation value is plotted on the horizontal axis and the response of the transfer function on the vertical axis.

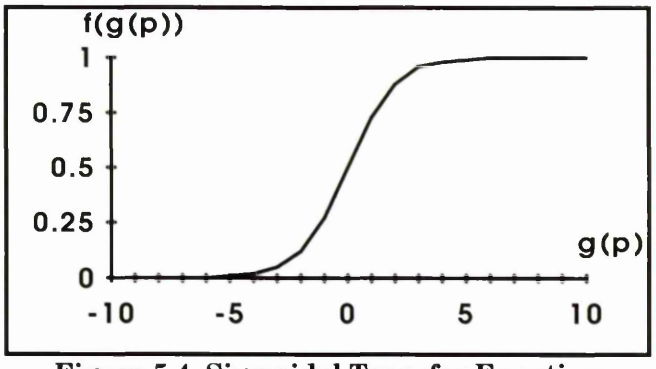

Figure 5.4 Sigmoidal Transfer Function

5.3.4 Normalisation Of Training Data

In order to train a network, the input data must be in a form which is appropriate for the activation and transfer functions being utilised within the network. When using the standard sigmoid transfer function, the input data to the activation function should consist of numerical values between 0 and 1 (Stanley & Luedeking, 1990). In order to translate the actual data into the required form, the data must be recoded. The recoding of the data in this case is performed by the following formula :

$$X_{new} = \frac{X_{old} - X_{min}}{X_{max} - X_{min}} \qquad (5.5)$$

where X_{old} is the original data point and X_{min} and X_{max} are the minimum and maximum values which X_{old} can take and X_{new} is the recoded value.

5.3.5 Back Propagation Learning Algorithm

Back propagation is the most commonly used type of supervised learning algorithm and, so is used in this study. Here, a pattern is sent through the layers of a feed-forward multi-layer network and an error value is propagated back through the network during training. As the error is fed back, the weights are altered, thus preventing the same error from happening. Eventually, an output pattern is produced which corresponds to the input pattern entered. The main aim is to minimise the mean square error between the actual output and the target output of each neuron in the network.

5.3.6 Network Parameters

Factors which have been seen to affect the time for a network to train successfully are listed below.

The **initial assignment of weights** has been shown to have a significant influence on the time taken for convergence (i.e. for the network to reach a stable state) (Kolen & Pollack, 1990). Those weights which are initially allocated introduce associations (connections/relationships) between certain input and output patterns. However, these associations may or may not be correct and it is therefore necessary that the algorithm is not only able to learn new associations but "unlearn" those which are incorrect.

The **learning rate** of a network is the measure of the speed of convergence of the initial weight pattern to the ideal (optimum) pattern. If the weight pattern is far from what it should be, the

changes can be made in fairly large steps. When the weight pattern is close to its target output, then the changes must be made in fairly small steps. A large learning rate (chosen by the user) may cause the algorithm to overshoot the target continually, thus causing wild fluctuations in the output. However, too small a learning rate may cause the network to take longer to converge. The convergence time of back propagation is ultimately related to the difficulty of the problem to be solved and the nature of the training data (Stanley & Luedeking, 1990).

The **momentum term** is implemented into the weight change process to average out oscillating weight changes and give an idea of the direction and magnitude of the next weight change. This can be any real value between 0 and 1.

The **tolerance** is the measure by which the actual output from the network is allowed to differ from the target output, whilst still being close enough to be correct. The tolerance can also be any real number between 0 and 1. However it is unwise to choose values of exactly 0 or 1.

5.4 LOCATING THE QRS ONSET

5.4.1 Introduction

Due to the success of the application of artificial neural networks for cases such as ECG signal detection where a feed-forward multi-layer perceptron was used as a pattern classifier to distinguish between normal and abnormal beats, as well as to classify different abnormal beat morphologies (Hu, Tompkins, Afonso et al., 1993), it was of

interest to see how well software-based neural networks would perform when locating ECG wave fiducial points. The QRS waveform, being the dominant wave type in an ECG signal, was the natural choice for investigating the use of neural networks in identifying fiducial points. Only if the neural network were to be successful in locating a QRS fiducial point, would it be worthwhile to look at estimating the fiducial points of the smaller waveforms of the ECG signal by neural networks. In this chapter the performance of artificial neural networks in estimating the location of the QRS onset was investigated.

The type of network used in this investigation required the use of the feed-forward back propagation algorithm. The criteria behind this type of algorithm is to minimise the mean square error between the actual output and the target output of each neuron in a multi-layer network. The software for this network was already available within the department (Devine, 1990).

5.4.2 The Training Set

A total of 75 ECGs from the CSE multi-lead measurement study were used as the training set. Since the aim of this study was to locate the QRS onset, it was necessary to obtain the true QRS onsets of the 75 ECGs. These were 'visually' estimated by an expert electrocardiographer, who examined the spatial velocity and the modal beat of each ECG and used the reference CSE QRS durations as a guide to maintain an exact correspondence between the onsets/offsets and the corresponding durations. These onsets were then used as the true onsets in the training process of the neural network.

5.4.3 Training the Neural Networks

The training process involved the neural network being trained with QRS data for which the QRS onset was specified. The input data used here was 21 spatial velocity points extracted from the QRS waveform data. This formed a small window of sample points in which the true QRS onset would be known to lie. The 21 points were selected by using an approximate estimate of the QRS onset point as an indication of the centre of the window from which the range of points would be extracted. The preliminary QRS onset located by the conventional Glasgow program (Macfarlane et al., 1990) was taken to be this estimate. The 21 points were made up by extracting 10 spatial velocity values on either side of this preliminary estimate. For each sample point two additional 'inputs' were used, namely the slopes of linear regressions based on 5 points to the left and 5 points to the right of each of the 21 sample points. These slopes provided the neural network with additional information in terms of how the signal was changing with time and therefore allowed the network to identify common patterns in the 75 sets of input data (i.e. the 75 cases from the CSE data set) presented to the network.

The networks investigated were fully connected and are listed in Table 5.1 along with the network configurations. The performance of the networks was compared using, as input data, the 21 spatial velocities as the only inputs, the 42 gradients as the only inputs and both of these combined as the input (i.e. 63 inputs). Networks with one or more hidden layers were used in the hope that the addition of an extra layer would increase the capacity of the network to learn and store associations and therefore improve its overall effectiveness. Each training file also contained the location of the 'true' QRS onset in order

that the network could learn where the true onset lay. Training was completed when all of the onsets had been 'learned' by the networks. For those networks which did not fully complete training, if the number of iterations exceeded 1000000, then the training process was interrupted in case of overtraining and the weights at that point were stored. The weight files for each type of network contained a list of the final weights which represented the associations between the neurons in adjacent layers and which were required to produce the desired outputs.

A learning rate of 1 and 1.5 was set so as not to be too large in case the network did not sufficiently learn the patterns in the data presented and not too small in case the process took too long for the network to reach a stable state (i.e. to train effectively). A tolerance of 0.2 was chosen implying that the network would keep training with the selected training patterns until the outputs from the network differed by no more than 0.2 from the target output. The momentum parameter was set arbitrarily at 0.4 or 0.5.

During the testing phase, the output field for each case consisted of 21 neurons whose values all lay in the range [0,1]. Each value was an estimate of how likely each neuron was the true QRS-onset location. The higher the value of an output neuron, the more likely that this was the location of the QRS onset. In an ideal situation, there would be twenty neurons which had the value 0 and only one with output 1, implying that this point was the true QRS onset predicted by the neural network. In this study, the highest value regardless of the magnitude was taken to be the best estimate of the QRS onset. Whichever network configuration was used, the number of output neurons remained constant throughout at 21.

Network	Description
21-33-21	21 inputs, 33 hidden neurons (1 hidden layer), 21 output neurons. Learning rate = 1.0 Momentum = 0.4 Tolerance = 0.2
42-33-21	42 inputs, 33 hidden neurons (1 hidden layer), 21 output neurons. Learning rate = 1.0 Momentum = 0.4 Tolerance = 0.2
63-33-21	63 inputs, 33 hidden neurons (1 hidden layer), 21 output neurons. Learning rate = 1.0 Momentum = 0.4 Tolerance = 0.2
63-45-21	63 inputs, 45 hidden neurons (1 hidden layer), 21 output neurons. Learning rate = 1.0 Momentum = 0.4 Tolerance = 0.2
63-50-21 (1)	63 inputs, 50 hidden neurons (1 hidden layer), 21 output neurons. Learning rate = 1.0 Momentum = 0.4 Tolerance = 0.2
63-50-21 (2)	Learning rate = 1.0 Momentum = 0.5 Tolerance = 0.2
63-50-21 (3)	Learning rate = 1.5 Momentum = 0.4 Tolerance = 0.2
63-55-21	63 inputs, 55 hidden neurons (1 hidden layer), 21 output neurons. Learning rate = 1.0 Momentum = 0.4 Tolerance = 0.2
63-63-21	63 inputs, 63 hidden neurons (1 hidden layer), 21 output neurons. Learning rate = 1.0 Momentum = 0.4 Tolerance = 0.2
63-33-33-21	63 inputs, 33*2 hidden neurons (2 hidden layer), 21 output nuerons. Learning rate = 1.0 Momentum = 0.4 Tolerance = 0.2
63-50-33-21	63 inputs, 50 and 33 hidden neurons (2 hidden layers), 21 output neurons. Learning rate = 1.0 Momentum = 0.4 Tolerance = 0.2

Table 5.1 Types of Neural Networks Trained

5.4.4 Testing the Neural Networks

5.4.4.1 The Validation Set

The initial validation set consisted of 50 randomly chosen ECGs from the training set which were deliberately contaminated by the addition of high frequency 25μV RMS noise in order to change their appearance. It may be arguable as to whether this could be considered as an actual "test" set since, although noise was added to distort the appearance of the ECGs, they were still taken from the original training set. However, in the absence of an independent validation set at this time, this was considered a viable first attempt. Before presentation of the ECG data to the network, the ECGs were filtered using the method discussed in Chapter 3, which involved splitting the ECG and averaging the final waveforms, the Glasgow smoothing filter. The various networks specified in Table 5.1 were then applied to the 50 cases and the resulting estimates of the QRS onsets summarised (Table 5.2).

Results from the conventional program as well as those produced by introducing the Glasgow smoothing filter into the program are included in Table 5.2 for comparison. As mentioned previously, the sample point with maximum output was taken to be the 'network' estimate of the QRS onset. As an overall summary of performance, each case was scored by the difference of the 'true' QRS onset and the 'actual' estimated onset. A summation of all the scores over all 50 cases in the test set was used as a performance indicator for each method and type of network. From the performance scores in Table 5.2, it is clear that the Glasgow smoothing filter very significantly outperformed the conventional program. This was only slightly bettered by some of

the neural networks with the network performing best having 63 inputs (21 sample points and 42 slopes), a single hidden layer with 50 neurons and 21 output neurons (learning rate=1.5, momentum=0.4 and tolerance=0.2). The three '63-50-21' networks (using different momentums and learning rates) all performed consistently well on the validation set in terms of the overall score. Other combinations of learning rates and momentums for networks with fewer hidden neurons did not perform consistently well - hence the reason they are not included in Table 5.2.

The number of exact QRS onset locations by the best performing network improved by 60% (i.e. 10 to 16) when compared to the Glasgow smoothing filter alone. However, closer inspection of the results showed that in the case of the filter alone, the maximum number of sample points by which a particular QRS onset deviated from the 'true value' was five, whereas for the best trained network there were three cases which deviated from this by six sample points. Therefore, although the number of cases which were correctly located improved, there was also substantial increases in the differences between the corresponding true and network estimates for some ECGs in the test set. Figure 5.5 depicts the output response for the neural network which performed best i.e. 63-50-21, in terms of the network output at each of the estimates of the QRS onsets for the 50 ECGs tested. Each case has been represented by a different symbol. In general there was no obvious pattern with just 32% of cases being correctly located ($\frac{16}{50}$). It was seen that out of the 16 onsets which were correctly detected, just over 43% of the onsets were determined with a network output of between 0.9 and 1.0, 25% between 0.8 and 0.9, just over 12% between 0.6 and 0.8 and similarly between 0.3 and 0.6. One out of the sixteen

cases was correctly located with a network output of only 0.1. Moreover, there were cases (out of the 50 ECGs) where the network determined onsets with an output between 0.8 to 1 but was inaccurate with its estimation when compared to the 'true' QRS onset. It could therefore be concluded that there was little suggestion from the data that the network output at the predicted QRS onset was proportional to the accuracy of the estimation of the QRS onset for this, the best performing network.

Difference (samples)	GP	GSF	21-33-21	42-33-21	63-33-21	63-45-21	63-50-21 (1)	63-50-21 (2)	63-50-21 (3)	63-55-21	63-63-21	63-33-33 -21	63-50-33 -21
0	2	10	15	9	16	10	12	14	16	11	15	12	12
1	18	19	16	20	14	15	18	17	17	21	17	18	18
2	15	13	9	8	13	15	12	10	11	10	12	10	11
3	6	4	8	5	1	3	3	2	2	3	0	5	4
4	5	3	0	2	1	1	1	2	1	1	3	1	0
5	1	1	1	1	1	2	2	1	0	1	1	0	0
6	0	0	0	4	3	3	2	2	3	2	2	2	3
7	0	0	0	0	1	0	0	1	0	0	0	1	2
≥8	3	0	1	1	0	1	0	1	0	1	0	1	0
Total	**50**	**50**	**50**	**50**	**50**	**50**	**50**	**50**	**50**	**50**	**50**	**50**	**50**
Score	**162**	**74**	**71**	**105**	**77**	**94**	**77**	**83**	**67**	**79**	**70**	**84**	**84**

Table 5.2 **Neural Networks Test Results - Validation Set**
Difference = |Estimated QRS onset - Referee/True QRS onset|
GP = Conventional Glasgow Program ; GSF = Glasgow Smoothing filter
See Table 6.1 for descriptions of (1), (2) and (3)

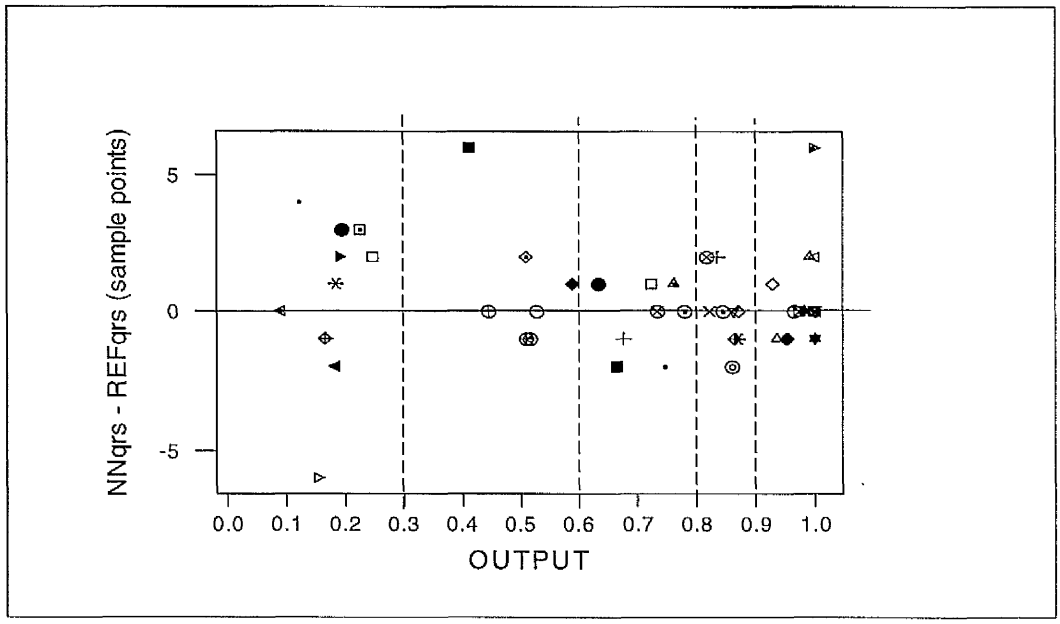

Figure 5.5 **Results produced by network 63-50-21**
NNqrs - QRS onset determined by the neural network
REFqrs - Referee/True QRS onset

5.4.4.2 The Test Set

The test data consisted of 48 "new" CSE ECGs with the true values provided by an electrocardiographer (see section 5.2.2). This test set of CSE ECGs was a completely fresh set of data, independent of the training set. The lead data for each ECG was again filtered using the new Glasgow smoothing filter, before forming the spatial velocity and extracting the data for presentation to the network. All the networks (in Table 5.1) were then tested using the new input data (21 spatial velocities and 42 slopes). The results were recorded and summarised in the same manner as before in Table 5.3.

The method which performed best overall was the Glasgow smoothing filter i.e. none of the neural networks performed as well as the Glasgow smoothing filter. Second to this was the two hidden layer network 63-33-33-21. From Table 5.3 it can be seen that, although this

network did not perform as well as the Glasgow smoothing filter, in terms of the overall score it did, however, estimate more exactly correct QRS-onsets (i.e. difference=0) than any other method or network. While this may be true, it is also apparent that from the remaining results of the '63-33-33-21' network, that it estimates more QRS onsets 3 and 4 samples away from the "true" onset than the Glasgow smoothing filter. This is also true for the networks: '43-32-21', '63-63-21' and '63-50-33-21'. All these networks located more correct QRS onsets than the Glasgow smoothing filter, but these too produced in general a wider spread of estimates than the Glasgow smoothing filter. All in all, it was clear that the overall performance of the Glasgow smoothing filter was superior to that of any of the artificial neural networks. Moreover, the network which performed best in the initial validation data set (63-50-21) was now ranked only 7th in this "new" test set.

Difference (samples)	GP	GSF	21-33-21	42-33-21	63-33-21	63-45-21	63-50-21 (1)	63-50-21 (2)	63-50-21 (3)	63-55-21	63-63-21	63-33-33 -21	63-50-33 -21
0	6	9	8	11	8	8	9	8	8	9	11	15	11
1	14	18	13	14	10	10	13	9	11	11	10	11	12
2	11	10	14	9	10	9	10	11	10	13	12	7	9
3	10	6	6	5	11	10	8	11	11	9	8	7	9
4	5	3	3	6	4	5	5	5	4	3	2	6	4
5	1	1	2	2	4	4	2	3	4	2	3	1	3
6	1	1	0	0	1	1	1	0	0	0	1	0	0
7	0	0	1	1	0	1	0	1	0	1	1	1	0
≥8	0	0	1	0	0	0	0	0	0	0	0	0	0
Total	**48**	**48**	**48**	**48**	**48**	**48**	**48**	**48**	**48**	**48**	**48**	**48**	**48**
Score	**97**	**79**	**97**	**88**	**105**	**111**	**93**	**106**	**100**	**93**	**94**	**82**	**88**

Table 5.3 **Neural Networks Test Results - Test Set**
Difference = |Estimated QRS onset - Referee/True QRS onset|
GP=Conventional Glasgow Program ; GSF =Glasgow Smoothing Filter
See Table 6.1 for descriptions of (1), (2) and (3)

5.5 DISCUSSION

In this study, the design of the artificial network was such as to keep the run time of the testing phase to a minimum. The choice of network 63-X-21 meant that there was no need to implement a moving window technique, which would require numerous 'passes' over a region of the ECG. This would have been the case if a network had been designed to have a single output neuron, i.e. 63-X-1. It may be argued, however, that the number of hidden neurons and hence 'connections' to the output neuron would have been far less and thus less time consuming using the 63-X-1 network. Another possible issue which can arise is that too many hidden neurons may cause a network to overtrain (i.e. memorise the training set). However, it is possible to overtrain with any network and so, as in the case of the 63-X-21 network in this study, intervention is required to stop the process of overtraining by interrupting the training process.

5.6 SUMMARY

It has been shown that this particular application of neural networks has not entirely proved to be successful in estimating the QRS onset. However, although the results may not have been encouraging, it should be noted that the networks were trained and tested with a relatively small sample size. Ideally, a much larger training set would have been available when developing the neural networks but this would have needed corresponding true onsets, something which was too difficult to achieve. This would require preferably more than one experienced cardiologist to pick out wave onsets visually, a task which is tedious and time consuming.

Evaluation of the networks using a validation set based on contaminated member of the training set indicated that certain networks performed better than both the conventional Glasgow program and the Glasgow smoothing filter in terms of the number of QRS onsets 'correctly' located (i.e. zero deviation between the estimated and 'true' QRS onset). However, there was evidence that the networks produced more cases which deviated from the 'true' QRS onset by over 5 sample points compared to the other methods.

Based on an actual test set, the performance of the 'best' network ('best' from the results of the validation set), was not maintained when applied to the current test set ECGs. In fact, the Glasgow smoothing filter scored best overall, and although some networks estimated more exactly correct onsets, once again, there was more variability in the estimates based on the networks than in the Glasgow smoothing filter.

It has thus been shown that with the introduction of the new Glasgow smoothing filter alone, the amount of deviation between the estimated and the true onset decreased considerably when compared to the corresponding results produced by the conventional Glasgow program. This also suggests that the referee/true QRS onset was not unreasonable. Any improvement (at the very least) which was seen with the addition of the neural networks was not consistent from one test set to another.

Although this chapter has concentrated on QRS onset location, the initial aim had been to eventually apply the technique of neural networks to locate the fiducial points of the most difficult of the

waveforms, the P-wave. However, since this method did not prove successful for the most dominant of the waveforms, it seemed a pointless exercise to study the accuracy of P-wave onset location using the time-consuming method of neural networks.

CHAPTER SIX

FIDUCIAL POINT LOCATION USING METHODS OF LINEAR TEMPLATES

6.1 INTRODUCTION

Fiducial point location within the conventional Glasgow program involves the use of thresholds or critical values. Spatial velocities (see section 1.7) are compared to these critical values within the appropriate waveform regions (windows) and if the critical value is exceeded, then the onset or offset point is considered to have been located. An alternative method proposed in this chapter is the construction of a template to be used on the appropriate spatial velocity or lead data in an attempt to estimate wave onsets and terminations. An early method developed (van Bemmel, Duisterhout, van Herpen et al., 1971) involved the construction of a template through averaging a series of spatial velocity curves from a sample of 500 visually analysed VCGs. The sample points averaged were those preceding and following the visually defined P-onsets of the 500 VCGs. The aim of this template was to facilitate accurate location of the P-onset in routine automated ECG analysis.

6.2 CONSTRUCTION OF GOLD STANDARDS

The aim of using templates was to improve the accuracy of locating the overall onset and offset points of the individual waveforms of an ECG signal. Once again, the CSE multilead measurement database was used for constructing and testing the templates. As in the case of

neural networks, it was necessary to determine fiducial points which represented the 'true reference' as accurately as was possible. A set of the 'true' values for the P, QRS and T wave fiducial points was estimated as follows :

From the CSE database of 125 ECGs, every fifth ECG from the first ECG onwards had the P-onset, P-termination, QRS-onset, QRS-termination and T-end visually estimated by an experienced electrocardiographer. This produced 24 sets of 'true' fiducial points. It was expected that there would be 25 sets of points. However, one ECG was excluded due to the absence of a P-wave (atrial fibrillation). For the remaining 100 ECGs, only the QRS onsets and terminations were visually estimated by the same electrocardiographer. The P- and T-wave fiducial points were then determined as follows using the CSE median program estimates provided with the CSE database for each fiducial point .

If CSE program median QRS onset - CSE program median P onset = X then New P onset = New QRS onset - X .

Here, the new QRS onset was that determined earlier by the electrocardiographer. This procedure was repeated for each ECG. A similar calculation was used to compute the P termination. The T end was calculated as follows :

If CSE program median T end - CSE program median QRS Onset = Y then New T end = New QRS onset + Y.

ECGs which exhibited signs of atrial fibrillation were excluded, leaving 88 out of 100 with 'true' estimates (the Gold standard) for each fiducial point, resulting in a total of 112 visually analysed ECGs (24+88).

6.3 TEMPLATE LOCATION OF THE P ONSET

6.3.1 Training Set

The first step in creating a template was to select a series of ECGs. A total of 24 ECGs was chosen from the 112 gold standard ECGs described above. For consistency, it was thought best to use, as the training set, only those 24 ECGs which had been analysed visually, and the remaining 88, as a test set.

In order to create a template for the location of the P-onset, the visually selected P onset values were used to extract a range of spatial velocity points from the training set ECG data. For each ECG, 10 spatial velocity points (at 2ms intervals) on either side of the 'true' P onset were extracted. The choice of 10 points was somewhat arbitrary. This produced a set of 21 spatial velocities for each of the 24 ECGs. These 24 sets of spatial velocities have been plotted (in μV) in Figures 6.1(a),(b)&(c). At first glance, the choice of some onsets may seem odd. However, it should be noted that each plot is a magnified subset of points taken from the region of the P-wave onset and so the peak of the P-wave will be of much greater amplitude than the range shown in these diagrams. In addition, the ECGs were processed with the inclusion of the new Glasgow smoothing filter discussed in Chapter 3. The data were again extracted and can be seen in Figures 6.2(a),(b)&(c). It is clear when comparing the corresponding plots that the filtered signals are much smoother than the originals. Initial

filtering of the data was performed in the hope that it would improve the performance of the template when compared to the unfiltered case. The 11th point, marked in each plot by a vertical line, represents the 'true' onset of the P-wave as determined by the electrocardiographer (from plots of unsmoothed spatial velocities at lower resolution).

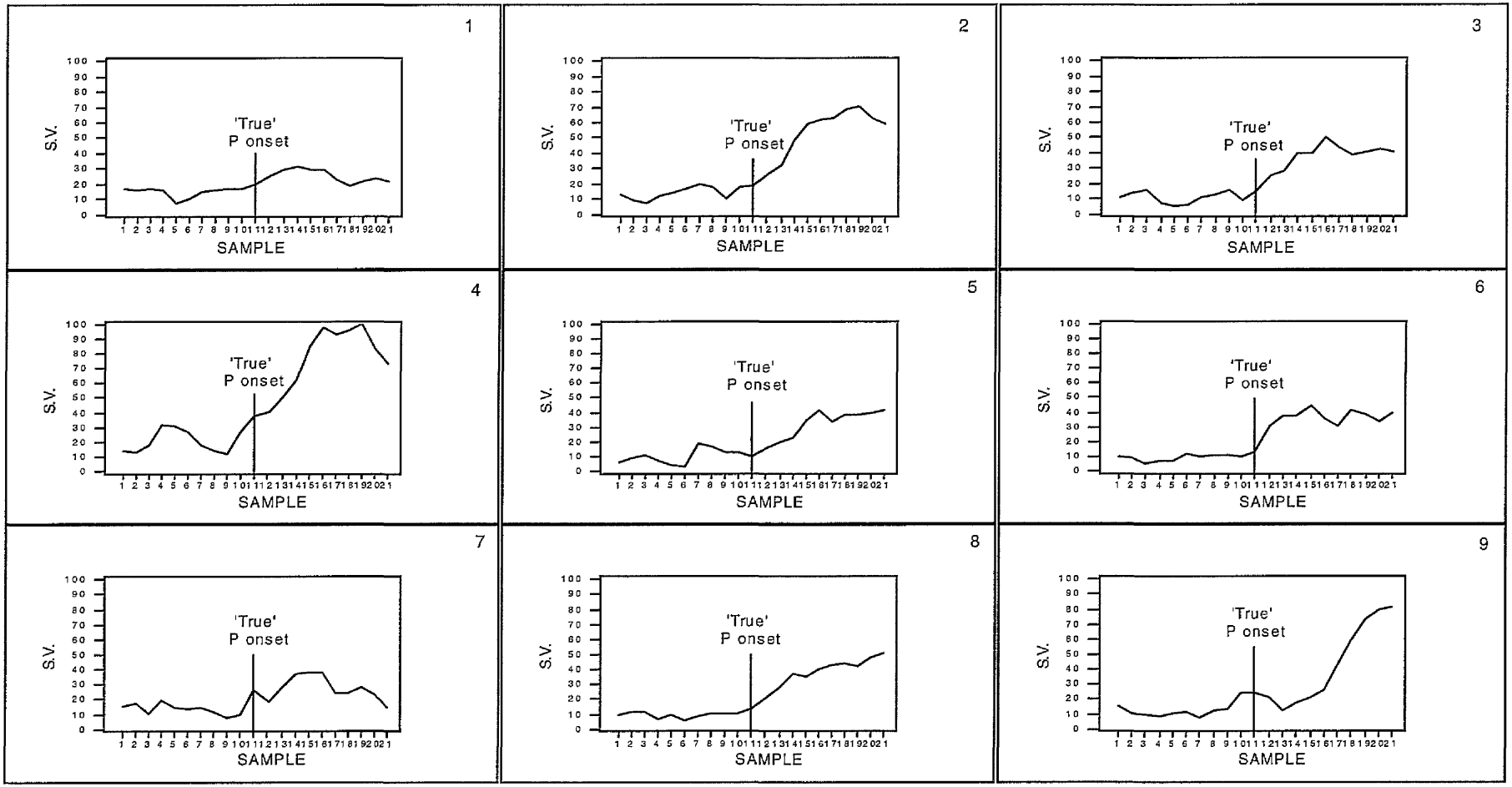

Figure 6.1(a) Subset of P-wave spatial velocity data (μV) used for the construction of a template for the P-onset (ECGs 1-9)

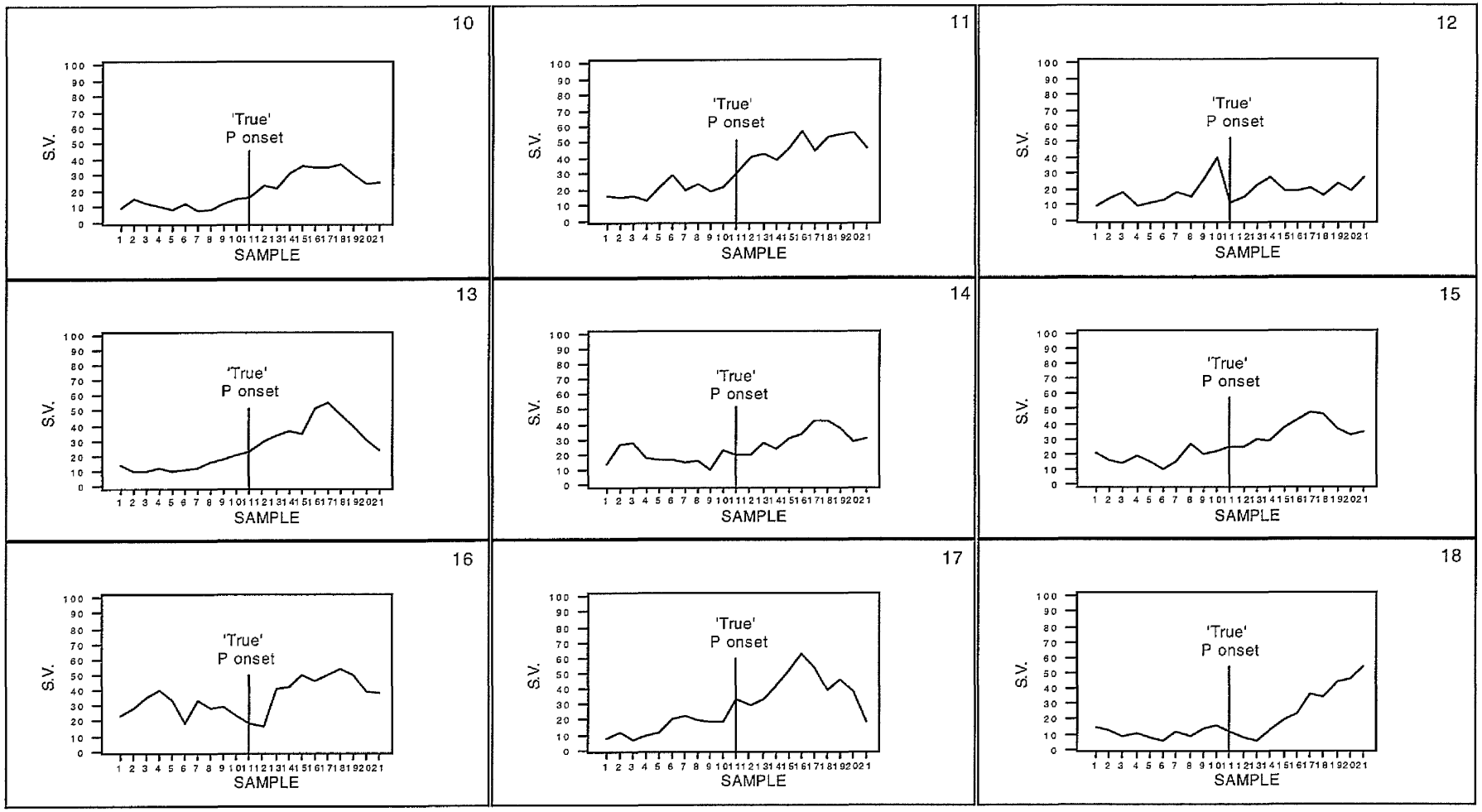

Figure 6.1(b) Subset of P-wave spatial velocity data (μV) used for the construction of a template for the P-onset (ECGs 10-18)

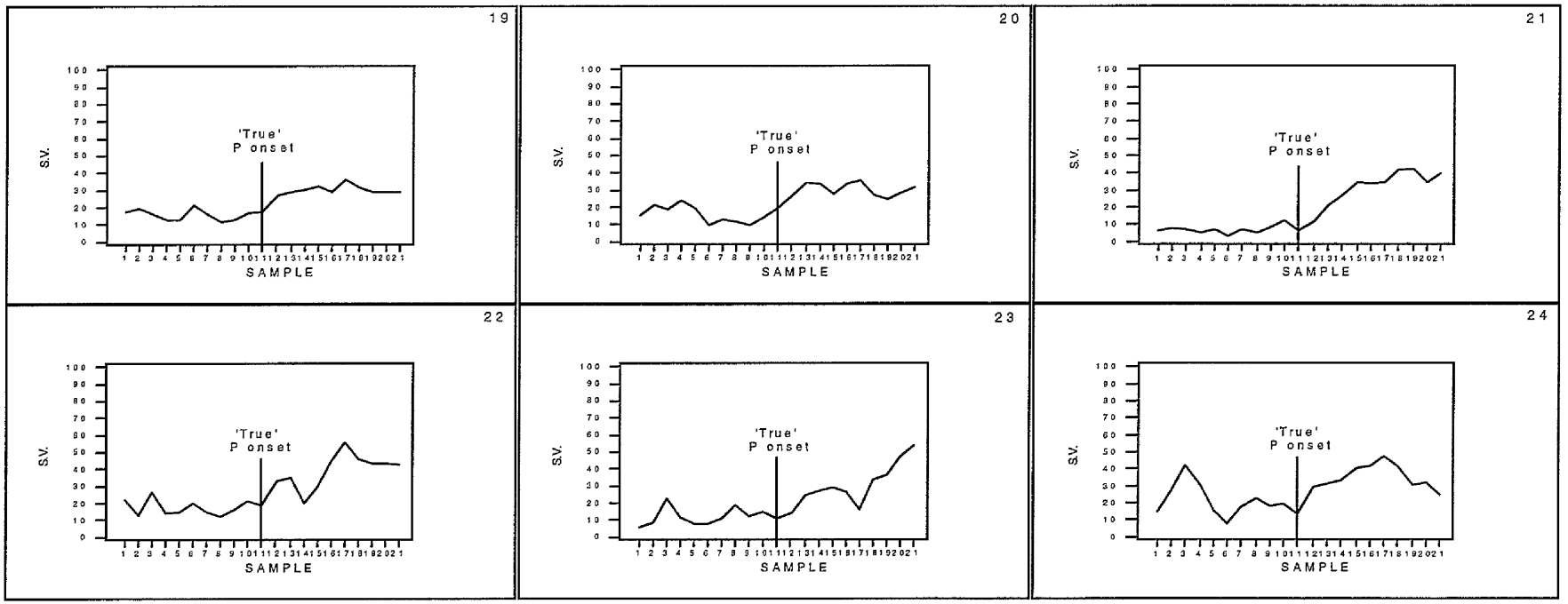

Figure 6.1(c) Subset of P-wave spatial velocity data (μV) used for the construction of a template for the P-onset (ECGs 19-24)

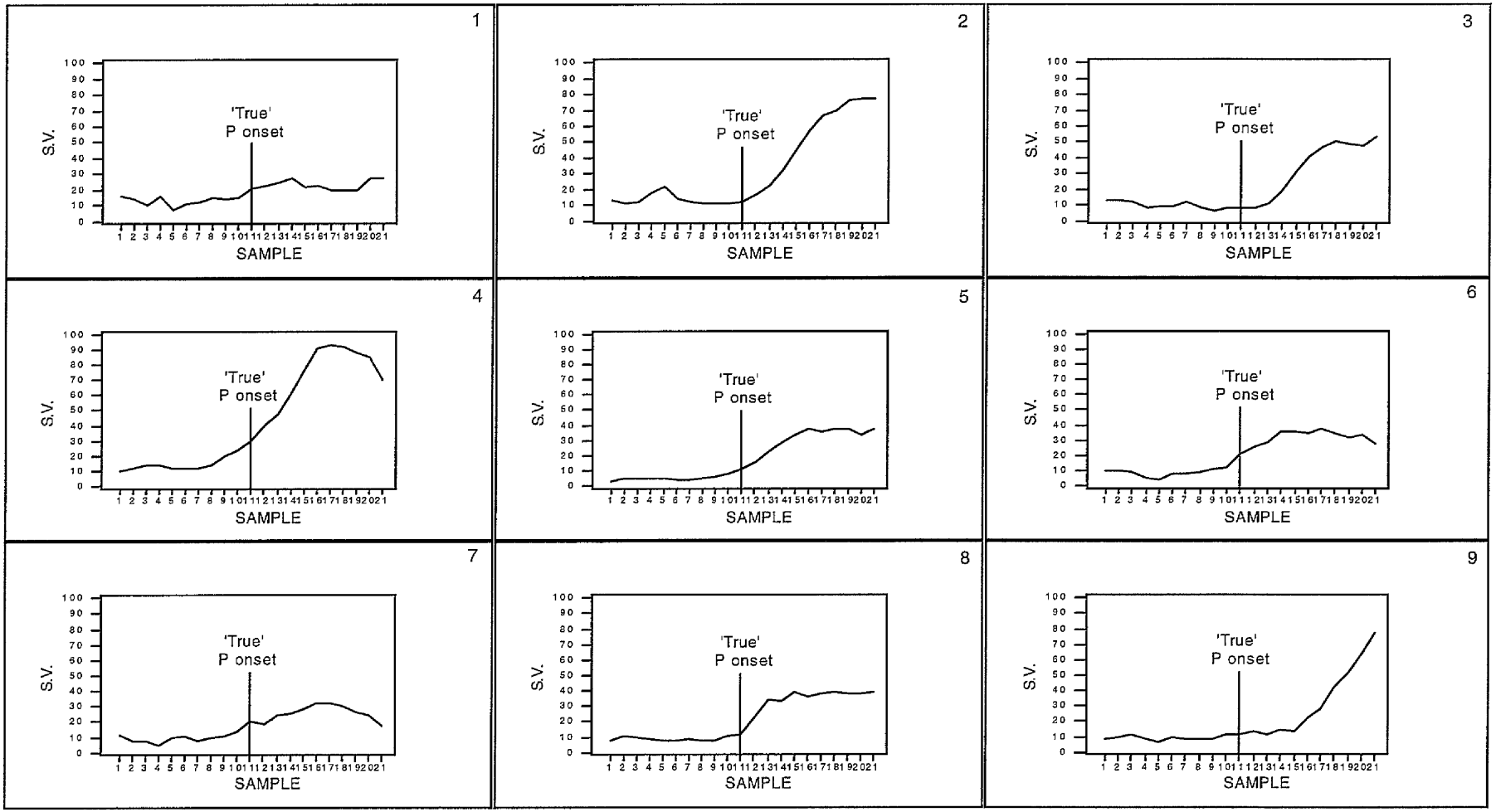

Figure 6.2(a) Subset of filtered P wave spatial velocity data (μV) used for the construction of a template for the P onset (ECGs 1-9)

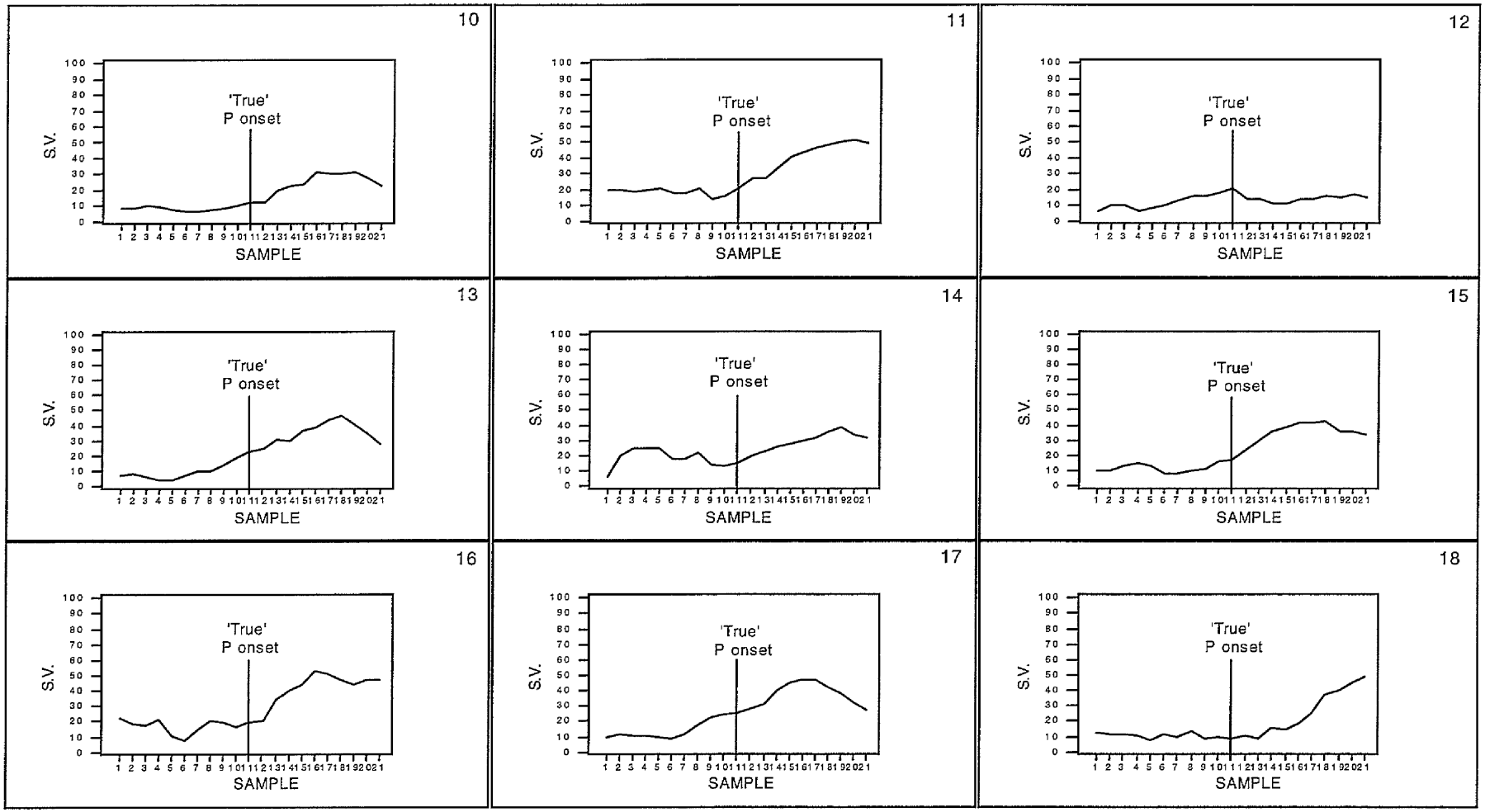

Figure 6.2(b) Subset of filtered P wave spatial velocity data (μV) used for the construction of a template for the P onset (ECGs 10-18)

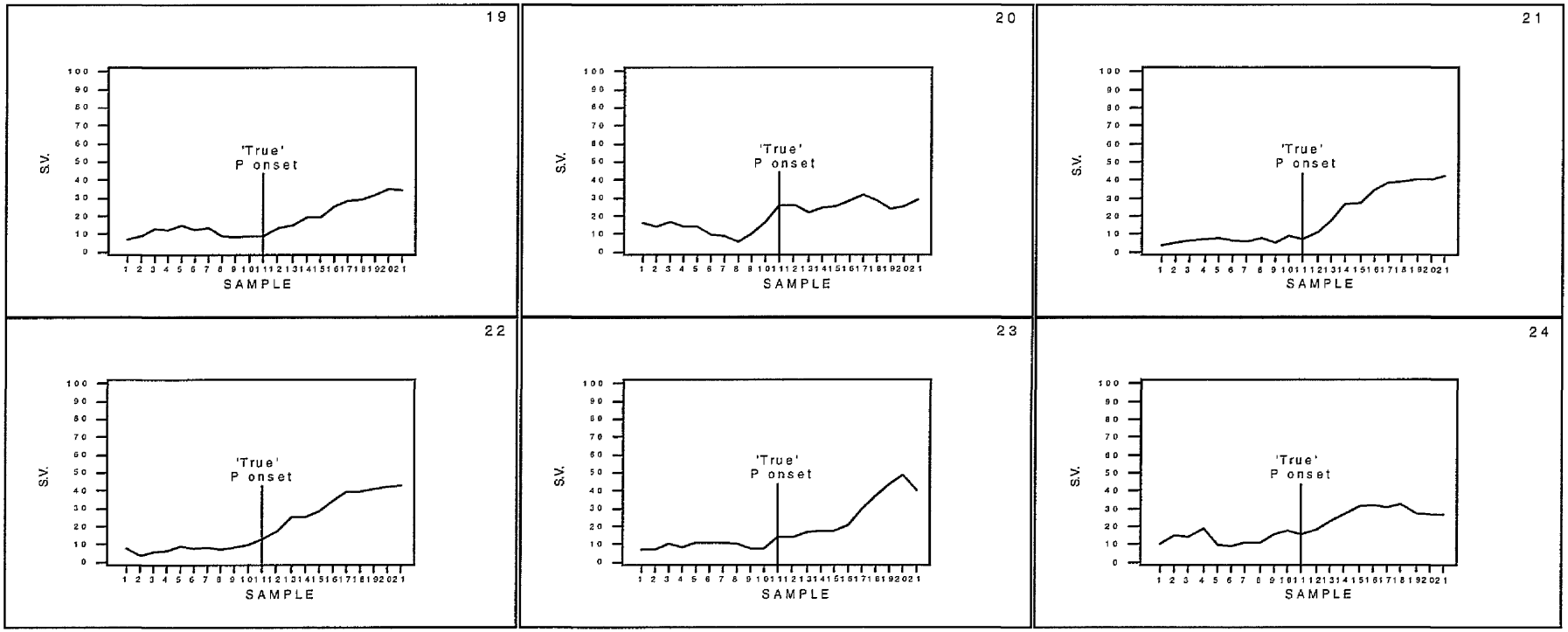

Figure 6.2(c) Subset of filtered P wave spatial velocity data (μV) used for the construction of a template for the P onset (ECGs 19-24)

6.3.2 Design of the Templates

Two versions of possible template were considered in this study. The first was a global template while the second was individualised to the ECG being analysed. Each of the two templates was 'passed' over all the potential P-onset values in a specific search region and a simple sum of squares criterion was used to estimate the 'true' P-onset.

Global Non-Linear Template

The first template was constructed by aligning the 24 ECGs and simply averaging across these for each of the 21 sample points. This formed the required 21 point global non-linear template where the 11th point was the 'true' P onset.

Individualised Linear Template

The second template involved the estimation of individual parameters for the training set. These were the slopes, β_1 and β_2, on either side of the 'true' P-onset and the value of the spatial velocity, α, at the onset (see Figure 6.3). Each onset was approximated by a 'change-point' linear regression where the onset was the change point.

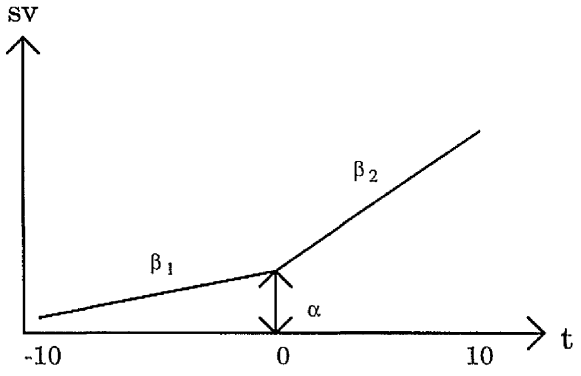

Figure 6.3 Schematic representation of the parameters in an individualised linear template for the P-onset

The scale on the t-axis (i.e. sample point) in Figure 6.3 is numbered -10 to 10 and sv represents the spatial velocity. The true P-onset lies on the point 0 with 10 points on either side of it.

In order to estimate the three parameters, standard least squares was used on the following model

$$\underline{X} = A\underline{\theta} + \underline{\varepsilon} \tag{6.1}$$

where $\underline{X}$ is the set of 21 'observed' spatial velocities and A (21x3 matrix) is as follows

$$A = \begin{bmatrix} 1 & -10 & 0 \\ 1 & -9 & 0 \\ & \vdots & \\ & \vdots & \\ 1 & 0 & 0 \\ 1 & 0 & 1 \\ & \vdots & \\ & \vdots & \\ 1 & 0 & 10 \end{bmatrix}$$

and $\underline{\theta} = \begin{bmatrix} \alpha \\ \beta_1 \\ \beta_2 \end{bmatrix}$ the vector of the unknown parameters α, β_1 and β_2. Also $\underline{\varepsilon}$ is a vector of independent random errors where each $\varepsilon_i \sim N(0,\sigma^2)$.

Based on least squares, parameter estimates were produced for each of the 24 ECG cases. These individual parameter estimates were then investigated as to whether or not they were dependent on certain aspects of each individual's ECG signal, such as heart rate,

approximate estimate for P-duration (determined by the Glasgow program) and the maximum spatial velocity of the P-wave. Each of these variables was thought to be of possible importance in determining the appearance of the P-wave. For example, a high heart rate may produce steeper sloped P-waves; similarly the greater the magnitude of the maximum spatial velocity, the steeper the gradient (β_2) while a long P-duration may suggest a less steep gradient (β_2) following the P-onset compared to a shorter P-duration.

In order to obtain an initial impression, each of the "response variables" $\hat{\alpha}$, $\hat{\beta}_1$ and $\hat{\beta}_2$ was plotted against each of these 3 possible explanatory variables (P-duration, maximum spatial velocity and heart rate). These plots can be seen in Figure 6.4 with the sample correlations between each "parameter estimate" and each "possible explanatory variable". Here HR represents the heart rate for each of the 24 cases and P-Dur, the P-duration. The only clear conclusion from these plots is that there is a strong positive relationship between the "variables" $\hat{\beta}_2$ and MaxSV, the maximum spatial velocity (μV), although $\hat{\beta}_2$ and HR look mildly related.

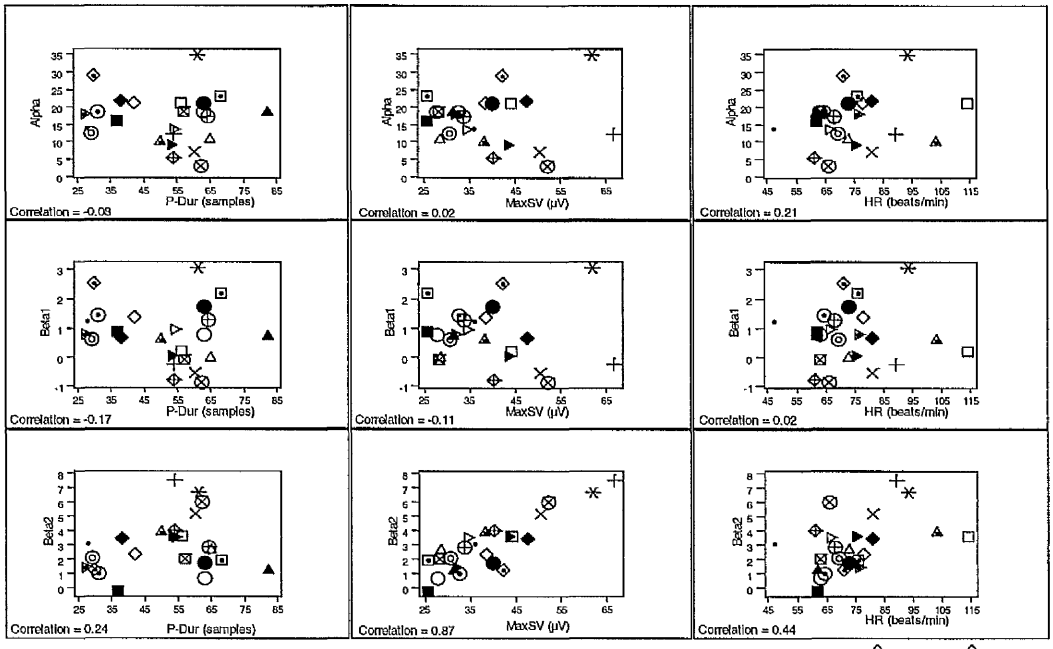

Figure 6.4 **Relationships between the response variables $\hat{\alpha}$, $\hat{\beta}_1$ and $\hat{\beta}_2$ and explanatory variables P-duration (sample points), maximum spatial velocity (µV) and heart rate.**

More formally, each set of "response variables", $\hat{\alpha}$, $\hat{\beta}_1$ and $\hat{\beta}_2$, was assessed for its potential dependency on the possible explanatory variables by means of stepwise variable selection. The results for each response variable are tabulated in Table 6.1(a).

"Response Variable"	Significant Explanatory Variable(s)
$\hat{\alpha}$	None
$\hat{\beta}_1$	None
$\hat{\beta}_2$	Maximum Spatial Velocity

Table 6.1(a) Results of the Stepwise Variable Selection Techniques

The corresponding p-values for the variable selection procedure are presented in Table 6.1(b). The significance of the relationships of the individual response and explanatory variables is presented as well as the relationship between $\hat{\beta}_2$ and P-Dur and $\hat{\beta}_2$ and HR, having corrected for the effect of MaxSV. It is clear that MaxSV has a significant effect on $\hat{\beta}_2$, the slope proceeding the P-onset and that

having corrected for MaxSV, neither P-Dur or HR are significant in the regression model.

Response Variable	P-Dur	MaxSV	HR
$\hat{\alpha}$	p-value= 0.7	p-value = 0.9	p-value = 0.3
$\hat{\beta}_1$	p-value = 0.4	p-value = 0.6	p-value = 0.9
$\hat{\beta}_2$	p-value = 0.3	p-value < 0.001	p-value = 0.03
Corrected for MaxSV	p-value = 0.09	--	p-value = 0.9

Table 6.1(b) Corresponding p-values for the stepwise variable selection procedure.

The only "significant result" in Table 6.1(a) was not surprising since it was understandable that the slope following the P-onset would be influenced by the maximum spatial velocity of the P-wave. To quantify this relationship for test purposes (of future patients), the regression equation was

$$\hat{\beta}_2 = -3.00 + 0.15*\text{MaxSV} + \text{random error} \qquad (6.2)$$

Since there was no relationship between the other two response variables and any of the explanatory variables, the obvious choices for estimates, $\hat{\alpha}$ and $\hat{\beta}_1$, for future use, were the sample means of the corresponding terms for the 24 ECGs in the training set, i.e. "global estimates" for $\hat{\alpha}$ of 16.48 and for $\hat{\beta}_1$ of 0.79 for every future patient.

The following vector of 21 fitted spatial velocity values represented the required template for any future patient :

$$\begin{bmatrix} \hat{\alpha} - 10\hat{\beta}_1 \\ : \\ : \\ \hat{\alpha} - \hat{\beta}_1 \\ \hat{\alpha} \\ \hat{\alpha} + \hat{\beta}_2 \\ : \\ : \\ \hat{\alpha} + 10\hat{\beta}_2 \end{bmatrix}$$

with corresponding estimates based on the above results taking

$$\hat{\alpha} = 16.48, \ \hat{\beta}_1 = 0.79$$

$$\text{and } \hat{\beta}_2 = -3.00 + 0.15*\text{MaxSV} \tag{6.3}$$

where MaxSV is the P-wave maximum spatial velocity of the future patient and so

$$\text{Fit}(\text{MaxSV}) = \begin{bmatrix} 8.58 \\ 9.37 \\ 10.16 \\ 10.95 \\ 11.74 \\ 12.53 \\ 13.32 \\ 14.11 \\ 14.90 \\ 15.69 \\ 16.48 \\ 13.48 + .0.15 * \text{MaxSV} \\ 10.48 + 0.30 * \text{MaxSV} \\ 7.48 + 0.45 * \text{MaxSV} \\ 4.48 + 0.60 * \text{MaxSV} \\ 1.48 + 0.75 * \text{MaxSV} \\ -1.52 + 0.90 * \text{MaxSV} \\ -4.52 + 1.05 * \text{MaxSV} \\ -7.52 + 1.20 * \text{MaxSV} \\ -10.52 + 1.35 * \text{MaxSV} \\ -13.52 + 1.50 * \text{MaxSV} \end{bmatrix}$$

The form of the global non-linear template is depicted in Figure 6.5(a) whereas an example of the individualised template is shown in Figure 6.5(b). A MaxSV equal to 40.2 (an acceptable value for the maximum spatial velocity of a P-wave) was substituted into the above template and the resulting values were plotted. The 11th sample point of each template represents the 'true' P-onset.

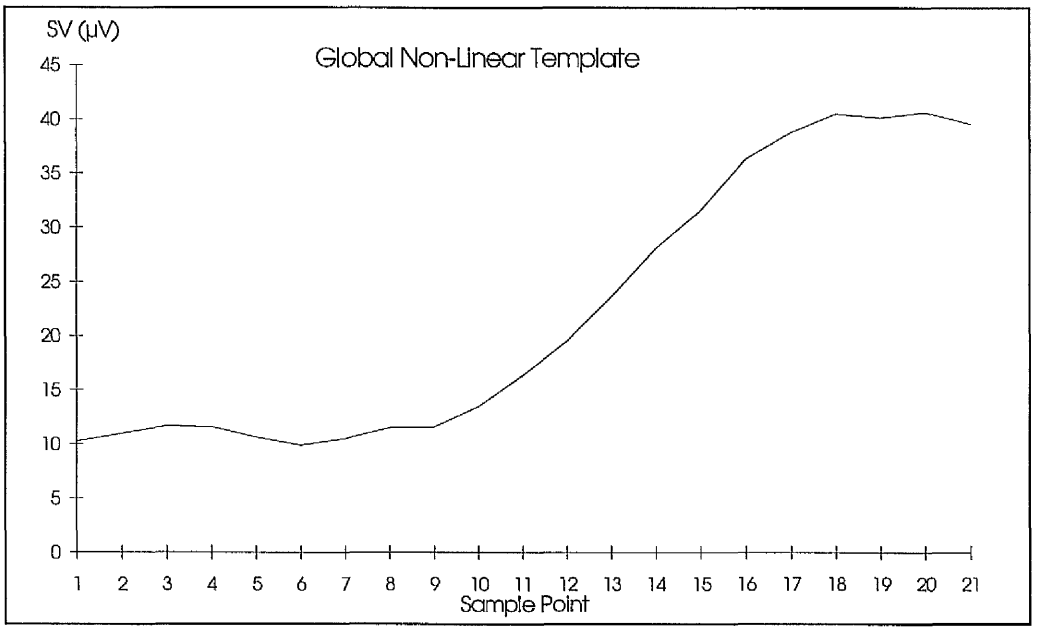

Figure 6.5(a) The Global Non-Linear Template used for P-onset location

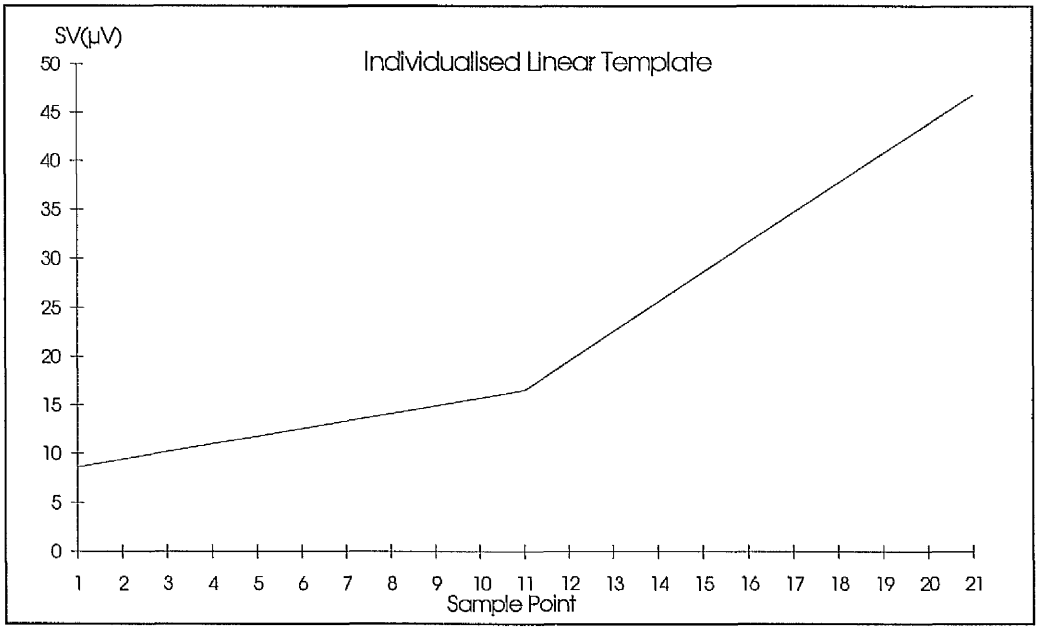

Figure 6.5(b) The Individualised Linear Template used for P-onset Location (MaxSV=40.2μV)

Creation of a Search Region for P-onset Location

In order to assess the performance of the global and individualised templates, they must be applied to an appropriate "search region" of an ECG. It is assumed within the Glasgow program

that the general morphology of a P-wave, in terms of the spatial velocity data, takes the form of an M-shape and so the search region was selected as shown in Figure 6.6, where m samples before and n samples after the first peak of the P-wave spatial velocity (P1) were included.

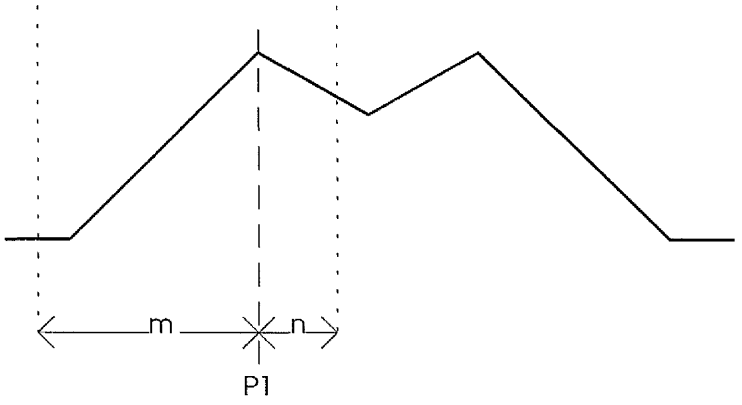

Figure 6.6 Demonstration of the selection of the search region for P-onset location

The search region therefore consisted of m+n samples. Initially m was assigned to be 40. However if the location of the peak lay too close to the beginning of the record resulting in P1-m<1 then the starting point of the search region was assigned to be the first sample point. The value of n was arbitrarily fixed to be 10. The onset was therefore located as follows :

Let t be a sample point in the chosen "search region", i.e. $t=sp_1,sp_2,.....,sp_{50}$, where

sp_1=sample point 1 in the search region

sp_2=sample point 2 in the search region

.

.

sp_{50}=sample point 50 in the search region

Also, let $SV_i(t)$ be the spatial velocity at the point t+i (for i=0,...,20 and $t=sp_1,...,sp_{50}$) for the j^{th} patient (j=1,...,n, where n is the total number of patients in a test set). Moreover, the true onset is represented by the point i=10.

Then for each patient define

$$SS_j(t) = \sum_{i=0}^{20} (SV_i(t) - Fit_i(MaxSV_j))^2 \qquad (6.4)$$

where $MaxSV_j$ is the maximum spatial velocity for the P-wave of the j^{th} patient and Fit_i are the elements of $Fit(MaxSV_j)$.

The P-onset for the j^{th} patient is then estimated as $\hat{Pt}_j+10$ (since the onset is located 10 sample points from the beginning of the template), by minimising $SS_j(t)$ over t in the defined search region, i.e.

$$SS_j(\hat{Pt}_j) = \min_{sp_1 \le t \le sp_{50}} SS_j(t) \qquad (6.5)$$

6.3.3 Results for P-Onset Template Estimation

The test set consisted of the remaining 88 CSE ECGs from the multilead measurement reference library. All 88 ECGs were analysed first by using the global template and then by the individualised template (incorporated into the Glasgow program). The two sets of templates constructed using the unfiltered data and corresponding filtered data (using the Glasgow smoothing filter) were passed over unfiltered and filtered ECG data, respectively. All the results were

compared to the 'true' reference results determined previously (see section 6.2), by taking the corresponding differences in fiducial points. Tables 6.2(a) and 6.2(b) summarise the results for both non-filtered and filtered cases respectively. Results for the conventional program, unfiltered and filtered (using the Glasgow smoothing filter) have also been included in order to compare any improvements through the use of the templates.

Statistics	GP	GT	IT
$\sum_{1}^{88}(\text{Diff})^2/88$	38.63	47.95	51.31
Median	2.00	1.00	0.00
S.D.	5.17	6.92	7.20
U.Q.	5.75	3.00	2.00
L.Q.	0.00	-2.00	-2.75

Table 6.2(a) **Summary statistics (including the mean sum of squares) for the P-onset difference (estimated-true in sample points) determined by the conventional Glasgow Program, global template and individualised template - unfiltered data.**
GP=Conventional Glasgow Program,
GT=Global Template, IT=Individualised Template
S.D. = standard deviation
U.Q. = upper quartile and L.Q. = lower quartile

Statistics	GSF	GT	IT
$\sum_{1}^{88}(\text{Diff})^2/88$	44.94	28.16	22.42
Median	3.00	0.00	0.00
S.D.	5.50	5.32	4.71
U.Q.	5.00	3.00	3.00
L.Q.	1.00	-2.00	-1.00

Table 6.2(b) **Summary statistics (including the mean sum of squares) for the P-onset difference (estimated-true)**
GSF=Glasgow Program & Glasgow smoothing filter
GT=Global Template, IT=Individualised Template
S.D. = Standard Deviation
U.Q. = upper quartile and L.Q. = lower quartile

When observing both tables, it is apparent that the individualised template on the filtered data performs best. From Table 6.2(b) it is seen that the median difference for both templates is zero, implying the absence of a bias. This is illustrated in Figure 6.7, where the last two boxplots in the diagram represent the results obtained using the filtered templates. Figure 6.7 also highlights that there is a clear bias present when using the conventional Glasgow program and the Glasgow smoothing filter. Both versions of the Glasgow program seem to produce later P onsets in comparison to the 'true' onsets. However for both cases (unfiltered and filtered), the bias is eliminated when the individualised template is used. Table 6.3 summarises the total number of P-onsets located accurately by each method relative to the 'true' values. It is seen that the individualised template locates more P-onsets than any of the other methods.

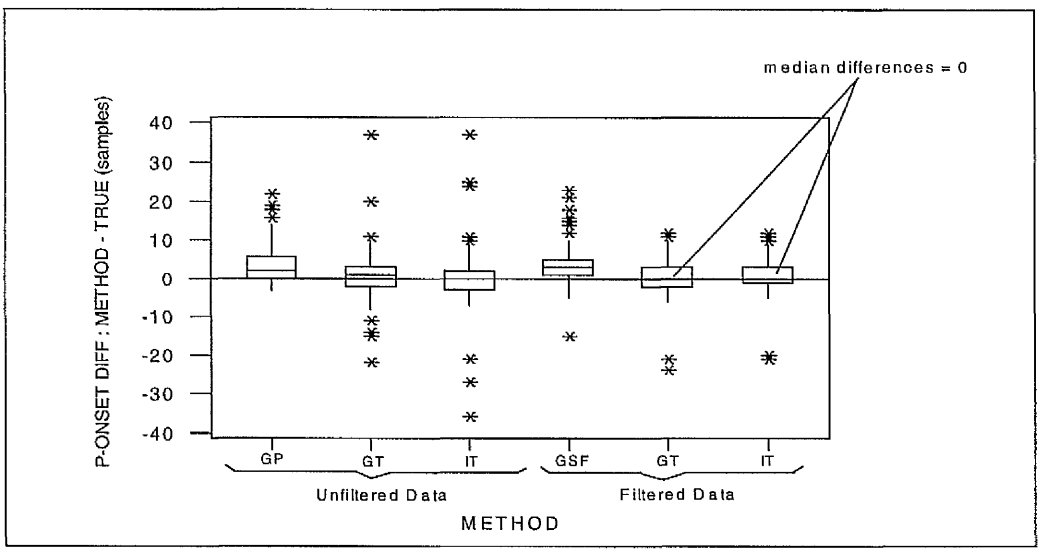

Figure 6.7 **Performance of the Glasgow Program (GP), Glasgow smoothing Filter (GSF), Global Template (GT) and Individualised Template (IT) when estimating the P-Onset for unfiltered and filtered data.**

Statistic	CGP	GSF	GT	IT
# Correctly Estimated	10	6	9	16

Table 6.3 Number of P onsets correctly located (n=88)

6.4 TEMPLATE LOCATION OF THE P-OFFSET

6.4.1 Training Set

Since the procedure using the individualised template, constructed using the Glasgow smoothing filter data, provided the best estimates of the P-onset, it was decided to use this procedure for the remaining fiducial points. In order to estimate an appropriate template for the offset of the P-wave, 21 spatial velocity points around the referee-determined P-offset were extracted for the same 24 ECGs as before. The resulting data are presented in Figures 6.8(a),(b)&(c). As with the P-onset, some of the choices for the 'true' P-offsets may seem somewhat unlikely, but this is again due to the magnification of the region surrounding the "true" offset being "small" compared to the P-wave magnitude itself.

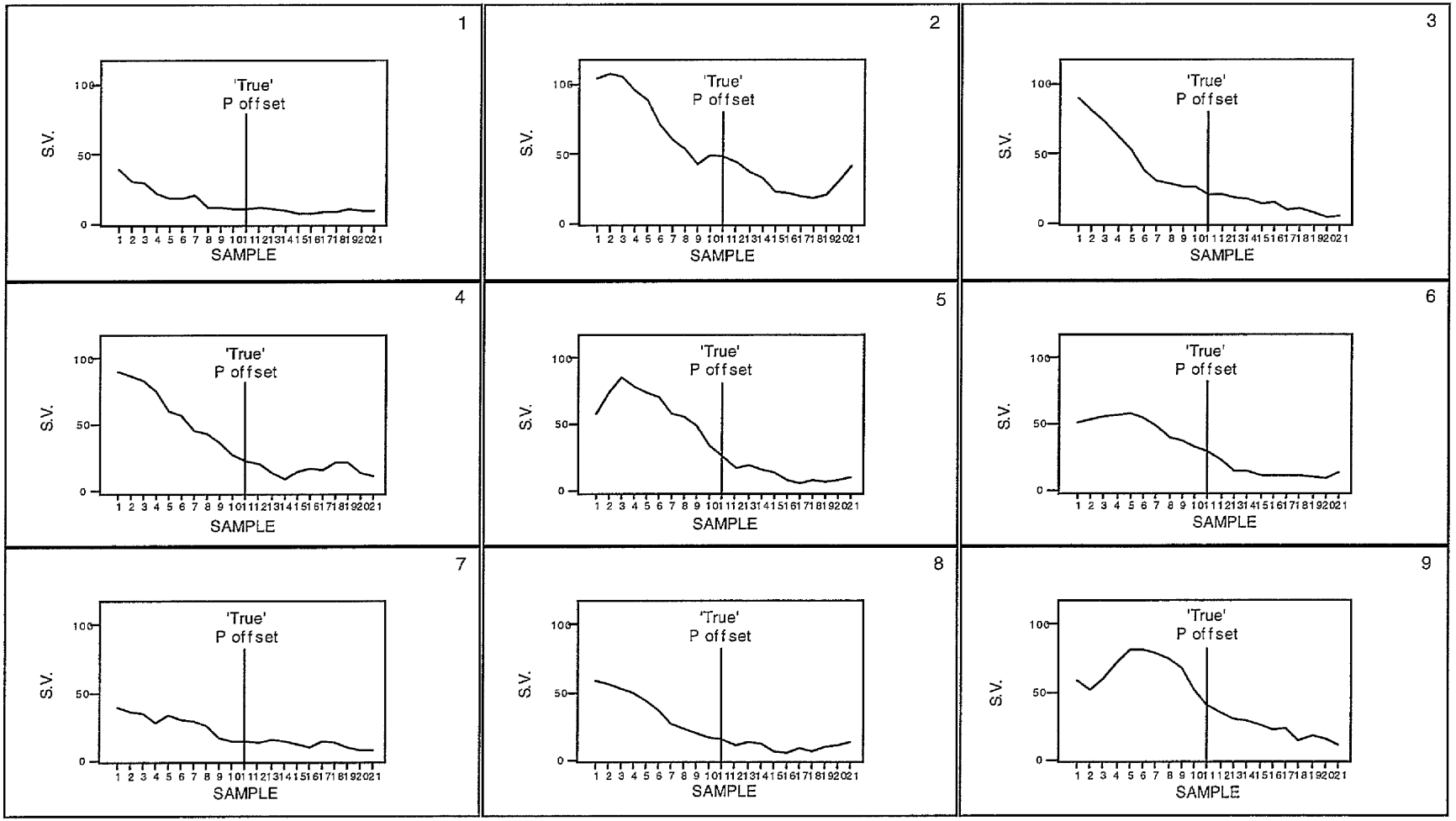

Figure 6.8(a) Subset of filtered P wave spatial velocity data (μV) used for the construction of a template for the P offset(ECGs 1-9)

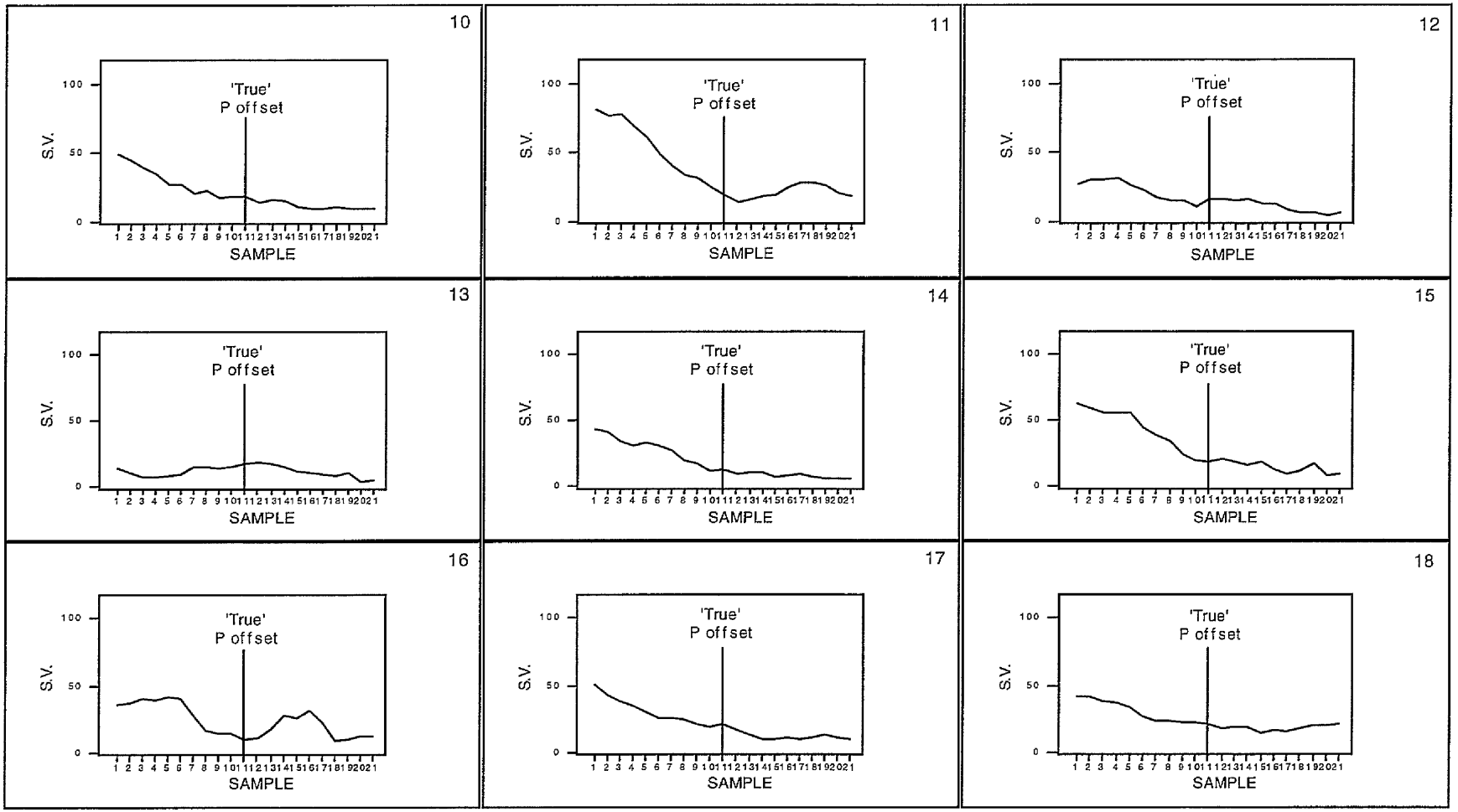

Figure 6.8(b) Subset of filtered P wave spatial velocity data (μV) used for the construction of a template for the P offset(ECGs 10-18)

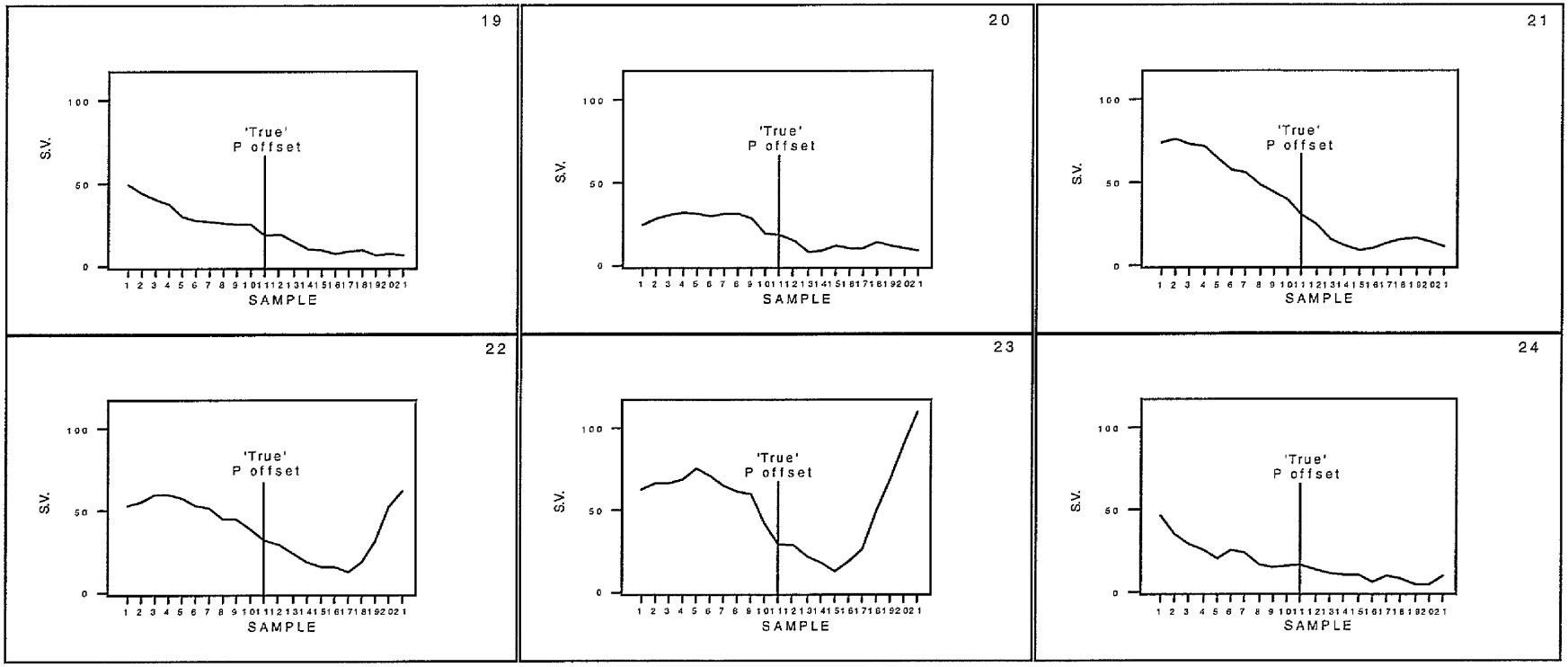

Figure 6.8(c) Subset of filtered P wave spatial velocity data (μV) used for the construction of a template for the P offset(ECGs 19-24)

6.4.2 Construction of the Templates

As with the P-onset, global and individualised templates were constructed using the same procedure described in section 6.3.2.

In the case of the individualised linear template, by using methods of standard least squares as in section 6.3.2, it was possible to determine estimates for α, β_1 and β_2 for each of the 24 ECGs in the training set (see Figure 6.9). Each "response variable", $\hat{\alpha}$, $\hat{\beta}_1$ and $\hat{\beta}_2$ was then plotted against each of the explanatory variables, P-duration, maximum spatial velocity and heart rate (Figure 6.10).

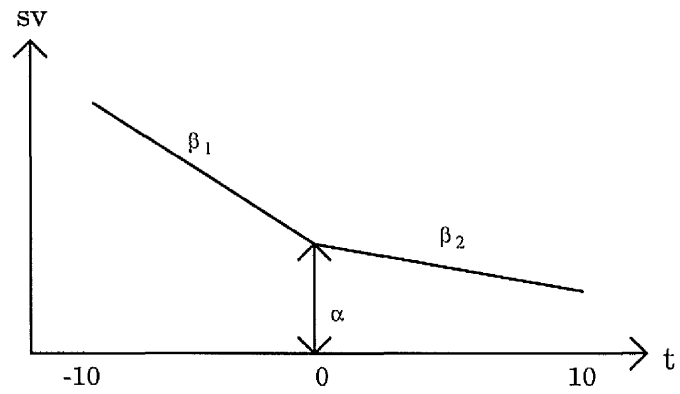

Figure 6.9 Schematic representation of the parameters in an individualised linear template for the P-offset

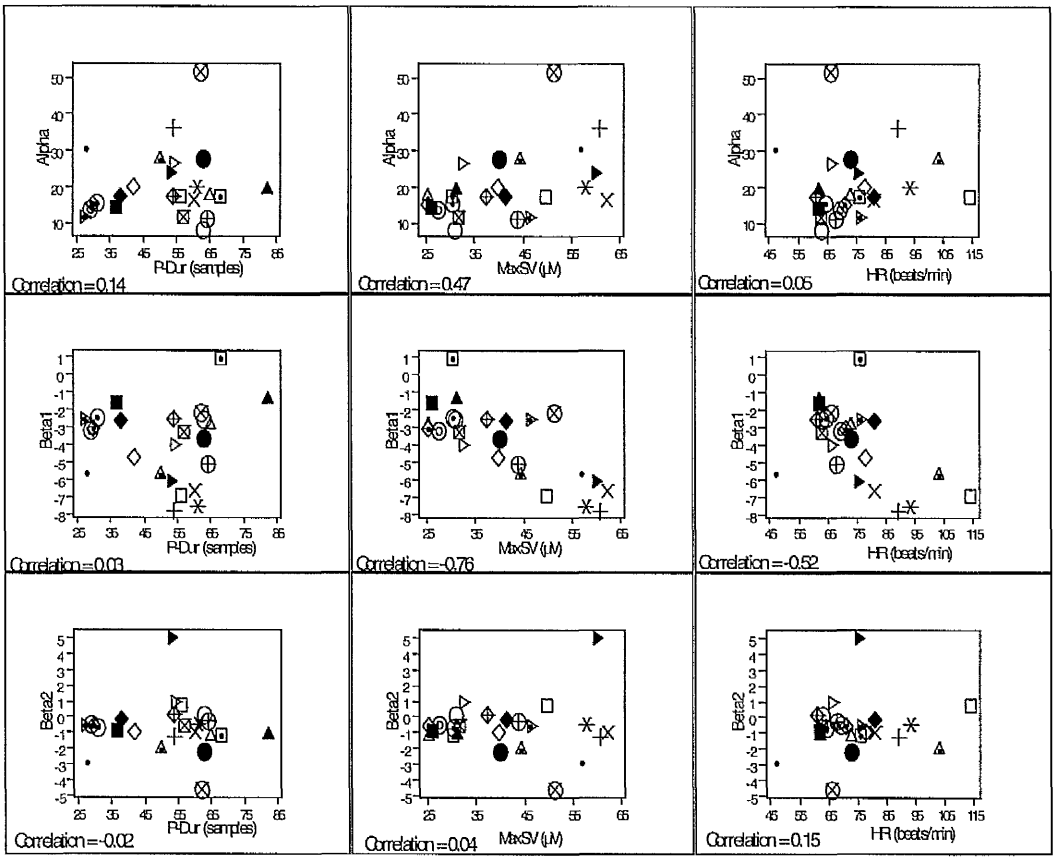

Figure 6.10 **Relationships between the response variables $\hat{\alpha}$, $\hat{\beta}_1$ and $\hat{\beta}_2$ and explanatory variables P-duration, maximum spatial velocity and heart rate.**

From Figure 6.10, there appears to be reasonably strong negative relationships between $\hat{\beta}_1$ and both the maximum spatial velocity of the P-wave and the heart rate. This implies that as the value of the maximum spatial velocity and heart rate increases the corresponding slope preceding the P-offset increases. There also appears to be a positive relationship between $\hat{\alpha}$ and the maximum spatial velocity.

Once again, stepwise variable selection techniques were used to investigate the dependency of each of the three "response variables" on the potential explanatory variables. The results are presented in Table 6.4(a).

Response Variable	Significant Explanatory Variable(s)
$\hat{\alpha}$	Maximum Spatial Velocity
$\hat{\beta}_1$	Maximum Spatial Velocity
$\hat{\beta}_2$	None

Table 6.4(a) Results of the Stepwise Variable Selection Techniques

Table 6.4(b) contains the respective p-values for the stepwise selection technique. From the individual correlations, it can be seen that $\hat{\alpha}$ is dependent on MaxSV. The other individual significant relationships are between $\hat{\beta}_1$ and MaxSV and $\hat{\beta}_1$ and HR. However, it can be seen that after having corrected for MaxSV, HR become marginally non-significant, leaving MaxSV as the only significant variable.

Response Variable	P-Dur	MaxSV	HR
$\hat{\alpha}$	p-value= 0.5	p-value= 0.02	p-value= 0.8
Corrected for MaxSV	p-value= 0.6	--	p-value= 0.5
$\hat{\beta}_1$	p-value= 0.9	p-value < 0.001	p-value= 0.009
Corrected for MasSV	p-value= 0.6	--	p-value= 0.06
$\hat{\beta}_2$	p-value= 0.9	p-value= 0.8	p-value= 0.5

Table 6.4(b) Corresponding p-values for the stepwise variable selection procedure.

These results suggest that the spatial velocity at the true P-offset and the slope preceding the P-offset are both related to the maximum spatial velocity of the P-wave. Although there was a suggestion that this slope was also dependent on the heart rate, the variable selection procedures showed that the effect of heart rate on $\hat{\beta}_1$ proved non-significant when corrected for maximum spatial velocity.

The following equations represent the fitted relationships :

$$\hat{\alpha} = 5.37 + 0.36*\text{MaxSV} \quad (6.6)$$

$$\hat{\beta}_1 = 1.57 - 0.13*\text{MaxSV} \quad (6.7)$$

A "global estimate" for β_2 was obtained by taking the sample mean of the corresponding term for the 24 ECGs in the training set, i.e. $\hat{\beta}_2$=-0.69. The resulting template for the P-offset was therefore estimated as :

$$\text{Fit}(\text{MaxSV}) = \begin{bmatrix} -10.33 + 1.66 * \text{MaxSV} \\ -8.76 + 1.53 * \text{MaxSV} \\ -7.19 + 1.40 * \text{MaxSV} \\ -5.62 + 1.27 * \text{MaxSV} \\ -4.05 + 1.14 * \text{MaxSV} \\ -2.48 + 1.01 * \text{MaxSV} \\ -0.91 + 0.88 * \text{MaxSV} \\ 0.66 + 0.75 * \text{MaxSV} \\ 2.23 + 0.62 * \text{MaxSV} \\ 3.80 + 0.49 * \text{MaxSV} \\ 5.37 + 0.36 * \text{MaxSV} \\ 4.68 + .0.36 * \text{MaxSV} \\ 3.99 + 0.36 * \text{MaxSV} \\ 3.30 + 0.36 * \text{MaxSV} \\ 2.61 + 0.36 * \text{MaxSV} \\ 1.92 + 0.36 * \text{MaxSV} \\ 1.23 + 0.36 * \text{MaxSV} \\ 0.54 + 0.36 * \text{MaxSV} \\ -0.15 + 0.36 * \text{MaxSV} \\ -0.84 + 0.36 * \text{MaxSV} \\ -1.53 + 0.36 * \text{MaxSV} \end{bmatrix}$$

Creation of a Search Region for P-offset Location

As in the case of the P-onset, to assess the performance of the global and individualised templates, it was necessary to apply them to an

appropriate search region of and ECG. The search region used is shown in Figure 6.11. The size of the search region was such, that it was wide enough to cover all potential offset points. As in section 6.3.2, the corresponding sum of squares functions were computed for each of the two templates and the P-offsets were considered to be located when this function was minimised for each ECG.

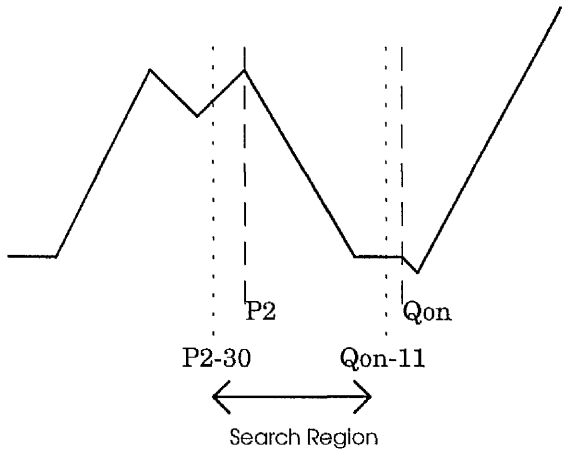

Figure 6.11 Demonstration of the selection of the search region for P-offset location - P2 = Peak2 and Qon = QRS onset.

6.4.3 Results for P-Offset Template Estimation

Both the global and individualised templates were tested on the same 88 ECGs as in the previous case. All the lead data were filtered initially using the Glasgow smoothing filter. Differences (in samples points) between the estimated and 'true' P-offsets were computed, for both templates, conventional Glasgow program and Glasgow smoothing filter. The results are summarised in Table 6.5, from which it is clear that the program incorporating the Glasgow smoothing filter seems to perform best, with the median difference being 1 sample point (i.e. 2 milliseconds). Although this indicates the presence of a slight

positive bias, such biases appear in all the other methods. This can be seen more clearly in Figure 6.12. All four of the methods used, produce estimates of the P-offset slightly later than the 'true' P-offset. The number of P-offsets correctly located by each method is given in Table 6.6. It appears that the conventional program, Glasgow smoothing filter and the program incorporating the individualised template locate approximately the same number of P-offsets correctly but the global template performs less well.

Statistics	GP	GSF	GT	IT
$\sum_{1}^{88} (\text{Diff})^2 / 88$	36.75	19.11	25.70	21.51
Median	2.00	1.00	2.00	2.00
S.D.	5.48	4.14	4.90	4.07
U.Q.	4.75	3.00	4.00	4.00
L.Q.	0.00	-1.00	0.00	0.00

Table 6.5 **Summary statistics (including the mean sum of squares) for the P-offset difference (estimated-true). GP=Glasgow Program; GSF=Glasgow Program & Glasgow smoothing filter; GT=Global Template, IT=Individualised Template S.D. = standard deviation U.Q. = upper quartile and L.Q. = lower quartile**

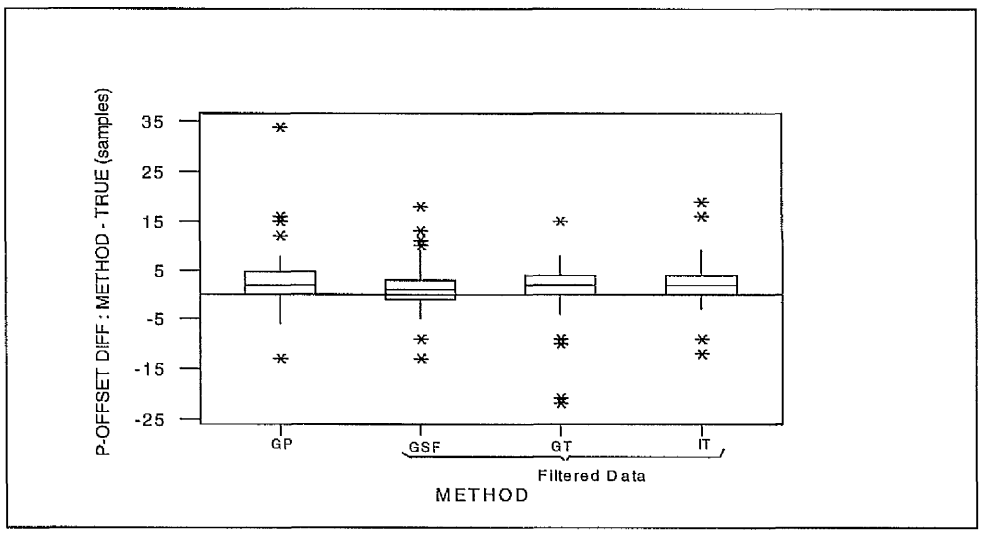

Figure 6.12 **Performance of the Glasgow Program (GP), Glasgow smoothing Filter (GSF), Global Template (GT) and Individualised Template (IT) when estimating the P-Offset.**

Statistic	GP	GSF	GT	IT
# Correctly Estimated	11	10	5	11

Table 6.6 Number of P offsets correctly located (n=88)

6.5 TEMPLATE LOCATION OF THE QRS-ONSET

6.5.1 Construction of the Templates

As before, 10 spatial velocity points were extracted from both sides of the "true" QRS-onset (Glasgow smoothing filter data) for the 24 training set ECGs. These are shown in Figures 6.13(a),(b)&(c).

A non-linear global template and individualised linear template was once again constructed. In the case of the individualised template dependency of the 24 sets of estimates, $\hat{\alpha}$, $\hat{\beta}_1$ and $\hat{\beta}_2$ on the potential explanatory variables: heart rate, an approximate estimate for the QRS-duration determined by the Glasgow Program (sample points) and maximum spatial velocity (μV) of the QRS complex, was assessed by stepwise variable selection techniques. A plot of each of the three parameters against each explanatory variable can be seen in Figure 6.14 while the results from the stepwise variable selection techniques are presented in Table 6.7(a).

A significant relationship between the gradient of the line ***preceding*** the QRS onset, $\hat{\beta}_1$, and the maximum spatial velocity of the QRS complex was found. However the significance of this relationship appears due to one outlier (see Figure 6.14). In fact, if the outlier were to be excluded, then the effect of MaxSV on the response variable would be non-significant. However, the outlier had to be kept in the data set. It will be seen later that the global template does not perform any worse than the individualised template suggesting that MaxSV

should to be excluded from the final model for the linear template. There was however, no significant relationship between the gradient of the slope following the QRS onset, $\hat{\beta}_2$, and the maximum spatial velocity, as in the case of the P-onset. A significant relationship between $\hat{\alpha}$, the spatial velocity at the QRS onset and the maximum spatial velocity was also discovered from the stepwise approach, once again most likely heavily influenced by the presence of the 'outlier'.

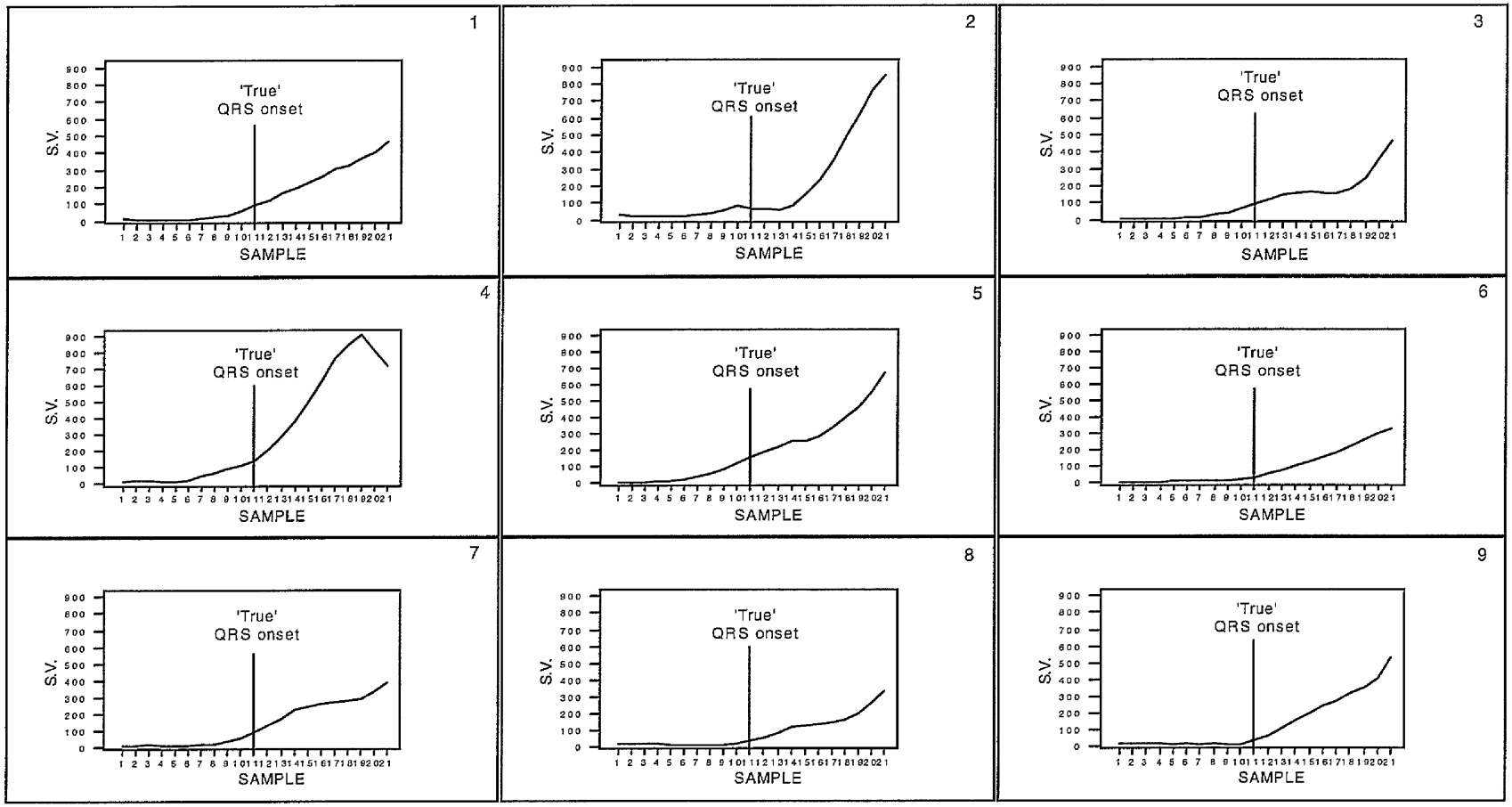

Figure 6.13(a)Subset of QRS-complex spatial velocity data (μV) used for the construction of a template for the QRS-onset (ECGs 1-9)

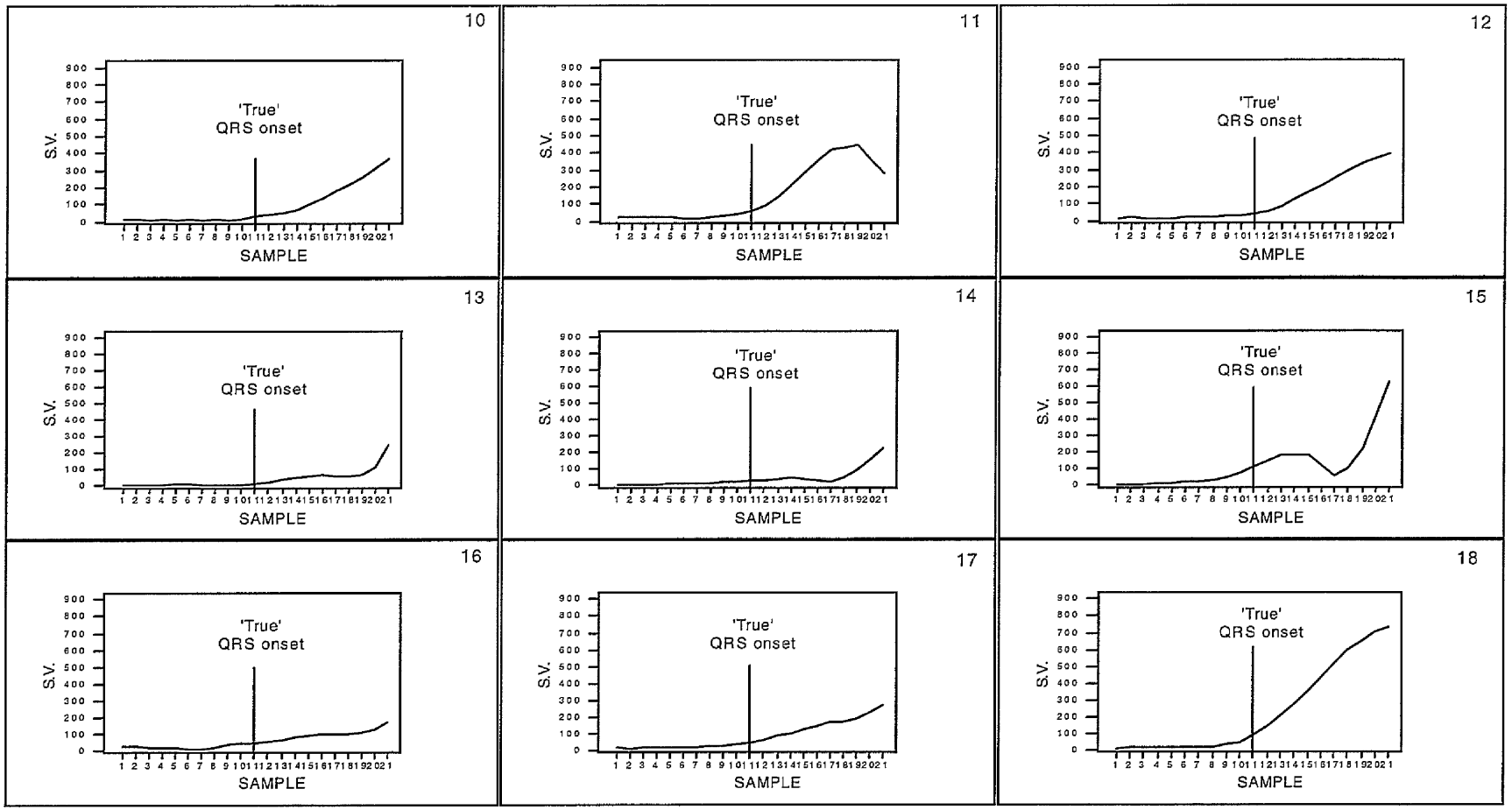

Figure 6.13(b) Subset of QRS-complex spatial velocity data used (μV) for the construction of a template for the QRS-onset (ECGs 10-18)

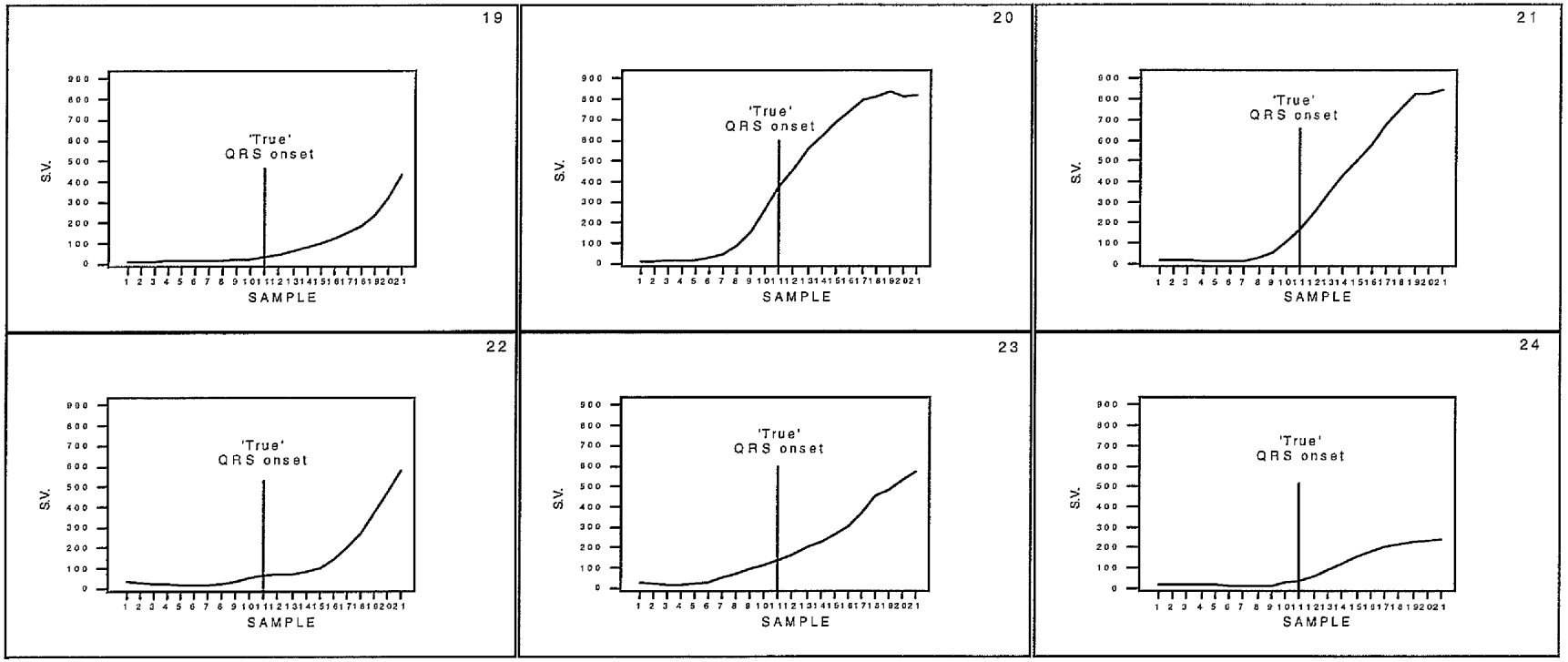

Figure 6.13(c) Subset of QRS-complex spatial velocity data (μV) used for the construction of a template for the QRS-onset (E CGs 19-24)

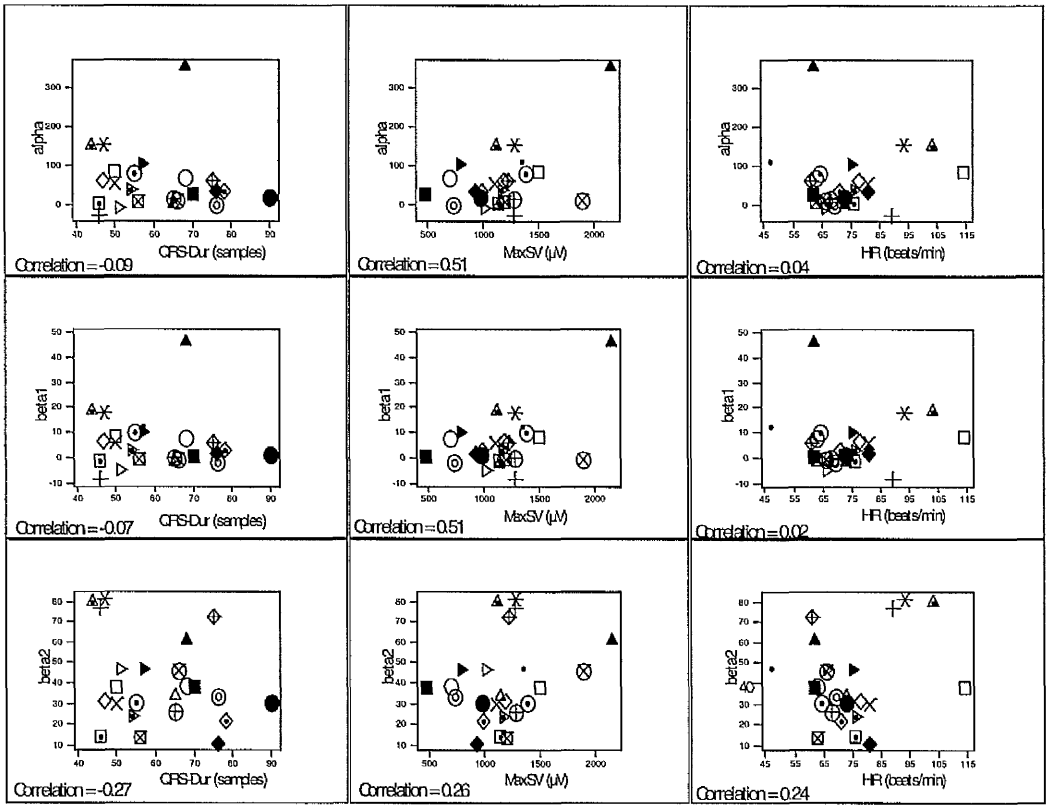

Figure 6.14 **Relationships between the response variables $\hat{\alpha}$, $\hat{\beta}_1$ and $\hat{\beta}_2$ and explanatory variables QRS-duration, maximum spatial and heart rate.**

Response Variable	Significant Explanatory Variable(s)
$\hat{\alpha}$	Maximum Spatial Velocity
$\hat{\beta}_1$	Maximum Spatial Velocity
$\hat{\beta}_2$	None

Table 6.7(a) **Results of the Stepwise Variable Selection Techniques**

The p-values in Table 6.7(b) support the outcome of the stepwise selection procedure. Clearly $\hat{\alpha}$ and $\hat{\beta}_1$ were dependent only on MaxSV and, after adjusting for MaxSV, no other variable was significant.

Response Variable	QRS-Dur	MaxSV	HR
$\hat{\alpha}$	p-value= 0.7	p-value= 0.01	p-value= 0.8
Corrected for MaxSV	p-value= 0.9	--	p-value= 0.9
$\hat{\beta}_1$	p-value= 0.8	p-value = 0.01	p-value= 0.9
Corrected for MaxSV	p-value= 0.8	--	p-value= 0.9
$\hat{\beta}_2$	p-value= 0.2	p-value= 0.2	p-value= 0.3

Table 6.7(b) Corresponding p-values for the stepwise variable selection procedure.

As a result the regression equations were:

$$\hat{\alpha} = -72.96 + 0.11*\text{MaxSV} \quad (6.8)$$

$$\hat{\beta}_1 = -11.84 + 0.015*\text{MaxSV} \quad (6.9)$$

By taking $\hat{\beta}_2$ as the sample mean of the corresponding terms for the 24 ECGs in the training set. i.e. $\hat{\beta}_2 = 40.37$, the resulting individualised 21-point template was

$$\text{Fit}(\text{MaxSV}) = \begin{bmatrix} 45.44 - 0.037 * \text{MaxSV} \\ 33.60 - 0.022 * \text{MaxSV} \\ 21.76 - 0.0070 * \text{MaxSV} \\ 9.92 + 0.0080 * \text{MaxSV} \\ -1.92 + 0.023 * \text{MaxSV} \\ -13.76 + 0.038 * \text{MaxSV} \\ -25.60 + 0.053 * \text{MaxSV} \\ -37.44 + 0.068 * \text{MaxSV} \\ -49.28 + 0.083 * \text{MaxSV} \\ -61.12 + 0.098 * \text{MaxSV} \\ -72.96 + 0.113 * \text{MaxSV} \\ -32.59 + 0.113 * \text{MaxSV} \\ 7.78 + 0.113 * \text{MaxSV} \\ 48.15 + 0.113 * \text{MaxSV} \\ 88.52 + 0.113 * \text{MaxSV} \\ 128.89 + 0.113 * \text{MaxSV} \\ 169.26 + 0.113 * \text{MaxSV} \\ 209.63 + 0.113 * \text{MaxSV} \\ 250.00 + 0.113 * \text{MaxSV} \\ 290.37 + 0.113 * \text{MaxSV} \\ 330.74 + 0.113 * \text{MaxSV} \end{bmatrix}$$

Creation of a Search Region for QRS-onset Location

The search region for the QRS-onset consisted of the subset of points illustrated in Figure 6.15 where a schematic representation of a QRS complex has been depicted. The approximate QRS-onset shown in Figure 6.15 was determined by the Glasgow program. Once again, the QRS-onset for each of the 88 ECGs was considered located once the sum of squares function for each ECG was minimised (see section 6.3.2).

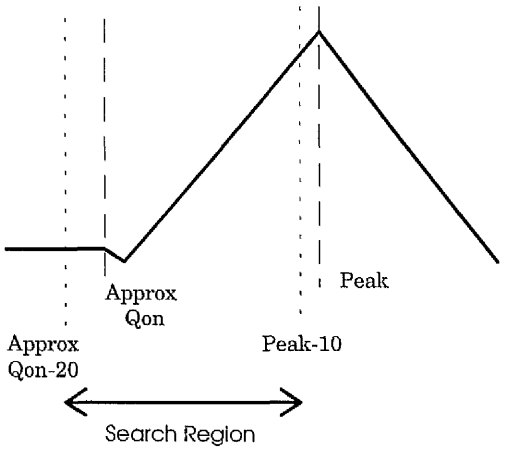

Figure 6.15 **Demonstration of the selection of the search region for QRS-onset location - Peak = peak of QRS complex and Approx Qon = Approximate QRS-onset.**

6.5.2 Results for QRS-Onset Template Location

Differences were once again computed between each methods estimate of the QRS-onset and the corresponding 'true' value. The results (in sample points) are summarised in Table 6.8.

Statistics	GP	GSF	GT	IT
$\sum_{1}^{88} (\text{Diff})^2 / 88$	5.52	3.81	7.24	5.40
Median	1.50	1.00	0.00	0.00
S.D.	1.74	1.65	2.69	2.29
U.Q.	3.00	2.00	2.00	2.00
L.Q.	1.00	0.00	-1.00	-1.00

Table 6.8 **Summary statistics (including mean sum of squares) for the QRS-onset difference (estimated-true).**
GP=Glasgow Program;
GSF=Glasgow Program & Glasgow smoothing filter;
GT=Global Template, IT=Individualised Template
S.D.=standard deviation
U.Q. = upper quartile and L.Q. = lower quartile

Table 6.8 shows that the median difference across the 88 test cases for both template methods was zero which implies that the templates

neither under- or over-estimate the QRS onset. Both the Glasgow program and Glasgow smoothing filter, show evidence of overestimation. However, it is clear from Figure 6.16 that both templates show slightly greater variability than the conventional program and Glasgow smoothing filter. The number of QRS-onsets correctly located by each method is summarised in Table 6.9. It is evident that the individualised template performed best, correctly locating more QRS-onsets than the other three methods.

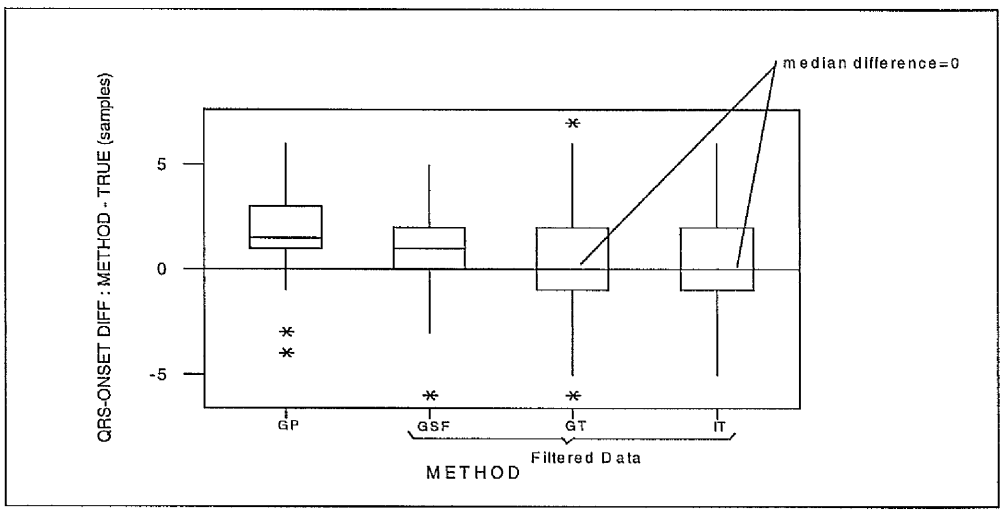

Figure 6.16 **Performance of the Glasgow Program (GP), Glasgow smoothing Filter (GSF), Global Template (GT) and Individualised Template (IT) when estimating the QRS-Onset.**

Statistic	GP	GSF	GT	IT
# Correctly Estimated	12	16	15	30

Table 6.9 **Number of QRS-onsets correctly located (n=88)**

6.6 TEMPLATE LOCATION OF THE QRS-OFFSET

6.6.1 Construction of Templates

The 24 subsets of filtered spatial velocity data (using the Glasgow smoothing filter) are shown in Figures 6.17(a),(b)&(c). Once again a global non-linear and an individualised linear template were formed. As in the case of the QRS onset, a plot of $\hat{\alpha}$, $\hat{\beta}_1$ and $\hat{\beta}_2$ against each possible explanatory variable is depicted in Figure 6.18 while the results from the stepwise variable selection procedures are presented in Table 6.10. The correlations in Figure 6.18 suggest that there is no significant relationship between any of the variables. Table 6.10(a) confirms that none of the response variables ($\hat{\alpha}$, $\hat{\beta}_1$ and $\hat{\beta}_2$) were dependent on any of the explanatory variables.

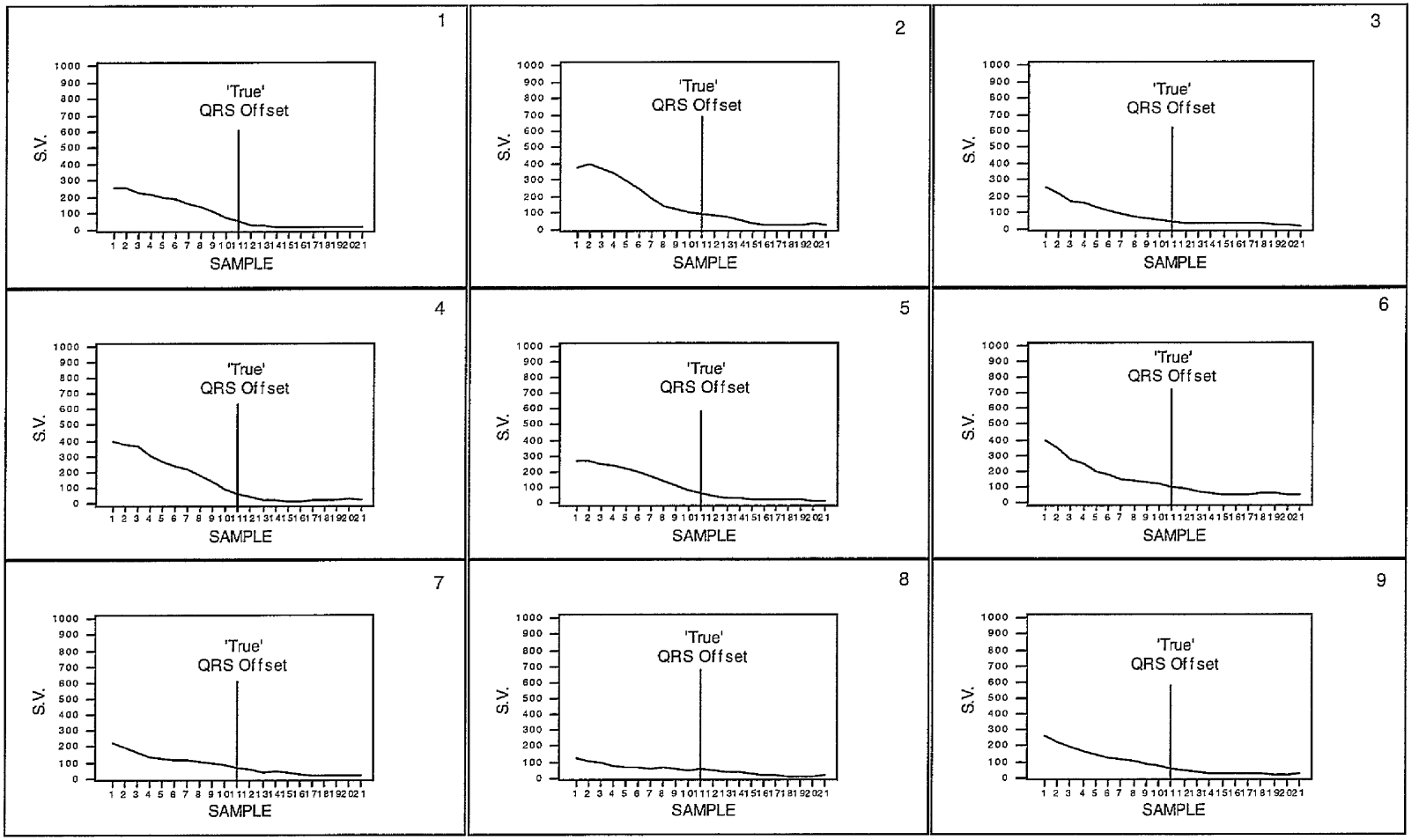

Figure 6.17(a)Subset of filtered QRS complex spatial velocity data (μV) used for the construction of a template for the QRS offset (1-9)

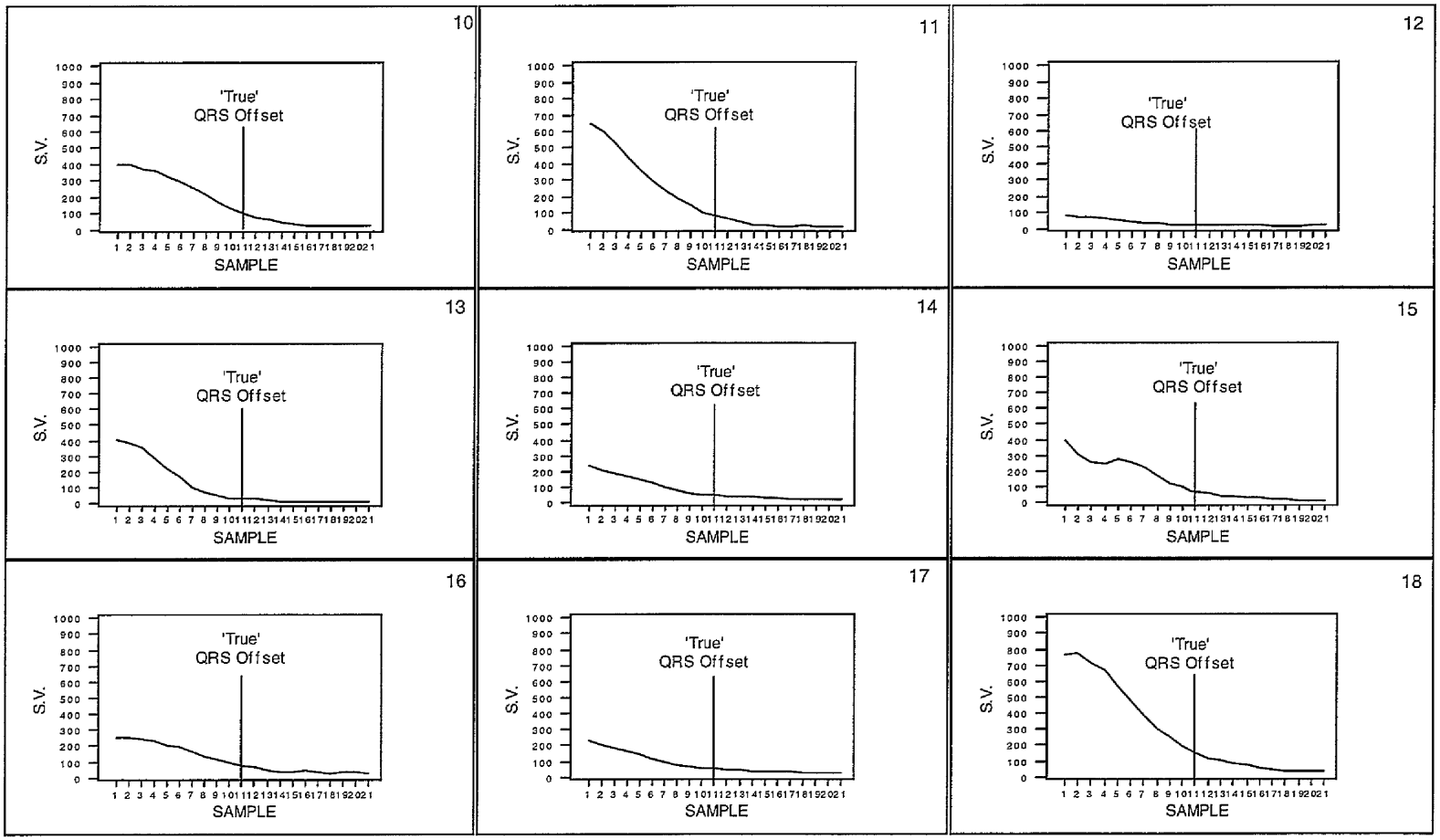

Figure 6.17(b) Subset of filtered QRS complex spatial velocity data (μV) used for the construction of a template for the QRS offset (10-18)

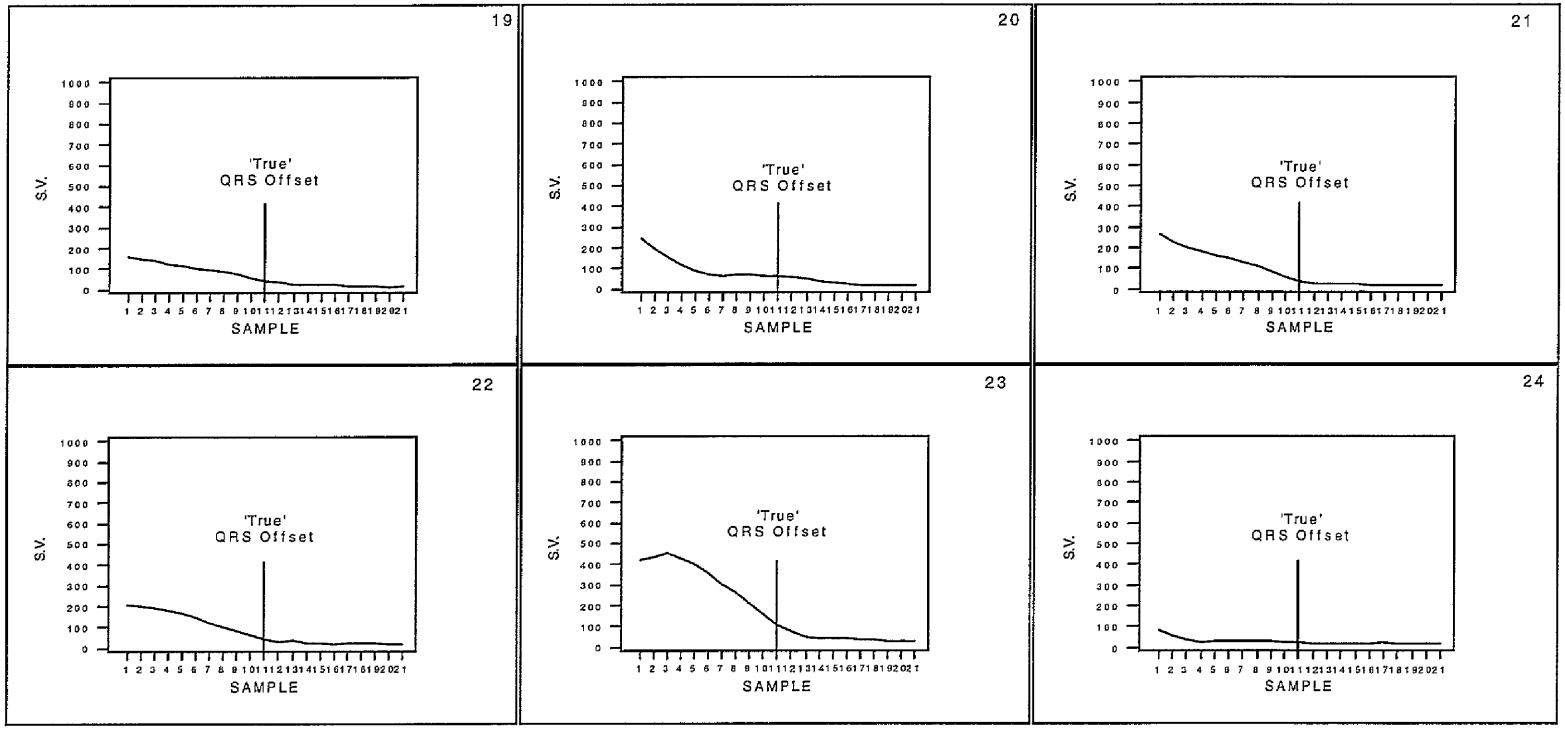

Figure 6.17(c) Subset of filtered QRS complex spatial velocity data (μV) used for the construction of a template for the QRS offset (19-24)

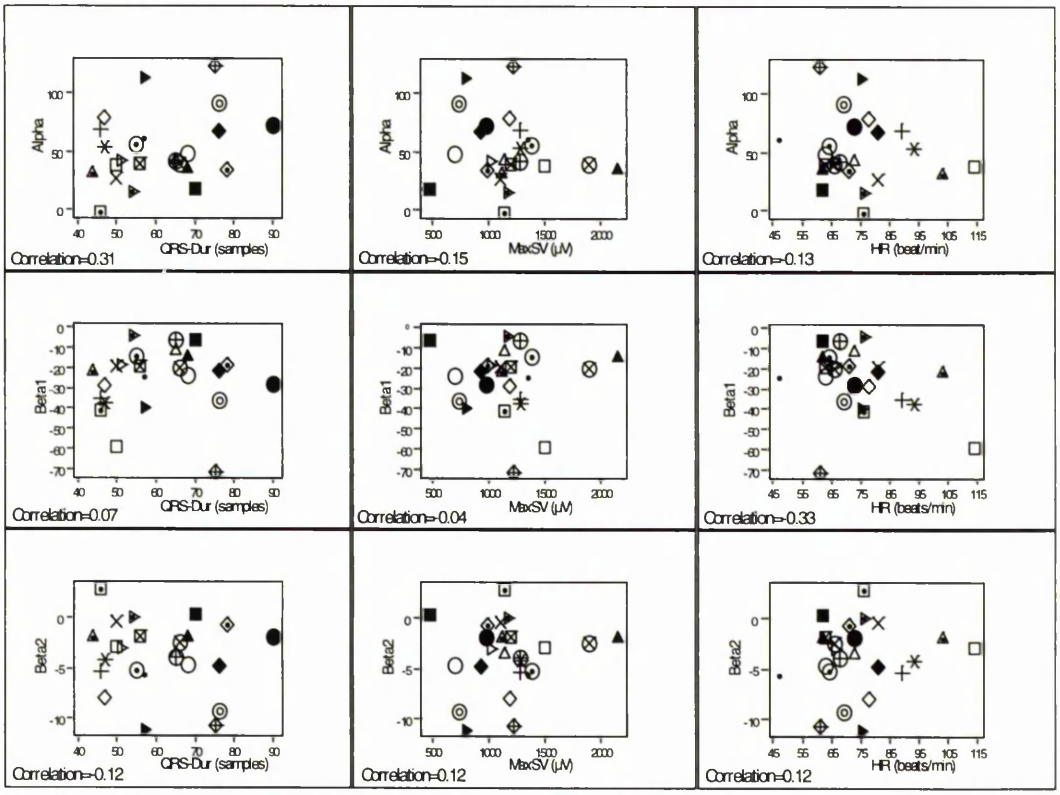

Figure 6.18 **Relationships between the response variables $\hat{\alpha}$, $\hat{\beta}_1$ and $\hat{\beta}_2$ and explanatory variables QRS-duration, maximum spatial and heart rate.**

Response Variable	Significant Explanatory Variable(s)
$\hat{\alpha}$	None
$\hat{\beta}_1$	None
$\hat{\beta}_2$	None

Table 6.10(a) **Results of the Stepwise Variable Selection Techniques**

Table 6.10(b) shows the corresponding p-values for the stepwise technique.

Response Variable	QRS-Dur	MaxSV	HR
$\hat{\alpha}$	p-value= 0.1	p-value= 0.5	p-value= 0.5
$\hat{\beta}_1$	p-value= 0.8	p-value = 0.9	p-value= 0.1
$\hat{\beta}_2$	p-value= 0.6	p-value= 0.6	p-value= 0.6

Table 6.10(b) **Corresponding p-values for the stepwise variable selection procedure.**

Since there were no significant explanatory variables, the choice for the estimates, $\hat{\alpha}$, $\hat{\beta}_1$ and $\hat{\beta}_2$, was the sample mean of the corresponding terms for the 24 ECGs in the training set. These were: $\hat{\alpha}$ = 51.50, $\hat{\beta}_1$ = -25.73 and $\hat{\beta}_2$ = -3.76. Although this meant that the template would remain the same for further analyses (since it would not be adapted to an individual ECG), this template will still be referred to as 'individualised' in what follows. The resulting template was therefore

$$\text{Template} = \begin{bmatrix} 308.8 \\ 283.1 \\ 257.3 \\ 231.6 \\ 205.9 \\ 180.2 \\ 154.4 \\ 128.7 \\ 102.9 \\ 77.2 \\ 51.5 \\ 47.7 \\ 43.9 \\ 40.2 \\ 36.5 \\ 32.7 \\ 28.9 \\ 25.2 \\ 21.4 \\ 17.7 \\ 13.9 \end{bmatrix}$$

Creation of a Search Region for QRS-Offset Location

The search region is defined in Figure 6.19 in diagrammatic form.

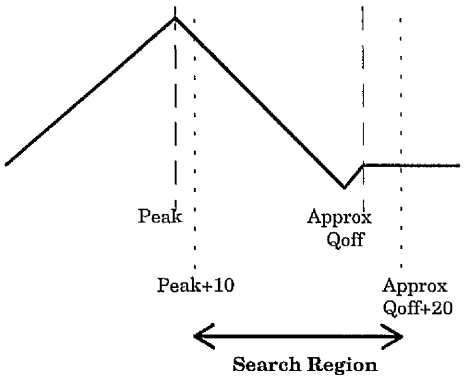

Figure 6.19 Definition of the search region for location of the QRS offset - Peak = peak of QRS complex and Approx Qoff = Approximate QRS Offset.

As with the case of the QRS-onset, the approximate QRS offset was also determined by the Glasgow program. The QRS offsets for each of the 88 ECGs were thus located using the procedures outlined in section 6.3.2.

6.6.2 Results for QRS-Offset Template Location

Differences were once again computed for each method with respect to the 'true' QRS-offset. The results (in sample points) are presented in Table 6.11.

Statistics	GP	GSF	GT	IT
$\sum_{1}^{88} (\text{Diff})^2 / 88$	19.13	9.19	11.65	11.68
Median	1.50	1.00	2.00	2.00
S.D.	3.78	2.91	3.09	3.10
U.Q.	5.00	3.00	3.00	3.00
L.Q.	-0.75	-1.00	0.00	0.00

Table 6.11 Summary statistics (including mean sum of squares) for the QRS-offset difference (estimated-true).
GP=Glasgow Program;
GSF=Glasgow Program & Glasgow smoothing filter;
GT=Global Template, IT=Individualised Template
S.D.=Standard deviation
U.Q. = upper quartile and L.Q. = lower quartile

From Table 6.11 it is clear that there is a bias present in the estimates produced by all the program versions. The bias is however reduced when incorporating the Glasgow smoothing filter into the Glasgow program. Addition of either template in conjunction with the smoothing filter did not enhance the performance of the program at all in terms of reducing the overall bias. It can be seen from Figure 6.20 that although the bias was greater for both the templates (compared to the Glasgow smoothing filter), the global and individualised templates showed least variation in their estimation of the QRS offset. The conventional Glasgow program performed poorest in comparison. It is apparent that all four versions of the program seemed to over-estimate the QRS-offset with respect to the 'true' offset. The number of correct QRS-offsets located by each of the programs is summarised in Table 6.12. The two templates appear to perform best in this case with the conventional program performing worst.

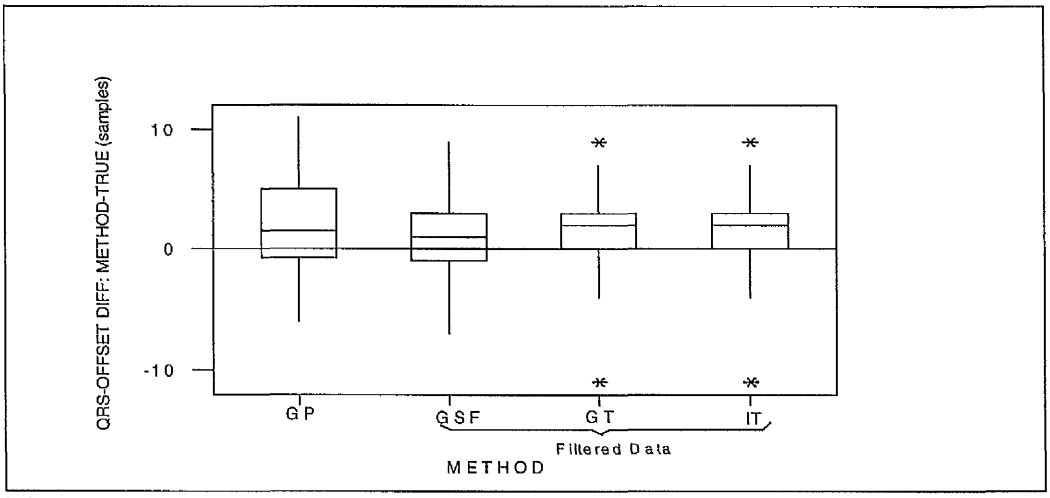

Figure 6.20 **Performance of the Glasgow Program (GP), Glasgow smoothing Filter (GSF), Global Template (GT) and Individualised Template (IT) when estimating the QRS-Offset.**

Statistic	GP	GSF	GT	IT
# Correctly Estimated	12	14	16	16

Table 6.12 Number of exact QRS-offsets correctly located (n=88)

6.7 TEMPLATE LOCATION OF THE T-END

6.7.1 The Training Set

Unlike the data used for the other fiducial points, the training set for the T-end did not consist of spatial velocity data but instead consisted of modal beat data for the individual leads. As a result there would be a T-end for each lead and eventually from these individual estimates an overall T-end would be obtained.

From the 24 training set ECGs (pre-filtered using the Glasgow smoothing filter), fifty average beats were visually selected with varying morphologies. There were four main types of wave morphologies. These are illustrated in Figure 6.21.

Upright T-wave

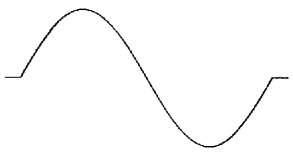

Biphasic T-wave (Type I)

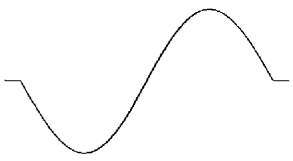

Biphasic T-wave (Type II)

Inverted T-wave

Figure 6.21 Examples of T-wave morphologies

In the training set there was a total of 25 upright T-waves, 18 inverted T-waves, 2 biphasic (Type I) and and 5 biphasic (Type II) T-waves.

Since the template would be concerned with the end of the T-wave, the process of constructing a template would involve only the end segment of both biphasic waveforms, where each took the form of either an inverted or an upright waveform. Therefore, there were two forms the template could take. For this case it was not sensible to create a global template since the T-waves for each lead would not have the same wave morphologies.

6.7.2 Construction of the Templates

Within the modal beat data, the (global) 'true' T-end points (see section 6.2) were used to extract the amplitudes of the 10 points on either side of the 'true' T-ends, producing a set 21 amplitudes for each of the 50 cases in the training set. These sets of data are plotted in Figures 6.22(a),(b),(c),(d),(e)&(f). Clearly, at first glance, some of the choices for the T-end seem odd. However, the amplitudes of these points are small in comparison to the entire T-wave. Small amounts of noise at the end of the T-wave will naturally appear worse when magnified, especially when concerned with individual lead data and not the spatial velocity, which has smoothing properties when constructed.

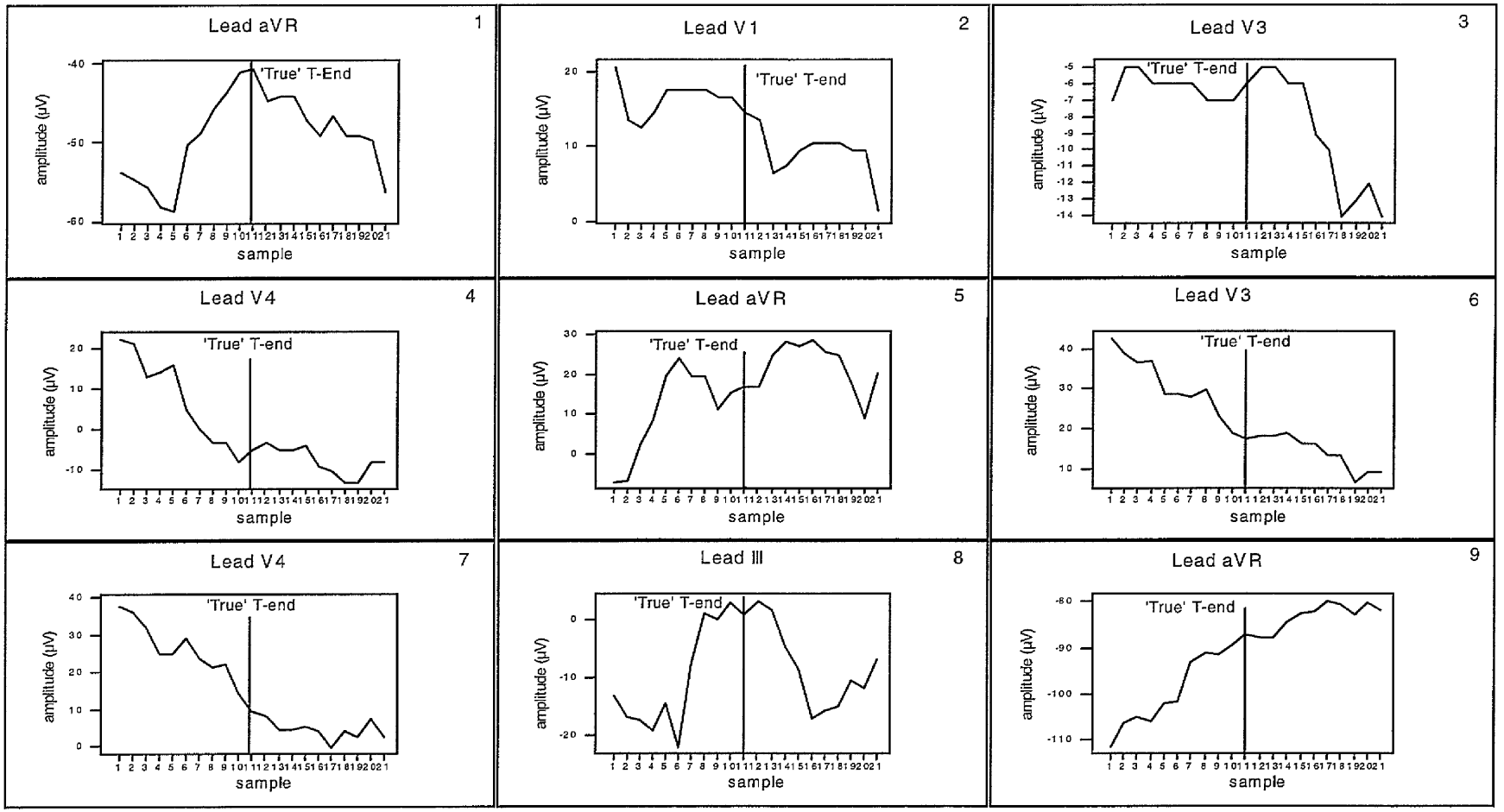

Figure 6.22(a)Subset of T-wave lead data used for the construction of a template for the T-end (1-9)

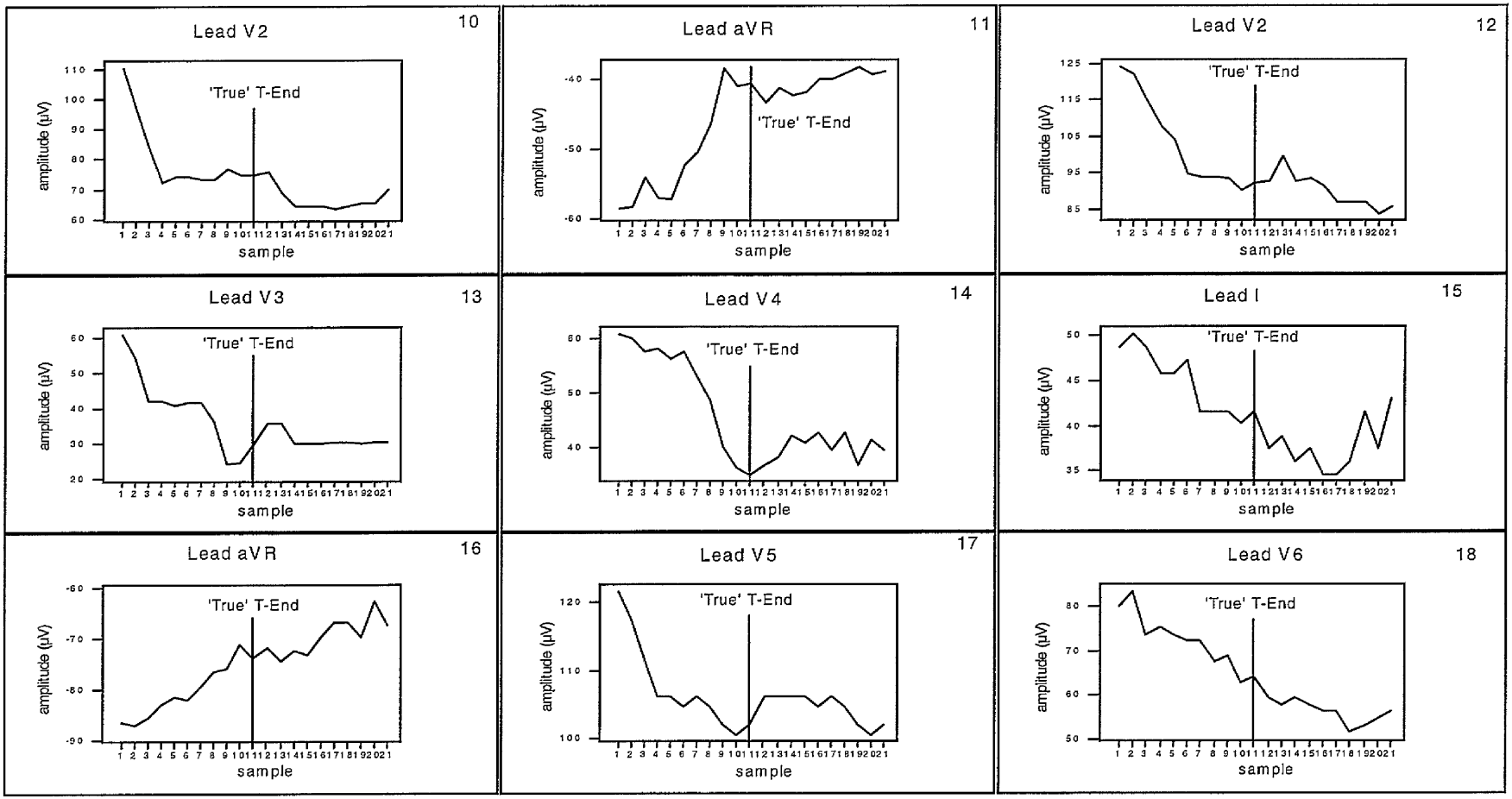

Figure 6.22(b) Subset of T-wave lead data used for the construction of a template for the T-end (10-18)

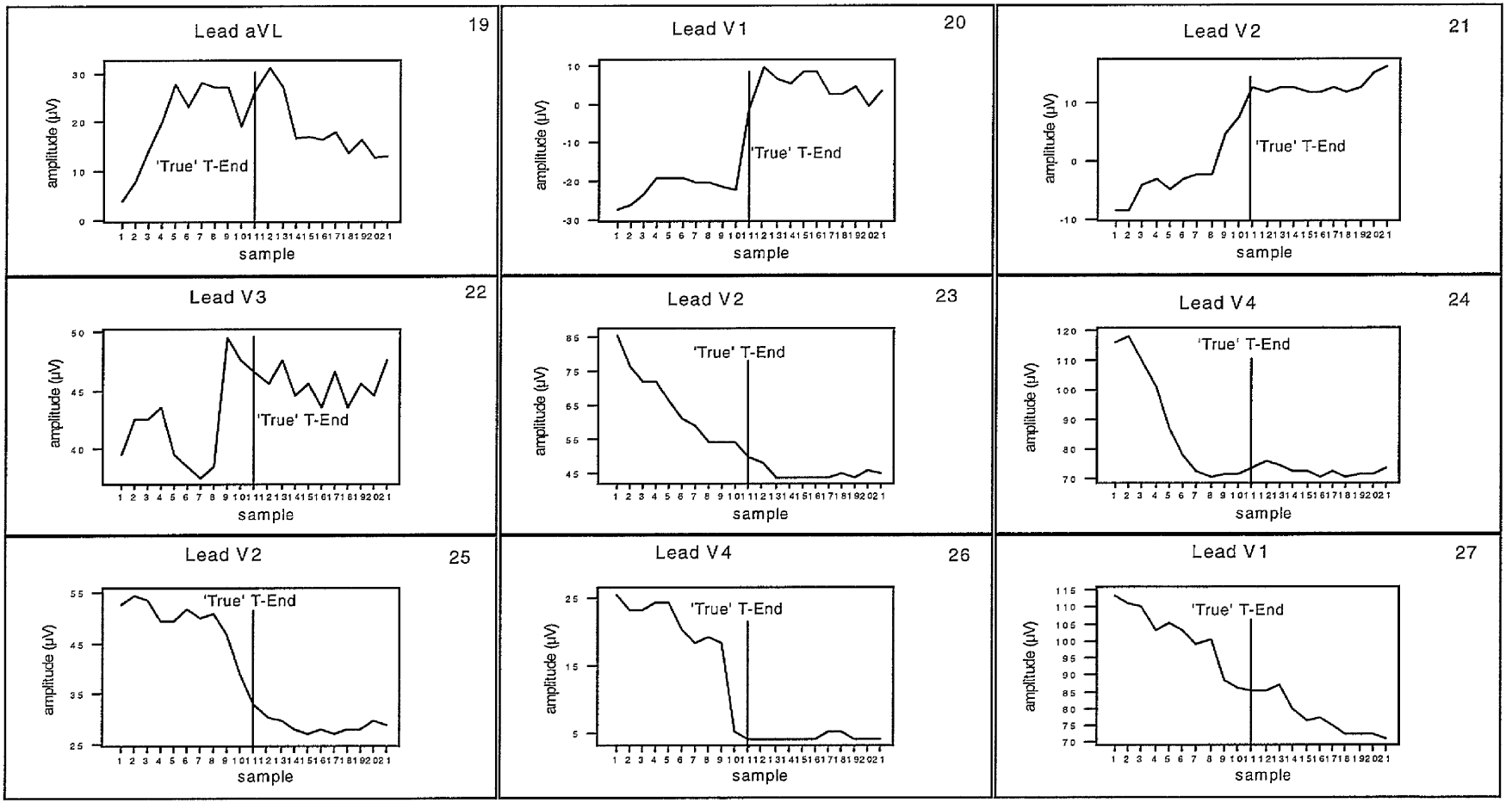

Figure 6.22(c) Subset of T-wave lead data used for the construction of a template for the T-end (19-27)

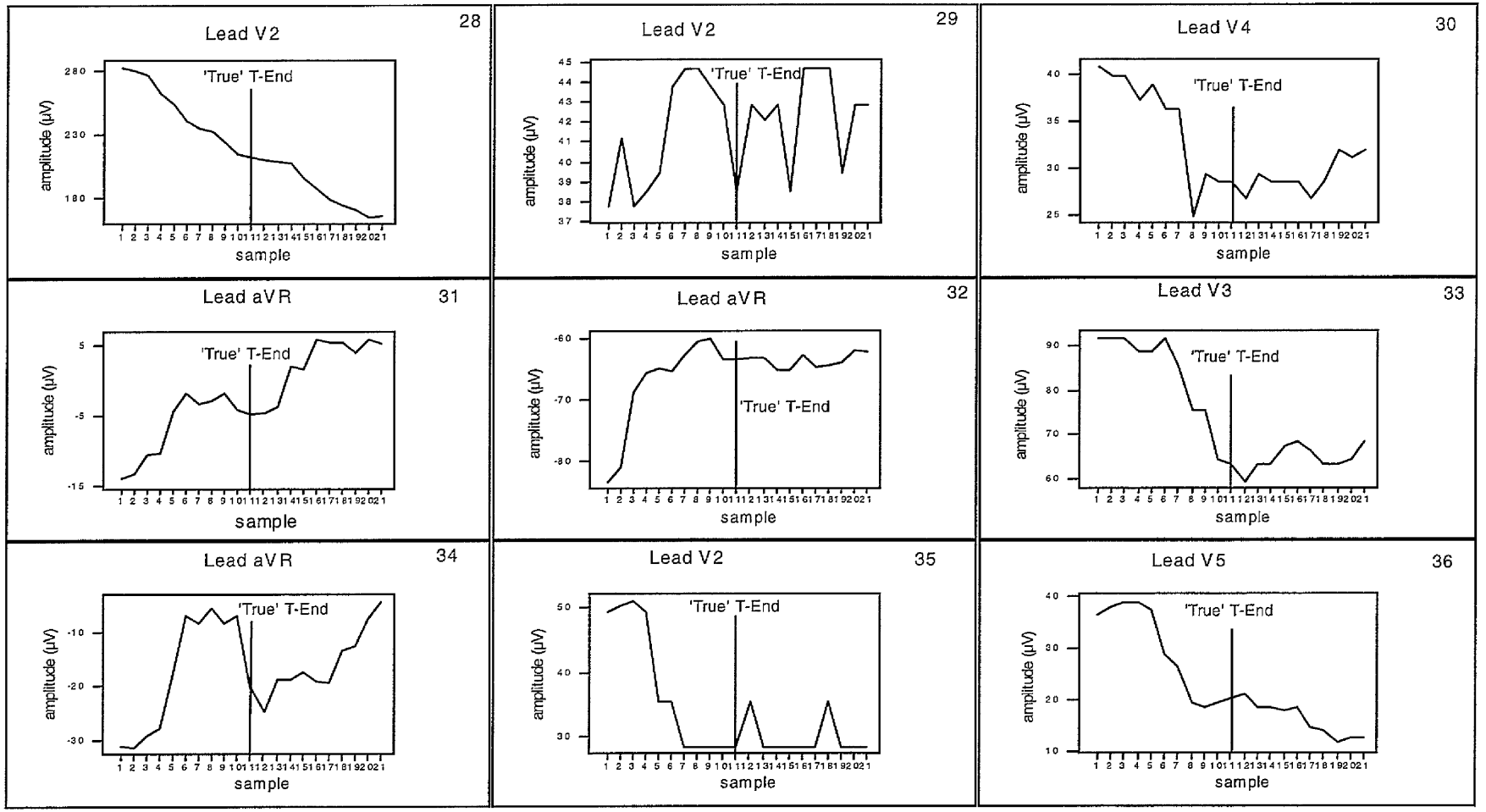

Figure 6.22(d) Subset of T-wave lead data used for the construction of a template for the T-end (28-36)

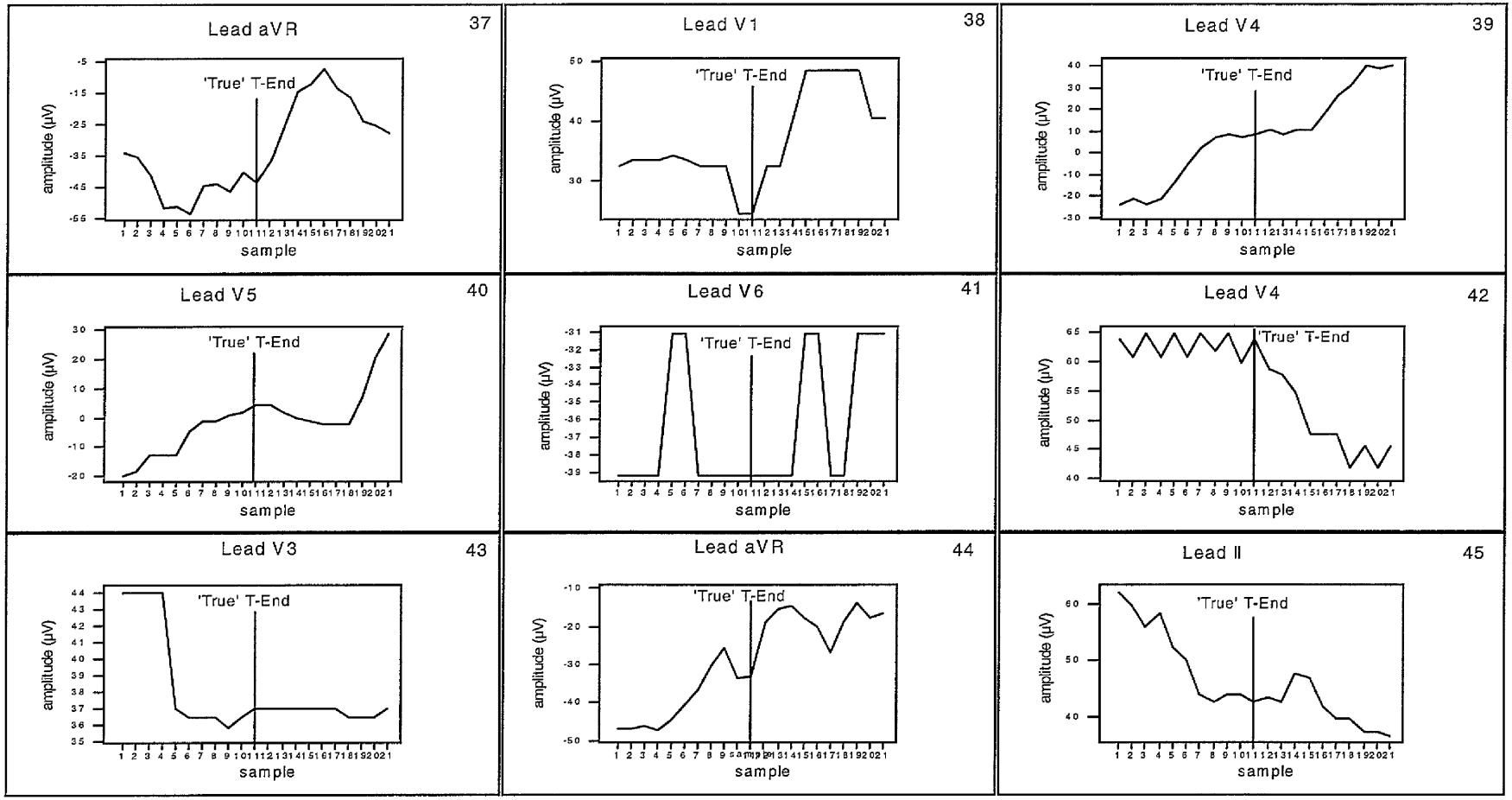

Figure 6.22(e) Subset of T-wave lead data used for the construction of a template for the T-end (37-45)

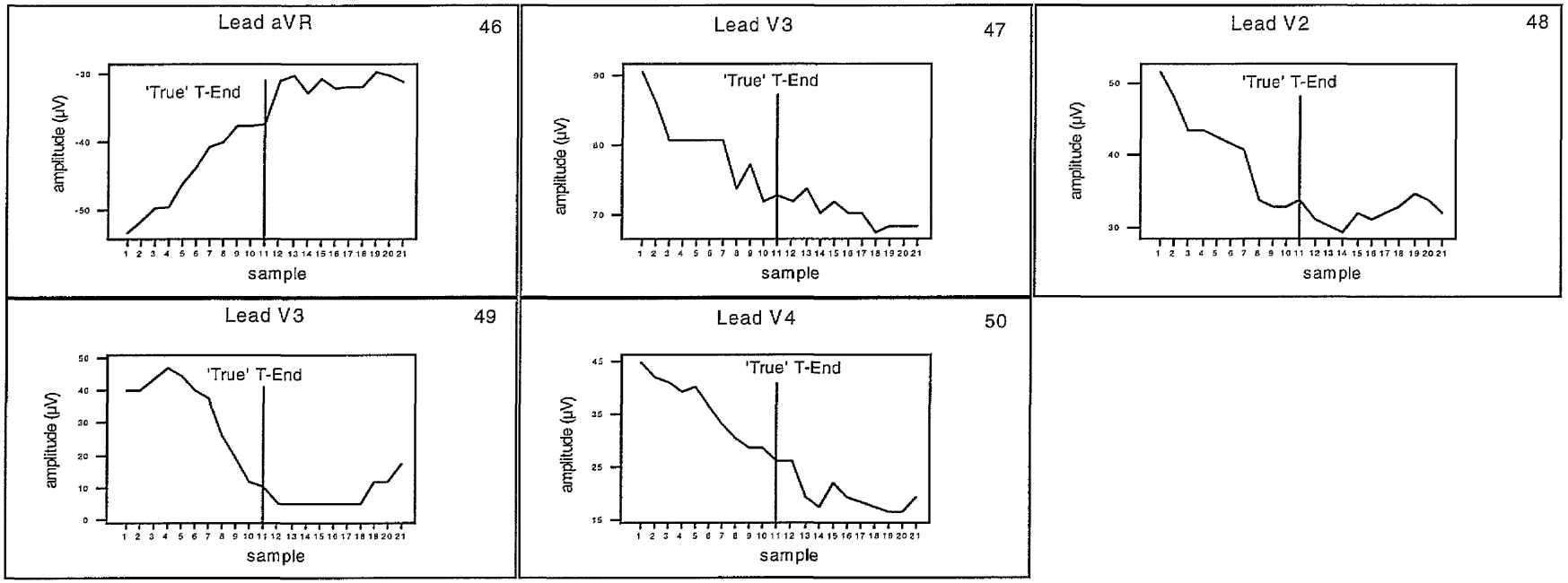

Figure 6.22(f) Subset of T-wave lead data used for the construction of a template for the T-end (46-50)

The model for template estimation could then be represented schematically as in Figure 6.23.

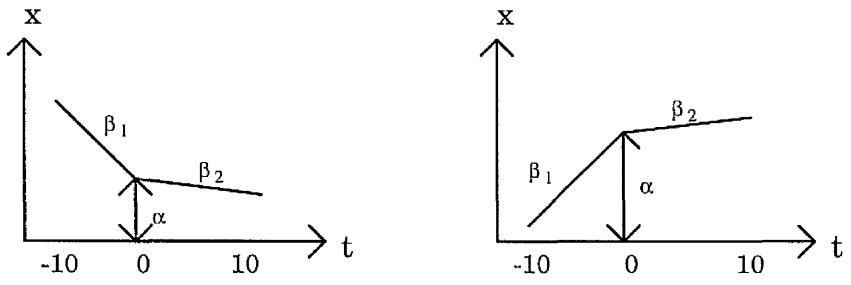

Figure 6.23 Schematic representation of the two forms of model used for the construction of the template

The first of the two diagrams represents the end section of all the upright and biphasic (type II) T-waves and the second, all inverted and biphasic (type I) T-waves in the training data. The common intercept and slope parameters, α, β_1 and β_2 were estimated for each of the 50 beats. Each (individually estimated) parameter was then assessed for its dependency on the three potential explanatory variables, i.e. approximate QT interval as determined by the Glasgow program (sample points), maximum amplitude of the T-wave in μV (if the wave were biphasic the amplitude of the second component was recorded, while the maximum amplitude could be positive or negative depending on the type of T-wave) and the heart rate. Plots illustrating these relationships are provided in Figure 6.24. Stepwise variable selection techniques were also used as previously and the results are shown in Table 6.13(a). The corresponding p-values are presented in Table 6.13(b).

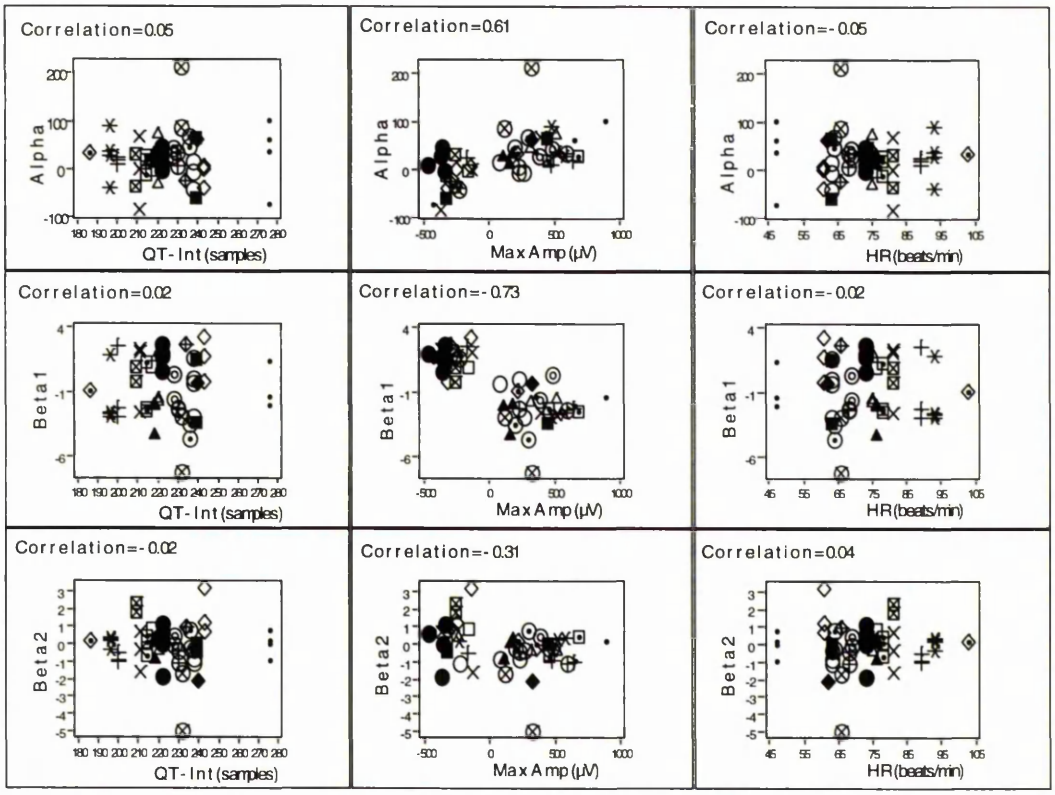

Figure 6.24 **Relationships between the response variables $\hat{\alpha}$, $\hat{\beta}_1$ and $\hat{\beta}_2$ and explanatory variables QT-Interval, maximum amplitude and heart rate.**

Response Variable	Significant Explanatory Variable(s)
$\hat{\alpha}$	Maximum Amplitude
$\hat{\beta}_1$	Maximum Amplitude
$\hat{\beta}_2$	Maximum Amplitude

Table 6.13(a) Results of the Stepwise Variable Selection Techniques

Response Variable	QT-Int	MaxAmp	HR
$\hat{\alpha}$	p-value= 0.7	p-value <0.001	p-value= 0.8
Corrected for MaxAmp	p-value= 0.8	--	p-value= 0.6
$\hat{\beta}_1$	p-value= 0.9	p-value < 0.001	p-value= 0.9
Corrected for MaxAmp	p-value= 0.7	--	p-value= 0.9
$\hat{\beta}_2$	p-value= 0.9	p-value= 0.03	p-value= 0.8
Corrected for MaxAmp	p-value= 0.9	--	p-value= 0.7

Table 6.13(b) Corresponding p-values for the stepwise variable selection procedure.

All three parameters were dependent on the maximum amplitude of the T-wave, and in particular, $\hat{\beta}_1$ was dependent on the maximum amplitude, implying that only one template would be required since the amplitude (and subsequent sign) of the T wave would determine the shape of the template. Neither of the two variables QT-interval or heart rate, were significant before or after having corrected for the maximum amplitude variable. The form of the relationships were therefore:

$$\hat{\alpha} = 11.74 + 0.083*\text{MaxAmp} \quad (6.10)$$

$$\hat{\beta}_1 = -0.14 - 0.0046*\text{MaxAmp} \quad (6.11)$$

$$\hat{\beta}_2 = -0.010 - 0.0010*\text{MaxAmp} \quad (6.12)$$

The final form of the template for the T-end was as follows:

$$\text{Fit}(\text{MaxAmp}) = \begin{bmatrix} 13.14 + 0.13 * \text{MaxAmp} \\ 13.00 + 0.12 * \text{MaxAmp} \\ 12.86 + 0.12 * \text{MaxAmp} \\ 12.72 + 0.12 * \text{MaxAmp} \\ 12.58 + 0.11 * \text{MaxAmp} \\ 12.44 + 0.11 * \text{MaxAmp} \\ 12.30 + 0.10 * \text{MaxAmp} \\ 12.16 + 0.097 * \text{MaxAmp} \\ 12.02 + 0.092 * \text{MaxAmp} \\ 11.88 + 0.088 * \text{MaxAmp} \\ 11.74 + 0.083 * \text{MaxAmp} \\ 11.73 + 0.082 * \text{MaxAmp} \\ 11.72 + 0.081 * \text{MaxAmp} \\ 11.71 + 0.080 * \text{MaxAmp} \\ 11.70 + 0.079 * \text{MaxAmp} \\ 11.69 + 0.078 * \text{MaxAmp} \\ 11.68 + 0.077 * \text{MaxAmp} \\ 11.67 + 0.076 * \text{MaxAmp} \\ 11.66 + 0.075 * \text{MaxAmp} \\ 11.65 + 0.074 * \text{MaxAmp} \\ 11.64 + 0.073 * \text{MaxAmp} \end{bmatrix}$$

Creation of a Search Region

A search region was constructed and was used to locate the T-end points for each of the leads for a 15-lead ECG. The selection of the search area is depicted in Figure 6.25.

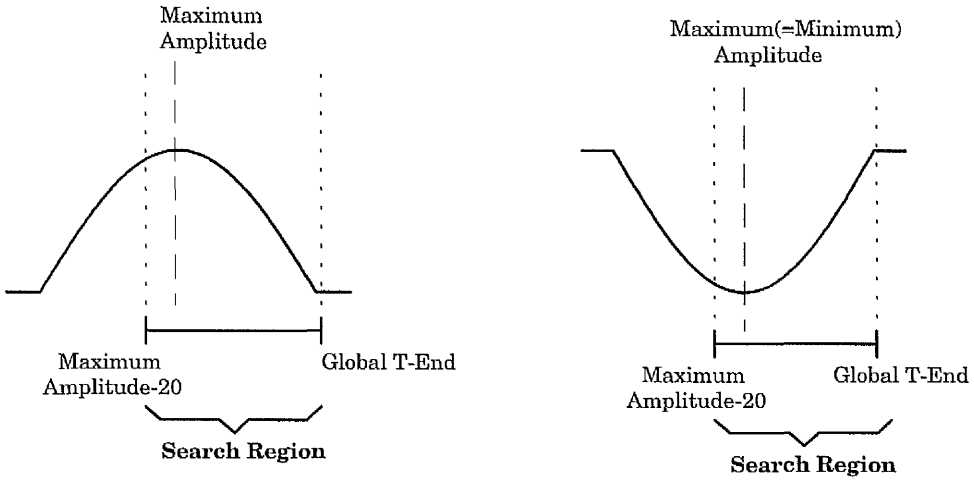

Figure 6.25 Definition of the search region for location of the T-End.

Initially the start of the search region was set as the location of the maximum/minimum amplitude-20. The end of the search region was set as the global T-end value estimated by the Glasgow program. However, if the difference between the location point of the maximum amplitude and the global T-end was considered too large then the starting point was adjusted so as to reduce the search area. Each lead was processed individually and differences between the fitted template values and the amplitude values within the search region were computed. The process of minimising the sum of squares error was once again performed using the procedures outlined earlier in the P-onset case. This process was repeated for all the other leads until all 15 T-end points were located. Finally, in order to test the performance of the template, a global T-end was selected from the fifteen estimated for each ECG, by applying the method used for global T-end location within the Glasgow program, briefly discussed in Chapter One.

6.7.3 Results for T-End Template Location

The same test set of 88 ECGs was used as before. After processing each ECG, the conventional and filtered (using the Glasgow smoothing filter) program T-end estimates were obtained. As before, the differences between each method and the "true" value were computed in sample points. The results are summarised in Table 6.14. It is clear that the template performed best, with a median difference of 1 sample point i.e. 2 milliseconds. There was a much greater bias present in the conventional program and in the Glasgow smoothing filter version. This can be seen graphically in the form of boxplots (Figure 6.26). This positive bias implied that both versions of the program were over-estimating the T-end. The improvement in the estimates, by first introducing the filter into the program and then the template, can be seen in the drop in standard deviation and the mean sum of squares value at each stage. Table 6.15 summarises the total number of correct T-ends located by each method. It is apparent the template performs far better than the other two methods.

Statistics	GP	GSF	IT
$\sum_{1}^{88} (\text{Diff})^2 / 88$	259.50	161.55	93.89
Median	5.50	5.00	1.00
S.D.	14.00	11.21	9.53
U.Q.	10.00	9.00	3.00
L.Q.	1.25	1.00	-1.00

Table 6.14 **Summary statistics (including mean sum of squares) for the T-End difference (estimated-true).**
GP=Glasgow Program;
GSF=Glasgow Program & Glasgow smoothing filter;
IT=Individualised Template
S.D=standard deviation
U.Q. = upper quartile and L.Q. = lower quartile

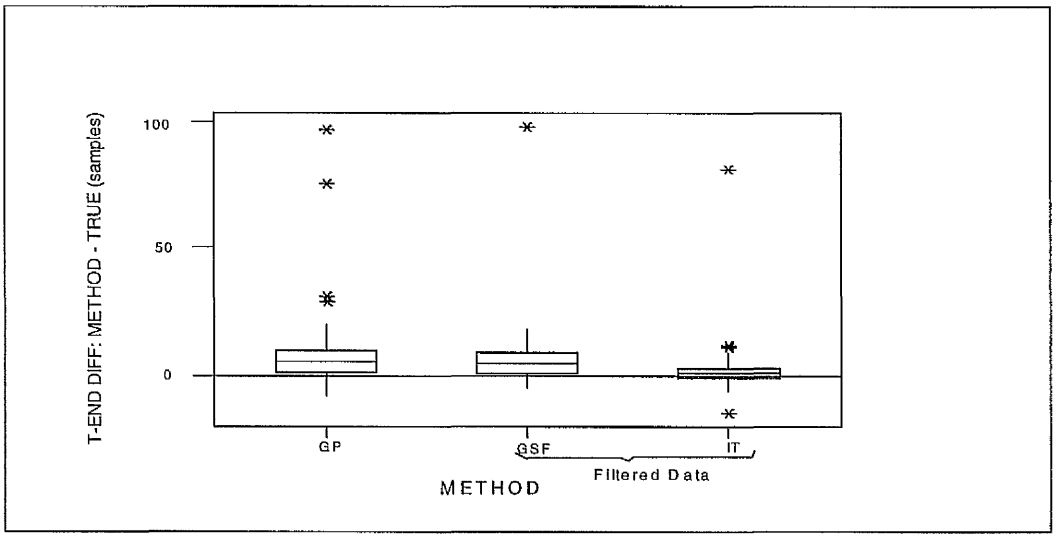

Figure 6.26 **Performance of the Glasgow Program (GP), Glasgow smoothing Filter (GSF) and Individualised Template (IT) when estimating the T-end.**

Statistic	GP	GSF	IT
# Correctly Estimated	6	8	17

Table 6.15 **Number of T-ends correctly located (n-88)**

From Figure 6.26, it was clear that there was one common outlier whose T-end point was grossly mis-estimated. Indeed, this ECG showed 2:1 A-V block which is generally caused when the sinus impulses are blocked so that not every P-wave is followed by a QRS complex. The PR-interval remains constant with intermittent dropped beats. From the ECG in Figure 6.27, it is apparent that every second QRS complex is missing hence the term "2:1" A-V block. It was deduced that the three methods seemed to pick up the end of the following P-wave which directly followed the previous T-wave, missing the T-end altogether. (i.e. the modal beat contained the P-wave of the next beat). The difference in the summary statistics after removing the outlier can be seen in Tables 6.16.

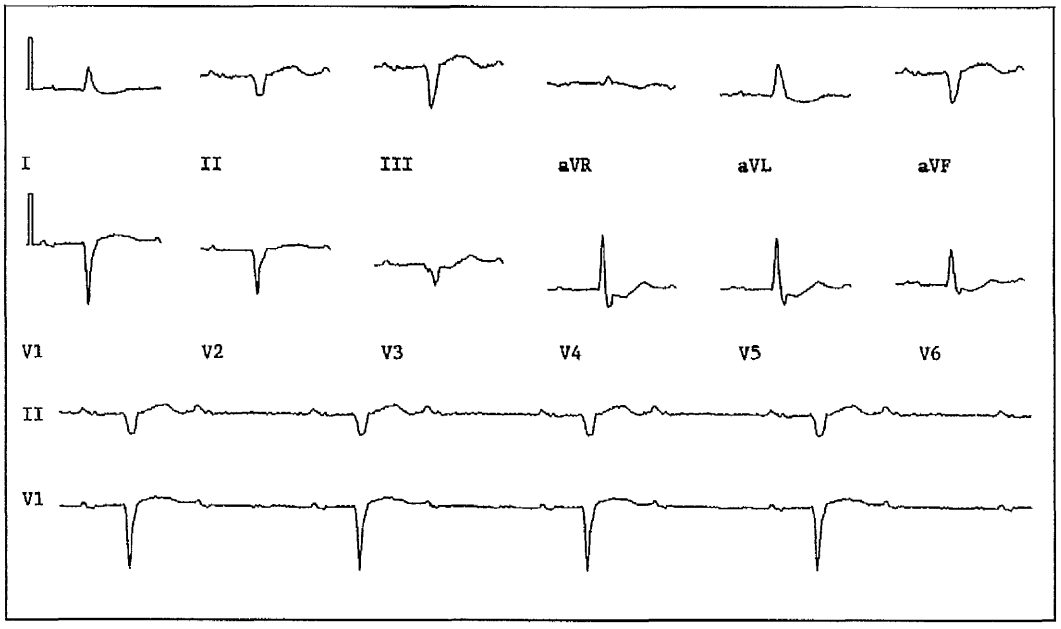

Figure 6.27 Common outlier in the test set - ECG showing 2-1 A-V block

Statistics	GP		GSF		IT	
	Signed	Absolute	Signed	Absolute	Signed	Absolute
$\sum_{1}^{87} (\text{Diff})^2 / 87$	154.33		53.01		19.55	
Median	5.00		5.00		1.00	
S.D.	10.26		5.27		4.30	
U.Q.	10.00		9.00		3.00	
L.Q.	1.00		1.00		-1.00	

Table 6.16 Summary statistics for the T-End difference (estimated-true) determined by the Glasgow Program & Glasgow smoothing filter and individualised template - outlier removed.

As would be expected, when Table 6.15 and Table 6.16 are compared, the significant drop in the mean sum of squares is very evident. There is also a clear drop in the standard deviation after omitting the outlier.

6.8 CONCLUSIONS CONCERNING FIDUCIAL POINT ESTIMATION

The tables below summarise the results obtained for each of the fiducial points in this chapter. Table 6.17 summarises the mean sum of squares across each method, while Tables 6.18 and 6.19 summarise the number of fiducial points located correctly and the standard deviation of the differences, estimated-true, (corrected for the bias) for each fiducial point respectively.

Mean Sum of Squares

Fiducial Point	GP	GSF	GT	IT
P-Onset	38.63	44.94	28.16	**22.42**
P-Offset	36.75	**19.11**	25.70	21.51
QRS-Onset	5.52	**3.81**	7.24	5.40
QRS-Offset	19.13	**9.19**	11.65	11.68
T-End	259.50	161.55	*	**93.89**

Table 6.17 **Mean sum of squares across the different methods of estimation for the five different fiducial points. GP=conventional Glasgow Program, GSF=Glasgow Smoothing Filter, GT=Global Template & IT=Individualised Template.**

 # Fiducial Points Correctly Located

Fiducial Point	GP	GSF	GT	IT
P-Onset	10	6	9	**16**
P-Offset	**11**	10	5	**11**
QRS-Onset	12	16	15	**30**
QRS-Offset	12	14	**16**	**16**
T-End	6	8	*	**17**

Table 6.18 **Number of fiducial points correctly located by each method .**

Standard Deviation

Fiducial Point	CGP	GSF	GT	IT
P-Onset	5.17	5.50	5.32	**4.71**
P-Offset	5.84	4.14	4.90	**4.07**
QRS-Onset	1.74	**1.65**	2.69	2.29
QRS-Offset	3.78	**2.91**	3.09	3.10
T-End	14.00	11.21	*	**9.53**

Table 6.19 Standard deviation of the differences (Estimate - True) across each method and for each fiducial point.

From the above Tables it is clear that the fiducial points are estimated best by using either the Glasgow smoothing filter on its own or combined with the individualised linear template. Table 6.20 below recommends the techniques (in conjunction with the original Glasgow program) which best estimated each fiducial point in the test set of 88 ECGs. It is suggested that the Glasgow smoothing filter alone be used when estimating the P-offset, QRS-onset and QRS-offset and then combined with the corresponding individualised templates when estimating the P-onset and T-end.

Fiducial Point	Recommended Technique
P Onset	GP & GSF & IT
P Offset	GP & GSF
QRS Onset	GP & GSF
QRS Offset	GP & GSF
T End	GP & GSF & IT

Table 6.20 Techniques recommended for fiducial point estimation

6.9 COMPARISON OF THE ESTIMATION METHODS

In order to compare the performance of one method of estimation to another in terms of the variability present in each set of fiducial point differences (estimate-true), a multiple comparisons procedure was used to construct confidence intervals for the ratio of the unknown standard deviations of the **differences** (estimate-true), $\frac{\sigma_{METHOD2}}{\sigma_{METHOD1}}$, with overall confidence of at least 95%. These intervals gave an indication of whether the variability using one method was significantly different than the other when estimating a particular fiducial point, relative to the 'true' estimate. However, these intervals were only approximations since the sets of data were not independent. In the calculations of the confidence intervals, the sample standard deviations about the mean of the differences were used, accounting for any biases present in the estimates. The confidence intervals were of the form:

$$\left(\frac{S_2}{S_1}\sqrt{F(n_1-1, n_2-1; 0.025/6)} \quad , \quad \frac{S_2}{S_1}\sqrt{F(n_1-1, n_2-1; 1-0.025/6)} \right)$$

where S_1 is the standard deviation say, for the Glasgow smoothing filter differences and S_2 is the sample standard deviation for the conventional Glasgow program differences, relative to the 'true' values. Also n_1 and n_2 are the number of subjects/ECGs in the test set for each method (n_1=n_2=88) and F is the test statistic. Confidence intervals for each pair of method comparisons (6 comparisons in total) are presented in Table 6.21 for the P-onset case only. These are further summarised in the standard multiple comparisons format in Figure 6.28 along with the other fiducial point multiple comparison results. The table lists all

the possible estimates for $\sigma_{\text{METHOD 2}}$ along the top of the table and the possible estimates for $\sigma_{\text{METHOD 1}}$ down the side of the table.

	σ_{GP}	σ_{GSF}	σ_{GT}
σ_{GSF}	(0.71, 1.25) includes 1	*	*
σ_{GT}	(0.73, 1.29) includes 1	(0.78, 1.37) includes 1	*
σ_{IT}	(0.82, 1.46) includes 1	(0.88, 1.55) includes 1	(0.85, 1.50) includes 1

Table 6.21 95% confidence intervals to quantify the variability in the P-onset differences produced by the Glasgow Program, Glasgow Smoothing Filter (GSF), Global Template (GT) and Individualised Template (IT) from the 'true' value.

Since all the intervals in Table 6.21 include the value 1, it can be concluded that there is no evidence to suggest a significant difference between the variability in the differences of the corresponding estimated and 'true' values of any of the methods investigated.

In Figure 6.28(a), the outcome of the P-onset estimation is summarised in the usual multiple comparison format where each method has been joined by a vertical line, indicating no significant differences between any of the methods. The sample standard deviations are also provided in ascending order. Also included are summarised versions of the remaining fiducial points. In the case of the P-offset, there was a significant difference between the variability of the individualised template and the conventional Glasgow program with respect to the 'true' P-offset. When the four methods were compared in terms of variability in the respective QRS-onset differences (relative to the 'true' onset) a significant difference between the Glasgow smoothing filter and both templates was observed. There was also evidence of a significant difference between the variability in

Glasgow program differences and the global template differences. With regards to the QRS-offset, there was no evidence of a significant difference in any of the four methods with regards to the variability. Finally, in the case of the T-end, it was found that there was clear evidence of a significant difference between the variability in the conventional Glasgow program differences (with respect to the 'true' value) and that of the individualised template.

(a) P-ONSET

Method	IT	GP	GT	GSF
S.D.	4.71	5.57	5.32	5.50

(b) P-OFFSET

Method	IT	GSF	GT	GP
S.D.	4.07	4.14	4.90	5.48

(c) QRS-ONSET

Method	GSF	GP	IT	GT
S.D.	1.65	1.74	2.29	2.69

(d) QRS-OFFSET

Method	GSF	GT	IT	GP
S.D.	2.91	3.09	3.10	3.78

(e) T-END

Method	IT	GSF	GP
S.D.	9.53	11.21	14.00

Figure 6.28 Summary of the multiple comparisons to identify differences in the methods of fiducial point estimation
Notes: (i) Low values of SD are 'good'
(ii) Methods with a 'common' overline are <u>not</u> significantly different from each other in terms of SD's.

6.10 PERFORMANCE OF THE INDIVIDUALISED LINEAR TEMPLATES IN THE PRESENCE OF NOISE

To investigate the performance of the conventional program, filter and individualised templates in the presence of noise, the five types of noise investigated in Chapter Four were added onto each of the 88 CSE ECGs. Due to problems related to compression of the noisy data, it was only possible to obtain results for 77 of these 88 ECGs. ECG data sent over the internal network in the Glasgow Royal Infirmary is compressed due to reasons such as reduction in transmission time, reduction in memory costs in the data acquisition device and for long-term storage of data (Peden; 1982). In order to process the CSE ECGs, the data would have to be compressed since the Glasgow program expects a compressed ECG file to be supplied.

The type of coding used to compress data within the Glasgow program is known as Huffman coding. This procedure involves computing residuals of the digitised ECG data since the variance of the residual sequence is very much less than the original sequence. These residuals are then assigned specific binary codes, where the most frequently occurring residual is assigned say, code word 0 and the next most frequent residual, 100 and so on. However, when additional high frequency noise was added to the CSE ECG data, the combination of the original data for certain ECGs coupled with the high frequency noise resulted in the production of too many different residual values thus making it impossible for the data to be compressed effectively.

For each of the noise types, the performance of each of the methods at fiducial point estimation, was assessed in an identical manner to that described earlier in this chapter.

6.10.1 Results for the P-Onset

The results for the P-onset are summarised in Table 6.22. As before, all the measurements are in sample points. The summary statistics in each cell of the table are of the following form:

$\sum_{1}^{77}(\text{Diff})^2 / 77$
Median
Standard Deviation
Upper Quartile
Lower Quartile

Here the median, standard deviation, upper quartile and lower quartile are that of the estimate-true differences.

It was observed that the addition of excess noise did have a slight detrimental effect on each of the methods of estimation. In particular the Glasgow program performed worse in noise types 1, 3 and 5. The Glasgow smoothing filter performed worst in noise types 2 and 4 and the individualised template in the presence of noise 4 (see Figures 6.29(a),(b)&(c)). However, in some cases it was observed that the addition of noise improved the overall accuracy of the estimates, but this was not consistent over the three methods. e.g. Noise 1 improved the P-onset estimation vastly, yet the performance of the conventional Glasgow program worsened significantly.

In general, it was clear that the template once again performed better than both the conventional and smoothing filter program versions, except in the presence of noise type 4, where the standard deviation was higher for the template than the other two programs. This was due to one extreme observation. The reason for this outlier was that instead of the spatial velocity taking the form of an m-shape (two peaks), it consisted of three peaks. The 'true' location of the P-onset was situated at the beginning of the first peak, however, the template located the onset at the beginning of the third (see Figure 6.30; the example used is the original unfiltered waveform supplied only to illustrate the nature of the P-wave), even though the search region incorporated all three parts of the P-wave in its search for the P-onset. The true improvement using the individualised template over the other methods for noise 4 as well as the other noise types can be seen by the decrease in the median differences in the relevant row of Table 6.22. Note also that by adding noise types 1, 2, 3 and 5, any existing biases are eliminated using the template.

NOISE TYPE	GP	GSF	IT
NO NOISE	36.22 2.00 5.04 5.00 0.00	43.92 3.00 5.38 5.00 1.00	17.71 1.00 4.08 3.00 -1.00
NOISE 1 High Freq 25μV RMS	65.78 1.00 8.15 3.00 -3.00	36.19 2.00 5.20 4.00 0.00	10.23 0.00 3.22 1.00 -2.00
NOISE 2 Line Freq 50Hz, 25μV peak	32.78 2.00 5.20 4.00 0.00	55.69 2.00 6.67 4.00 0.00	17.61 0.00 4.22 2.00 -1.00
NOISE 3 Line Freq 60Hz, 25μV peak	43.64 2.00 6.03 3.00 0.00	23.61 2.00 4.03 4.00 0.00	22.96 0.00 4.77 2.00 -2.00
NOISE 4 Baseline 0.3Hz, 0.5mV peak	33.25 2.00 4.23 4.50 0.00	43.23 3.00 5.03 5.00 1.00	42.53 1.00 6.23 3.00 -1.00
NOISE 5 Baseline & High Freq 0.3Hz, 0.5mV peak; 15μV RMS	54.57 2.00 5.82 4.00 -1.50	37.52 3.00 4.93 5.00 1.00	18.13 0.00 4.27 1.50 -2.00

Table 6.22 **Performance of the conventional program, the filter and the template when estimating the P-onset in the presence of noise. Each of the above cells contains the following:**

$\sum_{1}^{77} (\text{Diff})^2 / 77$
Median
S.D.
U.Q.
L.Q.

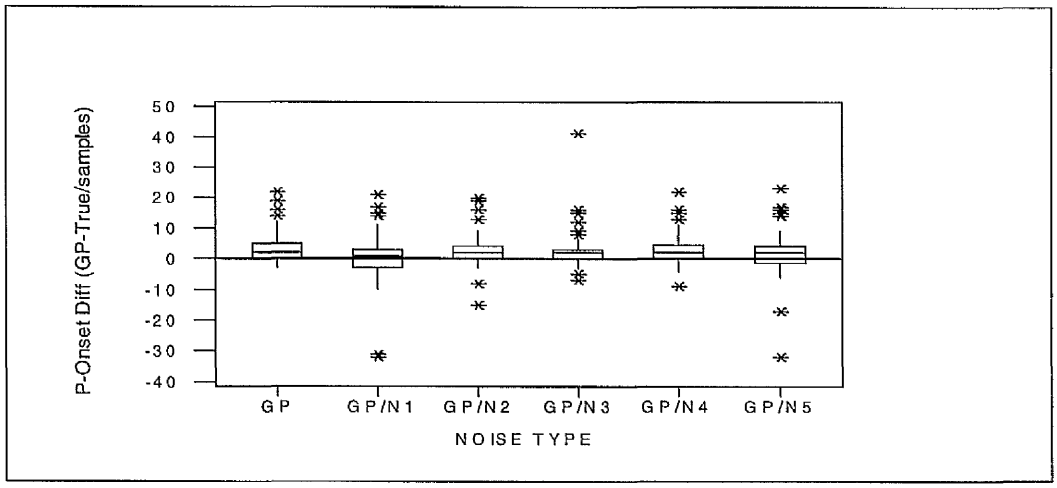

Figure 6.29(a) **Performance of the conventional Glasgow Program (GP) when estimating the P-onset in the absence and presence of noise. N1-N5 represents noise types 1-5.**

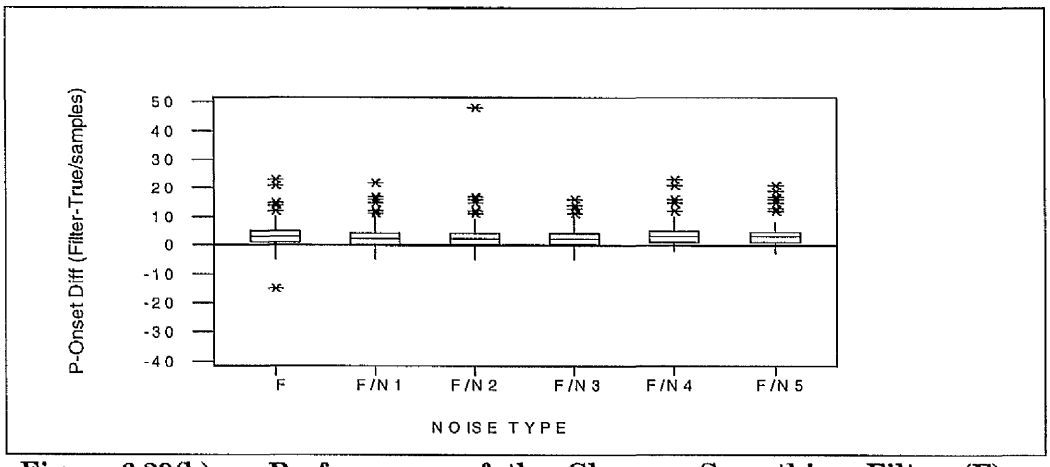

Figure 6.29(b) **Performance of the Glasgow Smoothing Filter (F) when estimating the P-onset in the absence and presence of noise. N1-N5 represents noise types 1-5.**

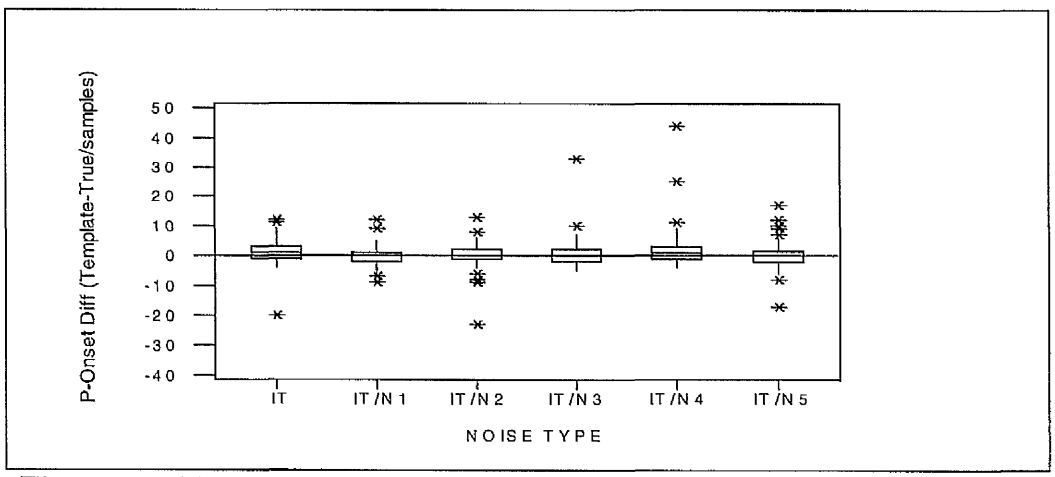

Figure 6.29(c) **Performance of the Individualised Template (IT) when estimating the P-onset in the absence and presence of noise. N1-N5 represents noise types 1-5.**

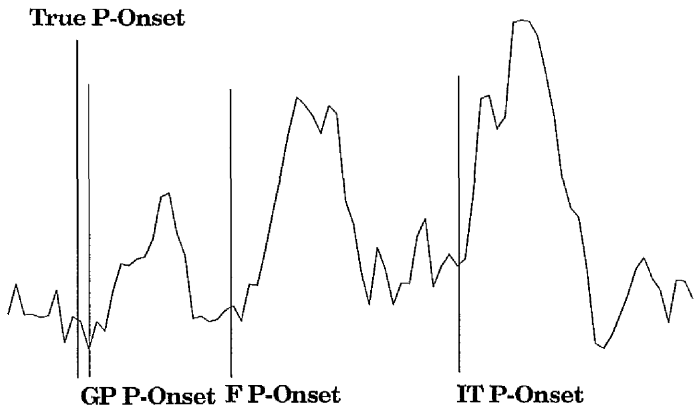

Figure 6.30 Spatial velocity of a P-wave to demonstrate the reason behind an outlying P-onset observation in the case of the Individualised template (unfiltered and not to scale).

6.10.2 Results for the P-Offset

Results for the P-offset are presented in Table 6.23, in sample points. With the addition of noise, there was again no dramatic deterioration in the estimation of the P-offset by any of the methods (see also Figures 6.31(a),(b)&(c)). From Table 6.23, the sum of squares criteria indicates that in general the Glasgow smoothing filter produces better estimates of the P-offset than the conventional program or the individualised template. However, it was apparent that, although the template was unsuccessful in improving the accuracy of the P-offset when compared to the filter alone, adding the various types of noise had no detrimental effect on its performance.

NOISE TYPE	GP	GSF	IT
NO NOISE	33.44 2.00 5.31 4.00 0.00	19.04 1.00 4.15 3.00 -1.00	21.38 2.00 4.07 4.00 0.00
NOISE 1 High Freq 25µV RMS	51.40 1.00 7.04 4.50 -2.00	26.61 2.00 4.87 3.00 -1.00	27.62 2.00 4.96 4.00 0.00
NOISE 2 Line Freq 50Hz, 25µV peak	37.25 2.00 5.73 4.00 0.00	25.43 1.00 4.75 3.00 0.00	16.12 2.00 3.67 4.00 0.00
NOISE 3 Line Freq 60Hz, 25µV peak	22.81 1.00 4.65 3.00 -1.00	15.14 1.00 3.76 3.00 -1.00	24.73 2.00 4.80 4.00 0.00
NOISE 4 Baseline 0.3Hz, 0.5mV peak	21.56 1.00 4.42 4.00 0.00	19.83 1.00 4.21 4.00 -0.50	24.45 2.00 4.61 4.00 0.00
NOISE 5 Baseline & High Freq 0.3Hz, 0.5mV peak; 15µV RMS	30.84 1.00 5.35 4.50 -1.00	14.00 1.00 3.41 4.00 0.00	16.08 2.00 3.48 4.00 0.00

Table 6.23 **Performance of the conventional program, the filter and the template when estimating the P-offset in the presence of noise. Each of the above cells contains the following:**

$\sum_{1}^{77}(\text{Diff})^2 / 77$
Median
S.D.
U.Q.
L.Q.

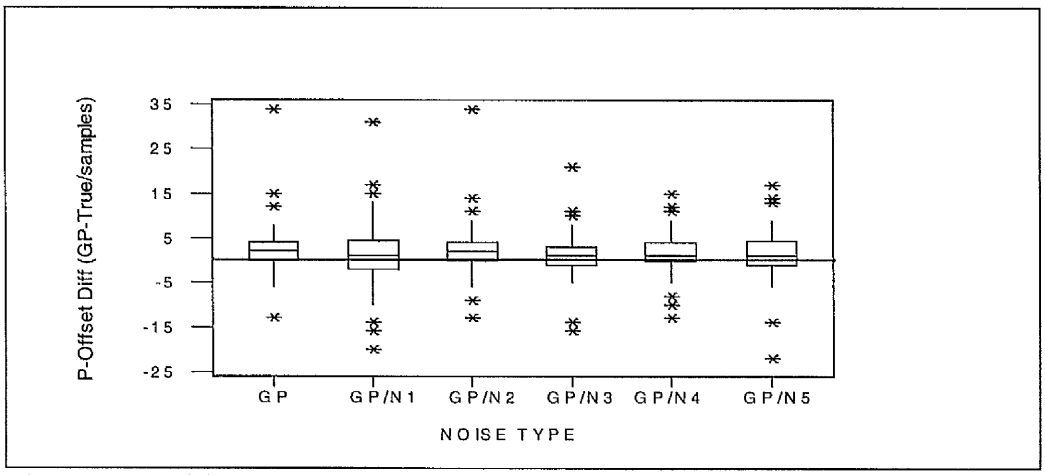

Figure 6.31(a) **Performance of the Conventional Glasgow Program (GP) when estimating the P-offset in the absence and presence of noise. N1-N5 represents noise types 1-5.**

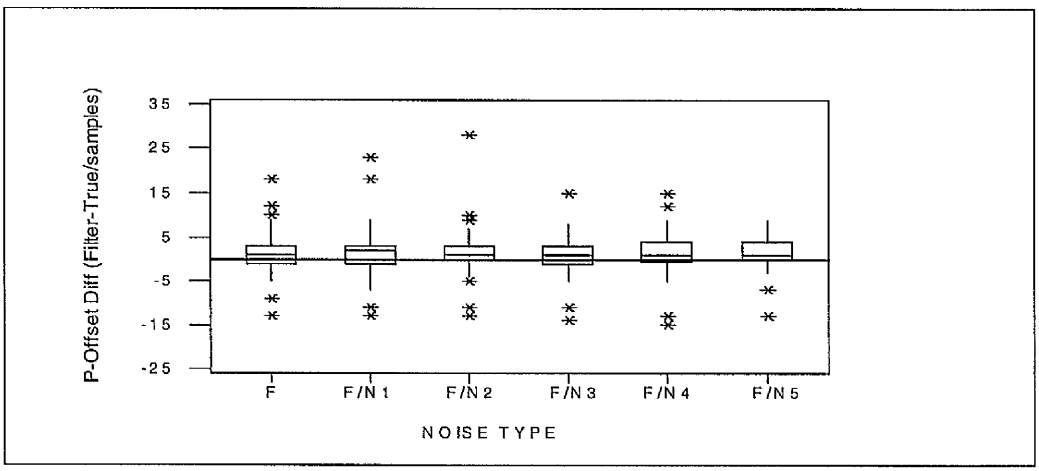

Figure 6.31(b) **Performance of the Glasgow Smoothing Filter (F) when estimating the P-offset in the absence and presence of noise. N1-N5 represents noise types 1-5.**

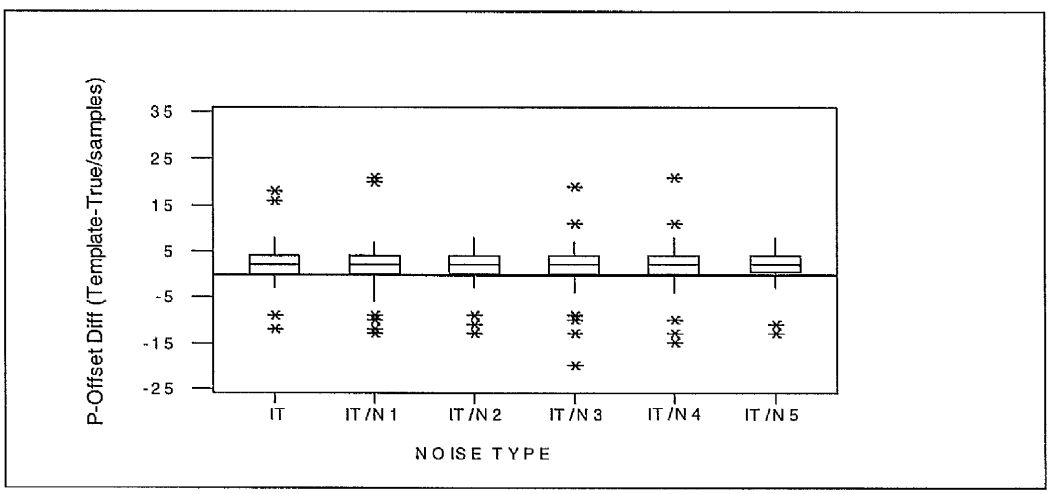

Figure 6.31(c) **Performance of the Individualised Template (IT) when estimating the P-offset in the absence and presence of noise. N1-N5 represents noise types 1-5.**

6.10.3 Results for the QRS Onset

The performance of the 77 test cases for each method of QRS-onset estimation are summarised in Table 6.24. The Glasgow smoothing filter clearly performed better than the conventional program and the individualised template. Although the use of the template eliminated any bias in the results for the noise-free ECGs, after the addition of excess noise, the results deteriorated. It was clear from the median of the signed differences that the QRS-onset was being consistently under-estimated by the template in the presence of the five noise types. Closer inspection of the spatial velocity data gave no explanation as to why this systematic bias was occurring. The only explanation was that a slight change in the data after adding noise and subsequent filtering, led to a better level of agreement between the template and spatial velocity data 3 sample points earlier than the location of the 'true' onset, for most of the 77 cases. It was apparent that both the Glasgow program and the Glasgow smoothing filter produced later QRS-onsets in the absence and presence of noise (see Figures 6.32(a),(b)&(c)). Although the addition of noise introduced a negative bias into the QRS-onset estimates determined by the template, the standard deviation of the differences about the 'true values' remained consistent across the different noise types.

	GP	GSF	IT
NO NOISE	5.68 2.00 1.76 3.00 0.50	3.99 1.00 1.72 2.00 0.00	5.53 0.00 2.33 2.00 -1.00
NOISE 1 High Freq 25μV RMS	15.74 2.00 3.85 3.00 0.00	4.49 1.00 1.95 2.00 0.00	11.52 -3.00 2.12 -1.00 -4.00
NOISE 2 Line Freq 50Hz, 25μV peak	5.97 1.00 2.02 3.00 0.00	3.65 1.00 1.57 2.00 1.00	11.48 -3.00 1.79 -1.00 -4.00
NOISE 3 Line Freq 60Hz, 25μV peak	7.79 1.00 1.96 2.50 1.00	3.96 1.00 1.73 2.00 0.00	12.26 -3.00 2.11 -1.50 - 4.00
NOISE 4 Baseline 0.3Hz, 0.5mV peak	8.34 2.00 2.36 3.00 1.00	6.48 1.00 2.41 2.00 0.00	11.18 -3.00 2.07 -1.00 -4.00
NOISE 5 Baseline & High Freq 0.3Hz, 0.5mV peak; 15μV RMS	6.58 2.00 2.22 3.00 0.00	4.56 1.00 1.91 2.00 0.00	11.84 -3.00 2.21 -1.00 -4.00

Table 6.24 **Performance of the conventional program, the filter and the template when estimating the QRS-onset in the presence of noise. Each of the above cells contains the following:**

$\sum_{1}^{77}(\text{Diff})^2 / 77$
Median
S.D.
U.Q.
L.Q.

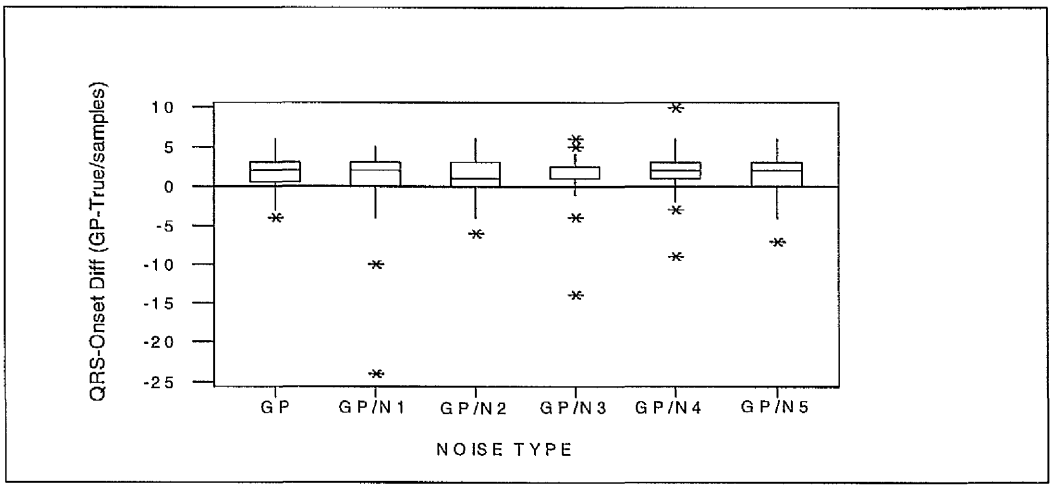

Figure 6.32(a) **Performance of the Conventional Glasgow Program (GP) when estimating the QRS-onset in the absence and presence of noise. N1-N5 represents noise types 1-5.**

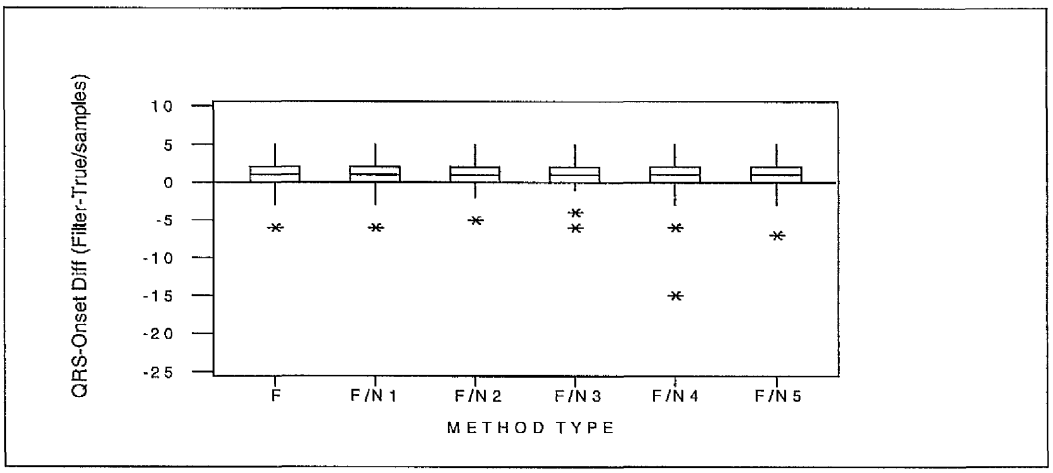

Figure 6.32(b) **Performance of the Glasgow Smoothing Filter (F) when estimating the QRS-onset in the absence and presence of noise. N1-N5 represents noise types 1-5.**

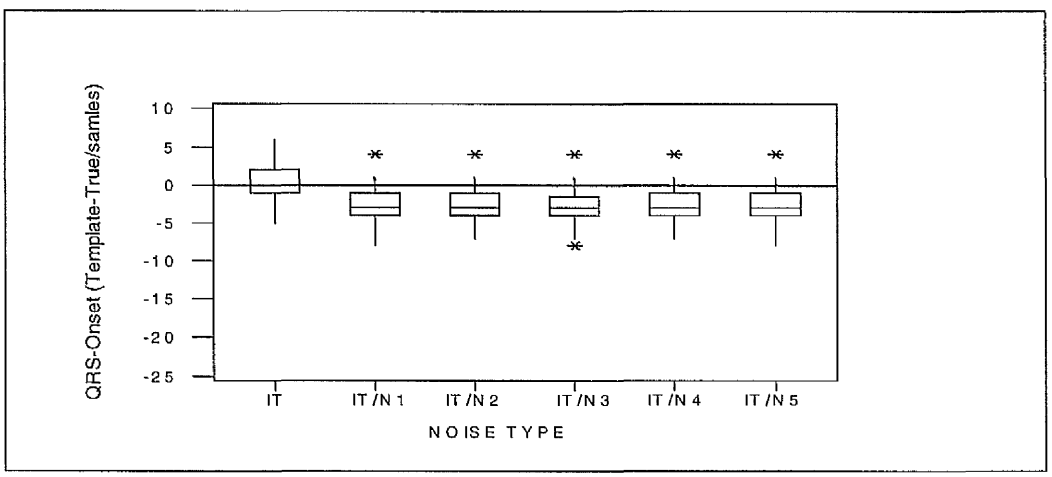

Figure 6.32(c) **Performance of the Individualised Template (IT) when estimating the QRS-onset in the absence and presence of noise. N1-N5 represents noise types 1-5.**

6.10.4 Results for the QRS Offset

Results for the estimation of the QRS-offset by each method are presented in Table 6.25. As with the case of the QRS-onset, the Glasgow smoothing filter produced the most accurate QRS-offset estimates. In the case of the conventional program, noise type 1 had a detrimental effect on the program's ability to estimate the offset (median difference=5 sample points from the true value). However, this bias was reduced greatly after applying the Glasgow smoothing filter as well as the template. Surprisingly, the addition of noise type 3 resulted in a median difference of zero for both the conventional program and smoothing filter. The template results were not affected in this manner, with a consistent median difference of 2 sample points across all the noise types (see also Figures 6.33(a),(b)&(c)).

	GP	GSF	IT
NO NOISE	19.88 1.00 3.91 5.00 -1.00	9.18 1.00 2.91 3.00 -1.00	12.47 2.00 3.18 3.00 0.00
NOISE 1 High Freq 25μV RMS	41.65 5.00 4.32 8.00 2.00	12.75 1.00 3.42 3.00 -1.00	13.40 2.00 3.37 3.00 0.00
NOISE 2 Line Freq 50Hz, 25μV peak	20.74 1.00 4.22 4.00 -1.00	10.48 1.00 3.15 3.00 -1.50	12.99 2.00 3.34 3.00 0.00
NOISE 3 Line Freq 60Hz, 25μV peak	42.97 0.00 6.59 3.00 -2.00	9.42 0.00 3.06 2.00 -1.00	13.48 2.00 3.41 3.00 0.00
NOISE 4 Baseline 0.3Hz, 0.5mV peak	20.42 2.00 4.13 4.50 -1.00	9.84 1.00 3.04 3.00 -1.00	13.55 2.00 3.30 4.00 0.00
NOISE 5 Baseline & High Freq 0.3Hz, 0.5mV peak; 15μV RMS	31.44 3.00 4.44 6.00 0.00	13.92 1.00 3.60 3.00 -1.00	14.58 2.00 3.53 3.50 0.00

Table 6.25 **Performance of the conventional program, the filter and the template when estimating the QRS-offset in the presence of noise. Each of the above cells contains the following:**

$\sum_{1}^{77}(\text{Diff})^2 / 77$
Median
S.D.
U.Q.
L.Q.

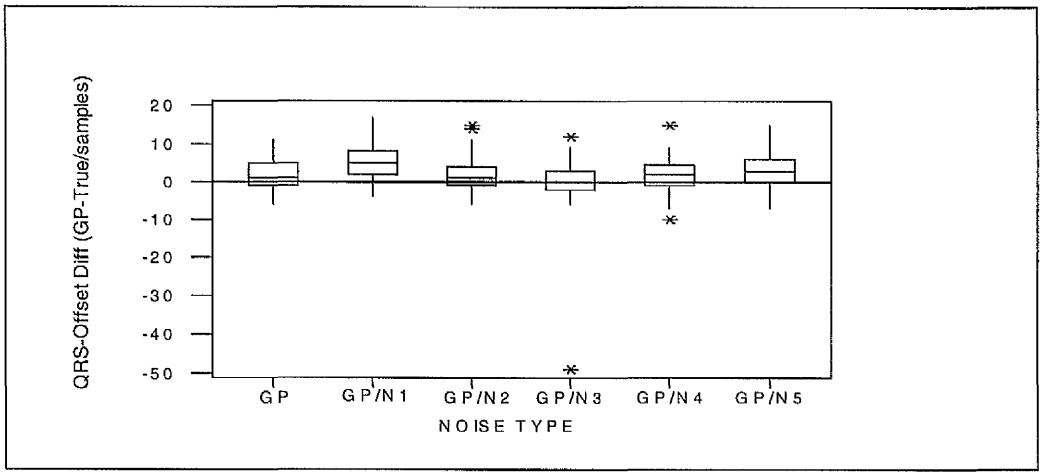

Figure 6.33(a) **Performance of the Conventional Glasgow Program (GP) when estimating the QRS-offset in the absence and presence of noise. N1-N5 represents noise types 1-5.**

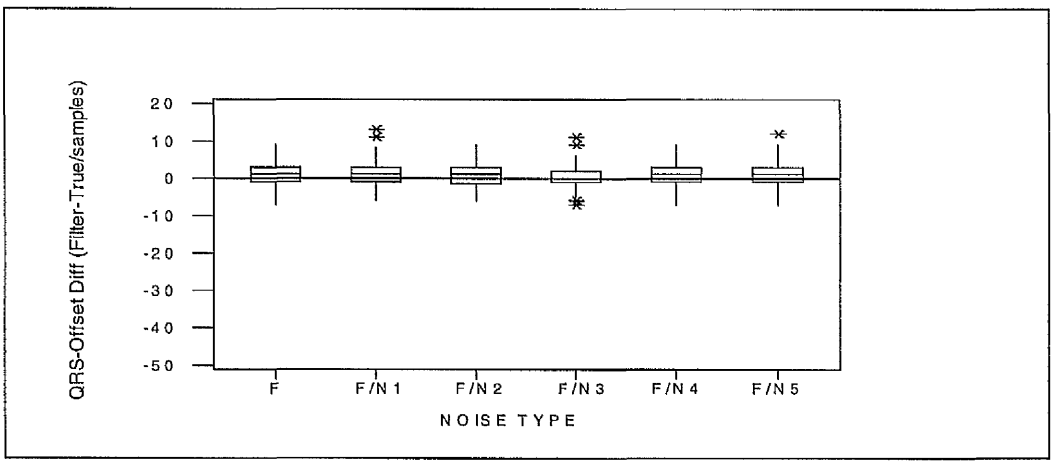

Figure 6.33(b) **Performance of the Glasgow Smoothing Filter (F) when estimating the QRS-offset in the absence and presence of noise. N1-N5 represents noise types 1-5.**

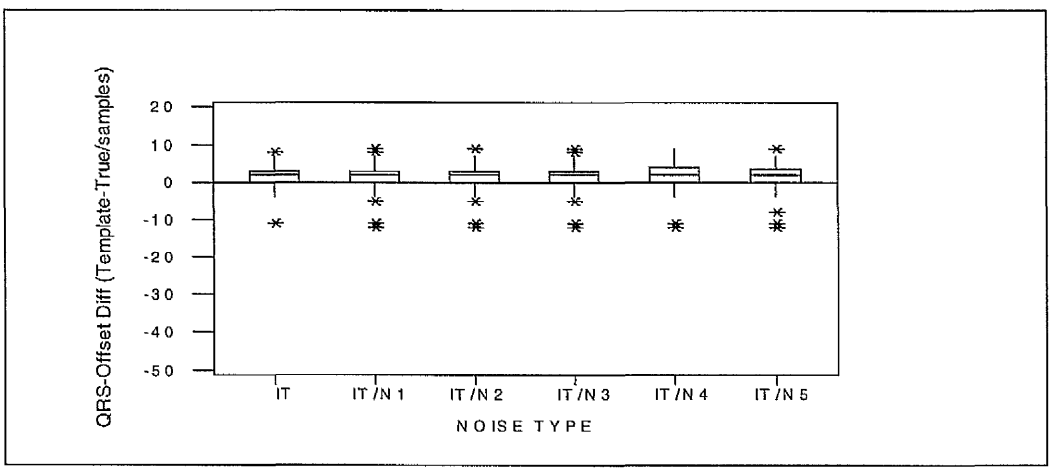

Figure 6.33(c) **Performance of the Individualised Template (IT) when estimating the QRS-offset in the absence and presence of noise. N1-N5 represents noise types 1-5.**

6.10.5 Results for the T-End

Table 6.26 summarises the performance of each method when estimating the T-ends in the presence of the different types of noise. It was clear that the individualised template performed best where the median difference remained consistent regardless of the type of noise. Although each method generally showed signs of a positive bias, this bias ranged from a maximum of 1 sample point about the true value for the individualised template, to a maximum of 6 sample points in the case of the conventional program. Overall, the results for each method remained fairly consistent across the different noise types (see Figures 6.34(a),(b)&(c)), leading to the conclusion that the addition of noise did not seem to affect the performance of any of the methods (for this set of ECGs at least).

	GP	GSF	IT
NO NOISE	274.09 6.00 14.55 9.50 3.00	174.66 5.00 11.76 9.00 1.00	103.83 1.00 10.01 3.00 -1.00
NOISE 1 High Freq 25μV RMS	215.61 6.00 12.67 10.00 3.00	181.58 5.00 11.99 8.00 2.00	108.69 1.00 10.23 4.00 -1.00
NOISE 2 Line Freq 50Hz, 25μV peak	215.91 6.00 12.21 9.00 3.00	179.71 5.00 11.96 9.00 1.00	101.03 1.00 9.88 4.00 -1.00
NOISE 3 Line Freq 60Hz, 25μV peak	239.03 5.00 13.78 9.00 3.00	184.61 5.00 12.26 9.00 1.00	111.81 1.00 10.50 3.00 -2.00
NOISE 4 Baseline 0.3Hz, 0.5mV peak	281.53 5.00 14.90 10.00 2.00	193.73 5.00 12.62 8.00 1.00	115.88 1.00 10.58 4.00 -1.00
NOISE 5 Baseline & High Freq 0.3Hz, 0.5mV peak; 15μV RMS	195.03 6.00 12.49 8.50 3.00	178.75 5.00 12.13 8.00 1.00	116.75 1.00 10.68 3.50 -1.50

Table 6.26 **Performance of the conventional program, the filter and the template when estimating the T-end in the presence of noise. Each of the above cells contains the following:**

$\sum_{1}^{77}(\text{Diff})^2 / 77$
Median
S.D.
U.Q.
L.Q.

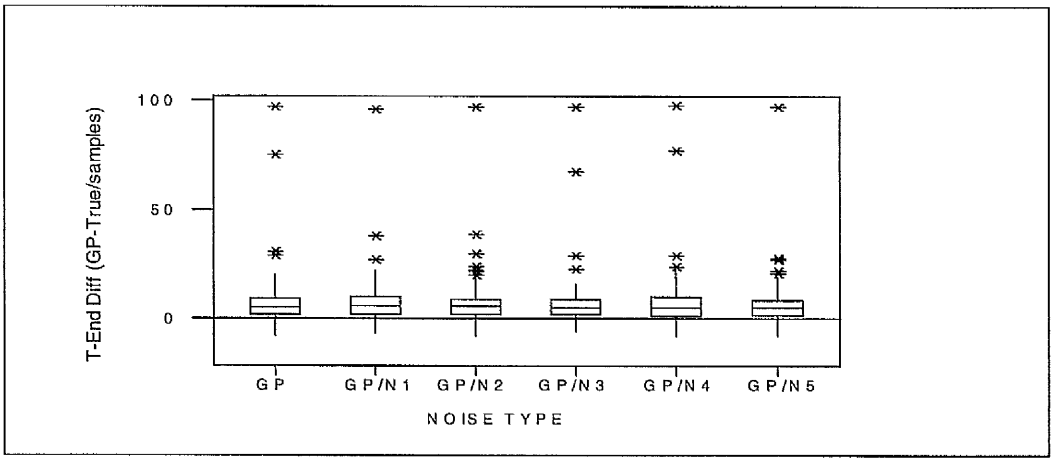

Figure 6.34(a) **Performance of the Conventional Glasgow Program (GP) when estimating the T-End in the absence and presence of noise. N1-N5 represents noise types 1-5.**

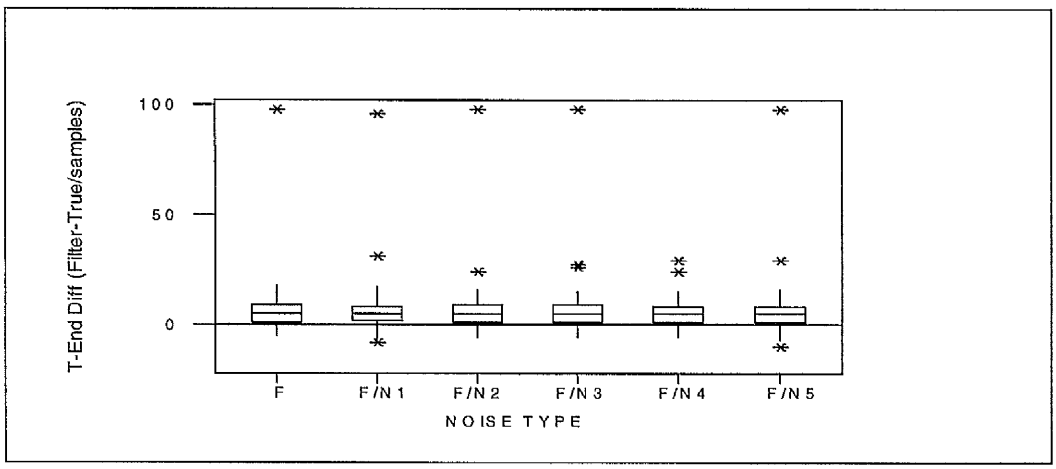

Figure 6.34(b) **Performance of the Glasgow Smoothing Filter (F) when estimating the T-End in the absence and presence of noise. N1-N5 represents noise types 1-5.**

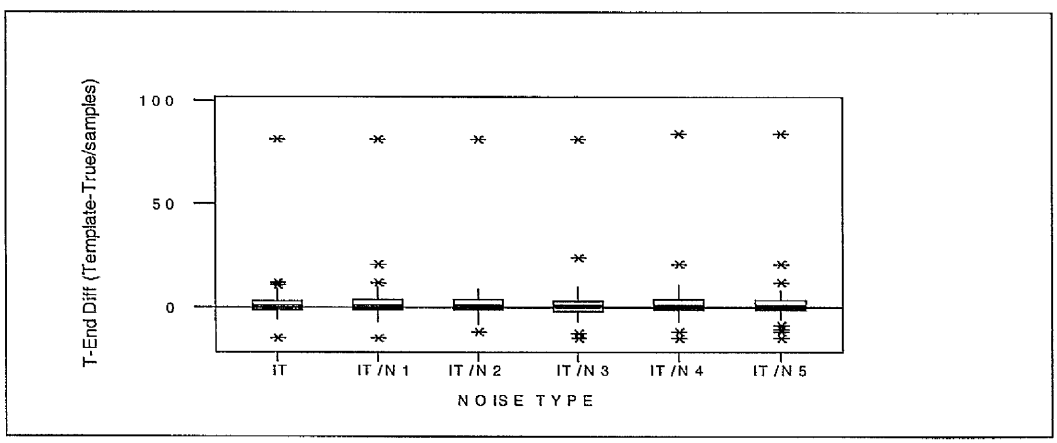

Figure 6.34(c) **Performance of the Individualised Template (IT) when estimating the T-End in the absence and presence of noise. N1-N5 represents noise types 1-5.**

6.11 CONCLUSIONS CONCERNING FIDUCIAL POINT ESTIMATION IN THE PRESENCE OF NOISE.

It has been shown that, for particular fiducial points the Glasgow smoothing filter coupled with the individualised template has improved the accuracy of ECG fiducial point location. For other fiducial points, the smoothing filter alone has been more successful. When the ECG signal was contaminated with excess noise, the Glasgow smoothing filter, once again, performed best when locating the P-offset, QRS-onset and QRS-offset of the 77 ECGs in the test set. With respect to estimating the P-onset and T-end, the individualised template combined with the Glasgow smoothing filter, performed best.

6.12 ESTIMATION OF THE FIDUCIAL POINT INTERVALS

In this section, interest is centred on the P-duration, QRS-duration, PR-interval and QT-interval. Each of the 88 durations/intervals was estimated from the conventional, filtered and template-determined estimates of the onsets and offsets of the 88 CSE ECGs. The relevant differences were computed forming the required durations and intervals. Boxplots of each type of fiducial interval difference (with respect to the true value) are depicted in Figures 6.35(a),(b),(c) and (d).

For the case of the P-duration (Figure 6.35(a)), the conventional Glasgow program performs better than the smoothing filter in terms of reducing the bias. This is due to the fact that there is a positive bias in both the onset and offset estimates produced by the conventional Glasgow program which almost cancel each other out, leaving only a slight negative bias. The performance of the filter is poorest in terms of

the bias, due to a large positive bias in the P-onset estimates and a small positive bias in the P-offsets. In the case of the template, although the bias is eliminated in the P-onset estimates there is a positive bias present in the offset data and so the resulting P-duration data shows signs of a slight positive bias. The overall variability appears to be smallest in the estimates produced by the template.

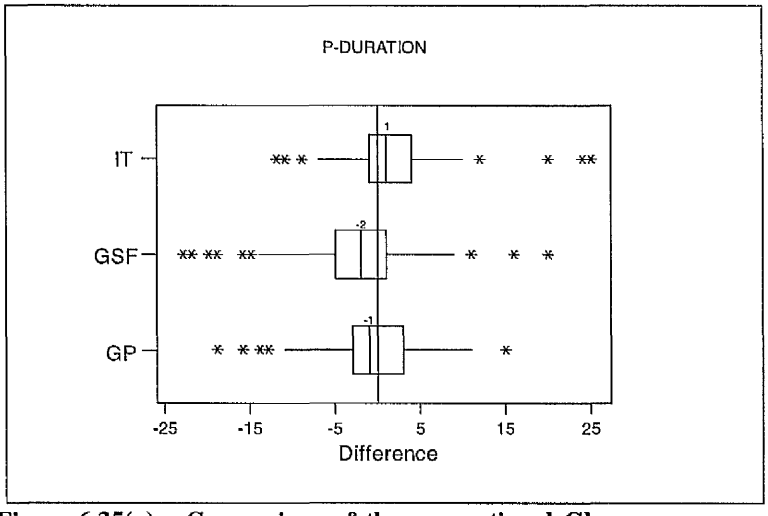

Figure 6.35(a) Comparison of the conventional Glasgow program (GP), Glasgow smoothing filter (GSF) and individualised template (IT) P-duration differences.
Difference = Estimate - True

From figure 6.35(b), it can be seen that although the bias in the QRS-duration estimates produced by the template is the greatest, the overall variability appears to be less than the other two methods of estimation. The Glasgow smoothing filter performs best in terms of exhibiting the smallest bias in the QRS-duration estimates.

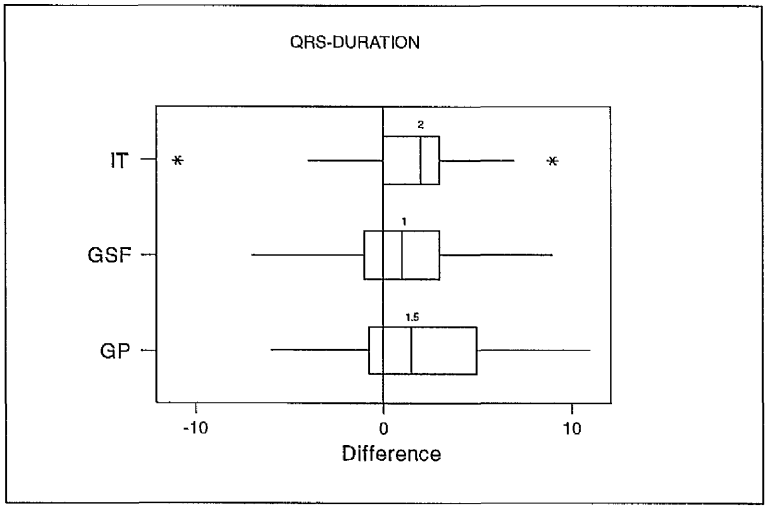

Figure 6.35(b) **Comparison of the conventional Glasgow program (GP), Glasgow smoothing filter (GSF) and individualised template (IT) QRS-duration differences.**
Difference = Estimate - True

From the boxplots of PR-interval estimation (Figure 6.35(c)), initial impressions are that the Glasgow smoothing filter does not perform as well as the conventional Glasgow program in terms of the variability and bias. However, by introducing the template into the program in addition to the smoothing filter, the bias is removed. The reason behind the poor performance of the smoothing filter is due to the poor estimation of the P-onset. Earlier in the chapter, the median difference between the smoothing filter QRS-onset estimate and 'true' onset was seen as being 1 sample point. However, the median difference for the P-onset was noted as being 3 sample points (6ms), thus resulting in poor PR-interval estimation (PR-interval=QRS-onset - P-onset).

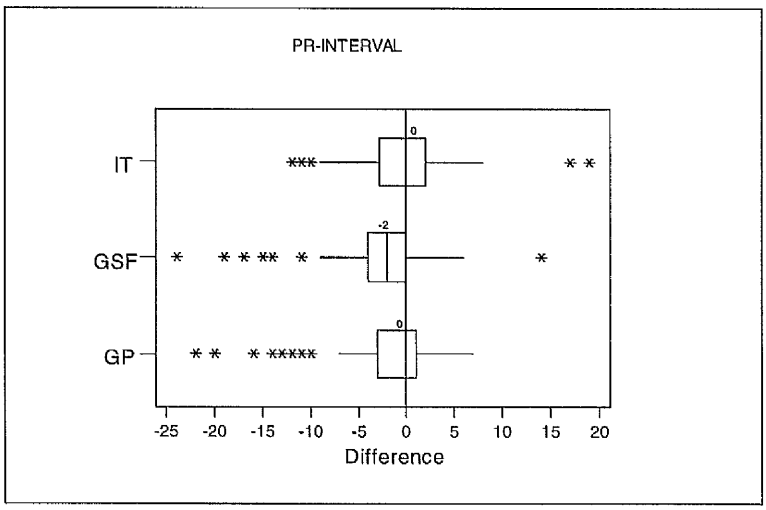

Figure 6.35(c) **Comparison of the conventional Glasgow program (GP), Glasgow smoothing filter (GSF) and individualised template (IT) PR-interval differences. Difference = Estimate - True**

When estimating the QT-interval, it is clear that the individualised template (combined with the Glasgow smoothing filter) performs best when estimating the QT interval (see Figure 6.35(d)). This is not surprising since the template has been far more successful in estimating the T-end, than the Glasgow smoothing filter and Glasgow program, respectively. The reason for the common outlier in Figure 6.35(d) is due to 2:1 A-V block, which has been explained in detail in section 6.7.3.

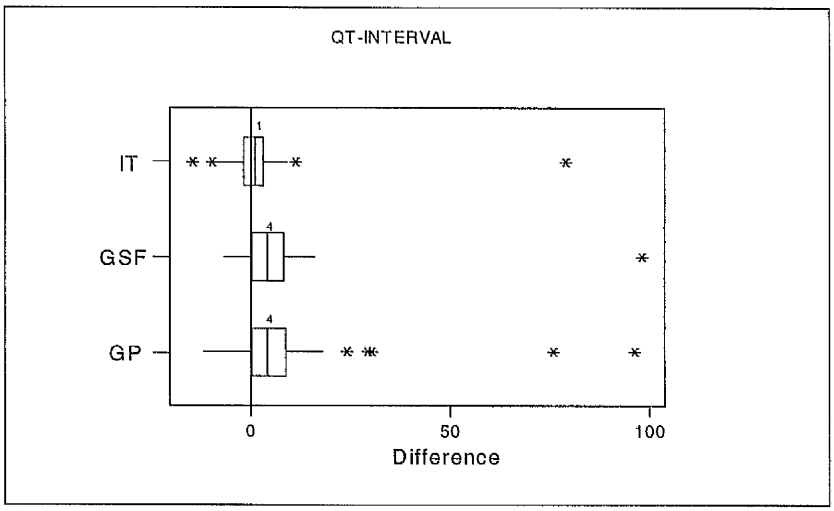

Figure 6.35(d) **Comparison of the conventional Glasgow program (GP), Glasgow smoothing filter (GSF) and individualised template (IT) QT-interval differences. Difference = Estimate - True**

Summary statistics (of the difference=estimate-true) for each methods performance in estimating the four fiducial intervals are tabulated in Tables 6.27(a), (b), (c) and (d). All measurements are in sample points.

Table 6.27(a) summarises the results of the P-duration estimated by each method with respect to the 'true' P-duration. It is clear from the median differences and the standard deviations that there is in fact no real difference between the Glasgow program and the individualised template in terms of estimating the duration of the P-wave apart form a slightly smaller inter-quartile range in the case of the individualised template, which was observed earlier from the boxplots in Figure 6.35(a).

Statistics	GP	GSF	IT
$\sum_{1}^{88} (\text{Diff})^2 / 88$	37.31	57.24	39.75
Median	-1.00	-2.00	1.00
S.D.	6.09	7.22	6.14
U.Q.	3.00	1.00	4.00
L.Q.	-3.00	-5.00	-1.00

Table 6.27(a) **Summary statistics (including the mean sum of squares) for the P-duration difference (estimated-true) for each method.**
GP=Glasgow Program; GSF=Glasgow smoothing filter; IT=Individualised Template
S.D. = standard deviation
U.Q. = upper quartile and L.Q. = lower quartile

Summary statistics of the QRS-duration differences for each method relative to the 'true' values are shown in Table 6.27(b). The standard deviation for the Glasgow smoothing filter is seen to be less than that of the individualised template with the conventional program performing worst. The inter-quartile range of the estimates for each method does, however, suggest that the template showed less variability in its QRS-duration estimates when compared to the other two methods.

Statistics	GP	GSF	IT
$\sum_{1}^{88} (\text{Diff})^2 / 88$	19.13	9.19	11.68
Median	1.50	1.00	2.00
S.D.	3.78	2.91	3.10
U.Q.	5.00	3.00	3.00
L.Q.	-0.75	-1.00	0.00

Table 6.27(b) **Summary statistics (including the mean sum of squares) for the QRS-duration difference (estimated-true) for each method.**
GP=Glasgow Program; GSF=Glasgow smoothing filter; IT=Individualised Template
S.D. = standard deviation
U.Q. = upper quartile and L.Q. = lower quartile

A summary of the results for the differences between each of the three versions of the Glasgow program and the corresponding 'true' values for the PR-interval are shown in Table 6.27(c). It was evident that the individualised template in conjunction with the smoothing filter seemed to perform best out of the three methods with the filter performing worst in terms of the amount of bias in the estimates.

Statistics	GP	GSF	IT
$\sum_{1}^{88} (\text{Diff})^2 / 88$	32.38	39.68	22.74
Median	0.00	-2.00	0.00
S.D.	5.40	5.67	4.79
U.Q.	1.00	0.00	2.00
L.Q.	-3.00	-4.00	-2.75

Table 6.27(c) **Summary statistics (including the mean sum of squares) for the PR-interval difference (estimated-true) for each method.**
GP=Glasgow Program; GSF=Glasgow smoothing filter; IT=Individualised Template
S.D. = standard deviation
U.Q. = upper quartile and L.Q. = lower quartile

Results for the QT-interval difference estimated by each method with respect to the 'true' value, are summarised in Table 6.27(d). There is clearly a vast improvement in QT-interval estimation, particularly between the conventional Glasgow program algorithm and that which combines the Glasgow smoothing filter with the template technique. Indeed, it is observed that the median difference between the Glasgow program and corresponding 'true' values drops from 4 sample points (8ms) to 1 sample point (2ms) when the smoothing filter is coupled with the template. Likewise, the sample standard deviation of the differences drops from 14.1 to 9.4 sample points. In general, the smoothing filter on it own also performs better than the conventional program with a drop in the sample standard deviation.

Statistics	GP	GSF	IT
$\sum_{1}^{88} (\text{Diff})^2 / 88$	240.09	151.81	90.02
Median	4.00	4.00	1.00
S.D.	14.14	11.30	9.41
U.Q.	8.75	8.00	3.00
L.Q.	-3.00	-4.00	-2.75

Table 6.27(d) **Summary statistics (including the mean sum of squares) for the QT-interval difference (estimated-true) for each method.**
GP=Glasgow Program; GSF=Glasgow smoothing filter; IT=Individualised Template
S.D. = standard deviation
U.Q. = upper quartile and L.Q. = lower quartile

6.13 CONCLUSIONS CONCERNING FIDUCIAL INTERVAL ESTIMATION

Table 6.28 below, summarises the methods which performed best when estimating each of the four fiducial intervals/durations.

Interval/Duration	Best Method
P-Duration	GP & GSF & IT
QRS-Duration	GP & GSF
PR-Interval	GP & GSF & IT
QT-Interval	GP & GSF & IT

Table 6.28 Methods which performed best when estimating fiducial intervals/durations.

It is clear that the individualised template (combined with the smoothing filter) performs best when estimating the P-duration, PR-interval and QT-interval. The Glasgow smoothing filter appears to perform best when estimating the QRS duration. These results are consistent with those observed earlier in the chapter where the actual fiducial points were estimated.

6.14 EVALUATION OF THE CONVENTIONAL AND MODIFIED PROGRAMS USING THE CSE TOLERANCE LIMITS

6.14.1 The CSE Standards/Tolerance Limits

Recommendations made in 1985 by the CSE working party stated that for measurements to be acceptable, the results should approach the referee (true) results as closely as possible. This resulted in the publication of a set of standards with which all future results would be compared. It was suggested that any program where the standard

deviation of the differences of its estimates from the 'true' values exceeded these standards, should be improved with respect to its wave recognition. These standards/tolerance limits are shown in Table 6.29.

FIDUCIAL POINT	TOLERANCE LIMIT (samples points)
P ONSET	5
P OFFSET	6
QRS ONSET	3
QRS OFFSET	6
T END	15

Table 6.29 CSE Tolerance Limits

6.14.2 Evaluation of the Methods of Estimation

Table 6.30 summarises the noise-free standard deviations of the estimated-true differences for the 88 CSE ECGs in sample points.. Results are presented for each of the three versions of the Glasgow program (conventional, smoothing filter and template) where each fiducial point is compared to the declared tolerance limit. Most of the standard deviations fell within the required limits, except for the case of the P-onset, where the standard deviations for the conventional program and filter both were just greater than the tolerance limit. Once again it was found that the individualised template performed best when estimating the T-end and P-onset.

88 ECGS IN THE ABSENCE OF NOISE

FIDUCIAL POINT	TOLERANCE LIMIT	GP	GSF	IT
P ONSET	5.00	5.17	5.50	4.71
P OFFSET	6.00	5.48	4.14	4.07
QRS ONSET	3.00	1.74	1.65	2.29
QRS OFFSET	6.00	3.78	2.91	3.10
T END	15.00	14.00	11.21	9.53

Table 6.30 Comparison of the conventional Glasgow program (GP), Glasgow smoothing filter (GSF) and individualised template (IT) standard deviations of the differences (with respect to the 'true' values) with CSE tolerance limits (in sample points).

The standard deviations (in sample points) for the 77 noisy CSE ECGs (in the presence of five noise types) along with the tolerance limit for each fiducial point are presented in Tables 7.31(a), (b) and (c). It can be seen that most of the standard deviations in the case of the Glasgow program and the Glasgow smoothing filter exceeded the stated tolerance limit for P-onset. The individualised template performed best, with only the P-onset in the presence of noise type 4 being estimated poorly.

Both the smoothing filter and the individualised template perform well in the case of the P-offset, where the standard deviations of the differences (with respect to the true values) all lay below the tolerance limit. The Glasgow program performed poorly when estimating the P-offset in the presence of noise type 1.

The results for the QRS onset and QRS offset in the absence and presence of noise all fell below the CSE tolerance limits in the case of the Glasgow smoothing filter and the individualised template. The conventional program estimated the QRS onset and offset poorly in the presence of noise types 1 and 3 respectively.

Finally, it can be seen from each of the three tables that the T-end results produced by each program version fell below the required limit, although in the presence of noise type 4, the standard deviation of the conventional program difference (with respect to the 'true value') only just fell inside the stated limit.

Conventional Glasgow Program

FIDUCIAL POINT	TOLERANCE LIMIT	NO NOISE	NOISE 1	NOISE 2	NOISE 3	NOISE 4	NOISE 5
P ONSET	5.00	5.04	8.15	5.20	6.03	4.93	7.20
P OFFSET	6.00	5.31	7.04	5.73	4.65	4.42	5.35
QRS ONSET	3.00	1.76	3.85	2.02	2.47	2.36	2.22
QRS OFFSET	6.00	3.91	4.32	4.22	6.59	4.13	4.22
T END	15.00	14.55	12.67	12.69	13.78	14.90	12.49

Table 6.31(a) **Standard Deviations (in sample points) of the differences (Glasgow program - 'true') in the absence and presence of noise.**

Glasgow Smoothing Filter

FIDUCIAL POINT	TOLERANCE LIMIT	NO NOISE	NOISE 1	NOISE 2	NOISE 3	NOISE 4	NOISE 5
P ONSET	5.00	5.38	5.20	6.67	4.03	5.30	4.93
P OFFSET	6.00	4.15	4.87	4.75	3.76	4.21	3.41
QRS ONSET	3.00	1.72	1.95	1.57	1.73	2.41	1.91
QRS OFFSET	6.00	2.91	3.42	3.15	3.06	3.04	3.60
T END	15.00	11.76	11.99	11.96	12.26	12.62	12.13

Table 6.31(b) **Standard Deviations (in sample points) of the differences (Glasgow smoothing filter - 'true') in the absence and presence of noise.**

Individualised Template

FIDUCIAL POINT	TOLERANCE LIMIT	NO NOISE	NOISE 1	NOISE 2	NOISE 3	NOISE 4	NOISE 5
P ONSET	5.00	4.08	3.22	4.22	4.77	6.23	4.27
P OFFSET	6.00	4.07	4.96	3.67	4.80	4.61	3.48
QRS ONSET	3.00	2.33	2.12	2.06	2.11	2.07	2.21
QRS OFFSET	6.00	3.18	3.37	3.34	3.41	3.30	3.53
T END	15.00	10.01	10.23	9.88	10.50	10.58	10.68

Table 6.31(c) **Standard Deviations (in sample points) of the differences (Individualised template - 'true') in the absence and presence of noise.**

6.15 CONCLUSIONS CONCERNING PROGRAM EVALUATIONS

It has been shown that the Glasgow smoothing filter and the individualised template perform well when estimating fiducial points, in terms of remaining within the required standards/tolerance limits,

in the absence as well as in the presence of certain noise types. It has been seen that both methods, in conjunction with the existing Glasgow logic, have shown considerable improvement in the estimation of **all** the fiducial points compared to the conventional Glasgow program, when tested on the CSE data set.

6.16 DISCUSSION

The number of ECGs used in each of the training sets was limited which has obvious implications on the reliability of the conclusions. However, due to the fact that only 24 ECGs had been visually analysed in full, circumstances did not allow for a larger training set.

The procedure of stepwise regression used for the construction of the linear templates is not without pitfalls. Any variable selection procedure is prone to overfit the data in a model. However, the advantage of forward stepwise regression (as in this case) is that the model starts with 'nothing' and then incorporates the variables one step at a time. This is the opposite to backwards stepwise regression which include multiple variables from the start. If, in this chapter, 2 or more variables had been selected for the final model then it could be argued that the choice of variables was not necessarily the best fit. However, in this case, at most one explanatory variable was chosen in the selection procedure and so in fact there was no problem of overfitting in the model.

Templates based on 21 points were used here to locate the fiducial points of the different components of an ECG (i.e. P-wave, QRS-complex and T-wave). Experience suggested that for a waveform of

greater magnitude, a bigger template should have been employed. This would therefore involve constructing a template incorporating more than 21 sample points or alternatively a template still consisting of 21 points, but where each sample point used for the template was separated by 6 or more milliseconds. The number of sample points separating the template points would be arbitrary and would involve a process of trial and error. This could prove to be a time consuming process. Another option could be to construct a flexible template which would incorporate the magnitude of the waveform. so that a larger template would be applied to those waveforms with steeper slopes and vice versa for those with less steep slopes.

6.17 SUMMARY

The technique of individualised linear templates has proved to be successful when estimating the P-onset and T-end of an ECG waveform both in the absence and presence of noise. The Glasgow smoothing filter has been shown to perform best of all when estimating the P-offset, QRS-onset and QRS offset. When each estimated fiducial point was compared to a set of standards published by the CSE working party, it was found that most of the estimates produced by the Glasgow smoothing filter (in the absence and presence of noise) lay within the required tolerance limits. Almost all the template-determined estimates remained within the limit while the conventional Glasgow program, once again, performed poorest.

When the fiducial points determined by the conventional Glasgow program, Glasgow smoothing filter and template were used to construct the corresponding duration and interval estimates it was

found that the P-duration, PR-interval and QT -interval were best estimated using the template-determined fiducial point estimates. The QRS duration was best estimated using the Glasgow smoothing filter-determined fiducial points.

CHAPTER SEVEN

CONCLUSIONS

7.1 METHODS TESTED

The main objective of this study was to improve the ECG wave measurement system within the Glasgow Program. There were three main techniques investigated. These were:

(i) Methods of splitting

(ii) Software based neural networks

(iii) Methods of linear templates

In chapters 3, 4 and 6 it was seen that, overall, the idea of splitting and averaging ECGs improved the quality of the signal. However, due to the lack of accurate P-onset estimation when utilising the new Glasgow smoothing filter, the resulting P-durations and PR-intervals were poorly estimated when compared to the conventional program. In fact, late P-onset detection compared to the reference value resulted in shorter P-durations and PR-intervals. There was, however, an improvement in the estimation of the P-offset, QRS-onset, QRS-offset and the T-end when the Glasgow smoothing filter was incorporated. This meant that when compared to the conventional Glasgow program, there was an increase in the accuracy of QRS-duration and QT-interval estimation.

Software based neural networks were trained to locate the QRS-onset using a training set of 75 filtered CSE ECGs (using the

Glasgow smoothing filter). It was concluded that although the network with 63 input neurons, 50 hidden neurons and 21 output neurons performed best on a validation set of 50 ECGs (taken from the training set and deliberately contaminated with high frequency 25μV RMS noise), the performance was not consistent when the networks were evaluated using an independent test set consisting of 48 "new" CSE ECGs. It was evident that with the implementation of the Glasgow smoothing filter without the use of neural networks, there was less difference between the estimated and the true QRS-onsets than those produced by the conventional Glasgow program.

Investigation of the use of linear templates in fiducial point estimation led to the conclusion that, for a set of 88 CSE ECGs, by combining an adjustable linear template with the Glasgow smoothing filter and conventional program, it was possible to improve on the accuracy of the P-onset and particularly the T-end location when compared to the conventional Glasgow program and the Glasgow smoothing filter. Whilst the template improved the estimation of the P-onset and T-end, the Glasgow smoothing filter performed best when estimating the P-offset and QRS-onset and QRS-offset. When the relevant duration and interval measurements were calculated for each method, it was seen that in the case of the P-duration, there was not much of a difference between the template-determined estimates and the conventional Glasgow program. The template did, however, improve the estimation of the of the PR-interval and QT-interval when compared to the Glasgow smoothing filter and conventional program. In the case of the QRS-duration, the Glasgow smoothing filter produced the best estimates. Tables 7.1 and 7.2 summarise the standard deviations of the differences observed between each of the

methods and the corresponding reference values for each fiducial point and duration/interval respectively in sample points. Recommendations for the best method for estimating each fiducial point are summarised in Table 7.3. Also included are the tolerance limits set by the CSE working party and the corresponding standard deviations of the differences between the estimated fiducial points and the 'true' values in sample points.

Difference	GP	GSF	IT
P Onset	5.71	5.50	4.71
P Offset	5.48	4.14	4.07
QRS Onset	1.74	1.65	2.29
QRS Offset	3.78	2.91	3.10
T End	14.00	11.21	9.53

Table 7.1 Standard deviations of the estimated-true fiducial point differences (in sample points) for the conventional Glasgow program (GP), Glasgow smoothing filter (GSF) and the individualised template (IT).

Difference	GP	GSF	IT
P Duration	6.09	7.22	6.14
QRS Duration	3.78	2.91	3.10
QT Interval	14.14	11.30	9.41
PR Interval	5.40	5.67	4.79

Table 7.2 Standard deviations of the estimated-true duration/interval differences (in sample points) for the conventional Glasgow program (GP), Glasgow smoothing filter (GSF) and the individualised template (IT).

Fiducial Point	Recommended Technique	CSE Tolerance Limit	S.D. of Difference Estimated-True
P Onset	GP+GSF & IT	5.00	4.71
P Offset	GP+GSF	6.00	4.07
QRS Onset	GP+GSF	3.00	1.65
QRS Offset	GP+GSF	6.00	2.91
T End	GP+GSF & IT	15.00	9.53

Table 7.3 Recommendations for the estimation of ECG wave fiducial points within the Glasgow program. Also included are the CSE tolerance limits and the corresponding standard deviations (S.D.) of the differences in sample points (estimated-true). GSF=Glasgow smoothing filter and IT=individualised template

7.2 LIMITATIONS

The main problem with this study was the limited number of ECGs available with complete 'true' values for the fiducial points. Much effort is required to obtain estimates of these by visual identification for a training or intended test set. A problem encountered with the Glasgow smoothing filter was that the alignment points required for averaging the individual beats within the Glasgow program were shifted for some cases. This was due to the fact that the waveform became smoother after filtering, shifting the maximum spatial velocity. It was these 'shifted' maximum spatial velocities which were then used within the Glasgow program criteria for locating each of the alignment points, in turn shifting these points. Due to this discrepancy, not only would the original recording have to be visually analysed for fiducial point selection but so would the filtered recording.

7.3 FUTURE DEVELOPMENT

The techniques used in the study have shown that it is possible to enhance the performance of automated analysis programs through methods of filtering and template matching. It would, however, be desirable to eventually construct a large multilead database of ECGs complete with reference duration and interval measurements for future testing.

Further work into template location of fiducial points is currently being undertaken in order to construct a more flexible template. This would involve an initial check on the size of the waveform being examined. The steeper the slope of the waveform the greater would be

the number of points in the template. Also being investigated is a search region with an undefined endpoint, where template matching will continue until an overall minimum sum of squares function is located rather than locating one in a defined search region.

Locating wave measurements is only a small part of the Glasgow program. However, improvements in the estimation of wave measurements and diagnostic criteria within the program will clearly lead to a more enhanced and effective version of the Glasgow Program.

REFERENCES

Adli, Yamamoto, Y., Nakamura, T. (1999)
Studies on eliminating interference by electromagnetic induction from power lines in ECG signals.
Front Med Biol Eng; 9(3): 229-239.

Alraun, W., Zywietz, C., Borovsky, D., Willems, J. L. (1983)
Methods for Noise Testing of ECG Analysis Programs.
In : Computers in Cardiology. ed. Ripley, K. L.
IEEE Computer Society, Long Beach, CA : pp253

Anderson, J. (1995)
An Introduction to Neural Networks.
MIT Press, Massachusetts.

Bailey, J. J., Horton, M., Itscoitz, S. B. (1974)
A Method for Evaluating Computer Programs for Electrocardiographic Interpretation.
III. Reproducibility Testing and the Sources of Program Errors.
Circulation; **50** : 88-93

Biomedical Digital Processing (1993)
Tompkins, W. J., Ed.
Prentice Hall, New Jersey.

Bourdillon, P. J., Denis, B., Harms, F. M. A., Mazzocca, G., Meyer, J., Robles de Medina, E. O., Ritsema van Eck, H. J., Willems, J. L. (1982)
European experience in the standardisation of measurements and of definitions of the Electrocardiogram.
In : Computerised interpretation of electrocardiograms VII. ed. Laks,M
New York, Engineering Foundation : p9.

Branscombe, M. (1990)
Modelling the Brain
Program Now, June : 28-30

Burdon Sanderson, J., Page, F. J. M. (1878)
Experimental results relating to the rhythmical and excitatory motions of the ventricle of the heart of the frog and the electrical phenomena which accompany them.
Proceedings of the Royal Society of London; **27** : 410-414.

Burger, H. C., van Milaan, J. B. (1946), (1947), (1948)
Heart vector and leads I, II and III.
British Heart Journal; (1946) **8** : 157-161, (1947) **9** : 154-160,
(1948) **10** : 229-233.

Caceres, C. A., Steinberg, C. A., Abraham, S., Carberry, W. J.,
McBride, J. M, Tolles W. E., Rikli E.D. (1962)
Computer extraction of electrocardiographic parameters.
Circulation; **25**: 356-362.

Cady, L.D. Jr, Woodburgy, M.A., Tick, L.J., Gelertner, M.M. (1961)
A Method for Electrocardiogram Wave Pattern Estimation.
Example : Left Ventricular Hypertrophy.
Circulation Research; **9** : 1078-82.

Committee of the American Heart Association for the Standardisation
of Precordial Leads.
(a) Supplementary report. (1938)
American Heart Journal; **15**: 235-239
(b) Second supplementary report. (1943)
Journal of American Medical Association; **121**: 1349-1351.

Committee of the American Heart Association for Standardisation of
Electrocardiographic Nomenclature. The standardisation of
electrocardiographic nomenclature. (1943)
JAMA; **121**, 1347-49.

Daskalov, I. K., Christov, I. I.
Automatic detection of electrocardiogram T-wave end.
Medical & Biological Engineering and Computing; 37(3): 348-53.

Devine, B. (1990)
Neural Networks in Electrocardiography
MSc Dissertation, University of Glasgow.

Edenbrandt, L., Devine, B., Macfarlane, P. W. (1992)
Neural Networks for Classification of ECG ST-T Segments
Journal of Electrocardiography; 25(3): 167-173.

Einthoven, W. (1901)
Un nouveau galvanometre.
Arch. Neerl. Sci. Exactes Nat.; **6** : 625-633.

Einthoven, W. (1903)
Die galvanometrische Registrirung des menschlichen Elektrokardiogramms, Zugleich eine Beurtheilung der Anwendung des capilar-Elektrometers in der Physiologie.
Pfluegers Arch; **99**: 472-480.

Einthoven, W., Fahr, G. E., De Waart, A. (1913)
Uber die Richtung und die manifeste Grosse der potentialschwankungen im menschlichen Herzen und uber den Einfluss der Herzlage auf die Form des Elektrokardiogramms.
Pfluegers Arch.; **150** : 275-315.
(Translation : Hoff H. E., Sekelj P. American Heart Journal (1950); **40** : 163-211).

Engelmann, T. W. (1878)
Ueber das electrische Verhalten des thatigen Herzens.
Pfluegers Arch; **17**: 68-99.

Fisch, C. (1980)
The Clinical Electrocardiogram : A Classic.
Circulation; **62** (suppl. III): 1-4.

Forbes, A. D., Jimison, H. B. (1987)
A QRS detection algorithm.
Journal of Clinical Monitoring; 3(1): 53-63.

Frank, E. (1956)
An accurate, clinically practical system for spatial vectorcardiography.
Circulation; **13** : 737-749.

Goldberger, E. (1942)
A simple, indifferent, electrocardiographic electrode of zero potential and a technique of obtaining augmented, unipolar, extremity leads.
American Heart Journal; **23** : 483-492.

Hebb, D. O. (1949)
The Organisation of Behaviour : A Neuropsychological Theory.
New York : John Wiley

Hu, Y. H., Tompkins, W. J., Urrusti, J. L., Afonso, V. X. (1993)
Applications of Artificial Neural Networks for ECG Signal Detection and Classification.
Journal of Electrocardiology; **26**, 66-73.

Hughes, H.C., Bertolet, R.D., Brownlee, R. R. (1983)
A new atrial lead with improved stability and P-wave detection.
Pacing & Clinical Electrophysiology; 6(4): 726-34.

Joint Recommendations of the American Heart Association and the Cardiac Society of Great Britain and Ireland: Standardisation of precordial leads. (1938)
American Heart Journal; **15**, 107-8, 235-9.

Kadambe, S., Murray, R., Boudreaux-Bartels, G. F. (1999)
Wavelet transform-based QRS complex detector.
IEEE Transactions on Biomedical Engineering; 46(7): 838-48.

Kolen, J. F., Pollack, J. B. (1990)
Back Propagation is Sensitive to Initial Conditions.
Complex Systems; **4**, 269-80.

Kolliker, A., Muller, H. (1856)
Nachweis der negativen schwankung des Muskelstroms am naturlich sich contrahirenden Muskel.
Verh. Phys. Med. Ges. Wurzburg; **6**: 528-33.

Korrs, J. A., Herpen, M. D., van Bemmel, J. H. (1999)
QT dispersion as an Attribute of T-Loop Morphology.
Ciculation; 99: 1458-1463.

Kossman, C. E., Brody, D. A. Burch, G. E. et al. (1967)
American Heart Association Committee on Electrocardiography.
Recommendations for standardisation of leads and specifications of instruments in electrocardiography and vectorcardiography.
Circulation; **35**, 583-602.

Lawrie, T.D.V., Macfarlane, P.W. (1968)
Towards Automated ECG Interpretation.
In: Computers in the Service of Medicine. eds. McLachlan G. & Shegog R.A.
London Oxford Press : 101-12.

Li, Z. A., Han, J. Y., Yang, X. T. (1986)
Analysis of complicated arrhythmias using a new system for P-wave detection.
Chinese Journal of Internal Medicine; 25(8): 469-71.

Macfarlane, P. W., Lorimer, A. R., Lawrie, T. D. V. (1971)
3 and 12-lead electrocardiogram interpretation by computer. A comparison on 1093 patients.
British Heart Journal; **3** : 366-374.

Macfarlane, P. W., Lawrie, T. D. V. (1974)
An Introduction to Automated Electrocardiogram Interpretation.
London, Butterworths.

Macfarlane, P. W., Watts, M. P., Peden, J., Lenox, G., Lawrie, T. D. V. (1976)
Computer assisted ECG interpretation.
British Journal of Clinical Equipment; **1** : 61-67.

Macfarlane, P. W., Peden, J., Lennox, G., Watts, M. P., Lawrie, T. D. V. (1977)
The Glasgow System
In : Trends in Computer Processed Electrocardiograms eds. van Bemmel J. H. & Willems J. L.
North Holland, Amsterdam : pp143-150

Macfarlane, P. W. (1979)
A hybrid lead system for routine electrocardiography.
In : Progress in Electrocardiology. ed. Macfarlane P. W.
Tumbridge Wells : Pittman Medical : 1-5.

Macfarlane, P. W., Willems, J. L. on the behalf of the CSE Working Party, (1983)
The CSE Project : progress as viewed by the co-operating centers.
In : Computerised interpretation of electrocardiograms VIII. ed. Selvester, R.
New York, Engineering Foundation.

Macfarlane , P. W., Watts, M. P., Podolski, M., Shoat, D., Lawrie, T. D. V. (1986)
The New Glasgow System
In: Computer ECG Analysis: Towards Standardization. ed. Willems, J. L., van Bemmel, J. H. & Zywietz, C.
Elsevier Science Publishers B.V. (North-Holland)

Macfarlane, P. W. (1989)
In : Comprehensive Electrocardiology. eds. Macfarlane, P. W. & Lawrie T. D. V. The Coming of Age of Electrocardiology, pp 3-40.
Oxford, Pergamon Press.

Macfarlane, P. W. (1989)
In : Comprehensive Electrocardiology. eds. Macfarlane, P. W. & Lawrie T. D. V. Lead Systems, pp 315-352.
Oxford, Pergamon Press.

Macfarlane, P.W. (1990)
A Brief History of Computer Assisted Electrocardiography.
Methods of Information in Medicine; **29** : 272-281.

Macfarlane, P. W., Devine, B., Latif, S., McLaughlin, S. C., Shoat, D. B., Watts, M. P. (1990)
Methodology of ECG Interpretation in the Glasgow Program
Methods of Information in Medicine; **29** : 354-361.

Mann, H. (1920)
A method of analyzing the electrocardiogram.
Arch. Intern. Med.; **25** : pp283-94.

Marey, E. J. (1876)
Des variations electriques des muscles et du coeur en particulier etudies au moyen de l'electrometre de M. Lippmann.
Comptes Rendus de l'Academie des Sciences; **82**: 975-977.

McCulloch, W. S., Pitts, W. H. (1943)
A Logical Calculus for the Ideas Immanent in Nervous Activity.
Bulletin of Mathematical Biophysics; **5** : 115-133.

McLaughlin, N. B., Campbell, R. W. F., Murray, A. (1995)
Comparison of automatic QT measurement techniques in the normal 12 lead electrocardiograms.
British Heart Journal; 74: 84-89.

McLaughlin, N. B., Campbell, R. W. F., Murray, A. (1996)
Accuracy of four automatic QT measurement techniques in cardiac patients and healthy subjects.
Heart; 76: 422-426.

Minsky, M. L., Papert, S. A. (1969)
Perceptrons: An introduction to computational geometry.
Cambridge, MA : MIT Press.

Mortara, D. W. (1977)
Digital Filters for ECG Signals.
In : Computers in Cardiology. eds. Ostrow, H. G. & Ripley, K. L.
IEEE Computer Society, Long Beach, CA : 511-514.

Murray, A., McLaughlin, N. B., Campbell, R. W. F. (1997)
Measuring QT disersion: man versus machine.
Heart; 77: 539-542.

Okajima, M., Stark L., Whipple, G., Yasui, S. (1963)
Computer Pattern Recognition Techniques : Some results with real electrocardiographic data.
IEEE Trans BME; **10** : 106-14.

Peden, J. C. M. (1982)
ECG Data Compression: Some practical considerations.
In: Computing in Medicine. eds. Paul, J. D., Jordan, M. M., Ferguson-Pell, M. W. & Andrews, B. J.
London: MacMillan : pp 62-7.

Pipberger, H.V., Freis, E.D., Taback, L., Mason, H.L. (1960)
Preparation of Electrocardiographic Data for Analysis by Digital Electronic Computer.
Circulation; **21** : 413-8

Pipberger, .V., Arms, R.J., Stallmann, F.W. (1961)
Automatic Screening of Normal and Abnormal Electrocardiograms by Means of a Digital Electronic Computer.
Proc. Soc. Exp. Biol. Med.; **106** : 130-2

Pipberger, H. V., Arzbaecher, R. C., Berson, A. S. et al. (1975)
Recommendations for standardization of leads and specifications of instruments in electrocardiography and vectorcardiography.
Circulation; **52**, 11-31.

Plokker, H. W. M. (1978)
Cardiac Rhythm diagnosis by digital computer
PhD Thesis, Free University, Amsterdam.

Rosenblatt, F. (1958)
The Perceptron, A Probabilistic Model for Information Storage and Organization in the Brain.
Psychological Review; **65** : pp 386-408

Ruha, A., Sallinen, S., Nissila, S. (1997)
A real-time microprocessor QRS detector system with a 1-ms timing accuracy fo the measurement of ambulatory HRV.
IEEE Transactions on Biomedical Engineering; 44(3): 159-67.

Rumelhart, D. E., Hinton, G. E., Williams, R. J. (1987)
Learning Internal Representations by Error Propagation
In : Parallel Distributed Processing : Explorations in the Microstructures of Cognition, eds. Rumelhart, D. E. & McClelland, J. L.
Cambridge, MA : MIT Press; **Vol. I** : pp. 318-362

Shusterman, V., Shah, S. I., Beigel, A., Anderson, K. P. (2000)
Enhancing the precision of ECG baseline correction: selective filtering and removal of residual error.
Comput Biomed Res; 33(2): 144-60.

Snellen, H. A. (1984)
A History of Cardiology.
Rotterdam : Donker.

Stallmann, F. W., Pipberger, H. V. (1961)
Automatic recognition of electrocardiographic waves by digital computer.
Circulation Research; **9**: 1138-1143.

Stanley, J., Luedeking, S. (1990)
Introduction to Neural Networks.
California Scientific Software, Sierra Madre, CA.

Sun, Y., Suppappola, S., Wrublewski, T.A. (1992)
Microcontroller-based real-time QRS detection.
Biomedical Instrumentation & Technology; 26(6): 477-84.

Suppappola, S., Sun, Y. (1995)
Automated performance evaluation of real-time QRS-detection devices.
Biomedical Instrumentation & Technology; 29(1): 41-9.

Taddei, A., Distante, G., Emdin, M., Pisani, P., Moody, G.B., Zeelenberg, C., Marchesi, C. (1992)
The European ST-T database; standard for evaluating systems for the analysis of ST-T changes in ambulatory electrocardiography.
European Heart Journal; 13:1164-1172.

Talmon, J. L. (1983)
A Structured Analysis
PhD Thesis, Free University, Amsterdam.

Thakor, N.V., Zhu, Y. S. (1991)
Applications of adaptive filtering to ECG analysis: nise cancellation and arrhythmia detection.
IEE Transactions on Biomedical Engineering; 38(8): 785-94.

Van Bemmel, J.H., Duisterhout, J.S., Van Herpen, G., Bierwolf, L.G., Hengeveld, S.J., Versteeg, B. (1971)
Statistical Processing Methods for Recognition and Classification of Vectorcardiograms.
In:Vectorcardiography 2. eds. Hoffman, I., Hamby, R.I. & Glassman, E. Amsterdam, North Holland Publ. Comp. : 207-15.

Van Bemmel, J. H. (1982)
Recognition of electrocardiographic patterns.
In : Handbook of Statistics. eds. Krishnaiah, P. R. & Kanal, L. N. Amsterdam : North Holland; **Vol 2** : 501-26.

Vemuri, V. (1988)
Artificial Neural Networks : An Introduction
IEEE Computer Society, Washington, D.C.

Vijaya, G., Kumar, V., Verma, H. K. (1998)
ANN-based QRS complex analysis of ECG.
Journal of Medical Engineering & Technology; 22(4): 160-7.

Waller, A. D. (1887)
A demonstration on man of electromotive changes accompanying the heart's beat.
Journal of Physiology; **8** : 229-234.

Willems J. L, Pipberger H. V. (1972)
Arrhythmia detection by digital computer.
Computer Biomedical Research; **5** : 263-278.

Willems J. L., Arnaud P., Degani R., Macfarlane P.W., van Bemmel J. H., Zywietz C. H. R. (1980)
Protocol for the concerted action project "Common Standards for Quantitative Electrocardiography".
2nd R&D programme in the field of Medical and Public Health Research of the EEC (80/344/EEC), CSE Ref. 80-06-00.
Acco Publ., Leuven : p152.

Willems, J. L., Arnaud, P., Degani, R., Macfarlane, P.W., van Bemmel, J. H., Zywietz, C. H. R. (1980)
An approach to measurement standards in computer ECG analysis.
In: Optimization of computer ECG Processing. eds. Wolf, H. K. & Macfarlane, P. W.
North Holland, Amsterdam : p135.

Willems, J. L., Arnaud, P., Degani, R., Macfarlane, P.W., van Bemmel, J. H., Zywietz, C. H. R. (1981)
The CSE European Working Party. Common Standards for Quantitative Electrocardiography. The CSE Pilot Study.
In : Proceedings of Medical Informatics Europe 81. eds. Gremy, F., Degoulet, P., Barber, B. & Salamon, R.
Springer-Verlag, Heidelberg : p319.

Willems, J. L.
In: Common Standards for Quantitative Electrocardiography.
1st progress report (1981), p242
2nd progress report (1982), CSE Ref. 82-11-20 : p246
3rd progress report (1983), p275
4th progress report (1984), p277
5th progress report (1985), p327
Acco Publ., Leuven.

Willems, J. L., Arnaud, P., Degani, R., Macfarlane, P.W., van Bemmel, J. H., Zywietz, C. H. R. (1982)
The CSE European Working Party. Common Standards for Quantitative Electrocardiography. CSE project phase one.
In: Computers in Cardiology. ed. Ripley, K. L.
Long Beach, CA, IEEE Computer Society : p69.

Willems, J. L., Arnaud, P., Degani, R., Macfarlane, P.W., van Bemmel, J. H., Zywietz C. H. R. (1985)
Establishment of a reference library for evaluating computer ECG measurement programs.
Computing Biomedical Research; **18** : 439-457.

Willems, J. L., Arnaud, P., Degani, R., Macfarlane, P.W., van Bemmel, J. H., Zywietz, C. H. R. (1985)
Assessment of the performance of electrocardiographic computer programs with the use of a reference data base.
Circulation; **71** : 523-534.

Willems, J. L., Arnaud, P., Degani, R., Macfarlane, P.W., van Bemmel, J. H., Zywietz, C. H. R. (1985)
Recommendations for measurement standards in quantitative electrocardiography.
European Heart Journal; **6**, 815-825.

Willems, J. L., Arnaud, P., Degani, R., Macfarlane, P.W., van Bemmel, J. H., Zywietz, C. H. R. (1987)
Development of a reference library for multi-lead ECG measurement programs.
Journal of Electrocardiology, **20**(suppl) : p56-61.

Willems, J. L., Arnaud, P., Degani, R., Macfarlane, P.W., van Bemmel, J. H., Zywietz, C. H. R. (1987)
A reference Data Base for Multilead Electrocardiographic Computer measurement programs.
Journal of the American College of Cardiology; **10** : 1313-1321.

Willems, J. L., Zywietz, C. H. R., Arnaud, P., van Bemmel, J. H., Degani, R., Macfarlane, P.W. (1987)
Influence of Noise on Wave Boundary Recognition by ECG Measurement Programs.
Computing Biomedical Research; **20** : 543-562.

Willems, J. L. (1989)
In : Comprehensive Electrocardiology. eds. Macfarlane P. W. & Lawrie T. D. V. Computer Analysis of the Electrocardiogram, pp1139-1176. Oxford, Pergamon Press.

Willems, J. L. (1993)
Common Standards for Quantitative Electrocardiography.
In: CSE Atlas. Ref. 83.05.13.
ACCP Publ., Leuven : p655.

Wilson, F. N., Johnson, F. D., Macleod, A. G., Barker, P.S. (1934)
Electrocardiograms that represent the potential variations of a single electrode.
American Heart Journal; **9** : 447-458.

Wilson, F. N., Johnston, F. D. (1938)
The Vectorcardiogram
American Heart Journal; **16**, pp14-28

Wilson, F. N., Kossman, C. E., Burch, G. E. et al. (1954)
American Heart Association Committee on Electrocardiography.
Recommendations for standardisation of electrocardiographic and vectorcardiographic leads.
Circulation; **10**, 564-73.

Xue, Q., Hu, Y.H., Tompkins, W. J. (1992)
Neural-network-based adaptive matched filtering for QRS detection.
IEE Trans BME; 39(4): 317-29.

Yang, T.F. (1995)
Artificial Neural Networks in Computerised Electrocardiography
Phd Thesis, University of Glasgow

Young, T.Y., Huggins, W.H. (1964)
Computer Analysis of Electrocardiograms using a Linear Regression Technique.
IEEE Trans BME; **11** : 60-7.

Zywietz, C., Schneider, B. (1977)
Computer Application on ECG and VCG Analysis. eds. Zywietz, C. & Schneider, B.
Amsterdam : North Holland Publ. Comp. : 1-153.

Zywietz, C. H. R., Willems, J. L., Arnaud, P., van Bemmel, J. H., Degani, R., Macfarlane, P.W. (1990)
Stability of Computer ECG Amplitude Measurements in the Presence of Noise[1].
Computing Biomedical Research; **23** : 10-31.